

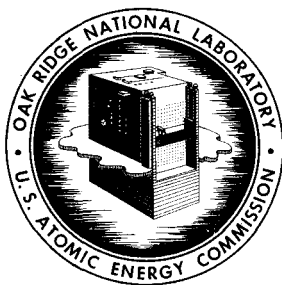
OAK RIDGE NATIONAL LABORATORY LIBRARIES



DOCUMENT COLLECTION

21

3 4456 0549089 4



**OAK RIDGE NATIONAL LABORATORY**

operated by

**UNION CARBIDE CORPORATION**

for the

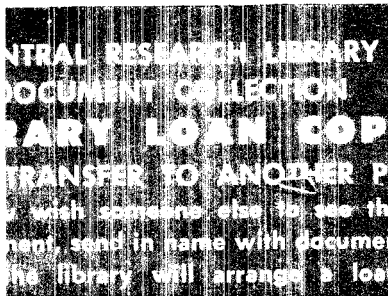
**U.S. ATOMIC ENERGY COMMISSION**



ORNL - TM - 1204

MEASUREMENT OF THE NEUTRON DIFFUSION PARAMETERS IN ORDINARY ICE  
AS A FUNCTION OF THE TEMPERATURE BY THE METHOD OF  
TIME-DEPENDENT NEUTRON DIFFUSION

E. G. Silver  
(Thesis)



Presented to the Graduate Council of the University of Tennessee in partial fulfillment of the requirements for the degree of Doctor of Philosophy.

Neutron Physics Division

MEASUREMENT OF THE NEUTRON DIFFUSION PARAMETERS IN ORDINARY ICE  
AS A FUNCTION OF THE TEMPERATURE BY THE METHOD OF  
TIME-DEPENDENT NEUTRON DIFFUSION\*

E. G. Silver

SEPTEMBER 1965

\*Presented to the Graduate Council of the University of Tennessee in  
partial fulfillment of the requirements for the degree of Doctor of  
Philosophy.

OAK RIDGE NATIONAL LABORATORY  
Oak Ridge, Tennessee  
operated by  
UNION CARBIDE CORPORATION  
for the  
U.S. ATOMIC ENERGY COMMISSION



3 4456 0549089 4

## ACKNOWLEDGEMENTS

The author wishes to thank the staff of Oak Ridge National Laboratory, operated by Union Carbide Corporation for the U.S. Atomic Energy Commission, for their assistance during the performance of the work covered in this thesis.

Heartfelt thanks are especially extended to Dr. Gerard deSaussure for many helpful discussions concerning the formulation and execution of the work. Gratitude also goes to Dr. Fred C. Maienschein and Mr. Everitt P. Blizard for their continuing interest and cooperation which provided encouragement and impetus to carry this work to its conclusion. The author also thanks Mrs. Joan Kobisk, Miss Lenna Lovette, Mrs. Lorraine Abbott, Mrs. Virginia Hamrick, and Mrs. Virginia Glidewell for their efforts in producing a finished dissertation under severe time limits.

Thanks also are due to Dr. M. J. Ohanian of the University of Florida for the numerical calculations of the diffusion parameters in ice, and to Dr. R. P. Belles, also of the University of Florida, for his interest in making such calculations possible.

Most of all the author wishes to acknowledge the indispensable support and never-failing confidence of his wife during the years since the commencement of this work. To her this thesis is dedicated.

TABLE OF CONTENTS

| CHAPTER  | PAGE |
|--|------|
| I. INTRODUCTION . . . . .  | 1    |
| General background . . . . .   | 1    |
| First-order theory of time-dependent diffusion . . . . .   | 3    |
| Historical review of pulsed neutron method . . . . .   | 5    |
| The asymptotic spectrum problem . . . . .  | 16   |
| Goal and scope of the present work . . . . .   | 34   |
| II. THEORETICAL CONSIDERATIONS . . . . .   | 36   |
| The Boltzmann equation . . . . .   | 36   |
| The spherical harmonic expansion of the Boltzmann<br>equation; reduction to diffusion theory . . . . . | 41   |
| Solutions of the one-velocity diffusion equation, and<br>optimization of experiment geometry . . . . . | 51   |
| Spectrum effects . . . . .   | 62   |
| $B^4$ coefficient in one-velocity $P_1$ approximation . . . . .  | 71   |
| The energy-dependent transport theory diffusion<br>cooling . . . . .                                   | 73   |
| The extrapolation distance . . . . .   | 78   |
| Scattering kernels: The Nelkin kernel . . . . .  | 84   |
| Numerical calculations of the ice diffusion parameters . . . . .                                       | 89   |
| III. THE EXPERIMENT . . . . .  | 101  |
| The Experimental Arrangement . . . . .   | 101  |
| The time analyzer and switching circuit . . . . .  | 109  |
| The detector and amplifier system . . . . .  | 119  |

| CHAPTER   | PAGE |
|---|------|
| Secondary pulse deflection system . . . . .                 | 127  |
| The test chamber . . . . .                                  | 128  |
| The target . . . . .  | 135  |
| Ice Cylinder Preparation . . . . .                          | 143  |
| Early trials . . . . .                                      | 144  |
| Large cylinders . . . . .                                   | 145  |
| Small cylinders . . . . .                                   | 147  |
| Data Collection . . . . .                                   | 151  |
| IV. DATA REDUCTION AND ANALYSIS . . . . .                   | 155  |
| Evaluation of the decay frequencies from the data . . . . . | 155  |
| Assignment of decay frequency errors . . . . .              | 192  |
| Calculation of the diffusion parameters . . . . .           | 203  |
| V. RESULTS AND DISCUSSION . . . . .                         | 221  |
| Attainment of Asymptotic Decay . . . . .                    | 221  |
| Diffusion Parameters; Comparison with Other                 |      |
| Experimental Results . . . . .                              | 224  |
| The absorption term, $v\Sigma_a$ . . . . .                  | 224  |
| The diffusion coefficient, $(vD)$ . . . . .                 | 228  |
| The diffusion cooling coefficient, $C$ . . . . .            | 235  |
| Discussion of Results . . . . .                             | 239  |
| Diffusion coefficient . . . . .                             | 240  |
| Diffusion cooling coefficient . . . . .                     | 249  |
| Comparison with Ohanian Calculations . . . . .              | 260  |
| BIBLIOGRAPHY . . . . .                                      | 265  |

| CHAPTER              | PAGE |
|----------------------|------|
| APPENDIX A . . . . . | 275  |
| APPENDIX B . . . . . | 283  |
| APPENDIX C . . . . . | 298  |
| APPENDIX D . . . . . | 360  |
| APPENDIX E . . . . . | 365  |
| APPENDIX F . . . . . | 375  |
| APPENDIX G . . . . . | 383  |

## ABSTRACT

In H<sub>2</sub>O-ice, in contrast to such crystalline moderators as beryllium and graphite, the ratio of the incoherent scattering cross section to the coherent scattering cross section is relatively large for all neutron energies. Therefore, despite its crystalline nature, ice should behave more like an amorphous medium than like crystalline beryllium or graphite. Thus the persistent spectrum-change effects that prevent establishment of a single-exponential decay following injection of neutrons into a small body of the moderator should be absent in ice, permitting the measurement of the diffusion parameters in ice by the method of time-dependent neutron diffusion. The present work was designed to test this hypothesis experimentally, and to measure the parameters  $v\Sigma_a$ , the absorption frequency;  $(vD)$ , the diffusion coefficient; and  $C$ , the diffusion cooling coefficient, assuming asymptotic spectra to be attained.

A series of accurately shaped uniform-density ice cylinders were therefore prepared by methods developed in the course of the work, and these cylinders were subjected to repeated neutron pulses from a 300,000 eV. deuteron accelerator using a deuterium target. The resulting decaying leakage flux was detected and its time-behavior examined by use of an eighteen-channel time-base analyzer. Analysis of the results reveals that asymptotic spectra are established, and therefore the diffusion parameters could be obtained.

The absorption frequency was found to be independent of temperature over the experimental range of  $-5^{\circ}$  to  $-85^{\circ}\text{C}$ . This was expected in view of the  $(1/v)$  behavior of the absorption cross section. The value of  $v\Sigma_a$

corresponds to  $\sigma_a(H)^{(2,200 \text{ m./sec.})} = (331.5 \pm 3.7) \times 10^{-3}$  b. in good agreement with other measurements.

The diffusion coefficient was found to vary linearly with absolute temperature according to the equation

$$(vD)(T^{\circ}K) = [(0.047 \pm 0.202) + (0.01225 \pm 0.0087) \cdot (T^{\circ}K)] \times 10^4 \text{ cm.}^2 \text{ sec.}^{-1} .$$

A small discontinuity in  $(vD)$  across the phase-boundary, inferred from this result, is explained in terms of known scattering cross sections.

The diffusion cooling coefficient was found, within large error limits, to fit either a linear or exponential model. The latter is of the form

$$C(T) = (1.047 \pm 0.173)T^{3/2} .$$

The values of  $C$  suggest that the energy-transfer parameter  $M_2$  is independent of temperature in the range measured. No large discontinuity in  $C$  across the phase boundary could be inferred from these results, in disagreement with results by two other investigators. Theoretical reasons for the observed behavior are suggested.



## CHAPTER I

### INTRODUCTION

#### I. GENERAL BACKGROUND

The interaction of thermal neutrons with non-fissioning matter can be characterized by any one of many possible sets of parameters whose complexity depends on the sophistication of the model employed. In addition to the 'microscopic' parameters which are usually given in cross section form (for example absorption cross section,  $\sigma_a$ , total scattering cross sections  $\sigma_s(E)$ , various partial scattering cross sections such as  $\sigma_{inc}$  and  $\sigma_{coh}$  the incoherent and coherent scattering cross section and  $\sigma_s(E' \rightarrow E, \vec{\Omega}', \vec{\Omega})$  (the cross section for scattering from energy  $E'$ , direction  $\vec{\Omega}'$  to energy  $E$  and direction  $\vec{\Omega}$ ) there have been defined various 'macroscopic' or 'integral' parameters such as the macroscopic cross sections, parameters relating neutron transport to the gradient of the neutron density, expressed variously as  $D$ , the diffusion coefficient,  $L$ , the diffusion length (defined by  $L = \sqrt{D/\Sigma_a}$ ) or  $\lambda_{tr}$  the transport mean free path (given by  $\lambda_{tr} = 3D$ ) and higher-order 'integral' parameters such as the diffusion cooling coefficient,  $C$ , and other terms deriving from transport models.

The diffusion parameters have been experimentally determined for many materials, especially those termed moderators. Moderators are materials characterized by high values of the moderating ratio ( $\Sigma_s \xi / \Sigma_a$ ) where  $\Sigma_s$  and  $\Sigma_a$  are the macroscopic scattering and absorption cross

sections and  $\xi$  is defined as  $\langle \ln \frac{E_1}{E_2} \rangle$  and is thus the mean logarithmic energy loss per collision (Glasstone and Edlund, 1952, see pages 143-145).

Three broad methods for measurements of the diffusion parameters have been employed. The oldest, 'classical' method involves the use of a localized steady-state source of thermal neutrons whose spatial variation in a large sample of the material is then determined. Examples of this type of measurement are the graphite experiments of Duggal and Martelly (1955) and Richey and Block (1956), the beryllium work by Gerasava et al. (1955), and the work in light water by Wilson, Bragden, and Kanner (1944), by Berthelot, Cohen, and Reel (1947), by Rockey and Skolnick (1960), and by Reier and deJuren (1961); as well as many others.

More recently the diffusion parameters have also been measured by the analysis of the changes with time in the neutron density due to a time-dependent source. Two types of experiments in this category may be distinguished. In one, a time-dependent (usually sinusoidally varying) thermal source generates a wave-like neutron density whose propagation through the medium is then observed (Weinberg and Wigner, 1958, page 212). Raievski and Horowitz (1955) and Droulers, Lacour, and Raievski (1958) measured the amplitude attenuation of the waves in graphite as a function of frequency. Later this method was extended by Perez and Uhrig (1963), who made measurements of both amplitude attenuation and phase lag in such wave propagation in various moderators.

The second type of time-dependent experiment for the determination of the diffusion parameters is the so-called 'pulsed-neutron

diffusion method' or 'time-dependent neutron diffusion method,' which is employed in the present work and bears more detailed discussion.

## II. FIRST-ORDER THEORY OF TIME-DEPENDENT NEUTRON DIFFUSION

In order to clarify the terminology to be used in discussing early work with the pulse-neutron technique it seems desirable to give at least a very simplified statement of the theory underlying the time-dependent diffusion experiments at the outset. We assume, then, a finite-sized volume of the moderator in question, characterized by an absorption cross section  $\Sigma_a$  cm.<sup>-1</sup> and a diffusion coefficient  $D$  cm. Assuming further a one-speed neutron population of density  $n(\vec{r}, t)$  at speed  $v$ , we write the source-free differential equation according to the diffusion-theory model as:

$$\frac{\partial n(\vec{r}, t)}{\partial t} = vD \nabla^2 n(\vec{r}, t) - vn(\vec{r}, t) \Sigma_a . \quad (1)$$

It is also assumed that space and time are separable, i.e.  $n(\vec{r}, t) = N(\vec{r})T(t)$ , and that the flux vanishes at the boundaries. The initial density may be written as

$$n(\vec{r}, 0) = \sum_i a_i F_i(\vec{r}) \quad (2)$$

where  $i$  represents the triplet of indices identifying each term in the triply infinite series representing the expansion of the arbitrary initial spatial distribution in terms of the appropriate orthogonal

functions  $F_i(\vec{r})$ .

The solution then is

$$n(r,t) = \sum_i a_i F_i(r) \exp \left\{ -[v\Sigma_a + vD B_i^2]t \right\} \quad (3)$$

where  $B_i^2$  is the eigenvalue corresponding to the  $i$ 'th eigenfunction in the expansion of the spatial initial distribution. It will be observed that the solution consists of a sum of exponentially decaying terms, each with a characteristic decay constant

$$\lambda_i = v\Sigma_a + vD B_i^2 . \quad (4)$$

It is generally true that in the denumerable set of eigenvalues  $B_i^2$  there must be a smallest one. The term with  $\lambda_i$  corresponding to this eigenvalue will then decay least rapidly, and will, in fact become the asymptotically dominant decay. That is to say, using  $j$  for this index

$$\lim_{t \rightarrow \infty} n(\vec{r},t) = a_j F_j(\vec{r}) e^{-(v\Sigma_a + (vD) B_j^2)t} . \quad (5)$$

It will be shown below that in general  $B_i^2$  increases with the indices,  $i$ , so that the asymptotic mode is, it turns out, the so-called fundamental mode which is the one having no nodes in the interior of the body, and which is therefore everywhere non-negative in the interior. The values of  $B_i^2$  depend only on the geometric dimensions of the test body and not on its properties, except for a small extrapolation

distance effect which will be discussed below.

If, therefore, the decay constant  $\lambda$  (when the index is omitted the fundamental eigenvalue case is to be understood) is experimentally determined for a variety of  $B^2$  values of the same material (differing in either size or shape or both) then Equation (4) may be regarded as a linear equation of  $\lambda$  as function of  $B^2$ .

As shown in Figure 1,  $\lambda_a = v\Sigma_a$  is given by the intercept of  $\lambda$  at  $B^2 = 0$ , and the slope of the curve corresponds to  $(vD)$ . On the same figure the dependence of the volume of material on the buckling (by buckling is meant the quantity  $B^2$  defined above) is also shown to emphasize that the volumes of the test material required for measurements close to zero buckling become very large.

### III. HISTORICAL REVIEW OF PULSED NEUTRON METHOD

With this much of an introduction to the time-dependent diffusion method some of the previous work in this field will now be briefly reviewed.

The earliest work involved interest in neutron time-of-flight spectrometers for measurements of absorption cross sections in the near-thermal region. In 1941 Baker and Bacher used a square-wave modulation of the ion source of a small cyclotron to produce a pulsed neutron source in an adjacent paraffin block in which the target was embedded. In order to calculate the effective time-shape of the thermal neutron burst leaving the paraffin block they calculated the correction to the 'true lifetime' (i.e. the absorption lifetime  $(v\Sigma_a)^{-1}$  caused by

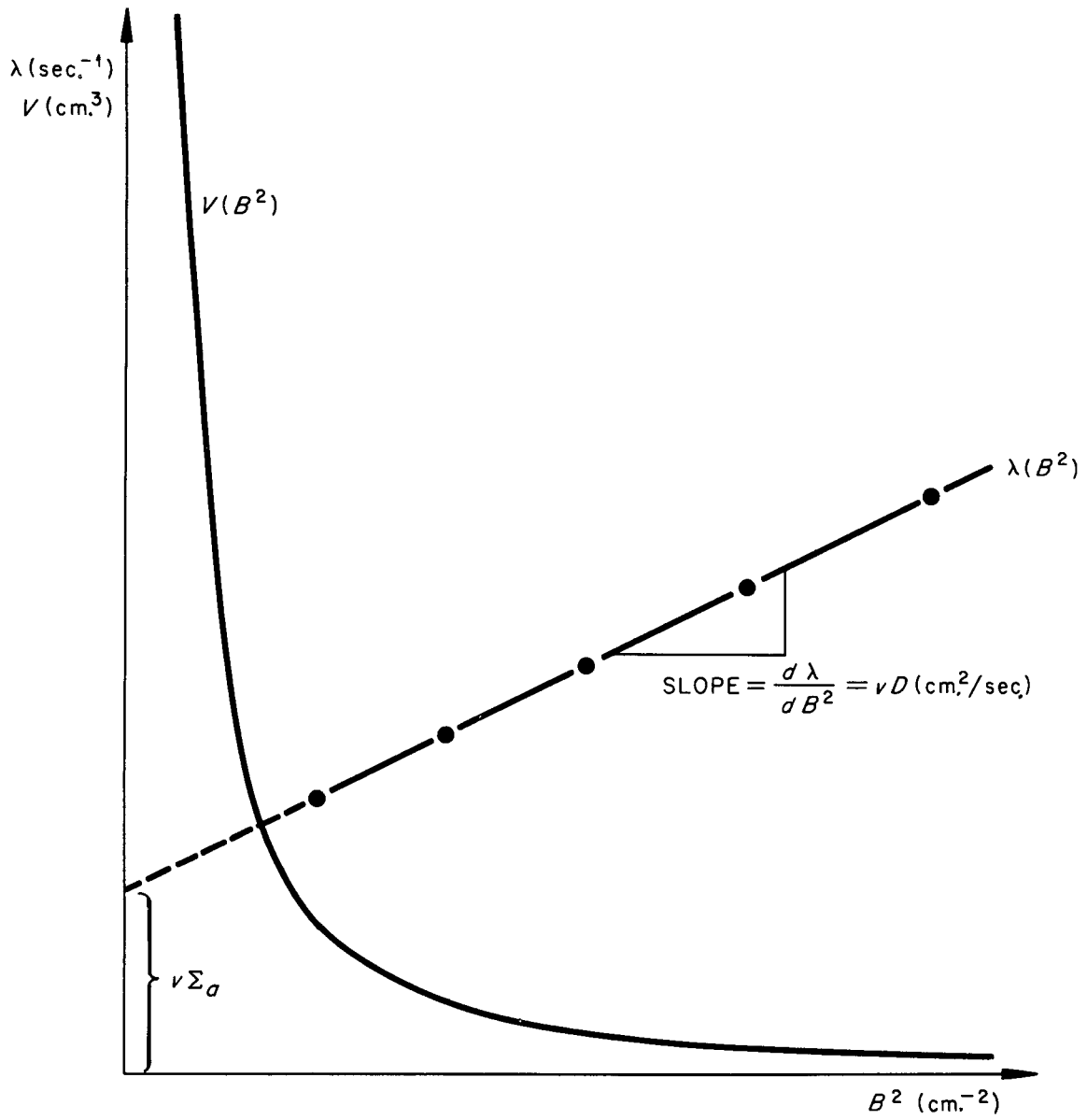


Figure 1. First-order dependence of decay constant,  $\lambda$ , and material volume,  $V$ , on the fundamental mode buckling,  $B^2$ . Scales are arbitrary.

diffusion of the neutrons out of the block. The paper quotes an unpublished calculation by Placek which gives the current from an infinite slab of thickness  $2a$ , with a uniform source throughout the slab as

$$j = (\text{const.}) \sum_{n \text{ odd}} \frac{e^{-(1 + n^2 r^2) \frac{t}{\tau}}}{1 + n^2 r^2} \quad (6)$$

where  $r$  is given by  $r = \pi L / 2a$ , and  $\tau = 1 / (v \Sigma_a)$ . By substituting  $L = (D / \Sigma_a)^{\frac{1}{2}}$ , the exponential term becomes

$$-\frac{t}{\tau} (1 + n^2 r^2) = -t [v \Sigma_a + n^2 (v \Sigma_a) \frac{\pi^2 (D / \Sigma_a)}{4a^2}] = -t [v \Sigma_a + B_n^2 v D] \quad (7)$$

where

$$B_n^2 = \frac{\pi^2 n^2}{4a^2} \quad (8)$$

In the year 1942 Manley, Haworth, and Luebke actually measured the exponential growth and decay of the thermal neutron population in a water tank for the first time, in order to obtain the absorption cross section of hydrogen. They alternately turned the ion source in a deuteron accelerator on and off and used a linear oscilloscope sweep to obtain, by photographic means, the time distribution of pulses observed in a  $\text{BF}_3$  counter immersed in a large tank of water (44-cm.-diam., 54-cm.-high). No attempt was made to separate the spatial distribution into modes, but a correction for diffusion was attempted as follows. An approximate solution for the source-free case with an

initial density distribution  $N(x)$  was obtained of the form:

$$N(x,t) = N(x)e^{-(v\Sigma_a - D \frac{N''}{N})t} \quad (9)$$

where the double prime denotes the second space derivative. These workers attempted experimentally to find a point in the tank where the spatial distribution would have an inflection point, i.e. a point where  $N'' = 0$ . Since  $N''(x) = \nabla^2 N(x) = B^2 N(x)$  the decay at such a point would be equivalent to the fundamental mode decay in an infinite body since effectively  $B^2 = 0$  at that point. However, it is clear now that when an asymptotic distribution is attained no such point exists, and at earlier times its location will shift as the relative amplitudes of the various modes alter in time. In this work, also, the measurements were restricted, by intensity considerations, to times of about 200  $\mu\text{sec}$ . after turning the source off, which is certainly too short for the purpose of attaining a time-invariant spatial distribution. Nonetheless, due to the fact that the tank was large, their reported value  $\sigma_a(H) = 0.33 \text{ b.}$  ("b." will be used for barn =  $10^{-24} \text{ cm.}^2$ ) is in good agreement with modern values.

A somewhat similar experiment was performed by Rainwater and Havens (1946) in 1943, but not published, due to security aspects until the later date. Their paper states that diffusion theory was applied to calculate the 'delayed thermal emission' from the paraffin source used for the time-of-flight experiments, but no quantitative results of the calculations are presented.

In 1953 Von Dardel and Waltner measured the neutron-proton capture cross section using a pulsed-neutron method with neutrons from a deuterium (heavy ice) target in a deuteron accelerator.

They avoided the problem of modes and leakage by using a very large vessel, 97 cm. by 97 cm. by 107 cm. with a central target, and measuring the variation of the neutron density with time at a large number of locations in the water.

Using the many measurements they thus found, in effect, the integral

$$n(t) = \int_{\text{vol.}} n(\vec{r}, t) d\vec{r} \quad (10)$$

to average out the changing shape of the flux distribution. Their value of the hydrogen absorption cross section was  $\sigma_a(\text{H}) = 0.321 \pm 0.005$  b. at  $2.2 \times 10^5$  cm./sec. velocity.

In 1954 Scott, Thompson and Wright employed the pulsed neutron method to determine the absorption cross sections of hydrogen, boron, and silver, the latter two by dissolving salts of these materials in water. They measured decay values over a buckling range from  $0.06 \text{ cm.}^{-2}$  to  $0.18 \text{ cm.}^{-2}$  and extrapolated the  $\lambda$  vs.  $B^2$  curves to  $B^2 = 0$  to obtain  $v\Sigma_a$ . As a neutron source they employed a uranium target bombarded by electrons from a betatron to produce  $(\gamma, n)$  and  $(\gamma, f)$  neutrons. No discussion of higher modes is given; the experimenters merely waited until apparently pure exponential curves were observed. They obtained a value of  $0.525 \pm 0.01$  cm. for  $\lambda_{\text{tr}}$  corresponding to  $D = 0.175$  cm. and

a hydrogen absorption cross section of 0.323 b. for a neutron velocity of  $2.2 \times 10^5$  cm./sec. This is apparently the first use of the pulsed neutron method to measure a value of the neutron diffusion coefficient of a moderator.

In 1954 Von Dardel published an extensive paper treating in detail for the first time the slowing down and thermal diffusion of neutrons in finite moderators. This paper was supplemented, later in the same year, by a paper together with N. G. Sjöstrand (Von Dardel and Sjöstrand, 1954). Von Dardel specifically recognized that the velocity dependence of the diffusion coefficient would lead to a shift in the spectrum of the asymptotic neutron population in a finite medium. Von Dardel termed this effect "diffusion cooling"; it appears as one or more correction terms to the first order equation for  $\lambda$  in  $B^2$  introducing terms of at least the order  $B^4$ . Von Dardel demonstrated the change in the effective temperature of the leakage neutrons directly by measuring the neutron transmission through a  $1/v$  filter.

Since that time many investigators have applied this method to various moderators, and much theoretical work has been done to interpret the results.

For example, graphite was studied by Beckurts (1957), Kuchle and Beckurts (1959), Antonov et al. (1955), and deSaussure and Silver (1957). Beryllium was investigated by Campbell and Stelson (1956), Antonov et al. (1956), Komoto and Kloverstrom (1958), Andrews (1960), and deSaussure and Silver (1958, 1959). Andrews (1960) and deSaussure and Silver (1959) also investigated the temperature dependence of the diffusion

parameters in beryllium. Andrews covered the range 19°C. to 205°C. and deSaussure and Silver measured from 500°C. to -100°C. The results of this work will be discussed in detail below since they bear on the present investigation. It is characteristic of these measurements in all the materials that they tend to agree well as to the absorption mean life and the diffusion coefficient, but disagree seriously concerning the magnitude, or even existence, of the diffusion cooling coefficient and higher order terms.

Pulsed experiments in heavy water have been reported by Sjöstrand (1959), Ganguly et al. (1963), Küssmaul and Meister (1963), and Daughtry and Waltner (1965). Measurements of the diffusion parameters by the pulsed neutron method have also been performed in beryllium oxide by Komoto and Kloverstrom [unpublished, quoted by Andrews (1960, page 197)], Ramanna et al. (1955), and Joshi et al. (1965); in paraffin by Dio (1958,1959) and Kuchle (1960a); in 'Dowtherm A'<sup>1</sup> by Kuchle (1960b); in zirconium hydride by Meadows and Whalen (1962); and in polyethylene by Sjöstrand, Mednis, and Nilsson (1959).

Pulsed-neutron measurements in water have been among the most intensively pursued right from the very beginning, due to the practical interest in water as a reactor moderator, its ready availability and convenient liquid state, and the inherent interest of its composition. As was discussed above, water was used in some of the very early work as medium for the measurement of the hydrogen-proton absorption cross section, and as a moderator and diluent for absorption cross section

---

<sup>1</sup>Registered Trademark for a mixture also called Diphyl.

measurements of dissolved substances.

Von Dardel's first work to obtain the diffusion coefficients directly included measurements in water (Von Dardel, 1954). Since then a number of other investigators have pulsed water to measure the diffusion parameters. In several instances the effect of temperature on D and C has been obtained in the domain from room temperature upwards. Room-temperature water measurements have been performed by Bracci and Coceva (1956), Lopes and Beyster (1961), Bretscher (1962), Dlouhý and Kvítek (1962), and Von Dardel and Sjöstrand (1954). The temperature dependence of the diffusion parameters in water was investigated by Dio and Schopper (1958), Kúchle (1960a, 1960b), and Antonov et al. (1960).

Three measurements on ice also have been published. One, interestingly enough, is included in Von Dardel's (1954) first paper; however this paper gives only a crude measurement of the variation of decay period with temperature in a single ice body having a shape intended mainly for transmission measurements and hence not very suitable for decay measurements. The ice was in a copper tank, and contained a 3.2-cm.-diam. hole in which the target was located, seven copper plates, 0.05-cm.-thick uniformly spaced, and a copper cup into which the detector could be inserted. Measurements were performed at  $98^{\circ}\text{K.}$ , and then, while the ice was warming up, further measurements were performed. Figure 2, taken from Von Dardel's paper (1954) shows the results obtained. Von Dardel states

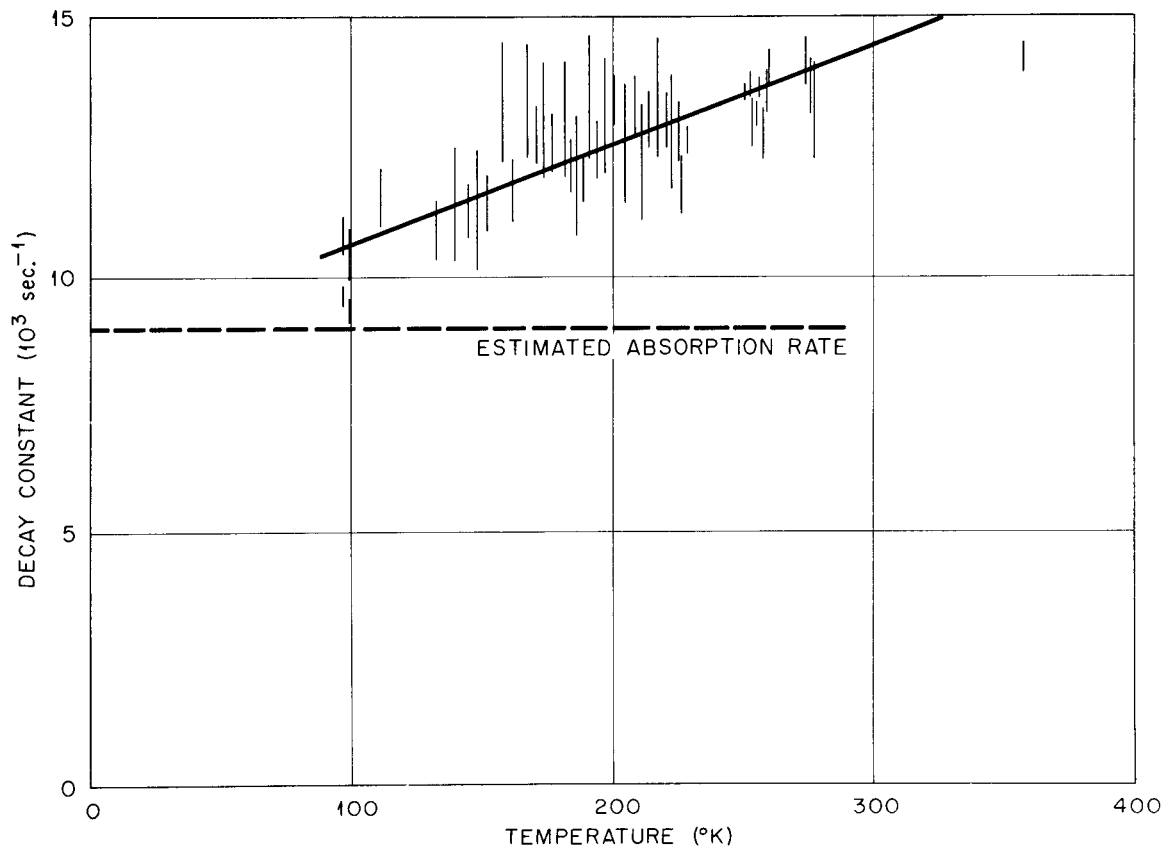


Figure 2. Asymptotic decay rate of the neutron intensity as a function of the absolute temperature of the moderator obtained by VonDardel (1954) p. 76.

". . . we find that the leakage rate is roughly proportional to the absolute temperature. This is in qualitative agreement with the temperature dependence of the diffusion length quoted by Fermi (1946):

$$L = 2.64 + 0.0061(T - 273) \text{ cm.} \quad (11)$$

which . . . will lead to a diffusion coefficient which is roughly proportional to the absolute temperature, since the mean life for absorption is temperature-independent."

The second reported pulsed-neutron measurement in H<sub>2</sub>O-ice was made by Antonov et al. (1962), who reported the ratios of the diffusion coefficients and diffusion cooling coefficients obtained in ice at 0°C., -80°C., and -196°C. to those obtained in water at 0°C. Using another report published by Antonov et al. (1960), absolute values for these quantities can be assigned from his work, though the error limits are large. A third measurement involving ice is the work of Dlouhý and Kvítek of the Czechoslovak Academy of Sciences (1962), who measured the diffusion parameters in water at 20°C. and at 0°C., and in ice at 0°C. However, the Letter to the Editor reporting these results contains little information on which to base an appraisal of the methods employed. Table I lists all the pulsed-neutron experiments performed in H<sub>2</sub>O by other experimenters.

The results of all the investigations in water will be discussed in detail in Chapter V, in comparison with results of the present work. A review article by Beckurts (1961), provides a good general review of the pulsed-neutron experiment field. More recently, symposia at Brookhaven (1962) and at Karlsruhe (1965) provided comprehensive surveys of the state of the field.

BUCKLING AND TEMPERATURE RANGES INVESTIGATED BY VARIOUS EXPERIMENTERS IN H<sub>2</sub>O

| Experimenter <sup>a</sup>     | Buckling Range                                    | Temperature Range                |
|-------------------------------|---|----------------------------------|
| VonDardel, 1954               | 19 cm. cube                                       | 98°K. → 0°C.<br>and room<br>room |
| Scott <u>et al.</u> , 1954    | ≈0  | room                             |
| VonDardel and Sjöstrand, 1954 | 0.11 cm. <sup>-2</sup> → 0.65 cm. <sup>-2</sup>   | room                             |
| Antonov <u>et al.</u> , 1955  | 0.12 cm. <sup>-2</sup> → 0.95 cm. <sup>-2</sup>   | 23°C. - 80°C.                    |
| Campbell and Stelson, 1955    | 0.08 cm. <sup>-2</sup> → 1.10 cm. <sup>-2</sup>   | room                             |
| Ramanna <u>et al.</u> , 1955  | ≈0  | room                             |
| Bracci and Coceva, 1956       | 0.09 cm. <sup>-2</sup> → 0.96 cm. <sup>-2</sup>   | room                             |
| Dio and Schopper, 1958        | 0.16 cm. <sup>-2</sup> → 0.87 cm. <sup>-2</sup>   | 19°C. - 75°C.                    |
| Küchle, 1960                  | 0.10 cm. <sup>-2</sup> → 0.75 cm. <sup>-2</sup>   | 22°C. → 80°C.                    |
| Antonov <u>et al.</u> , 1960  | ≈0.06 cm. <sup>-2</sup> → ≈0.5 cm. <sup>-2</sup>  | -196°C. → 286°C.                 |
| Lopez and Beyster, 1961       | 0.01 cm. <sup>-2</sup> → 0.59 cm. <sup>-2</sup>   | 26.7°C.                          |
| Bretscher, 1962               | ≈0.00 cm. <sup>-2</sup> → 0.60 cm. <sup>-2</sup>  | 26°C.                            |
| Antonov <u>et al.</u> , 1962  | not given   | -196°C. → 0°C.                   |
| Dlouhý and Kvítek, 1962       | ≈0.09 cm. <sup>-2</sup> → 0.79 cm. <sup>-2</sup>  | 0°C. → 20°C.                     |
| DeJuren, 1965                 | 0.031 cm. <sup>-2</sup> → 0.646 cm. <sup>-2</sup> | 23°C.                            |
| Pál, Bod, and Szatmáry, 1965  | not given   | 22°C.                            |

<sup>a</sup>References to these values will be found in the Bibliography.

## IV. THE ASYMPTOTIC SPECTRUM PROBLEM

At the outset of this discussion it will be well to define several terms which will be used with specific denotations throughout this discussion. When low-energy neutrons scatter by interaction with either a single nucleus, or with a system of scattering centers, then the process may be divided into two types, inelastic, and elastic. By inelastic processes is meant any process whereby the kinetic energy of the neutron changes. No change in the internal state of the scattering nucleus is implied, as is the case where the term is used at higher energies. The change in energy may be due to the translational energy taken up by the recoiling scatterer, or the scattering may change the internal state of a scattering molecule. Inelastic scattering can also result from a scattering process whereby a neutron either gives up or receives a quantum of vibration energy from a crystalline lattice, that is to say, phonon exchange. Bragg scattering off a plane of scattering centers in a crystal on the other hand is strictly elastic, since the mass of the lattice is in effect infinite, so that the momentum transfer involves no energy transfer. One may also divide scattering processes into incoherent and coherent types. These are different in that, in the former case the phase shifts are random so that all cross-terms vanish upon averaging; in the latter there is interference of the scattered wave amplitudes. It is easy to show that there is a minimum energy (or maximum neutron wave-length) with respect to any set of lattice parameters, beyond which coherent scattering is impossible. This minimum energy is called the Bragg cutoff, below which only

incoherent scattering processes are possible.

With these terms in mind, we now turn to a consideration of the effect of neutron velocity distribution on the first-order derivation given above. So far the discussion has assumed that at some instant in time the neutrons in a moderator, though arbitrarily distributed in space, all possess a single scalar speed,  $v$ , which would after that time remain unchanged. However, if the neutrons undergo any inelastic scattering, and if there is no absorption, then, in an infinite medium, the neutrons will, after a sufficiently long time, have the Maxwellian distribution as a consequence of the energy equipartition law, regardless of the details of the scattering processes. (See for example 'Kinetic Theory of Gases', (Present, 1958), pages 72-77.) In velocity terms this Maxwellian distribution is given by

$$n(v) dv = \frac{4n}{v_0^3 \sqrt{\pi}} v^2 e^{-v^2/v_0^2} dv \quad (12)$$

where  $v_0$  is the most probable velocity,

$$v_0 = \sqrt{\frac{2kT}{m}}, \quad (13)$$

$T$  is the temperature in Kelvin units,  $k$  is Boltzmann's constant, and  $m$  is the neutron mass. The equivalent distribution function in energy units is

$$n(E) dE = \frac{2\pi}{(\pi kT)^{3/2}} e^{-E/kT} \sqrt{E} dE \quad (14)$$

The principle of detailed balance on the energy transfer cross sections states

$$\Sigma_s(E \rightarrow E') M(E) = \Sigma_s(E' \rightarrow E) M(E') \quad (15)$$

where  $M(E)$  is the neutron density at energy  $E$  in a Maxwellian spectrum, and

$$\Sigma_s(E \rightarrow E') = 2\pi \int_0^\pi \Sigma_s(E \rightarrow E'; \theta) \sin \theta \, d\theta \quad (16)$$

where  $\theta$  is the angle through which the neutron is scattered. That is to say,  $\Sigma_s(E \rightarrow E')$  is the total scattering cross section from energy  $E$  to energy  $E'$ . This detailed balance condition (Nelkin, 1960) which applies strictly if there is no absorption or leakage guarantees that if the energy transfer cross section is nonvanishing the energy spectrum of the neutrons will, given sufficient time, become like that of the moderator atoms with which the neutrons are in contact.

In this situation (infinite medium, no absorption) there will be a true persisting asymptotic spectrum of neutrons with a Maxwellian velocity distribution. This is, indeed, the only condition under which a true asymptotic Maxwellian spectrum exists for infinitely long times (neglecting the free-neutron decay). If absorption is present, then not only will the spectrum decay in time, but in general it will not remain Maxwellian. In one particular case, however, the spectrum can be Maxwellian, even in the presence of absorption. This is the case if

the absorption has a  $1/v$  energy dependence. In that case, if the distribution  $M(v)$  is Maxwellian at time  $t$ , then the absorption rate at velocity  $v$ , defining  $\varphi(v)$  to be the total neutron flux at velocity  $v$ , is:

$$R(v) = \varphi(v) \Sigma_a(v) = N_N M(v) v N_A \frac{\sigma_{a,0} v_0}{v} = N_N N_A v_0 \sigma_{a,0} M(v) \quad (17)$$

where  $N_N$  and  $N_A$  are the densities of the neutrons and moderator atoms respectively,  $v_0$  is a reference velocity and  $\sigma_{a,0}$  is the microscopic absorption cross section at that velocity. The absorption is then proportional to the neutron spectrum amplitude at every velocity, and the spectrum is not distorted by the absorption. In this case, then, the spectrum will remain Maxwellian or become Maxwellian asymptotically. However, unless  $v\Sigma_a$  is small compared to  $(1/\tau)$ , where  $\tau$  is a measure of the time required to approach energy equilibrium, the population of neutrons will decay more rapidly due to absorption than it approaches a Maxwellian energy distribution so that the neutron flux amplitude will have effectively vanished before energy equilibrium is attained.

There is also a 'quasistable' situation in which an asymptotic spectrum is attained which is more or less distorted from the Maxwellian spectrum of the moderator atoms. This occurs if a constant source of neutrons of higher energy is present which compensates for the absorption losses (Weinberg and Wigner, 1950, pages 332-377). In that case an asymptotic spectrum will be established. However, since the neutrons are subject to absorption during the thermalization process, the low end of the population will be relatively attenuated, and the equilibrium

spectrum will be distorted, with its peak shifted upward. This is the so-called 'absorption hardening' effect met in reactor physics. If the absorption is weak the shape of the spectrum will not change materially, and the effect is mainly an upward shift in the effective temperature plus a "tail" proportional to  $1/E$  at the high-energy end. However, if the absorption is strong, or has strong resonances the spectrum distortion can be large.

Another, in the present instance, more interesting factor that can affect the equilibrium spectrum is the effect of leakage in a finite medium. The leakage term in the diffusion approximation is proportional to  $D$ , which generally increases with neutron velocity, and to  $v$ . So the faster neutrons will leak more rapidly than the slower ones, leaving the remaining distribution at a lower mean energy than that of the moderator atoms. This is the diffusion cooling effect, which adds a negative term of the order of  $B^4$  to the first-order solution of the diffusion equation [Equation (4)]. The magnitude of the energy shift for a given  $B^2$  depends on the velocity dependence of  $D$  and on the effectiveness of the energy exchange mechanisms that transfer energy from the moderator to the neutron population to compensate for the cooling effect. In the absence of any energy transfer and under the assumption made regarding the velocity dependence of  $D$  the spectrum would 'cool' continuously as long as any neutrons remain, since the faster component of the spectrum would at every time leak faster. If energy exchange scattering is present, then an equilibrium distribution may result when the two competing processes of diffusion cooling and energy exchange heating are in dynamic equilibrium.

Again, however, the time for such an equilibrium to be attained must be shorter than the neutron lifetime against leakage and absorption, or the neutron population will have decayed to the vanishing point before equilibrium is attained.

deSaussure and the present author (deSaussure and Silver, 1959; and Silver, 1962), in the process of investigating the diffusion parameters of beryllium metal found that at low temperatures and large bucklings the measured slope of the time-decay of the neutron population underwent continuous change over times as long as were accessible to measurement. (These times are limited by the available intensity of the pulsed neutron source and the counting background above which the decreasing count rate must be measured.) Figures 3 and 4 show the observed effect in two beryllium parallelepipeds. It will be observed that the effect is more pronounced with large buckling (small dimensions). Figures 5 and 6 show the apparent change in decay frequency in a beryllium block over longer periods of time, at 25°C. and at -25°C. The explanation, proposed by deSaussure (1962), rests on the particular shape and temperature dependence of the elastic and inelastic components of the scattering cross sections of beryllium, as calculated by Bhandari (1958), and shown in Figure 7. The transport cross section  $\sigma_{tr} = \sigma_s(1-\bar{\mu})$ , where  $\bar{\mu}$  is the mean cosine of the scattering angle, has typical Bragg peaks due to backward scattering of neutrons whose wavelength matches the spacing in a crystal plane. A very large peak at about 0.0068 eV. and several other peaks, are seen. The elastic scattering is only weakly temperature dependent. The inelastic contribution to the

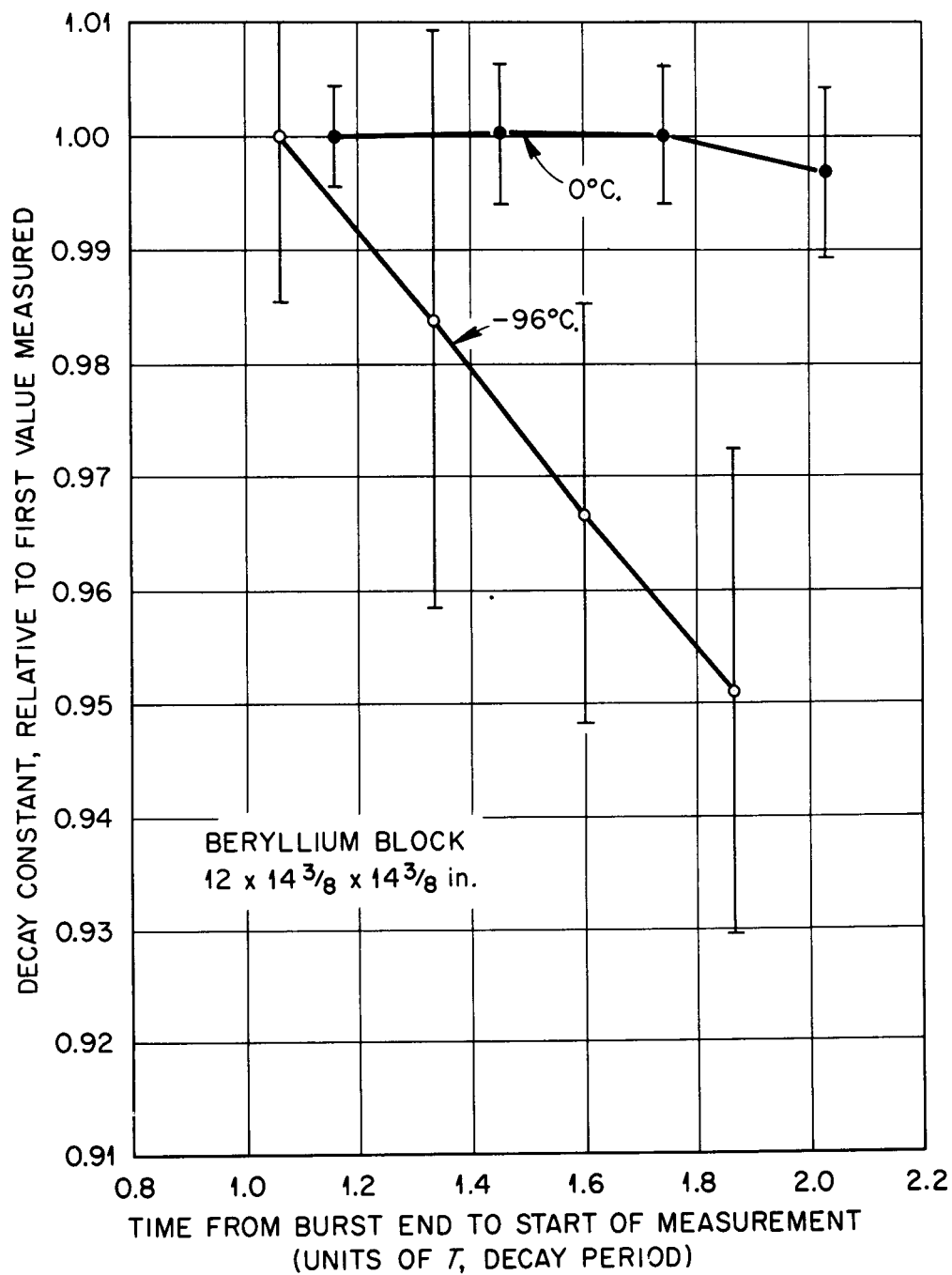


Figure 3. Relative values of decay constant,  $\lambda$ , as a function of time elapsed between end of neutron pulse and start of data analysis. Time is in units of  $T = 1/\lambda$ ;  $\lambda$  normalized to unity at about  $T = 1$ . The lines are drawn to connect points obtained from the same run and do not represent the rate of change in  $\lambda$ .

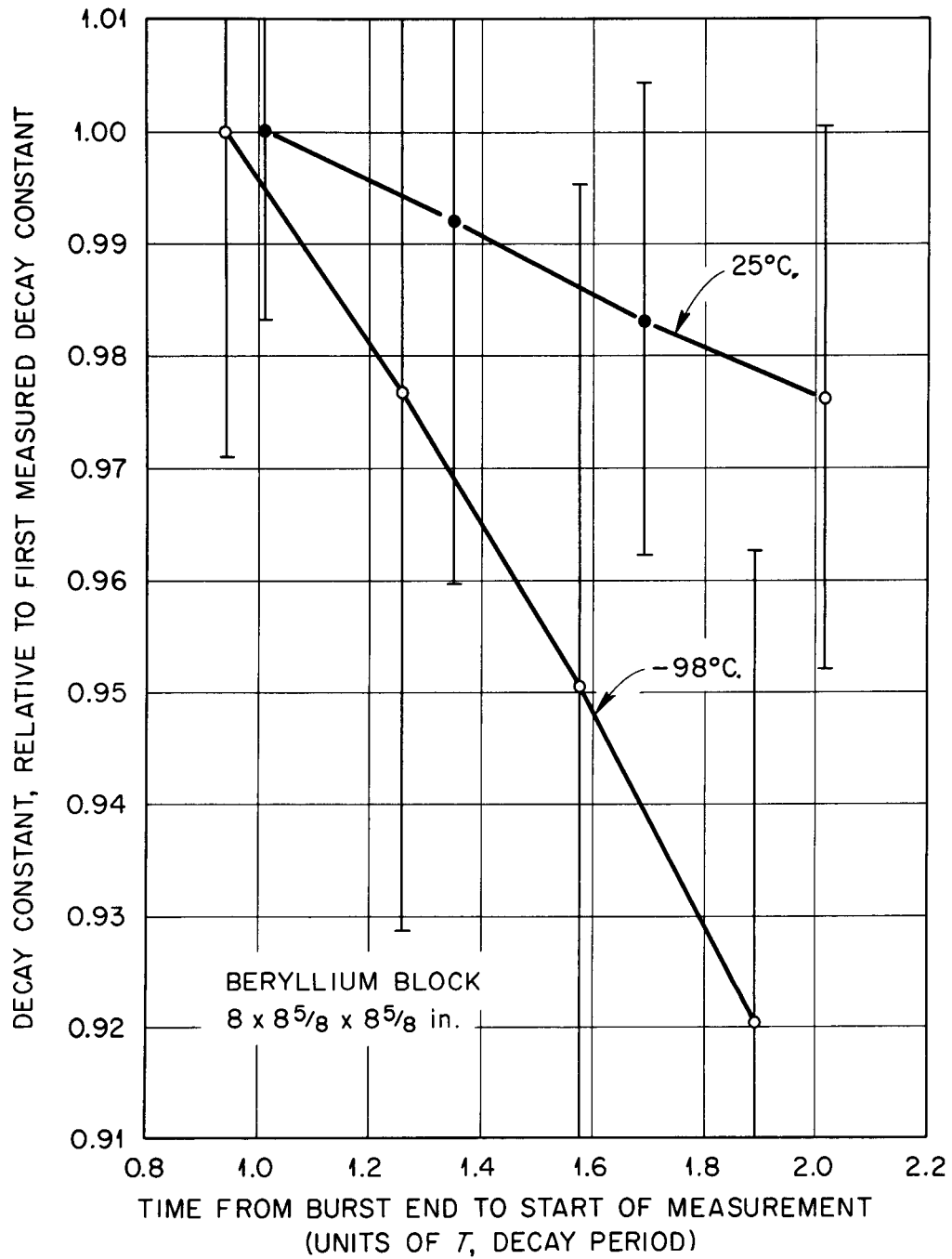


Figure 4. Relative values of decay constant,  $\lambda$ , as a function of time elapsed between end of neutron pulse and start of data analysis. Time is in units of  $T = 1/\lambda$ ;  $\lambda$  normalized to unity at about  $T = 1$ . The lines are drawn to connect points obtained from the same run and do not represent the rate of change in  $\lambda$ .

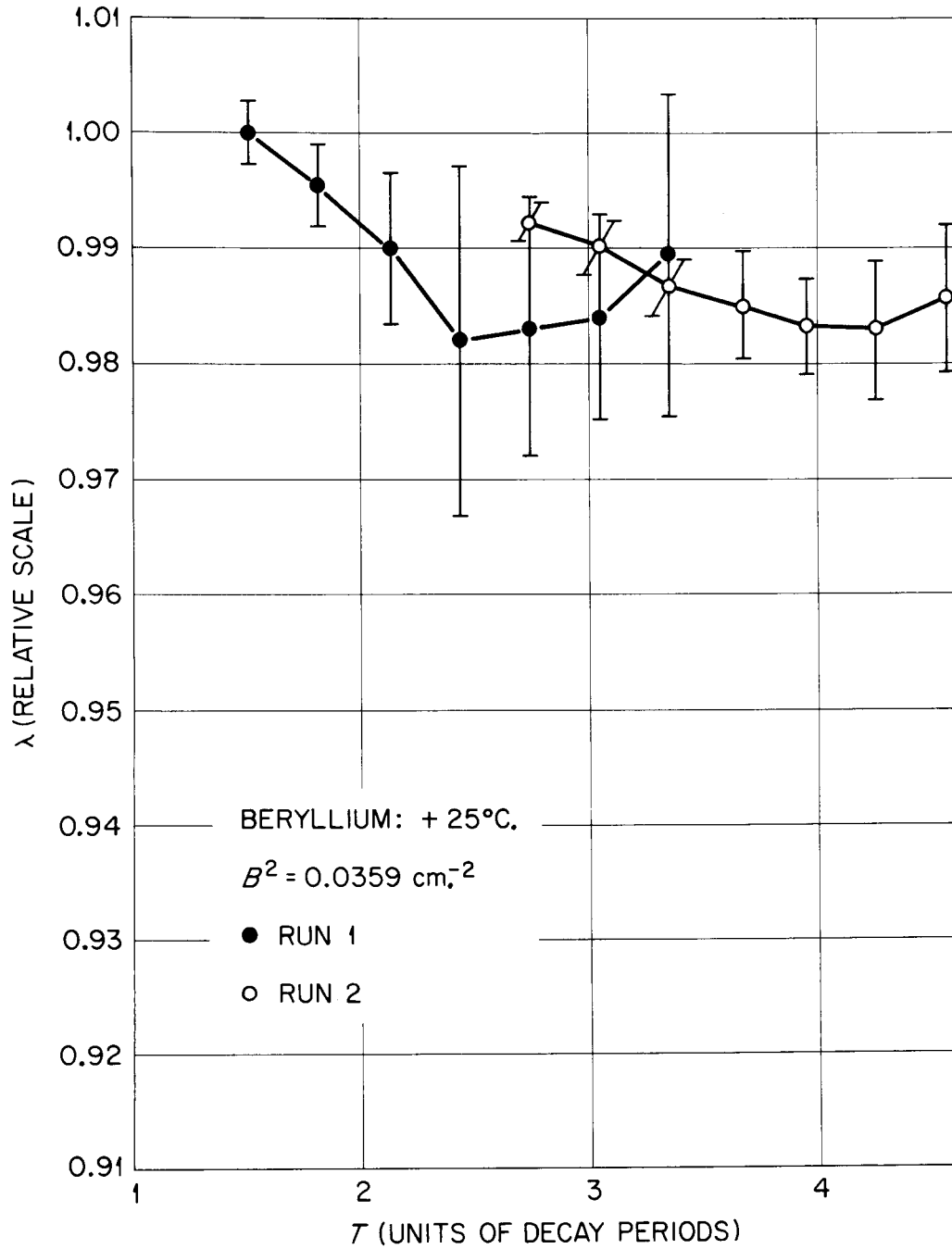


Figure 5. Relative values of decay constant,  $\lambda$ , as a function of time elapsed between end of neutron pulse and start of data analysis. Time is in units of  $T = 1/\lambda$ ;  $\lambda$  normalized to unity at about  $T = 1$ . The lines are drawn to connect points obtained from the same run and do not represent the rate of change in  $\lambda$ .

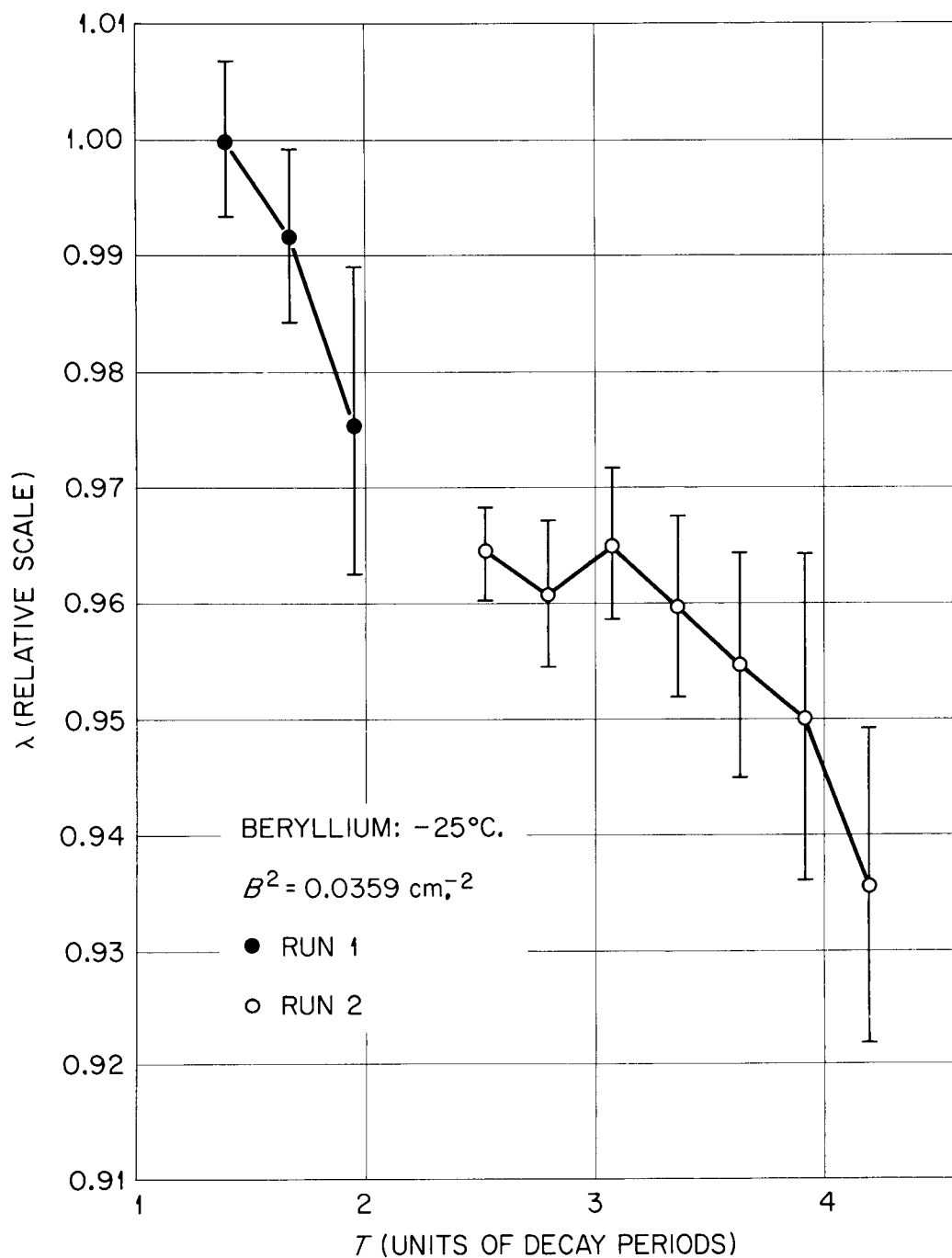


Figure 6. Relative values of decay constant,  $\lambda$ , as a function of time elapsed between end of neutron pulse and start of data analysis. Time is in units of  $T = 1/\lambda$ ;  $\lambda$  normalized to unity at about  $T = 1$ . The lines are drawn to connect points obtained from the same run and do not represent the rate of change in  $\lambda$ .

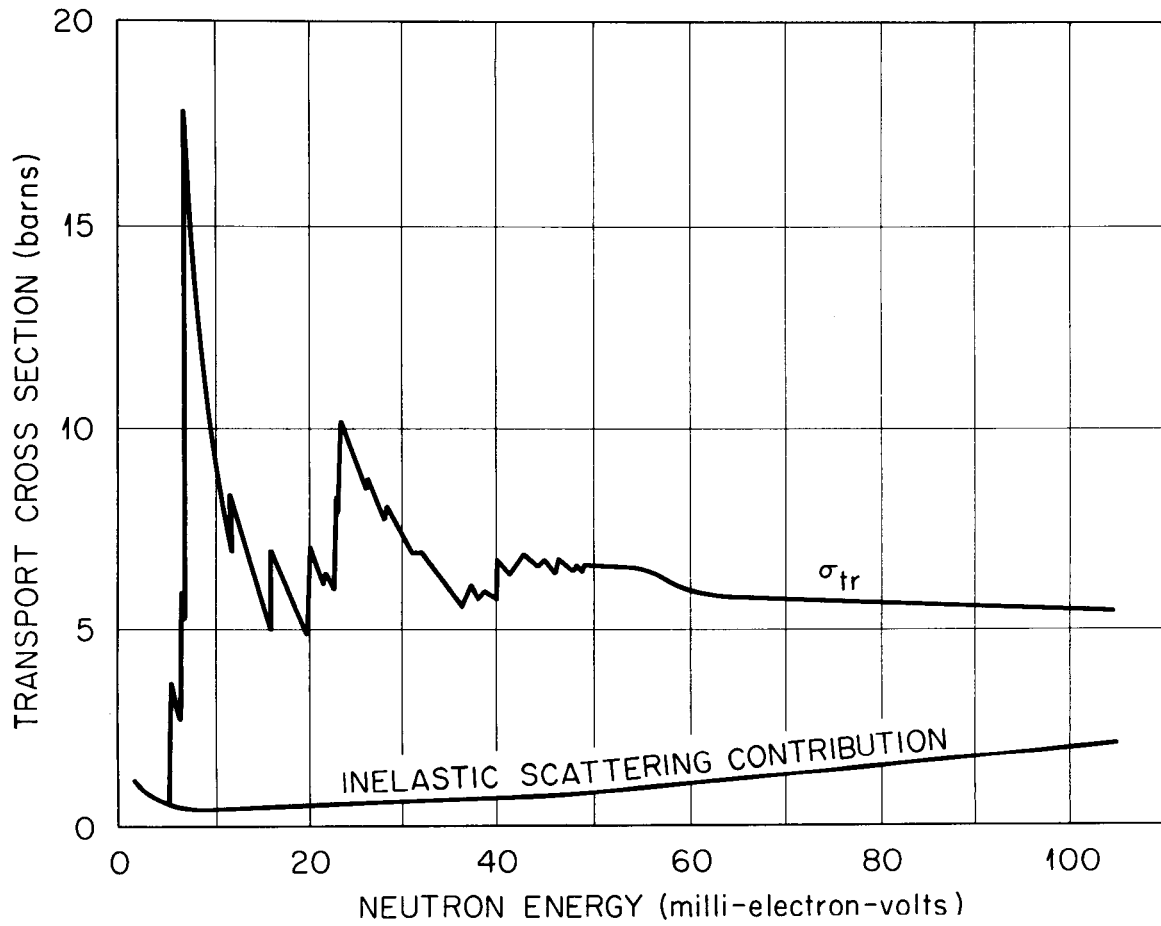


Figure 7. Transport cross section of beryllium calculated by R. C. Bhandari (1958).

scattering is also shown, and may be seen to be much smaller, at the energy of the peak, than the elastic component; however, the inelastic component of the scattering cross sections is strongly temperature dependent, as will be shown below. The very high peaking of the transport cross section is due to the strongly nonisotropic, and in fact dominantly backward scattering of neutrons of the energy corresponding to the elastic scattering peaks. At the 0.0068 eV. peak the inelastic component of the transport cross section is smaller by a factor of about 40 than the total cross section. The neutrons of that energy, then, may be considered to be a population with a very high probability of elastic, large-angle scattering, which in effect means small  $D$ , and a relatively small probability of scattering out of that energy per unit time. Since the energy-exchange mechanism is very ineffective for such neutrons, and the leakage losses are also low, these neutrons tend to persist as a separate, long-lived, subpopulation whose density continues to grow, relative to that of the total population, as time progresses. These 'trapped' neutrons, will therefore, be present in changing proportion, leading to changing measured effective decay periods. At high temperatures the higher inelastic cross section makes the "trap" much less effective. In an infinite beryllium moderator the spectrum would eventually become Maxwellian despite the cross section ratio, assuming the absorption were low enough, since the inelastic cross section does not vanish. However, in a small block, the spectrum continually sharpens as it decays, as the trapped neutrons become a more and more dominant component of the total population.

deSaussure (1962), showed, on the basis of a variational calculation, that an upper bound exists for the asymptotic beryllium decay frequency (not necessarily the least upper bound) of magnitude  $\lambda = (5.8 + 17.6 B^2) \text{ sec.}^{-1}$  which lies below the measured values obtained by various experimenters at large bucklings, demonstrating that the measured values do not represent asymptotic spectrum measurements.

If the measurement is performed before an asymptotic decay is established then the measured diffusion parameters would be expected to vary with such factors as the waiting time after the neutron injection, the background against which counting was done, and the mathematical method for fitting the data to an exponential decay. Figure 8, taken from deSaussure's, shows that, though the data of various workers agree well at small bucklings, there are serious discrepancies at large bucklings, with some points lying well above the calculated upper bound.

Jha (1960) has calculated the equilibrium spectrum in several small beryllium assemblies, using the correct transport cross section, and has shown that sharp peaks in the spectra occur. Recently Gaerttner, Daitch, and Fullwood (1965) have published experimental results demonstrating that in beryllium with  $B^2 \geq 0.0075 \text{ cm.}^{-2}$  asymptotic spectra are not established and that progressive peaking of the flux at the locations of the transport cross section maxima occurs.

If this explanation for the trapping effect is valid, then all crystalline materials in which energy domains with large ratios  $(\sigma_{tr})/(\sigma_{inel.})$  exist should exhibit such effects. Whereas a crystal with

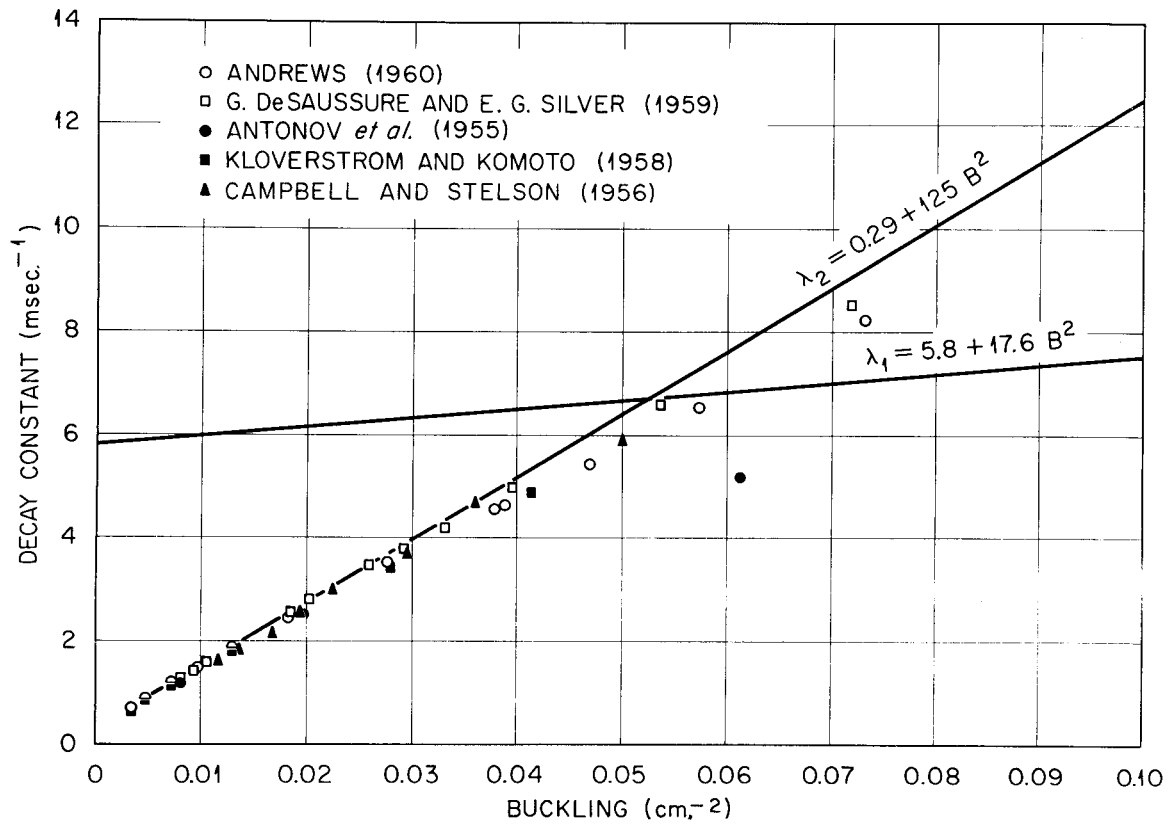


Figure 8. Measured values of decay frequency in Be, compared with calculated upper bounds.

much smaller elastic cross sections, i.e. small Bragg (coherent) scattering, should not exhibit such trapping behavior.

The scattering cross section for a bound atom scattering independently, i.e. with no coherent effects, cannot be measured directly; however, its magnitude can be found from measurements of the free-atom scattering cross section in the range of 10 to 20 eV, where binding effects are negligible. Since the incoherent 'hard-sphere' scattering is energy independent, applying a mass correction to the free-atom scattering cross section produces the 'bound-atom' scattering cross section,  $\sigma_{\text{bound-atom}}$ , which an infinite-mass atom with the same hard-sphere radius would possess:

$$\sigma_{\text{bound-atom}} = \sigma_{\text{free-atom}} \frac{(A + 1)^2}{A^2} . \quad (18)$$

In the absence of any mechanisms for inherently incoherent scattering, such as isotopic scattering or spin-dependent scattering, only the potential scattering cross section  $\sigma_p = 4\pi R^2$  exist, all of which can contribute to the coherent scattering. In the absence of such effects, then, one expects that  $(\sigma_{\text{free-atom}})(A + 1)^2/A^2$  should be equal to  $\sigma_{\text{coh.}}$ , the measured coherent cross section. Beryllium is such a material;  $\sigma_{\text{free-atom}}$  is quite flat from about 1.0 eV. to 30,000 eV. at 6.1 b. This gives  $\sigma_{\text{bound-atom}} = (10/9)^2 \times (6.1) = 7.5$  b., which agrees with the measured  $\sigma_{\text{coh.}} = 7.53 \pm 0.07$  b. (Hughes and Schwartz, 1958). The scattering in beryllium is then free of inherent incoherent scattering sources, except for the 'thermal diffuse' scattering from the lattice

displacements due to thermal agitation, which are strongly temperature dependent. This incoherent component may be observed directly as  $\sigma_{\text{tot.}} - \sigma_{\text{abs.}}$  for Be at 0.002 eV. which is below the Be Bragg cutoff energy of about 0.005 eV. The temperature effect is shown in Table II.

The situation in hydrogen is very different. Here  $\sigma_{\text{coh.}}$ , the cross section component capable of coherent scattering effects, is  $(1.78 \pm 0.02)$  b. (Stehn et al., 1964). This is much less than  $\sigma_{\text{bound-atom}} = (79.6 \pm 0.4)$  b. (Stehn et al., 1964), indicating that there is a large inherent source of incoherent scattering in hydrogen, which is due to the spin incoherence of the randomly aligned proton spins. There is also a contribution to the incoherent cross section due to the isotopic mixture of  $^1\text{H}$  and  $^2\text{H}$ , but the latter is so low that this contribution is negligible.

For a monoatomic scattering material of spin  $i$  there are two scattering amplitudes,  $a_+$  and  $a_-$ , depending on whether the compound spin of neutron and nucleus is  $(i + \frac{1}{2})$  or  $(i - \frac{1}{2})$ . Thus the coherent scattering amplitude will be (Hughes, 1953, pages 262-264):

$$a_{\text{coh.}} = \frac{i+1}{2i+1} a_+ + \frac{i}{2i+1} a_- \quad (19)$$

which is simply the average using the statistical weight ratio of  $(i+1)/i$  for the formation probabilities of the compound nucleus with  $(i + \frac{1}{2})$  and  $(i - \frac{1}{2})$  respectively. Since the scattering at thermal energies is purely s-wave scattering one has

$$\sigma = 4\pi\lambda^2 \sin^2 \delta \quad (20)$$

TABLE II  
 TOTAL CROSS SECTION AND INCOHERENT CROSS SECTION  
 IN BERYLLIUM FOR NEUTRONS WITH ENERGY  
 0.002 eV AT DIFFERENT TEMPERATURES

| Temperature<br>(°K) | $\sigma_T^a$<br>(barns) | $\sigma_{inc.} = \sigma_T - \sigma_a$ |
|---------------------|-------------------------|---------------------------------------|
| 100                 | 0.059                   | 0.050                                 |
| 300                 | 0.55                    | 0.53                                  |
| 440                 | 1.16                    | 1.15                                  |

<sup>a</sup>The values of  $\sigma_T$  are taken from the figure on page three of Hughes and Schwartz (1958).

And since the scattering amplitude  $a = (\lambda \sin \delta_o)$  one has simply

$$\sigma_{\text{coh.}} = 4\pi (a_{\text{coh.}})^2 = 4\pi \left( \frac{i+1}{2i+1} a_+ + \frac{i}{2i+1} a_- \right)^2. \quad (21)$$

The total scattering, on the other hand, is given by the sum of the weighted scattering intensities

$$\sigma_{\text{tot.}} = 4\pi \left[ \frac{i+1}{2i+1} a_+^2 + \frac{i}{2i+1} a_-^2 \right]. \quad (22)$$

Subtracting the coherent part leaves

$$\begin{aligned} \sigma_{\text{inc.}} &= 4\pi \left[ \frac{i+1}{2i+1} a_+^2 + \frac{i}{2i+1} a_-^2 - \left( \frac{i+1}{2i+1} a_+ + \frac{i}{2i+1} a_- \right)^2 \right] \\ &= 4\pi \frac{i(i+1)}{(2i+1)^2} (a_+ - a_-)^2 \end{aligned} \quad (23)$$

In hydrogen  $i = \frac{1}{2}$ , giving a 3:1 weight ratio in favor of  $a_+$ , and the measured values of the scattering amplitudes are (Sutton et al., 1947; Schull et al., 1948)

$$a_+ = 0.522 \times 10^{-12} \text{ cm.}$$

$$a_- = -2.34 \times 10^{-12} \text{ cm.}$$

which yields a bound-atom coherent cross section of 1.28 b. and a bound-atom total cross section of 79.0 b. in good agreement with the measured values quoted above.

It would therefore be expected that the 'trap' effect which was observed in crystalline beryllium should be absent in crystalline  $H_2O$ , since there would be no energy range with the large ratio of  $\sigma_{tr}/\sigma_{inc.}$  found in beryllium. Although some Bragg scattering in an ice crystal will occur since there is a coherent cross section, the much larger incoherent scattering, should be dominant and thus prevent any significant trap effect.

#### V. GOAL AND SCOPE OF THE PRESENT WORK

The motivations of this experiment were, then, to determine whether asymptotic spectrum neutron populations would be established in finite ice bodies in the buckling and temperature ranges accessible to measurement and, if so, to determine the neutron diffusion parameters carefully within that range. Although many measurements in  $H_2O$  liquid had been performed there were, at the time this work was begun, no reported results for the crystalline state of  $H_2O$  except for the very crude measurement by von Dardel described above and a single measured point by Antonov et al. (1962b), at liquid nitrogen temperature. To date the only additional data available are the publications by Antonov et al. (1960a, 1962), and by Dlouhý and Kvítek (1962) which were mentioned above. No information about the variation of the diffusion parameters in ice in the temperature range of  $0^{\circ}C.$  to  $-100^{\circ}C.$  has been published heretofore.

The following procedure was therefore undertaken: (1) make a number of suitably shaped ice bodies in which the neutron die-away can

be observed, (2) prepare a suitable pulsed source and detector system for measuring the time decay of the thermalized neutron populations resulting from injection of neutrons into the ice bodies, (3) obtain sufficient amounts of data to permit careful evaluation of the decay behavior, (4) develop or find suitable analytical methods for extracting the desired decay period from the data, (5) establish, by measurements with various bucklings and temperatures, whether an asymptotic spectrum can be obtained soon enough to permit measurements, (6) determine the proper extrapolation distances to employ in calculating the bucklings, (7) fit the decay parameters to a power series model in  $B^2$  to obtain the diffusion parameters, and (8) compare the results, as far as possible, with other measured and calculated data.

The equipment available, which will be described in more detail in the appropriate sections below, consisted primarily of a 300,000 v. power supply, a deuteron accelerator, an 18-channel time-base analyser, and a two-stage refrigerated test chamber with inside dimensions of about 20 in. by 20 in. by 20 in., capable of being cooled to  $-90^{\circ}\text{C}$ . Several additional components and modifications to existing equipment were developed or procured during the course of the work.

## CHAPTER II

### THEORETICAL CONSIDERATIONS

#### I. THE BOLTZMANN EQUATION

In order to provide a foundation for the equations used to describe the neutron transport in the particular case pertaining to this work the general equations governing the neutron density will be exhibited, and the various assumptions, simplifications, and approximations will be specifically introduced. The discussion is based mainly on the treatment by Weinberg and Wigner (1958), and makes extensive use of the derivations by Davisson (1957).

Certain assumptions can be made at the outset. First, it is assumed that neutron-neutron interactions are negligible. Even in high-flux reactors where the neutron flux may be as high as  $10^{14}$  cm.<sup>-2</sup> sec.<sup>-1</sup>, the neutron density is only of the order of  $5 \times 10^6$  neutrons/cm.<sup>3</sup>, which is a factor of  $10^{-14}$  smaller than the proton density in water ( $N(\text{H})_{\text{H}_2\text{O}} \approx 6 \times 10^{22}$  protons/cm.<sup>3</sup>). In the present work the neutron density is lower by another factor of at least  $10^{-5}$ , so if the neutron-neutron cross sections do not exceed those for neutron-proton interactions by many orders of magnitude, and they should not be very different, then the number of neutron-neutron interactions is negligible compared to the number of neutron-proton interactions to extremely high degree. It is also assumed that the neutron is free between collisions. Since the neutron has neither electric charge nor electric dipole moment, the

only forces that could affect it between collisions are gravity and inhomogeneous magnetic fields. (The latter because the neutron has a nonzero magnetic dipole moment.) It is assumed that no inhomogeneous magnetic fields are present, so that only gravity remains as a possibility. However, in water the neutron life-time is of the order of 200  $\mu\text{sec}$ . so that the effect of gravity would only displace a neutron by about  $2 \times 10^{-5}$  cm. even in an infinite medium, which is negligible compared to the system dimensions.

It is also assumed that the mechanics may be treated nonrelativistically, and that neutron orientation effects are of no significance.

The complete description of the neutron population requires not only that the density at every point in space  $(x,y,z) \equiv \vec{r}$ , be known, but also requires knowledge of the velocity of each neutron. One is then dealing with a six-dimensional phase space, which can be defined in terms of sets of six variables, such as  $(x,y,z,v_x,v_y,v_z)$  or  $(x,y,z,E,\theta,\varphi) \equiv (\vec{r},E,\vec{\Omega})$ . This latter representation will be employed in this discussion.

The fundamental quantity to be defined in terms of these variables may be chosen to be the directional flux which is defined as follows:  $f(\vec{r},E,\vec{\Omega},t) d\vec{r} d\vec{\Omega} dE \equiv$  the number of neutrons in the volume element  $d\vec{r}$  about  $\vec{r}$ , having energy between  $E$  and  $E + dE$ , moving into the element of solid angle  $d\vec{\Omega}$  about  $\vec{\Omega}$ , at time  $t$ , multiplied by their scalar speed  $v \equiv (2E/m)^{\frac{1}{2}}$ . By  $d\vec{\Omega}$  is meant  $(\sin \theta d\theta d\varphi)$ , where  $\theta$  and  $\varphi$  are spherical coordinate angles.

Then the neutron density is defined as

$$n(\vec{r}, t) \equiv \iiint (1/v) f(\vec{r}, E, \vec{\Omega}, t) dE d\vec{\Omega} \quad (24)$$

and the total neutron flux is defined as

$$\Phi(\vec{r}, t) \equiv \iiint f(\vec{r}, e, \vec{\Omega}, t) dE d\vec{\Omega} . \quad (25)$$

In these definitions  $\iiint dE d\vec{\Omega}$  is to be understood to mean

$$\iiint dE d\vec{\Omega} \equiv \int_0^{2\pi} \int_0^{\pi} \int_0^{\infty} dE \sin \theta d\theta d\varphi. \quad (26)$$

The Boltzmann equation describes the change, with time, of the neutron density in phase space. The local density at  $\vec{r}$  will change in two ways. One, because the neutrons "stream" i.e., move in straight lines from their instantaneous positions, and two, because of collisions, resulting in either change of angle and energy, or in absorption.

The streaming leaves  $E$  and  $\vec{\Omega}$  unchanged. It results in a current  $\vec{\Omega} f(\vec{r}, E, \vec{\Omega}, t)$ . The neutron density  $1/v f(\vec{r}, E, \vec{\Omega}, t)$  is reduced by the divergence of this current:

$$\begin{aligned} \frac{\partial}{\partial t} \left( \frac{1}{v} f(\vec{r}, E, \vec{\Omega}, t) \right)_{(1)} &= \frac{1}{v} \frac{\partial}{\partial t} f(\vec{r}, E, \vec{\Omega}, t) \\ &= - \nabla_{\vec{r}} \cdot (\vec{\Omega} f(\vec{r}, E, \vec{\Omega}, t)) = -\vec{\Omega} \cdot \nabla_{\vec{r}} f(\vec{r}, E, \vec{\Omega}, t) \quad (27) \end{aligned}$$

The subscript on the del operator signifies that differentiation with respect to the space variable, rather than the angle variables, is intended, and the subscript (1) on the left term is a reminder that this expression gives only one of two contributions to this term.

The second term  $\frac{\partial}{\partial t} \left( \frac{1}{v} f(\vec{r}, E, \vec{\Omega}, t) \right)_{(2)}$  is due to the collisions which may change the vector velocity,  $(E, \vec{\Omega})$  or may cause the neutron to be absorbed.

Such a process changes  $(E, \vec{\Omega})$  but leaves  $\vec{r}$  unchanged. There are, four contributions to this second type of change, 1) scattering into the phase-space volume element  $(d\vec{r}, dE, d\vec{\Omega})$ , 2) scattering out of the volume element, 3) absorption, and 4) source neutrons.

Thus, for example, the number of neutrons scattered into the phase-space volume element  $(d\vec{r} dE d\vec{\Omega})$  per unit time is given by

$$\int f(\vec{r}, E', \vec{\Omega}', t) \Sigma_s(\vec{r}, E' \rightarrow E, \vec{\Omega}' \rightarrow \vec{\Omega}, t) dE' d\vec{\Omega}' \quad (28)$$

where  $\Sigma_s(\vec{r}, E' \rightarrow E, \vec{\Omega}' \rightarrow \vec{\Omega}, t)$  is the macroscopic cross section for scattering neutrons at  $\vec{r}$ , with initial energy  $E'$  moving initially in direction  $\vec{\Omega}'$  to a final energy  $E$  and final direction  $\vec{\Omega}$ .

The number of neutrons absorbed and scattered out of the element per unit time is similarly given by

$$\int \left\{ f(\vec{r}, E, \vec{\Omega}, t) \left[ \Sigma_s(\vec{r}, E \rightarrow E', \vec{\Omega} \rightarrow \vec{\Omega}', t) + \Sigma_a(\vec{r}, E, t) \right] dE' d\vec{\Omega}' \right\} \quad (29)$$

where  $\Sigma_a(\vec{r}, E, t)$  is the absorption cross section for neutrons of energy  $E$  at  $\vec{r}$ , at time  $t$ . However

$$\int f(\vec{r}, E, \vec{\Omega}, t) \Sigma_s(\vec{r}, E \rightarrow E', \vec{\Omega} \rightarrow \vec{\Omega}', t) dE' d\Omega' = f(\vec{r}, E, \vec{\Omega}, t) \Sigma_s(\vec{r}, E, t) \quad (30)$$

where  $\Sigma_s(\vec{r}, E, t)$  is the total scattering cross section for neutrons with initial energy  $E$  at  $\vec{r}$  at time  $t$ . So we may rewrite expression (29) as

$$f(\vec{r}, E, \vec{\Omega}, t) [\Sigma_s(\vec{r}, E, t) + \Sigma_a(\vec{r}, E, t)] \quad (29a)$$

It is assumed that no  $(n, 2n)$  processes occur and no fission, so that scattering and absorption exhaust the neutron interaction possibilities. This also eliminates the complication of processes that occur at time  $t$  and give rise to neutrons at time  $t' > t$ , which is the case with delayed fission neutrons.

With these expressions the Boltzmann equation may be written as:

$$\frac{1}{v} \frac{\partial f(E, \vec{\Omega})}{\partial t} = - \vec{\Omega} \cdot \nabla_{\vec{r}} f(E, \vec{\Omega}) + S(E, \vec{\Omega}) - f(E, \vec{\Omega}) [\Sigma_s(E) + \Sigma_a(E)] + \int f(E', \Omega') \Sigma_s(E' \rightarrow E, \vec{\Omega}' \rightarrow \vec{\Omega}) dE' d\Omega'. \quad (31)$$

In this equation the variables  $r$  and  $t$ , which occur in  $f$ ,  $\Sigma_s$ ,  $\Sigma_a$ , and  $S$  have been suppressed.  $S(\vec{r}, E, \Omega, t)$  is defined to be the number of neutrons, due to an external source, which appear at  $\vec{r}$  at time  $t$  with energy  $E$  moving in direction  $\vec{\Omega}$ .

If the medium is isotropic, i.e. if  $\int dE d\vec{\Omega} \Sigma_s(\vec{r}, E' \rightarrow E, \vec{\Omega}' \rightarrow \vec{\Omega})$  is a function only of  $\vec{r}$  and  $E'$ , and if the neutrons are in thermal equilibrium with the medium (this implies  $\Sigma_a = 0$  and no sources) then the

time-derivative and divergence terms of the Boltzmann equation vanish and one has, from expressions (28), (29), and (31)

$$f(\vec{r}, E, \vec{\Omega}) \Sigma_s(\vec{r}, E \rightarrow E', \vec{\Omega} \rightarrow \vec{\Omega}') = f(\vec{r}, E', \vec{\Omega}') \Sigma_s(\vec{r}, E' \rightarrow E, \vec{\Omega}' \rightarrow \vec{\Omega}) \quad (32)$$

This is the so-called equation of detailed balance (Weinberg and Wigner, 1950, page 222). As shown, it holds, strictly, only for the case of no absorption and equilibrium.

## II. THE SPHERICAL HARMONIC EXPANSION OF THE BOLTZMANN EQUATION;

### REDUCTION TO DIFFUSION THEORY

In order to simplify Equation (31) and specify the terms, it is useful to expand the angles in spherical harmonics. For this expansion it will be assumed that the medium is constant in time, i.e. that  $\Sigma_s$  and  $\Sigma_a$  do not depend on  $t$ . Where they are not needed the coefficients  $\vec{r}$  and  $t$  will be suppressed in this discussion to simplify the notation.

Turning first to the scattering cross section, it is to be noted that  $\Sigma_s$  depends only on  $E$ ,  $E'$ , and the angle  $\theta_0$  between  $\vec{\Omega}$  and  $\vec{\Omega}'$ . This is based on the assumption that neither the neutrons nor the nuclei are polarized or oriented. So  $\cos \theta_0 = \vec{\Omega} \cdot \vec{\Omega}' = (\cos \theta)(\cos \theta') + (\sin \theta)(\sin \theta')(\cos(\varphi + \varphi'))$ .

Expanding the angular dependence of  $\Sigma_s$  in Legendre polynomials one writes

$$\Sigma_s(E' \rightarrow E, \vec{\Omega}' \rightarrow \vec{\Omega}) = \sum_l s_l(E' \rightarrow E) P_l(\cos \theta_0) \quad (33)$$

where the coefficients  $s_l(E' \rightarrow E)$  give the relative magnitudes of the terms in the expansion. Note that, in the case of infinitely heavy stationary nuclei (incoherent elastic scattering), the coefficients  $s_l(E \rightarrow E')$  are zero unless  $E = E'$ , and also due to the form of the Legendre polynomials, if the scattering is isotropic, that is, equally probable for all directions, then all the terms  $s_l(E \rightarrow E')$  are zero except the term for  $l = 0$ . It may be noted further that the total scattering cross section, which is obtained by integrating over all final angles  $\vec{\Omega}'$  and all final energies  $E'$ , becomes:

$$\begin{aligned} \Sigma_s(E) &= \sum_l \int_0^\infty dE' s_l(E \rightarrow E') \int_0^\pi 2\pi \sin \theta_0 d\theta_0 P_l(\cos \theta_0) \\ &= 4\pi \int_0^\infty s_0(E \rightarrow E') dE' \end{aligned} \quad (34)$$

The directional flux,  $f(\vec{r}, E, \vec{\Omega}, t)$  and the source term  $S(\vec{r}, E, \vec{\Omega}, t)$  are also expanded in spherical harmonics, but they must be expanded in the harmonics of the space angles  $\theta$  and  $\varphi$ . (Note: the angle  $\theta_0$  between  $\vec{\Omega}$  and  $\vec{\Omega}'$  is not the same as the polar angle  $\theta$ .) The expansions may be written as (Jahnke and Emde, 1945, page 115):

$$f(\vec{r}, E, \vec{\Omega}, t) = \sum_{l=0}^{\infty} \sum_{m=-l}^l f_{l,m}(\vec{r}, E, t) P_{l,m}(\vec{\Omega}) \quad (35)$$

and

$$S(\vec{r}, E, \vec{\Omega}, t) = \sum_{l=0}^{\infty} \sum_{m=-l}^l S_{l,m}(\vec{r}, E, t) P_{l,m}(\vec{\Omega}) \quad (36)$$

where

$$P_{\ell,m}(\vec{\Omega}) = e^{im\varphi} \frac{(\sin \theta)^{-m}}{\ell! 2^\ell} \left[ \frac{(\ell+m)!}{(\ell-m)!} \right]^{\frac{1}{2}} \frac{d^{\ell-m} (\cos^2 \theta - 1)^\ell}{(d \cos \theta)^{\ell-m}}. \quad (37)$$

The  $P_{\ell,m}(\vec{\Omega})$  are the so-called 'associated spherical harmonics'. Upon integrating the expansion of  $f(\vec{r}, E, \vec{\Omega}, t)$  over all angles, it is found that all terms except that for  $\ell = 0$  vanish. Therefore, the total flux at energy  $E$ , at location  $\vec{r}$ , at time  $t$  is given by:

$$f(\vec{r}, E, t) = \int d\vec{\Omega} f(\vec{r}, E, \vec{\Omega}, t) = 4\pi f_{0,0}(\vec{r}, E, t). \quad (38)$$

The associated spherical harmonics are orthogonal functions:

$$\int P_{\ell',m'}(\vec{\Omega}) P_{\ell,m}^*(\vec{\Omega}) d\Omega = \frac{4\pi}{2\ell+1} \delta_{\ell,\ell'} \delta_{m,m'}. \quad (39)$$

Thus, if the directional flux is multiplied by  $\cos \theta$  and integrated over all solid angles the result is

$$\int d\vec{\Omega} f(\vec{r}, E, \vec{\Omega}, t) \cos \theta = \frac{4\pi}{3} f_{1,0}(\vec{r}, E, t), \quad (40a)$$

since  $P_{1,0} = P_1 = \cos \theta$  and by orthogonality (Equation (40a)) all other terms vanish. But Equation (40a) is just the expression for  $j_z(\vec{r}, E, t)$ , the z-component of the neutron current vector. Similarly

$$\begin{aligned} j_x &= \int d\vec{\Omega} f(\vec{r}, E, \vec{\Omega}, t) \cos \theta \sin \varphi \\ j_y &= \int d\vec{\Omega} f(\vec{r}, E, \vec{\Omega}, t) \sin \theta \sin \varphi \end{aligned} \quad (40b)$$

Performing the integrations, and using the orthogonality conditions one obtains for the  $l = 1$  term:

$$\begin{aligned}
& f_{1,-1}(\vec{r}, E, t) P_{1,-1}(\vec{\Omega}) + f_{1,1}(\vec{r}, E, t) P_{1,1}(\vec{\Omega}) + f_{1,0}(\vec{r}, E, t) P_{1,0}(\vec{\Omega}) = \\
& f_{1,-1}(\vec{r}, E, t) \frac{1}{\sqrt{2}} e^{i\varphi} \sin \theta - f_{1,1}(\vec{r}, E, t) \frac{1}{\sqrt{2}} e^{i\varphi} \sin \theta + f_{1,0}(\vec{r}, E, t) \cos \theta = \\
& \frac{3}{4\pi} \vec{\Omega} \cdot \vec{j}(\vec{r}, E, t) . \tag{41}
\end{aligned}$$

So one may write

$$f(\vec{r}, E, \vec{\Omega}, t) = \frac{1}{4\pi} f(\vec{r}, E, t) + \frac{3}{4\pi} \vec{\Omega} \cdot \vec{j}(\vec{r}, E, t) + \sum_{l=2}^{\infty} \sum_{m=-l}^l f_{l,m}(\vec{r}, E, t) P_{l,m}(\vec{\Omega}) \tag{42}$$

Introducing these expansions into the Boltzmann equation one arrives (by multiplying each term by  $P_{l,m}(\vec{\Omega})^*$  and integrating) at the following form of the Boltzmann equation:

$$\begin{aligned}
\frac{1}{v} \frac{\partial f_{l,m}(\vec{r}, E, t)}{\partial t} = & - \left[ \frac{\sqrt{(l+2+m)(l+1+m)}}{2l+3} \left( -\frac{1}{2} \frac{\partial f_{l+1,m+1}}{\partial x} - \frac{i}{2} \frac{\partial f_{l+1,m+1}}{\partial y} \right) \right. \\
& + \frac{\sqrt{(l+1-m)(l+2-m)}}{2l+3} \left( \frac{1}{2} \frac{\partial f_{l+1,m-1}}{\partial x} - \frac{i}{2} \frac{\partial f_{l+1,m-1}}{\partial y} \right) \\
& + \frac{\sqrt{(l-m-1)(l-m)}}{2l-1} \left( \frac{1}{2} \frac{\partial f_{l-1,m+1}}{\partial x} + \frac{i}{2} \frac{\partial f_{l-1,m+1}}{\partial y} \right) \\
& \left. + \frac{\sqrt{(l+m)(l+m-1)}}{2l-1} \left( -\frac{1}{2} \frac{\partial f_{l-1,m-1}}{\partial x} + \frac{i}{2} \frac{\partial f_{l-1,m-1}}{\partial y} \right) \right]
\end{aligned}$$

$$\begin{aligned}
& + \left[ \frac{\sqrt{(\ell+1+m)(\ell+1-m)}}{2\ell+3} \frac{\partial f_{\ell+1,m}}{\partial z} + \frac{\sqrt{(\ell+m)(\ell-m)}}{2\ell-1} \frac{\partial f_{\ell-1,m}}{\partial z} \right] \\
& + \frac{4\pi}{2\ell+1} \int_0^\infty f_{\ell,m}(\vec{r}, E', t) s_\ell(E' \rightarrow E) dE' - \Sigma(E) f_{\ell,m}(\vec{r}, E, t) \\
& + S_{\ell,m}(E) . \tag{43}
\end{aligned}$$

where  $\Sigma(E) \equiv \Sigma_a(E) + \Sigma_s(E)$  and all variables not needed have been suppressed.

Note that the  $\ell$ 'th term of the expansion of the scattering cross section affects only the  $\ell$ 'th-order terms of the directional flux distribution. So if, for example, the scattering is spherically symmetric [ $\Sigma_s(E \rightarrow E') = S_0(E \rightarrow E')$ ] then only the equation for  $f_{0,0}$  contains an integral term.

The first order theory presented in Chapter I was based on the assumption that the neutron population could be approximately treated as one-velocity. Making this assumption the Boltzmann equation simplifies considerably:

$$\begin{aligned}
f(\vec{r}, E, \vec{\Omega}, t) & \rightarrow f(\vec{r}, \vec{\Omega}, t) \\
\Sigma(\vec{r}, E, \Omega, t) & \rightarrow \Sigma(r, \vec{\Omega}, t), \text{ etc.}
\end{aligned} \tag{44}$$

The Boltzmann equation thus becomes:

$$\begin{aligned}
\frac{1}{v} \frac{\partial}{\partial t} f(\vec{r}, \vec{\Omega}, t) + \vec{\Omega} \cdot \nabla_{\vec{r}} f(\vec{r}, \vec{\Omega}, t) & = \int d\vec{\Omega}' f(\vec{r}, \vec{\Omega}', t) \Sigma_s(\vec{r}, \vec{\Omega}' \rightarrow \vec{\Omega}) \\
& + S(\vec{r}, \vec{\Omega}) - \Sigma(\vec{r}) f(\vec{r}, \vec{\Omega}, t)
\end{aligned} \tag{45}$$

This equation can be expanded in spherical harmonics just as before, except that the coefficients now are not functions of energy.

The expansion yields, for each term

$$\frac{1}{v} \frac{\partial}{\partial t} f_{\ell,m}(\vec{r}, t) + [A] = \frac{4\pi}{2\ell + 1} f_{\ell,m}(\vec{r}, t) s_{\ell} - \Sigma(\vec{r}) f_{\ell,m}(\vec{r}, t) + S_{\ell,m} \quad (46)$$

where A represents the term in the brackets in Equation (43), except that the  $f_{\ell,m}$  are not functions of energy.

The same arguments as in the energy-dependent case can be applied to yield

$$\Phi_t = 4\pi f_{0,0} \quad (47a)$$

where  $\Phi_t$  is the total flux, and

$$J_x = \frac{4\pi}{3\sqrt{2}} (f_{1,-1} - f_{1,1}); \quad J_y = \frac{-4\pi i}{3\sqrt{2}} (f_{1,-1} + f_{1,1}); \quad J_z = \frac{4\pi}{3} f_{1,0} \quad (47b)$$

where  $\vec{J} = J_x \hat{i} + J_y \hat{j} + J_z \hat{h}$  is the total vector current.

To obtain the diffusion theory approximation one begins by neglecting all terms greater than  $\ell = 1$ .

Looking first at the  $\ell = 0$  form of Equation (43) one finds

$$\begin{aligned} \frac{1}{v} \frac{\partial f_{0,0}}{\partial t} + \frac{1}{3} \left[ \frac{1}{\sqrt{2}} \left( \frac{\partial f_{1,-1}}{\partial x} - \frac{\partial f_{1,1}}{\partial x} \right) - \frac{i}{\sqrt{2}} \left( \frac{\partial f_{1,1}}{\partial y} + \frac{\partial f_{1,-1}}{\partial y} \right) + \frac{\partial f_{1,0}}{\partial z} \right] \\ = 4\pi f_{0,0} s_0 - \Sigma(\vec{r}) f_{0,0} + S_{0,0} \end{aligned} \quad (48)$$

but  $\Sigma(\vec{r}) = \Sigma_s(\vec{r}) + \Sigma_a(\vec{r}) = 4\pi s_0 + \Sigma_a$  (see Equation (34)) and

$$(4\pi) \frac{1}{3} \left[ \frac{1}{\sqrt{2}} \left( \frac{\partial f_{1,-1}}{\partial x} - \frac{\partial f_{1,1}}{\partial x} \right) - \frac{i}{\sqrt{2}} \left( \frac{\partial f_{1,1}}{\partial y} + \frac{\partial f_{1,-1}}{\partial y} + \frac{\partial f_{1,0}}{\partial z} \right) \right] = \nabla \cdot \vec{J} \quad (49)$$

by Equation (41). So Equation (48) becomes:

$$\frac{1}{v} \frac{\partial \bar{\Phi}_t}{\partial t} + \nabla \cdot \vec{J} = - \Sigma_a \bar{\Phi}_t + S \quad (48a)$$

The equation for  $l = 1, m = 0$  is:

$$\begin{aligned} \frac{1}{v} \frac{\partial f_{1,0}}{\partial t} + \frac{\partial f_{0,0}}{\partial z} + \frac{1}{5} \left[ \sqrt{3/2} \left( - \frac{\partial f_{2,1}}{\partial x} + \frac{\partial f_{2,-1}}{\partial x} - i \frac{\partial f_{2,1}}{\partial y} - i \frac{\partial f_{2,-1}}{\partial y} \right) + 2 \frac{\partial f_{2,0}}{\partial z} \right] \\ = \frac{4\pi}{3} f_{1,0} s_1 - \Sigma f_{1,0} \end{aligned} \quad (50)$$

Since the diffusion theory assumption is based on the neglectability of terms with  $l > 1$ , the  $l = 2$  terms are dropped. This gives

$$\frac{1}{v} \frac{\partial J_z}{\partial t} + \frac{1}{3} \frac{\partial}{\partial z} \bar{\Phi}_t = \frac{4\pi}{3} s_1 J_z - \Sigma J_z \quad (50a)$$

or, solving for  $J_z$

$$J_z = \left( \frac{1}{v} \frac{\partial J_z}{\partial t} + \frac{1}{3} \frac{\partial \bar{\Phi}_t}{\partial z} \right) / \left( \frac{4\pi}{3} s_1 - \Sigma \right). \quad (50b)$$

Now if  $\bar{\mu}$ , the mean cosine of the scattering angle, is defined as

$$\bar{\mu} = \frac{\int d\vec{\Omega}' \cos \theta_o \Sigma_s(\vec{\Omega} \rightarrow \vec{\Omega}')}{\int d\vec{\Omega}' \Sigma_s(\vec{\Omega} \rightarrow \vec{\Omega}')} = \frac{s_1}{3s_o} = \frac{4\pi s_1}{3\Sigma_s} \quad (51)$$

then

$$J_z = \frac{1}{(\bar{\mu}\Sigma_s - \Sigma)} \left( \frac{1}{v} \frac{\partial J_z}{\partial t} + \frac{1}{3} \frac{\partial \Phi_t}{\partial z} \right) = - \left( \frac{3}{v} \frac{\partial J_z}{\partial t} + \frac{\partial \Phi_t}{\partial z} \right) \frac{1}{3(\Sigma - \bar{\mu}\Sigma_s)} \cdot \quad (52a)$$

The equations for  $l = 1, m = -1$  and  $l = 1, m = 1$  similarly give the expression

$$J_x = - \left( \frac{3}{v} \frac{\partial J_x}{\partial t} + \frac{\partial \Phi_t}{\partial x} \right) \frac{1}{3(\Sigma - \bar{\mu}\Sigma_s)} \quad (52b)$$

$$J_y = - \left( \frac{3}{v} \frac{\partial J_y}{\partial t} + \frac{\partial \Phi_t}{\partial y} \right) \frac{1}{3(\Sigma - \bar{\mu}\Sigma_s)} \quad (52c)$$

Combining the three components of Equation (52), one has

$$\vec{J} = - \left( \frac{3}{v} \frac{\partial \vec{J}}{\partial t} + \nabla \Phi_t \right) \frac{1}{3(\Sigma - \bar{\mu}\Sigma_s)}$$

The diffusion theory equation is obtained by assuming further that  $\frac{\partial \vec{J}}{\partial t} \ll \frac{v}{3} \nabla \Phi_t$  and therefore neglecting the term  $\frac{\partial \vec{J}}{\partial t}$ . Then

$$\vec{J} = \frac{-1}{3(\Sigma - \bar{\mu}\Sigma_s)} \nabla \Phi_t \cdot \quad (53)$$

This has the form of Fick's Law (Fick, 1855) where the term  $\frac{1}{3(\Sigma - \bar{\mu}\Sigma_s)} \equiv D$  is defined as the diffusion coefficient  $D$  in the diffusion approximation.

So:

$$\vec{J} = - D \nabla \Phi_t . \quad (54)$$

Substituting this expression in Equation (48) and assuming that no source is present, gives the equation:

$$\frac{1}{v} \frac{\partial \Phi_t}{\partial t} - \nabla \cdot (D \nabla \Phi_t) = - \Sigma_a \Phi_t . \quad (55)$$

In the one-velocity theory  $\Phi_t = nv$ , so in terms of neutron density this expression becomes:

$$\frac{\partial n(\vec{r}, t)}{\partial t} - \nabla \cdot (v D \nabla n) = - \Sigma_a v n . \quad (55a)$$

In a homogeneous medium,  $D$  is independent of  $\vec{r}$ , so the equation can be expressed as

$$\frac{\partial n(\vec{r}, t)}{\partial t} = (vD) \nabla^2 n(\vec{r}, t) - v \Sigma_a n(\vec{r}, t) \quad (56)$$

which is just the first order equation used in the arguments of Chapter I.

To summarize, the one-velocity diffusion-approximation equation was obtained from the general Boltzmann equation by the following assumptions, (1) the neutrons are all of the same scalar velocity,  $v$ , (2) the directional flux distribution is sufficiently close to isotropic so that terms with  $l \geq 2$  in the harmonic expansion can be neglected, (3) the

material is homogeneous and isotropic, and (4) the term  $\frac{\partial \vec{J}}{\partial t}$  can be neglected, because the change of neutron population with time is relatively slow. More sophisticated models, which remove some of these restrictions, will be considered later. However, it is convenient here to point out one aspect of assumption (4). In general, solving the spherical harmonics expansion of the Boltzmann equation by truncating after terms of order  $k$  in  $l$  one obtains the  $P_k$  approximation to the transport equation. Any such solution is not exact because, as we have seen in the case where  $l = 0$  and  $l = 1$ , the streaming term expression contains derivatives of  $f_{l+1,m}$ , and neglecting these is an approximation. In addition, the diffusion theory equation is not the true  $P_1$  approximation to the Boltzmann equation, because of the neglect of the term  $\frac{v}{3} \frac{\partial \vec{J}}{\partial t}$ . Including this term, Weinberg and Wigner (1958) point out, leads to a second-order equation in time:

$$\frac{3D}{v} \frac{\partial^2 n}{\partial t^2} + (1 + 3D\Sigma_a) \frac{\partial n}{\partial t} = (vD) \nabla^2 n - v\Sigma_a n \quad (57)$$

which is the 'telegrapher's equation' whose solutions are retarded in time so that a sudden local perturbation spreads with a finite velocity. Physically, this is true of course, because finite-velocity neutrons diffuse with finite velocities. Only in the limit of infinite velocity, zero diffusion coefficient, and zero absorption cross section, does the  $P_1$  approximation solution rigorously reduce to the diffusion approximation solution.

Thus, the diffusion approximation is a valid approximation to the  $P_1$  solution of the Boltzmann equation if any perturbations that occur are slow compared to the time it takes a 'neutron wave', i.e. the effect of the disturbance, to traverse the system under consideration.

### III. SOLUTIONS OF THE ONE-VELOCITY DIFFUSION EQUATION, AND OPTIMIZATION OF EXPERIMENT GEOMETRY

Before returning to the transport equations for more detailed solutions including velocity spectrum effects and nonisotropic scattering kernels, the solutions of the one-velocity diffusion equation in finite cylinders will be considered since they suffice to determine several significant design parameters for the experiment. Equation (56) is to be solved in cylindrical geometry. The  $\nabla^2$  operator in cylindrical coordinates has the form

$$\nabla^2 = \frac{1}{r} \frac{\partial}{\partial r} \left( r \frac{\partial}{\partial r} \right) + \frac{1}{r^2} \frac{\partial^2}{\partial \theta^2} + \frac{\partial^2}{\partial z^2} . \quad (58)$$

The usual assumption that the variables are separable is made:

$$n(r, \theta, z, t) = Q(r) \Theta(\theta) Z(z) T(t) . \quad (59)$$

With the origin of coordinates at the center of one plane face of a right circular cylinder of height  $H$  and radius  $R$  the following boundary conditions are assumed:

$$n(r = R, \theta, z, t) = 0 \quad (60a)$$

$$n(r, \theta, z = \left\{ \begin{matrix} 0 \\ H \end{matrix} \right\}, t) = 0 \quad (60b)$$

$$n(r, \theta, z, t) = n(r, \theta + 2\pi n, z, t) \quad (60c)$$

$$n(r, \theta, z, t = 0) = n_0(r, \theta, z) \quad (60d)$$

Conditions (60a) and (60b) state that the flux vanishes at the boundaries. Actually it is the return current which vanishes. However, as will be discussed later, the zero current condition can be equated to a zero-flux condition at an imaginary boundary beyond the actual boundary of the finite body. The boundaries at R and H are, therefore, to be understood as extrapolated boundaries which are a distance  $\delta H$  and  $\delta R$  beyond the physical vacuum interfaces.

Condition (60c) is the continuity condition for a complete cylinder, and condition (60d) gives the arbitrary spatial distribution of density at some time  $t = 0$ .

Substituting Equation (58) into Equation (57) and dividing by (vD)  $n(r, \theta, z, t)$  one obtains:

$$\frac{1}{(vD)} \left( \frac{T'(t)}{T(t)} + v\Sigma_a \right) = \left[ \frac{1}{rQ(r)} \frac{\partial}{\partial r} \left( r \frac{\partial Q(r)}{\partial r} \right) + \frac{1}{r^2} \frac{\Theta''(\theta)}{\Theta(\theta)} + \frac{Z''(z)}{Z(z)} \right] = k \quad (61)$$

where k is a constant to be determined. Primes denote differentiation.

The right hand equation yields

$$k - \frac{Q''}{R} - \frac{Q'}{rQ} - \frac{\Theta''}{r^2 Q} = \frac{Z''}{Z} = -w_n^2 \quad (62)$$

with  $\omega_n^2$  another separation constant. Therefore,  $Z'' = -\omega_n^2 Z$  with the solution

$$Z = A \cos \omega_n z + B \sin \omega_n z . \quad (63)$$

Applying boundary condition (60b) gives  $A = 0$ ;  $\omega_n = \frac{n\pi}{H}$ . So  $\omega_n^2 = \frac{n^2 \pi^2}{H^2}$ , where  $n = 1, 2, 3, \dots$ . Similarly the  $\theta$ -dependence can be separated:

$$r^2 k + \frac{\pi^2 n^2}{H^2} r^2 - \frac{r^2 Q''}{Q} - r \frac{Q'}{Q} = \frac{\Theta''}{\Theta} = -\nu^2 \quad (64)$$

where  $-\nu^2$  is a separation constant. The right-hand equation has solution

$$\Theta = C \cos \nu \theta + D \sin \nu \theta . \quad (65)$$

Boundary condition (60c) requires  $\nu$  to take on only the integer values  $\nu = l = 0, 1, 2, 3, \dots$ . This leaves the  $Q$ -equation in  $r$ :

$$r^2 Q'' + r Q' + (a^2 r^2 - l^2) Q = 0 \quad (66)$$

where

$$-a^2 = k + \frac{\pi^2 n^2}{H^2} . \quad (67)$$

The solution is

$$Q(r) = E J_\ell(ar) + FY_\ell(ar) \quad (68)$$

where  $J_\ell(ar)$  and  $Y_\ell(ar)$  are Bessel functions of the first and second kind of order  $\ell$ . Since  $\lim_{r \rightarrow 0} Y_\ell(ar) = \infty$  for all  $\ell$ ,  $F = 0$ . Boundary condition (60a) requires  $J_\ell(aR) = 0$  or  $aR = v_{\ell,m}$  where  $v_{\ell,m}$  is the  $m$ 'th zero of the  $J_\ell$  Bessel function. Therefore, one writes for the values of  $a$

$$a_{\ell,m} = \frac{v_{\ell,m}}{R} . \quad (69)$$

Putting this into Equation (67) gives

$$k = \frac{\pi^2 n^2}{H^2} + \frac{v_{\ell,m}^2}{R^2} \equiv B_{\ell,m,n}^2 . \quad (70)$$

$B_{\ell,m,n}^2$  is defined as the  $(\ell, n, m)$ -mode buckling of the cylinder.

The  $t$ -equation (left side of Equation (61)) then has the solution:

$$T = \exp \left\{ - \left[ v \Sigma_a + (vD) B_{\ell,m,n}^2 \right] t \right\} \quad (71)$$

The initial distribution  $n_0(r, \theta, z)$  can be expanded in the same orthogonal functions as the space part of the solution, since it obeys the same boundary conditions:

$$n_o(r, \theta, z) = \sum_{l, m, n}^{\infty} \sin \frac{n\pi z}{H} J_l(a_{l, m} r) [C_{l, m, n} \cos l\theta + D_{l, m, n} \sin l\theta] \quad (72)$$

where the amplitude factors  $C_{l, m, n}$  and  $D_{l, m, n}$  specify the initial distribution.

By assuming that the neutron source is an external point source the form of Equation (72) can be simplified by choosing the  $\theta = 0$  plane so that the source lies in this plane. Then, by symmetry,  $\Theta(\theta) = \Theta(-\theta)$  or

$$C \cos l\theta + D \sin l(\theta) = C \cos l(-\theta) + D \sin l(-\theta) . \quad (73)$$

But  $\cos(-\theta) = \cos(\theta)$  and  $\sin(-\theta) = -\sin \theta$ . Therefore,  $D = 0$  with this assumption, and the full solution becomes:

$$n(r, \theta, z, t) = \sum_{l, m, n} C_{l, m, n} \sin\left(\frac{n\pi z}{H}\right) J_l(a_{l, m} r) \cos l\theta \exp\left\{-\left[v\Sigma_a + vD B_{n, m, l}^2\right]t\right\} . \quad (74)$$

The nature of the solutions is then a triply infinite sum of terms each of which is associated with an exponential decay with decay frequency

$$\lambda_{l, m, n} = v\Sigma_a + (vD) B_{l, m, n}^2 . \quad (75)$$

Since the bucklings increase with increasing indices  $l, m, n$  the higher modes (for which  $l, m, n$  are greater than 0,1,1) will decay faster than the fundamental mode, and, whatever the initial spatial distribution, after sufficient time has elapsed the remaining amplitude of the

fundamental mode, relative to that of all the higher modes, will become as large as one wishes. The fundamental mode is that for which each index has its lowest allowed value, i.e.,  $l = 0$ ,  $m = 1$ ,  $n = 1$ . In practice, however, there is not an unlimited time available to wait for the higher modes to die away to sufficiently low levels. In particular, the lowest of the higher modes will be the most troublesome since they will decay relatively much more slowly than modes with still higher values of the modal indices.

It is, therefore, particularly desirable to maximize the difference in the buckling between the fundamental mode and the lowest detected higher mode. Two mechanisms are available to optimize this difference, one is use of symmetry considerations in the location of source and detector so as to avoid excitation of some modes by symmetry and avoid detection of others by detector placement at nodal points and the other is optimization of the cylinder proportions. With respect to the former, it will now be shown that either all 3 "first higher modes", i.e.,  $(0,1,2)$ ,  $(0,2,1)$ , and  $(1,1,1)$  can be effectively eliminated or, all  $l = 0$  modes and all even modes in  $m$ . The latter of these two will be shown to be preferable.

If the detector is placed at the center of one plane face of the cylinder, then only those radial modes ( $J_l$ ) that have non-zero amplitude at  $r = 0$  will be detected. However, all  $J_l$  modes except for  $J_0$  have 0-amplitude at  $r = 0$ . Therefore, this position eliminates all modes with  $l > 0$ , including the  $(1,1,1)$  mode.

By placing the source on the central plane, i.e., at  $z = \frac{H}{2}$ , all modes are eliminated which have a node at  $\frac{H}{2}$ , since symmetry requires an equal number of neutrons above and below this plane. That is, all modes for which  $\sin\left(\frac{n\pi}{H} \cdot \frac{H}{2}\right) = 0$  are eliminated by symmetry.  $\sin \frac{n\pi}{2} = 0$  for  $n = 2, 4, 6, \dots$ , etc.

This placement of source and detector was used in all experimental measurements. The allowed indices are then  $l = 0$ ;  $m = 1, 2, 3, \dots$ ;  $n = 1, 3, 5, \dots$ . Henceforth the buckling under these symmetry conditions will be designated as  $B_{m,n}^2 = h_n^2 + t_m^2$ , where

$$h_n^2 = \frac{n^2 \pi^2}{H^2} \text{ and } t_m^2 = \frac{v_{0,m}^2}{R^2}. \quad (76)$$

Note that  $h_3^2/h_1^2 = 9$  and  $t_{z/2}^2/t_1^2 = \frac{v_{0,2}^2}{v_{0,1}^2} = \frac{(5.5201)^2}{(2.4048)^2} = 5.269$ .

The optimum shape for a cylinder is thus that shape which maximizes the two lowest nonfundamental bucklings  $B_{2,1}^2$  and  $B_{1,3}^2$ .

For a given fundamental mode buckling

$$B^2 = \frac{\pi^2}{H^2} + \frac{v_0^2}{R^2} \quad (77)$$

it is clear that either one of the two first higher mode bucklings can be made as large as one desires by decreasing the respective cylinder dimension. However, this will decrease the other of the two disturbing bucklings since the other dimension must be increased to keep the fundamental buckling the same. The optimum shape is thus the one for which

$$B_{2,1}^2 = B_{1,3}^2, \text{ or } \frac{\pi^2}{H^2} + \frac{v_{0,2}^2}{R^2} = \frac{9\pi^2}{H^2} + \frac{v_{0,1}^2}{H^2} \quad (78)$$

Defining  $S \equiv \frac{H}{2R} = \frac{H}{D}$  one finds  $S = 0.894$  for the optimum cylinder proportions. With this proportion the ratio of buckling is:

$$\frac{B_{2,1}^2}{B_{1,1}^2} = \frac{B_{1,3}^2}{B_{1,1}^2} = 3.78 .$$

In order to determine the effects of less-than-optimum cylinder shapes the ratios  $\frac{B_{1,3}^2}{B_{1,1}^2}$  and  $\frac{B_{2,1}^2}{B_{1,1}^2}$  were computed as functions of  $S$  and are shown in Figure 9.

It is possible to find a detector position such that all 3 first higher modes are suppressed. This position is on the plane surface at the position shown in Figure 10, on the nodal line for  $l = 2$  at a distance from the center equal to  $R(v_{0,1}/v_{0,2})$ . In this case, however, the higher mode suppression is less advantageous. Since not all higher  $l$ -modes are suppressed by this position choice there are three first higher modes to consider:  $(2,1,1)$ ,  $(0,3,1)$ , and  $(0,1,3)$ . The effect of  $S$  on the ratios  $B_{2,1,1}^2/B_{0,1,1}^2$ ,  $B_{0,3,1}^2/B_{0,1,1}^2$ , and  $B_{0,1,3}^2/B_{0,1,1}^2$  was computed and is shown in Figure 11.

The optimum shape here is slightly longer and thinner since in this case the optimum value of  $\frac{H}{D}$  is 0.9795. However, the buckling ratio is only 3.49. This position is also less advantageous because the leakage flux is smaller, and because the position depends on the extrapolation distance and hence the temperature.

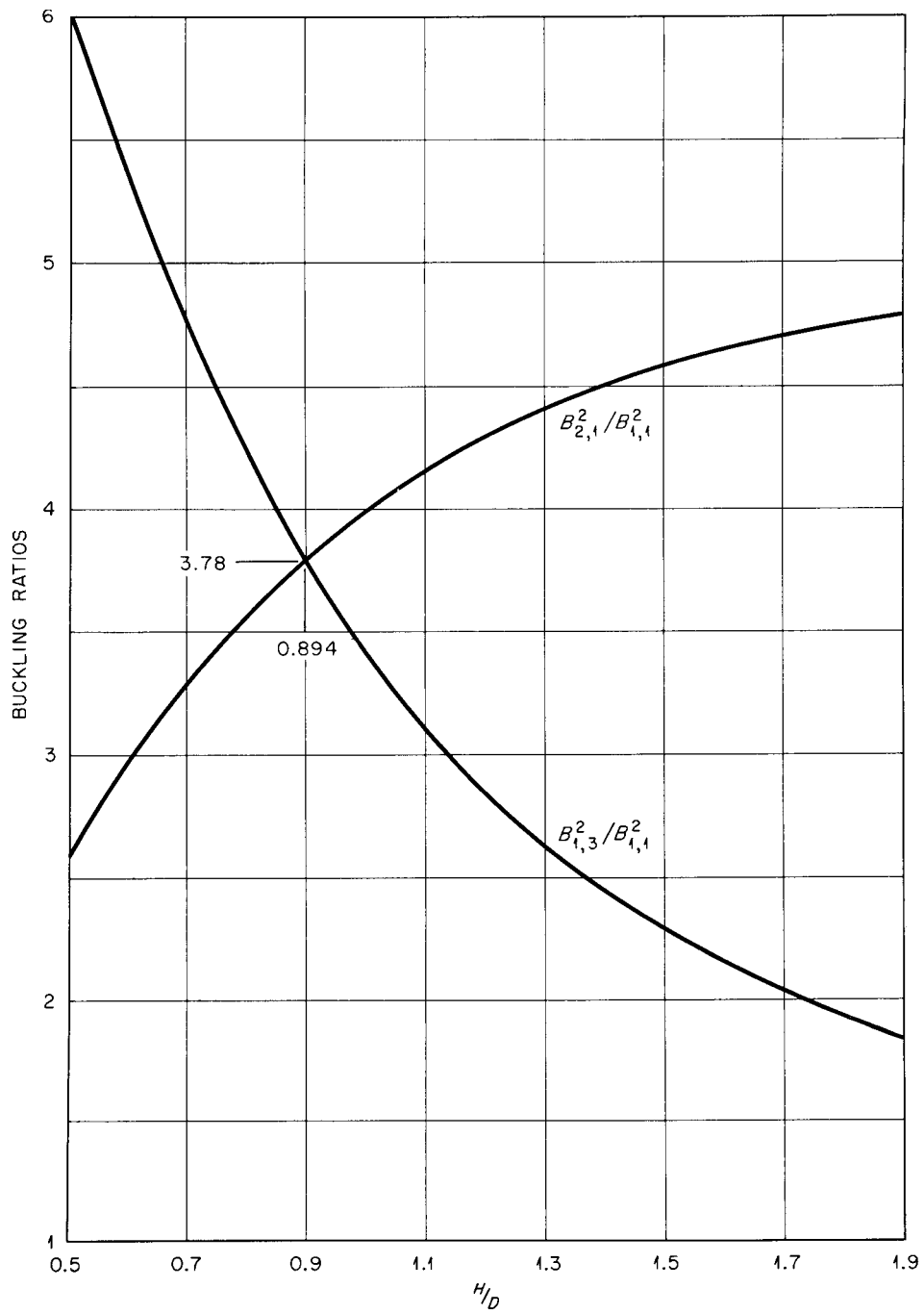


Figure 9. Ratios  $B_{1,2}^2 / B_{1,1}^2$  and  $B_{3,1}^2 / B_{1,1}^2$  as functions of  $H/2R$  where  $H$  and  $R$  are the extrapolated height and radius of the cylinder, respectively, and  $B_{m,n}^2 = \pi^2 n^2 / H^2 \cdot v_{m,n}^2 / R^2$ .

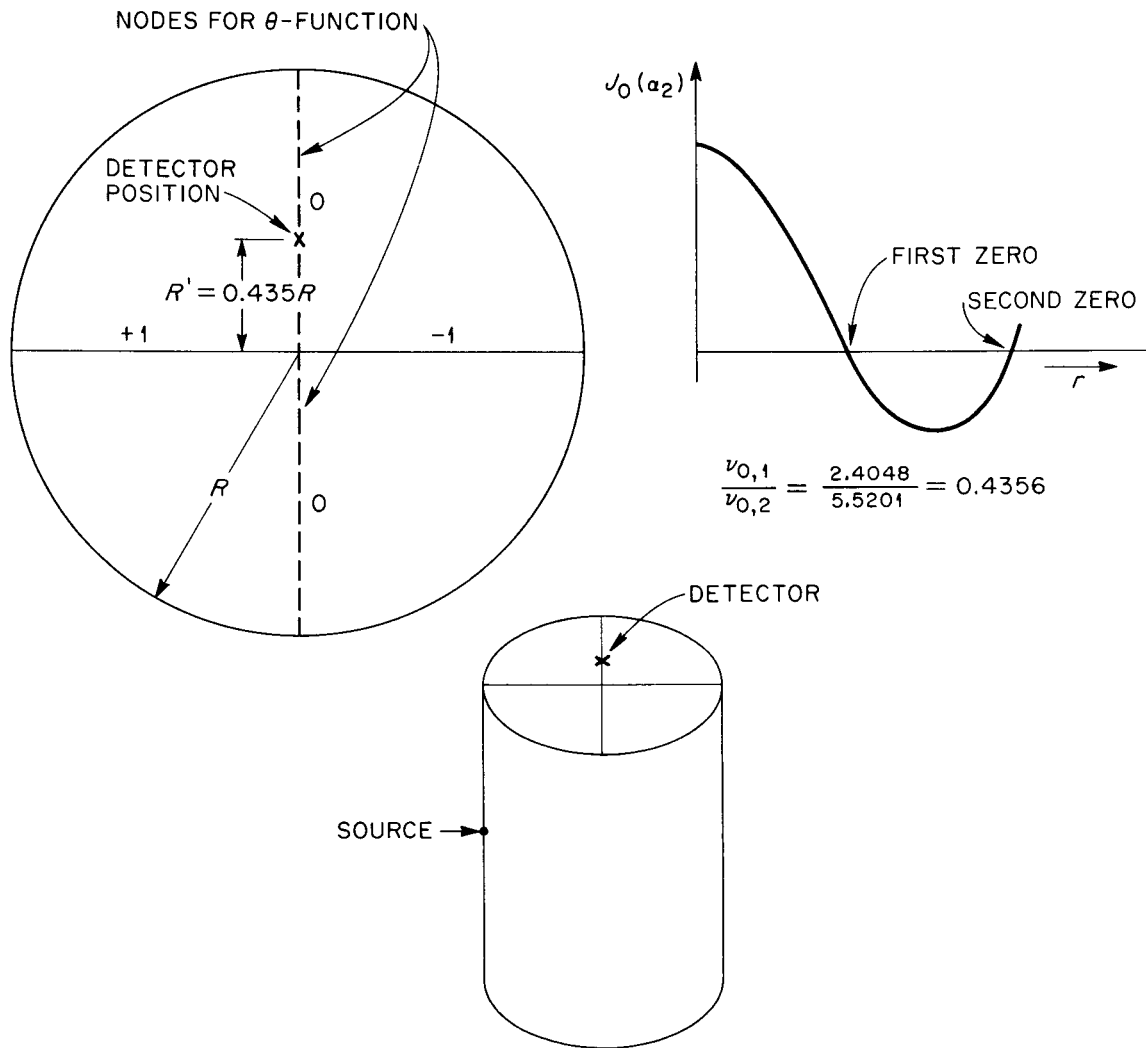


Figure 10. Position of detector for suppression of all three lowest higher modes.

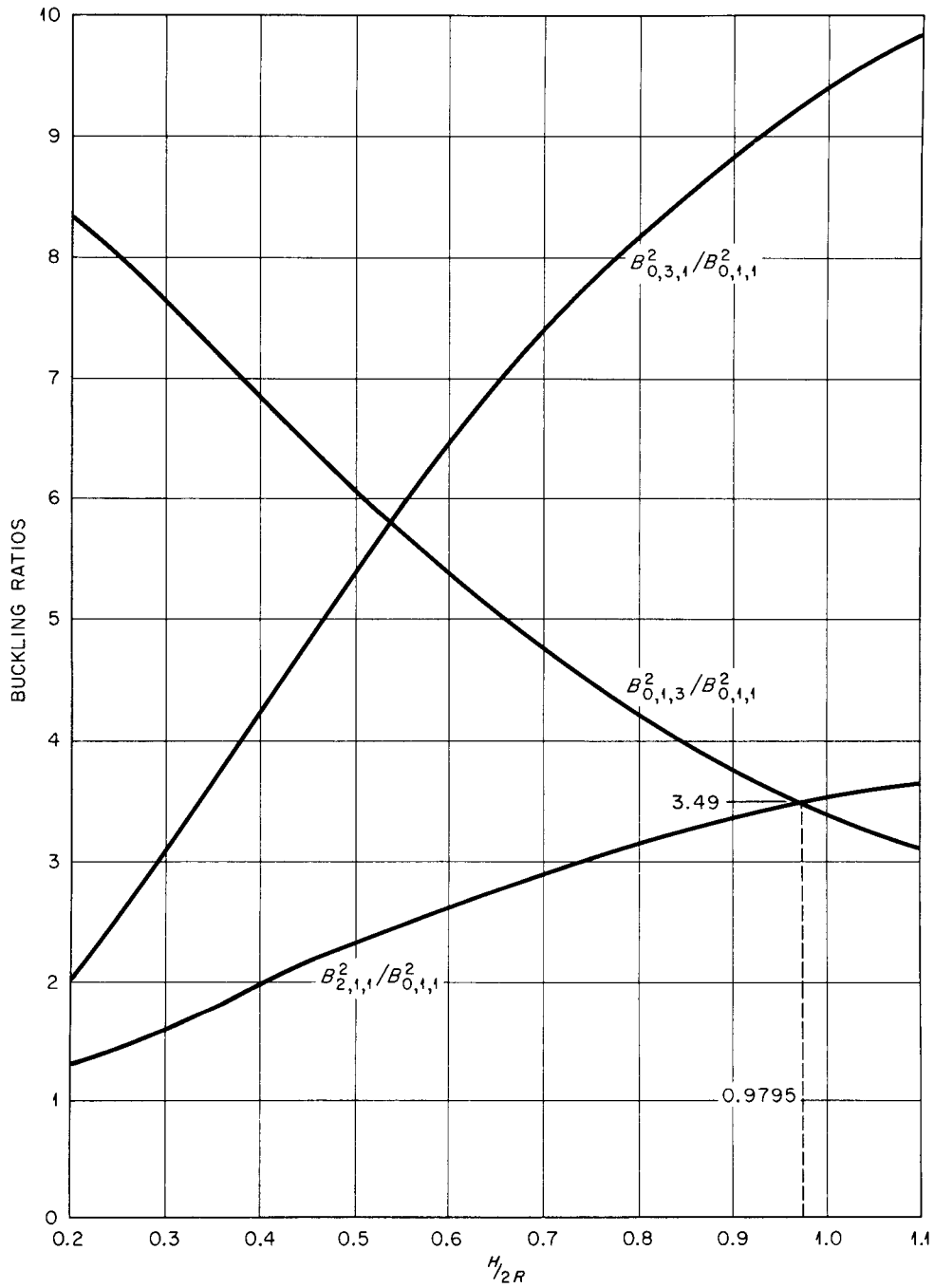


Figure 11. Ratios  $B_{0,3,1}^2 / B_{0,1,1}^2$ ,  $B_{0,1,3}^2 / B_{0,1,1}^2$ , and  $B_{2,1,1}^2 / B_{0,1,1}^2$  as functions of  $H/2R$ , where  $H$  and  $R$  are the extrapolated height and radius of the cylinder, respectively, and  $B_{1,m,n}^2 = \pi^2 n^2 / H^2 + \nu_{1,m}^2 / R^2$ .

It is perhaps worth emphasizing that the ratios described here are buckling ratios, not decay frequency ratios. The  $\lambda$ 's also include the term  $v\Sigma_a$ . In the present series of experiments  $v\Sigma_a$  constituted between 17 percent and 83 percent of the total decay frequency. The large proportions go with small bucklings, of course. Therefore, the higher-mode effects are apt to be more troublesome in large geometry than in the smaller cylinders.

#### IV. SPECTRUM EFFECTS

Consideration will now be given to the effect of the nonuniform neutron velocity on the present experiments. The main source for these considerations is the work of Beckurts and Wirtz (1964). The spectrum effect will be treated first in the diffusion theory approximation, using a series expansion in the energy.

In diffusion theory approximation the balance equation is:

$$\begin{aligned} \frac{1}{v} \frac{\partial \varphi(\vec{r}, E, t)}{\partial t} = & - \Sigma_a(E) \varphi(\vec{r}, E, t) + D(E) \nabla^2 \varphi(\vec{r}, E, t) \\ & + \int_0^{\infty} \Sigma_s(E' \rightarrow E) \varphi(\vec{r}, E', t) dE' - \Sigma_s(E) \varphi(\vec{r}, E, t). \end{aligned} \quad (79)$$

It is assumed that the flux is separable, i.e.

$$\varphi(\vec{r}, E, t) = \psi(\vec{r}, t) \varphi(E, T) \quad . \quad (80)$$

If the Equation (79) is integrated over all energies one gets

$$\frac{1}{\bar{v}} \frac{\partial \psi(\vec{r}, t)}{\partial t} = - \bar{\Sigma}_a \psi(\vec{r}, t) + \bar{D} \nabla^2 \psi(\vec{r}, t) \quad (81)$$

the averages  $\bar{v}$ ,  $\bar{\Sigma}_a$  and  $\bar{D}$  are spectrum-weighted averages. A balance equation for the energy density:

$$\bar{E} n(\vec{r}, t) = \int_0^{\infty} \frac{1}{\bar{v}} \varphi(E, \vec{r}, t) E dE ; \quad (82)$$

can be obtained by multiplying Equation (79) by  $E$  and integrating over energy, with the result:

$$\begin{aligned} \frac{\bar{E}}{\bar{v}} \frac{\partial \psi(\vec{r}, t)}{\partial t} &= - \bar{\Sigma}_a E_a \psi(\vec{r}, t) + \bar{D} E_D \nabla^2 \psi(\vec{r}, t) \\ &+ \psi(\vec{r}, t) \int_0^{\infty} E \left[ \int_0^{\infty} \Sigma_s(E' \rightarrow E) \varphi(E') dE' - \Sigma_s(E) \varphi(E) \right] dE \end{aligned} \quad (83)$$

where

$$E_a = \frac{\int_0^{\infty} E \Sigma_a(E) \varphi(E) dE}{\int_0^{\infty} \Sigma_a(E) \varphi(E) dE} \quad (84)$$

and

$$E_D = \frac{\int_0^{\infty} E D(E) \varphi(E) dE}{\int_0^{\infty} D(E) \varphi(E) dE} \quad (85)$$

Note that if  $\Sigma_a(E)$  goes as  $\frac{1}{v}$  then  $E_a = \bar{E}$ ; this will be assumed to be true. The last term in Equation (83) can be rewritten as

$$\int_0^{\infty} \int_0^{\infty} (E-E') \Sigma_s(E' \rightarrow E) \varphi(E') dE dE'. \quad (86)$$

If one multiplies Equation (81) by  $\bar{E}$  and subtracts it from Equation (83) one obtains:

$$\bar{D} \frac{\nabla^2 \psi}{\psi} (E_D - \bar{E}) = \int_0^{\infty} \int_0^{\infty} (E' - E) \Sigma_s(E' \rightarrow E) \varphi(E') dE' dE. \quad (87)$$

In a Maxwellian spectrum at the temperature of the moderator the right-hand expression of Equation (87) is zero because of the detailed-balance principle. But in a finite medium the left-hand side cannot be equal to zero (except in the physically unrealizable case where  $D(E)$  is proportional to  $1/v$ , thus making  $E_D = \bar{E}$ ). Thus, in a finite medium the spectrum will not be a Maxwellian at the temperature of the moderator. In an infinite medium on the other hand, the vanishing of the term  $\frac{\nabla^2 \psi}{\psi}$  guarantees that in the absence of a source the spectrum is a Maxwellian at the temperature of the medium, regardless of the energy dependence of  $D(E)$ .

It will now be assumed that the spectrum in such a case can be considered to be a Maxwellian at a shifted temperature  $T \neq T_0$ . Then  $\bar{E} = \frac{3}{2} k T$ , and

$$E_D = \frac{\int_0^{\infty} ED(E) \frac{E}{(kT)^2} e^{-E/kT} dE}{\int_0^{\infty} D(E) \frac{E}{(kT)^2} e^{-E/kT} dE} = 2kT + kT^2 \frac{d \ln \bar{D}}{dT} \quad (88)$$

$$\left(\text{since } \bar{D} = \int_0^{\infty} D(E) \frac{E}{(kT)^2} e^{-E/kT} dE, \frac{d\bar{D}}{dT} = \frac{-2\bar{D}}{T} + \frac{1}{kT^2} \int_0^{\infty} E D(E) \frac{E}{(kT)^2} e^{-E/kT} dE\right)$$

where the differentiation is with respect to the neutron temperature).

If, further,  $\frac{|T-T_0|}{T_0} \ll 1$ , which is the case in  $H_2O$  for reasonable bucklings, then one may expand  $\varphi(E)$  in a Taylor series about  $T = T_0$  and, keeping only 2 terms, obtain:

$$\varphi(E) = \frac{E}{(kT)^2} e^{-E/kT} = M(E) + \frac{T-T_0}{T_0} \left(\frac{E}{kT_0} - 2\right) M(E) \quad (89)$$

Then

$$\int_0^{\infty} \int_0^{\infty} (E'-E) \Sigma_s(E' \rightarrow E) \varphi(E') dE dE' = \frac{1}{2} k(T-T_0) \cdot N \cdot M_2 \quad (90)$$

where  $N$  is the number of atoms per unit volume and  $M_2$  is a measure of the mean squared energy exchanged per second by collisions between a neutron and the scattering atom, given by:

$$\begin{aligned} M_2 &= \frac{1}{(kT_0)^2} \int_0^{\infty} \int_0^{\infty} (E'-E)^2 M(E') \sigma_s(E' \rightarrow E) dE' dE \\ &= \frac{1}{(kT_0)^2} \int_0^{\infty} \int_0^{\infty} (E'^2 + E^2 - 2EE') M(E') \sigma_s(E' \rightarrow E) dE' dE \quad (91a) \end{aligned}$$

Making use of the principle of detailed balance  $M_2$  can also be written as:

$$M_2 = \frac{2}{(kT_0)^2} \int_0^\infty \int_0^\infty E'(E'-E) M(E') \sigma_s(E' \rightarrow E) dE' dE . \quad (91b)$$

Combining Equations (87), (88), and (90), one obtains

$$\bar{D} \frac{\nabla^2 \psi}{\psi} \frac{kT}{2} \left( 1 + 2 \frac{d \ln \bar{D}}{d \ln T} \right) = \frac{1}{2} k(T-T_0) N M_2 \quad (92)$$

or, since  $T \approx T_0$

$$\frac{T - T_0}{T_0} \approx \bar{D} \frac{\nabla^2 \psi}{\psi} \frac{1 + 2 \frac{d \ln \bar{D}}{d \ln T}}{N M_2} . \quad (93)$$

In the case of the asymptotically decaying neutron population one can write  $\psi(\vec{r}, t) = R(\vec{r}) e^{-\lambda t}$  where  $R(r)$  is the fundamental-mode eigenfunction of  $\nabla^2 R + B^2 R = 0$ , with the proper boundary conditions. Thus  $\frac{\nabla^2 \psi}{\psi} = -B^2$  and Equation (93) becomes

$$\frac{T - T_0}{T_0} = -DB^2 \frac{1 + d \frac{d \ln \bar{D}}{d \ln T}}{N M_2} \quad (94)$$

so that  $T$  is less than  $T_0$  and diffusion cooling occurs.

The solution of Equation (81) is

$$\lambda = \bar{v} \bar{\Sigma}_a + \bar{D} \bar{v} B^2 . \quad (95)$$

If, as is being assumed,  $\Sigma_a \propto \frac{1}{v}$  then  $\bar{v} \bar{\Sigma}_a = \overline{v\Sigma}_a = \alpha_o$ . The term  $\bar{D}\bar{v}$  depends on the spectrum and on  $B^2$  ( see Equation (94)). Expressing  $\bar{D}\bar{v}(T)$  as a Taylor series expansion about  $T_o$ , and keeping only two terms:

$$\bar{D}\bar{v}(T) = \bar{D}\bar{v}(T_o) + (T - T_o) \frac{d\bar{D}\bar{v}}{dT} \quad (96)$$

and defining  $\bar{D}\bar{v}(T_o) = (vD)_o$  and

$$C \equiv - T_o \bar{D} \frac{d\bar{D}\bar{v}}{dT} \frac{1 + 2 \frac{d \ln \bar{D}}{d \ln T}}{N M_2} \quad (97)$$

one gets  $\bar{D}\bar{v} = (vD)_o + CB^2$  from which it follows that:

$$\lambda = \alpha_o + (vD)_o B^2 + CB^4 \quad (98)$$

To eliminate the derivative  $\frac{d(\bar{v}\bar{D})}{dT}$  in Equation (97) one notes that

$$T \bar{D} \frac{d\bar{D}\bar{v}}{dT} = T \bar{D}^2 \frac{d\bar{v}}{dT} + T \bar{D}\bar{v} \frac{d\bar{D}}{dT} . \quad (99)$$

But  $\bar{v} = a \sqrt{T}$ , so the first term on the right becomes:

$$\frac{T \bar{D}^2}{2\sqrt{T}} a = \frac{\bar{D}^2}{2} a \sqrt{T} = \frac{\bar{v}\bar{D}^2}{2} . \quad (99a)$$

The second term can be expressed as:

$$\mathbb{T} \bar{D} \bar{v} \left( \frac{\bar{D}}{\mathbb{T}} \right) \frac{d \ln \bar{D}}{d \ln \mathbb{T}} = \bar{v} \bar{D}^2 \frac{d \ln \bar{D}}{d \ln \mathbb{T}}. \quad (99b)$$

Putting these expressions into Equation (99) one gets:

$$\mathbb{T} \bar{D} \frac{d \bar{D}}{d \mathbb{T}} = \frac{\bar{v} \bar{D}^2}{2} \left( 1 + 2 \frac{d \ln \bar{D}}{d \ln \mathbb{T}} \right) \quad (99c)$$

so that, making this substitution in Equation (97) one obtains:

$$C = \frac{\bar{v} \bar{D}^2}{2 \mathbb{N} M_2} \left( 1 + 2 \frac{d \ln \bar{D}}{d \ln \mathbb{T}} \right)^2. \quad (100)$$

Alternatively C can be expressed in different form:

$$C = \frac{2}{\bar{v} \mathbb{N} M_2} \left( \frac{\bar{v} \bar{D}}{2} + 2 \bar{v} \bar{D} \frac{d \ln \bar{D}}{d \ln \mathbb{T}} \right)^2 = \frac{2}{\bar{v} \mathbb{N} M_2} \left( \frac{\bar{v} \bar{D}}{2} + \bar{v} \frac{d \bar{D}}{d \ln \mathbb{T}} \right)^2. \quad (101)$$

But

$$\begin{aligned} \frac{d \bar{v} \bar{D}}{d \ln \mathbb{T}} &= \bar{v} \frac{d \bar{D}}{d \ln \mathbb{T}} + \bar{D} \frac{d \bar{v}}{d \ln \mathbb{T}} = \bar{v} \frac{d \bar{D}}{d \ln \mathbb{T}} + \bar{D} \mathbb{T} \frac{d \bar{v}}{d \mathbb{T}} \\ &= \bar{v} \frac{d \bar{D}}{d \ln \mathbb{T}} + \frac{\bar{D} \mathbb{T} a}{2 \sqrt{\mathbb{T}}} = \frac{\bar{v} d \bar{D}}{d \ln \mathbb{T}} + \frac{\bar{D} \bar{v}}{2} \end{aligned} \quad (102)$$

so

$$\bar{v} \frac{d \bar{D}}{d \ln \mathbb{T}} = \frac{d \bar{v} \bar{D}}{d \ln \mathbb{T}} - \frac{\bar{v} \bar{D}}{2} \quad (102a)$$

and

$$C = \frac{-2}{\bar{v} N M_2} \left( \frac{d\bar{v}\bar{D}}{d \ln T} \right)^2 \approx \frac{-2}{\bar{v} N M_2} \left( \frac{d(vD)_0}{d \ln T} \right)^2. \quad (103)$$

Beckurts and Wirtz (1964) present calculated values of  $C$  for water at  $20^\circ\text{C}$ . They assume that  $\frac{d \ln \bar{D}}{d \ln T} = 0.5$ . Using Nelkin's model for water (see below) to calculate  $M_2$  they find  $M_2(\text{Nelkin}) = 45.5 \text{ b./hydrogen molecule}$ . This leads to a value of  $C = - 3.4 \times 10^4 \text{ cm.}^4 \text{ sec.}^{-1}$ . If it is assumed that the hydrogen atoms form a free gas of mass 1.0, then the equation for  $M_2$  becomes:

$$M_2 = \frac{8 \sigma_s (\text{bound atom})}{A(1 + 1/A)^{7/2}}. \quad (104)$$

Inserting this value into the equation for  $C$  one obtains:

$$C = - 2.650 \times 10^3 \text{ cm.}^{-4} \text{ sec.}^{-1}.$$

Assuming that the hydrogen nuclei are rigidly bound to free water molecules one would obtain an effective "heavy gas" with  $A = 18$ , and then

$$C = - 4.250 \times 10^3 \text{ cm.}^{-4} \text{ sec.}^{-1}.$$

Beckurts and Wirtz (1964), have shown that expression (103) can also be obtained without the explicit assumption that the diffusion-

cooled spectrum shape remains Maxwellian, by expanding the spectrum in an orthogonal expansion

$$\varphi(E) = \sum_{m=0}^{\infty} A_m L_m^{(1)}\left(\frac{E}{kT_0}\right) M(E) . \quad (105)$$

With this expansion in the associated Laguerre polynomials of the first kind,  $L_m^{(1)}\left(\frac{E}{kT_0}\right)$ , a linear, homogeneous system of equations for the  $A_m$  is obtained:

$$\lambda \sum_{m=0}^{\infty} V_{im} A_m = B^2 \sum_{m=0}^{\infty} D_{im} A_m - \sum_{m=0}^{\infty} L_{im} A_m . \quad (106)$$

The  $V_{ik}$  factors were evaluated by Häfele and Dresner (1960). The  $D_{im}$  depend on the energy-dependence of  $D$ . If  $D$  is independent of  $E$  then

$$D_{im} = (m + 1) \delta_{im} . \quad (107)$$

The  $L_{im}$  depend on the scattering kernel. For the case of a heavy gas scatterer

$$L_{im} = -m(m + 1) \xi \Sigma_s \delta_{im} \quad (108)$$

However, even for an arbitrary scattering law  $L_{11} = \frac{NM_2}{2}$ , since the scattering-kernel dependence is in the  $M_2$ . Purohit (1961) and Takahashi (1962), have published general expressions for the  $L_{im}$ .

Solving these equations to the 2nd order in the polynomial expansion one obtains, for C:

$$C = \frac{-D_{oo}^2}{V_{oo} L_{11}} \left( \frac{V_{o1}}{V_{oo}} \right)^2 = \frac{-D^2 \left( \frac{2}{\sqrt{\pi}} v_T \right)}{2NM_2} = \frac{-D^2 \bar{v}}{2NM_2} \quad (109)$$

which is the same as the value found by assuming the spectrum to remain Maxwellian, for the case where  $\frac{d \ln D}{d \ln T} = 0$ , i.e., where D is a constant.

#### V. $B^4$ COEFFICIENT IN ONE-VELOCITY $P_1$ APPROXIMATION

Having observed that taking the spread of neutron velocities into account produces higher-order term in the  $\lambda$  vs  $(B^2)$  equation, it will now be shown that the effect of transport theory, even in the one-velocity, consistent  $P_1$  approximation also gives rise to such terms.

It has already been pointed out that the elementary diffusion approximation equations rest on neglecting the term  $d\vec{J}/dt$  in the first order expansion of the one-velocity transport equation, and that retention of this term results in the 'telegrapher's equation' (Equation (57)) which is of second order in the time derivative.

Let a homogeneous medium with no absorption and no source be assumed. Then one may separate the time and space part of the neutron flux and expand the spatial part into appropriate orthogonal functions:

$$\varphi(\vec{r}, t) = \sum_n S_n R_n(\vec{r}) T_n(t) \quad (110)$$

The equation in the time variable is then:

$$T_n'' + \frac{v}{3D} T_n' = \frac{v^2}{3} B_n^2 T_n \quad (111)$$

where  $B_n^2$  is the eigenvalue of the  $n$ 'th term of the spatial equation, i.e., of the  $n$ 'th mode buckling, and where primes denote derivatives. Assuming for  $T(n)$  solutions of the form:

$$T_n(t) = e^{-\lambda_n t} \quad (112)$$

one obtains the characteristic equation

$$\lambda_n^2 - \frac{v}{3D} \lambda_n + \frac{v^2}{3} B_n^2 = 0 \quad (113)$$

which has two solutions:

$$\left. \begin{array}{l} \lambda_{n,1} \\ \lambda_{n,2} \end{array} \right\} = \frac{v}{6D} \pm \frac{v}{6D} (1 - 12D^2 B_n^2)^{\frac{1}{2}}. \quad (114)$$

However, for large times only the smaller one will be significant; and only the fundamental-mode buckling term ( $n = 1$ ) is significant. For this asymptotic case, then, of large  $t$ , the decay frequency becomes

$$\lambda = \frac{v}{6D} [1 - (1 - 12 D^2 B^2)^{\frac{1}{2}}] \quad (114a)$$

which can be expanded in powers of  $B^2$  as follows:

$$\lambda = (vD) B^2 + 3(vD) D^2 B^4 - 18(vD) D^5 B^6 \dots \quad (115)$$

thus an effect in higher orders of  $B^2$  does exist in the  $P_1$  approximation, for one velocity. Note that this effect is of opposite sign than the diffusion cooling effect. It will also be noted that, if  $B_n^2 > \frac{1}{12D^2}$  there are no real solutions of Equation (113) which suggests that in very small systems no exponential time decay of the neutron flux exists. However, such a system has dimensions of the order of  $\lambda_{tr}$  and thus diffusion theory would not be applicable.

## VI. THE ENERGY-DEPENDENT TRANSPORT THEORY DIFFUSION COOLING

Having seen that both energy-dependent diffusion theory and one-velocity transport theory give rise to higher-power terms in the  $\lambda$  vs  $B^2$  equation, the method of the full energy-dependent transport theory will now be outlined. Details will not be given. This treatment is that of H. Honeck (1962), who has made numerical calculations of the diffusion cooling and  $B^6$  terms based on the analysis to be presented.

The transport equation for one-dimensional geometry, no source, homogeneous medium, and isotropic scattering can be written as:

$$\begin{aligned} \frac{1}{v} \frac{\partial f(x, E, \mu, t)}{\partial t} = & - \Sigma_t(E) f(x, E, \mu, t) - \mu \frac{\partial f(x, E, \mu, t)}{\partial x} \\ & + \frac{1}{2} \int_0^\infty \int_{-1}^{+1} \Sigma_s(E' \rightarrow E) f(x, E', \mu', t) dE' d\mu' \quad (116) \end{aligned}$$

where the angular dependence in this one-dimensional model is reduced to one angle, the angle made with respect to the x-axis, and the equation is in terms of  $\mu$ , the cosine of the angle. It will be assumed that the spectrum has attained equilibrium, and that the neutron population is, therefore, decaying exponentially. This assumption is expressed as:

$$f(x, E, \mu, t) = f(x, E, \mu) e^{-\lambda t} . \quad (117)$$

With this provision the transport equation becomes:

$$[\Sigma_t(E) - \frac{\lambda}{v}] f(x, E, \mu) = -\mu \frac{\partial F}{\partial x} + \frac{1}{2} \int_0^{\infty} \int_{-1}^{+1} \Sigma_s(E' \rightarrow E) f(x, E', \mu) dE' d\mu' . \quad (118)$$

Before going further, it is interesting to note that this equation implies an upper limit on the eigenvalues.  $f(x, E, \mu)$  is always  $\geq 0$ . Also the inscattering double integral on the right must be  $\geq 0$ . So, in the infinite medium case, where  $\frac{\partial F}{\partial x} = 0$ , it follows that  $\Sigma_t(E) - \lambda/v \geq 0$  or  $\lambda \leq (v\Sigma_t(E))_{\min}$ . Nelkin (1963), has shown that even in the case where  $\frac{\partial F}{\partial x} \neq 0$  the inequality holds. In crystalline moderators such as Be or graphite this limitation is a practically realizable one, because coherent scattering (Bragg scattering) is significant. In that case  $(v\Sigma_t(E))_{\min}$  occurs just below the Bragg cut-off, and this value of  $v\Sigma_a(E)$  determines the upper bound on  $\lambda$ . For example, in Be  $(v\Sigma_s)_{\min} = 3.8 \times 10^3 \text{ sec.}^{-1} \approx (v\Sigma_t)_{\min}$ . This says that for values of  $B^2 > B_c^2$ , where  $B_c^2$  is defined by

$$\lambda = 3.8 \times 10^3 \text{ sec.}^{-1} = v\Sigma_a + DB_c^2 + CB_c^4 + \dots \quad (119)$$

Equation (116) has no solution, that is, no asymptotic spectrum will exist. However, in  $H_2O$   $(v\Sigma_s)_{\min}$  occurs for very high energy and is of the order of  $3 \times 10^5 \text{ sec.}^{-1}$  so that asymptotic spectra should exist for, practically, all bucklings.

In ice, even though it is a crystalline solid, the relative magnitudes of  $\sigma_{\text{inc.}}/\sigma_{\text{coh.}}$  should cause the coherent scattering to be relatively unimportant so that, as in water, asymptotic spectra should be established. The confirmation of this supposition is one of the objectives of this work.

To return now to the discussion of the transport equation and its asymptotic spectrum solutions. Equation (118) cannot be reduced to a simple integral equation because of its space dependence. So a Fourier transformation is performed:

$$f(B,E,\mu) = \int_{-\infty}^{\infty} F(x,E,\mu) e^{-iBx} dx . \quad (120)$$

The transformed transport equation then becomes:

$$\left(\Sigma_t(E) - \frac{\lambda}{v}\right) f(B,E,\mu) = iB\mu f(B,E,\mu) + \frac{1}{2} \int_0^{\infty} \int_{-1}^1 \Sigma_s(E' \rightarrow E) f(B,E',\mu') dE' d\mu' . \quad (121)$$

Then integrating over angles:

$$\varphi(B,E) = \int_{-1}^1 f(B,E,\mu) d\mu \quad (122)$$

one obtains:

$$\varphi(B,E) = \frac{1}{B} \tan^{-1} \left\{ \frac{B}{\Sigma_t(E) - \frac{\lambda}{v}} \right\} \int_0^{\infty} \Sigma_s(E' \rightarrow E) \varphi(B,E') dE' . \quad (123)$$

So far, the assumption has been made that the scattering is isotropic. However, the nonisotropy can be taken into account by using, instead of  $\Sigma_s(E' \rightarrow E)$ , a Legendre polynomial expansion of the anisotropic scattering cross section. Honeck (1962), has performed a direct numerical integration of Equation (120) using the Nelkin model for water (adding a free gas kernel with mass 16 and  $\sigma_s = 3.76$  b. to account for the oxygen scattering) using terms up to  $l = 3$  in the expansion for the anisotropy of the scattering. He finds values of

$$\begin{aligned} (vD) &= 3.753 \times 10^4 \text{ cm.}^2 \text{ sec.}^{-1} \\ C &= -3.130 \times 10^3 \text{ cm.}^4 \text{ sec.}^{-1} \\ F &= 2.700 \times 10^2 \text{ cm.}^6 \text{ sec.}^{-1} \end{aligned}$$

where  $F$  is the coefficient of the  $B^6$  term.

Equation (123) can also be solved analytically, by making a power-series expansion. Equation (123) is written in the form:

$$\left\{ \left( B / \tan^{-1} \frac{B}{\Sigma_s(E) - \frac{\lambda}{v}} \right) - \Sigma_s(E) \right\} \varphi(B,E) = L \varphi \quad (124)$$

where  $L$  is the "thermalization operator" defined by

$$L \varphi = \int_0^{\infty} \Sigma_s(E' \rightarrow E) \varphi(B, E') dE' - \Sigma_s(E) \varphi(B, E) \quad . \quad (125)$$

Then the flux is expanded in a power series in  $B^2$ :

$$\varphi(B, E) = M(E) + B^2 \varphi_2(E) + B^4 \varphi_4(E) + \dots \quad (126)$$

$$\text{and } \lambda = (vD)_0 B^2 - CB^4 + FB^6 \dots$$

These series are inserted into Equation (124), the first term in the brackets is also expanded, and the coefficients of like powers of  $B$  are set separately equal.

From the zero-order term one obtains:

$$(vD)_0 = \frac{\int_0^{\infty} \frac{1}{3\Sigma_s(E)} M(E) dE}{\int_0^{\infty} \frac{1}{v} M(E) dE} \quad (127)$$

which is the expected result that  $\bar{D} = \bar{\lambda}_{tr}/3$ . More interestingly, the next order yields:

$$-C = \frac{\int_0^{\infty} \left[ \frac{(vD)_0}{v} - \frac{1}{3\Sigma_s(E)} \right] \varphi_2(E) dE}{\int_0^{\infty} \frac{1}{v} M(E) dE} + \frac{\int_0^{\infty} \left[ \frac{1}{3\Sigma_s^2(E)} \right] \left[ \frac{4}{15\Sigma_s(E)} - \frac{(vD)_0}{v} \right] M(E) dE}{\int_0^{\infty} \frac{1}{v} M(E) dE} \quad (128)$$

The first term is due to the energy-spectrum effect, which could have

been obtained by a similar power expansion of the diffusion equation. The second term is the transport effect. Honeck has calculated the diffusion cooling effect in  $H_2O$  by means of this expansion using numerical integration and, again, the Nelkin model to the same order in the angle-expansion as for the direct integration. His results for  $H_2O$  at  $20^\circ C$ . are as follows:

$$\begin{aligned}
 D_o &= 3.746 \times 10^4 \text{ cm.}^2 \text{ sec.}^{-1} \\
 C_E &= - 3.052 \times 10^3 \text{ cm.}^4 \text{ sec.}^{-1} \\
 C_T &= + 0.174 \times 10^3 \text{ cm.}^4 \text{ sec.}^{-1} \\
 C &= C_E + C_T = - 2.878 \times 10^3 \text{ cm.}^4 \text{ sec.}^{-1} \\
 F &= 1.80 \times 10^2 \text{ cm.}^6 \text{ sec.}^{-1}
 \end{aligned}$$

It will be observed that the transport part is only 0.057 times as large as the spectrum part of  $C$ , and that the  $B^6$  term coefficient is very small, as was confirmed for ice in the present experiments where no effect in  $B^6$  could be detected.

#### VII. THE EXTRAPOLATION DISTANCE

The boundary conditions assumed in all the equations discussed in either diffusion or transport theory are that the neutron flux (or the neutron density) vanish at the boundary. Since this is clearly not the case at the physical medium-vacuum interface, it is required to find the location of an imaginary surface, so located that the vanishing of the flux at this surface is equivalent to the actual conditions of

neutron leakage from the true surface.

In monoenergetic diffusion theory, assuming one-dimensional geometry, the neutron vector current  $\vec{J} = -D\nabla\phi$  can be broken into two partial currents in the plus-x and minus-x directions (Glasstone and Edlund, 1952, see pages 92 to 96):

$$\begin{aligned} J_- &= \frac{\phi}{4} + \frac{D}{2} \frac{\partial\phi}{\partial x} = \frac{\phi}{4} + \frac{\lambda_{tr}}{6} \left(\frac{\partial\phi}{\partial x}\right)_0 \\ J_+ &= \frac{\phi}{4} - \frac{D}{2} \frac{\partial\phi}{\partial x} = \frac{\phi}{4} - \frac{\lambda_{tr}}{6} \left(\frac{\partial\phi}{\partial x}\right)_0 \end{aligned} \tag{129}$$

If the point under consideration,  $x_0 = 0$  is a vacuum boundary (or the boundary between moderator and "black" absorber) then  $J_- = \frac{\phi}{4} + \frac{\lambda_{tr}}{6} \left(\frac{\partial\phi}{\partial x}\right)_0 = 0$ . Therefore, the slope of the flux at the surface is  $\frac{\partial\phi}{\partial x} = \frac{-6\phi_0}{4\lambda_{tr}}$ . Assuming a linear extrapolation one would then have a linear extrapolation distance  $d = \frac{2}{3} \lambda_{tr}$ .

Since the diffusion theory is not valid near such a boundary, the linear extrapolation distance is more accurately given by a  $P_n$  approximation to the one-velocity transport equation. Weinberg and Wigner (1958), show that in the limit of high-order approximation, for a very weak absorber, the linear extrapolation distance would be  $d = 0.71045 \lambda_{tr}$ .

However, this is strictly valid only in the case of a single velocity, isotropic scattering, plane surfaces, and no absorption. Moreover, since the modal flux shapes are curved (cosines or Bessel functions) the use of linear extrapolation distances is not quite

correct but tends to overestimate the correction.

In order to make suitable corrections to apply to the experiment analysis, including the effects of the velocity distribution and surface curvature, the effective dimensions were obtained by the relation

$$\begin{aligned}\tilde{H} &= H + 2(0.7104 \text{ (3D)}) P(B^2) \\ \tilde{R} &= R + (0.7104 \text{ (3D)}) Q(B^2)\end{aligned}\tag{130}$$

where  $P(B^2)$  and  $Q(B^2)$  are correction factors for the plane and curved surfaces of the cylinders respectively.

The factors  $P(B^2)$  and  $Q(B^2)$  were obtained from the results of Gelbard and Davis (1962), in which they performed computations with a multi-group thermal neutron computer program using the empirically adjusted Radkowsky bound-hydrogen scattering kernel (Radkowsky, 1950) (see below). They solved the slab and spherical-geometry cases in the  $P_3$  approximation and the cylindrical geometry case in both  $P_1$  and diffusion-theory approximations. Interestingly enough they find that neglecting both the  $\frac{d\vec{J}}{dt}$  term and the  $P_3$  corrections in the diffusion approximation gives rise to compensating errors, which make the result more accurate in the diffusion approximation than in the  $P_1$  approximation.

Gelbard and Davis first show that the diffusion parameters obtained in their calculations using the Radkowsky kernel are in agreement with experimental results for water.

The decay constants for slabs of various thicknesses,  $L$ , were then calculated and the augmentation distance  $d(B^2)$  was obtained by

$$d(B^2) = \frac{1}{2} \left( \frac{\pi}{B} - L \right) . \quad (131)$$

The calculations also produce a value of

$$D(B^2) = \frac{\int J(E, B^2) dE}{\int \nu \varphi(E, B^2) dE} . \quad (132)$$

For very large slabs ( $B^2 = 0$ ) Equation (132) gives  $D(0) = \left( \frac{\bar{1}}{\bar{v}} \right) (vD)_0$ . The ratio  $d(B^2)/3D(0) = d(B^2)/\lambda_{tr}(0)$  then gives the numerical ratio between extrapolation distance and transport mean free path. Figure 12 shows the values of  $d(B^2)/\lambda_{tr}(0)$  as function of  $B^2$ .

It is to be noted that in the 0-buckling limit  $d(0) = 0.76 \lambda_{tr}$ , rather than  $0.7104 \lambda_{tr}$ . This value also agrees with that found by Nelkin (1960) who made a variational-method calculation using the model  $D(E) \propto v$  and also obtained  $d \approx 0.76 \lambda_{tr}$ .

For use in the present work  $H(B^2)$  was calculated by the relation

$$H(B^2) = \frac{\pi}{B} - 2d(B^2) , \quad (133)$$

using the values of Figure 12 for  $d(B^2)$ . Then the correction factor  $P(B^2) = \frac{d(B^2)/\lambda_{tr}(0)}{0.7104}$  was plotted versus  $H(B^2)$  as shown in Figure 13.

This correction was then applied to each value of  $H$  by way of Equation (130).

Gelbard and Davis also give values for  $d(B^2)$  in infinite cylinders, and curve  $Q(B^2)$  was obtained for cylinders in the same way as  $P(B^2)$  was obtained for slabs. As expected, for large dimensions the cylinder

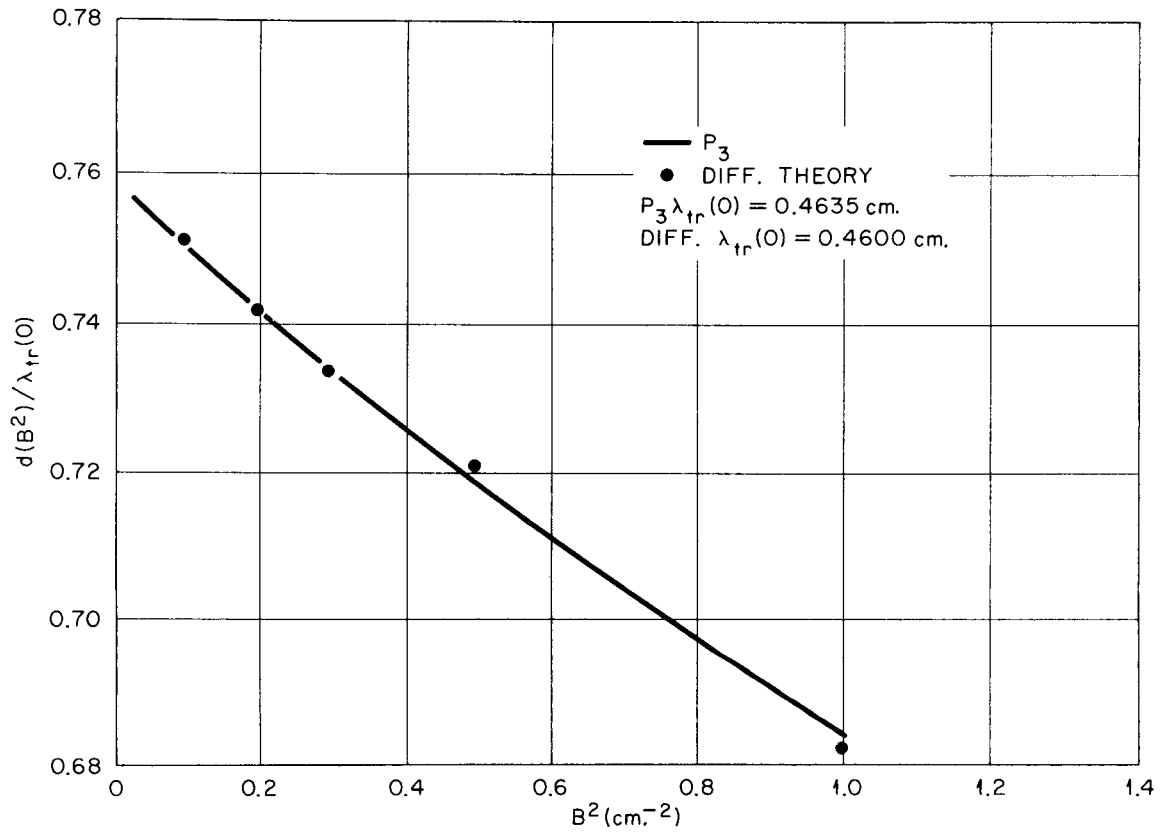


Figure 12. Ratio of augmentation distance  $d(B^2)$  to  $(vD)_0$  versus  $B^2$  calculated by Gelbard and Davis (1962), for Slab geometry.

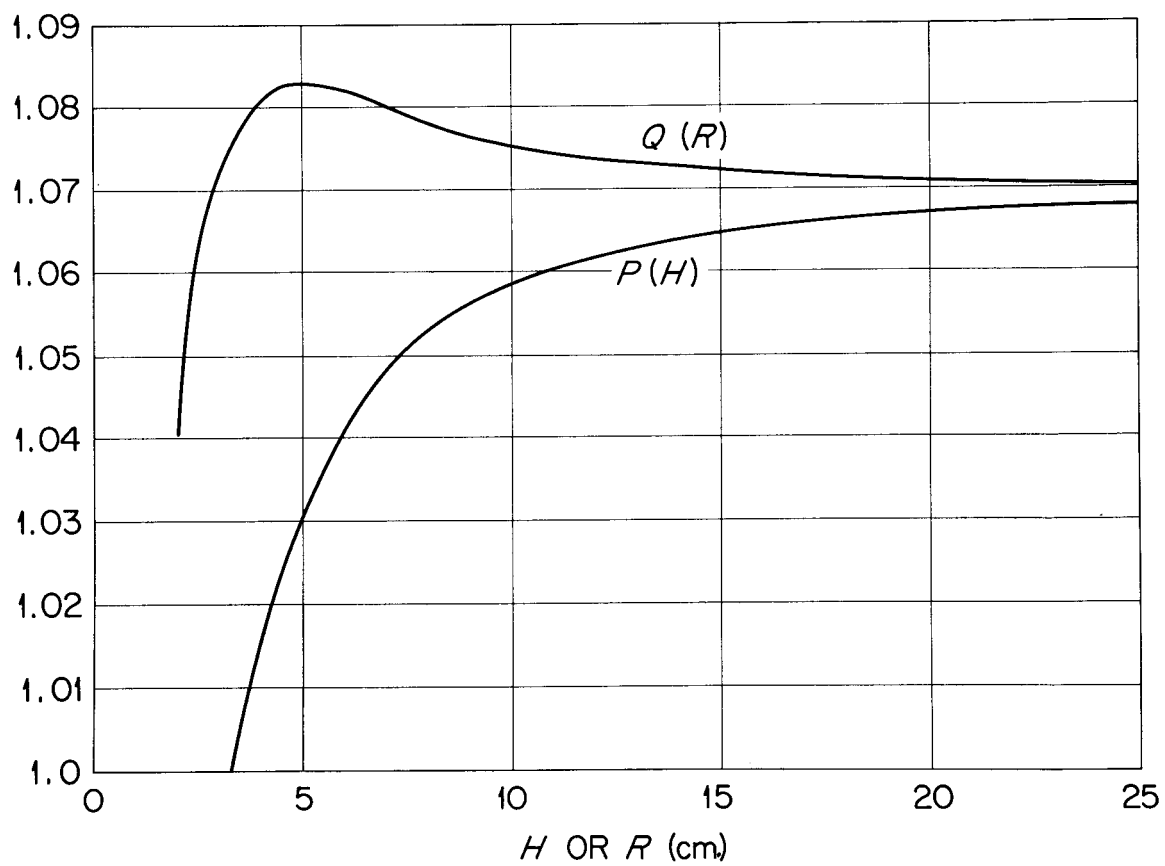


Figure 13. The extrapolation distance correction factors used to determine effective cylinder dimensions.  $P(H)$  and  $Q(R)$  are defined in the text.

values become identical with those for the slab since the curvature of the surface becomes negligible in the limit. Note that the distances  $d(B^2)$  are not linear extrapolation distances, but rather what Gelbard and Davis call "augmentation distances," which are just the distances to be added to the physical dimensions to yield the proper buckling for pulsed-neutron experiments.

In the present work the aluminum-ice interface was considered to be a black boundary. However, some neutrons may scatter from the aluminum or the cadmium back into the ice. However, a conservative calculation assuming (1) neutrons normally incident on a plane interface, and (2) half of all scattered neutrons scatter through  $180^\circ$  (the other half forward) shows that the return probability reduces to 0.003. The outer ice surfaces were, therefore, treated as vacuum interfaces.

#### VIII. SCATTERING KERNELS; THE NELKIN KERNEL

In many of the discussion presented so far the analysis of the equations requires that a specific form for  $\Sigma_s(E' \rightarrow E, \vec{\Omega}' \rightarrow \vec{\Omega})$  be used to evaluate the parameters. In a real sense the physics of the entire neutron transport theory resides in this scattering "kernel", and the various experiments measuring macroscopic and extensive parameters also must, finally, reduce to their connection with the basic physical interaction of neutrons with nuclei through the effect of the scattering kernel.

As has already been stated, the scattering kernels in most crystalline solids have contributions from two sources, the incoherent

component, due to interactions with single scattering centers, and coherent effects due to constructive and destructive interference of scattering amplitudes caused by the regular spacing of the scattering center in lattice regions.

However, in hydrogen the inelastic scattering is dominant by far so that only the incoherent scattering processes are important.

The question then arises as to the scattering kernel in ice, assuming incoherent scattering only. Under the incoherence assumption the only difference between water and ice would be the hindrance that the solid-state bonding offers to those motions that are available in the liquid state. Therefore, the scattering kernel for the liquid state will now be briefly considered.

A number of "experimental" kernels have been used which rest, not on the physics of the water molecule, but on agreement between numerical results with experiments. Of these only the "Radkowsky prescription" will be mentioned (Radkowsky, 1950). Essentially the Radkowsky prescription consists of treating the  $P_0$  and  $P_1$  components of the numerical transfer matrix (specifying neutron transfer cross sections from group  $i$  to group  $(i \pm k)$  in a given multigroup structure) as those for free protons, and treating the  $P_3$  matrix as diagonal (i.e., no group transfer) using values chosen so that the values of  $\sum_{tr}^m$  agree with those obtained by a code using experimental data. This method is useful for numerical calculations, such as those used by Gelbard and Davis and can give good results, but offers little insight into the fundamental processes. This prescription is

equivalent to assuming an energy-dependent effective mass, which is fitted to the experimental energy dependence of the scattering cross section by the formula

$$\sigma_s(E) = [(M_{\text{eff}})/(1 + M_{\text{eff}})]^2 . \quad (134)$$

Nelkin has constructed a model for scattering in water which yields excellent agreement with most macroscopic measurements. (Nelkin, 1960).

The basic assumptions of the Nelkin model are that the water molecule can perform vibrations, hindered rotations, and hindered translations. It is assumed that the various degrees of freedom carry out simple harmonic oscillations. Nelkin starts by assuming that the motion of the scattering proton is a superposition of normal modes described by harmonic oscillator coordinates and obtains the exact scattering kernel:

$$\sigma(E_0, E, \theta) = \left(\frac{\sigma_b}{8\pi^2}\right) \sqrt{\frac{E}{E_0}} \int_{-\infty}^{\infty} e^{-i\epsilon t} q(\vec{K}, T, t) dt \quad (135)$$

where  $\sigma_b = 81.2$  b. is the bound-hydrogen cross section  $\epsilon \equiv (E - E_0)$  is the energy transferred in the scattering,  $\vec{K}$  is the momentum transferred,  $T$  is the absolute temperature and

$$q(\vec{K}, T, t) = \langle \exp \left[ \sum_{p=1}^N (\vec{K} \cdot \xi_p)^2 f(\omega_p, T, t) \right] \rangle \quad (136)$$

where

$$f(\omega, T, t) = [(n + 1)(e^{-i\omega t} - 1) + n(e^{i\omega t} - 1)]/2\omega ,$$

$n = [e^{-\omega/T} - 1]^{-1}$ ,  $\vec{\xi}_p$  is the amplitude and  $\omega_p$  the frequency of the p'th normal mode.

The normal modes of motion are then approximated as follows: the frequencies of internal vibration are assumed "free", i.e., the same as those of the vapor molecule. The translation and rotation are assumed to be those of the rigid molecule.

The translation is treated in the high-energy limit, i.e., as "free". Nelkin points out that in a solid lattice the translation motion about the mean position gives rise to a purely elastic scattering component which decreases with increasing momentum transfer as  $\exp(-K^2 u^2)$  where

$$K^2 = \sum_{p=1}^3 (K \cdot \xi_p)^2 \quad (138)$$

and  $u^2$  is the mean square displacement. Nelkin states that most of the contribution to  $u^2$  is due to translation, and that thus the measured value of  $u$  can be used to give a crude measure of the Debye temperature for the translational motion. For a Debye frequency distribution  $u^2$  is:

$$u^2 = \frac{3}{2 M \Theta^3} \int_0^{\Theta} \omega \coth(\omega/2T) d\omega \quad (139)$$

where  $\Theta$  is the Debye temperature. For  $u^2 = 0.14 \times 10^{-16} \text{ cm.}^2$  (the measured value) one obtains a Debye temperature of 0.011 eV. This characteristic energy associated with the hindrance of translational motions is small enough so that the translational motions can be considered free. This gives a  $q$  function equivalent to that of an ideal monoatomic gas of mass 18 at temperature  $T$

$$q_t \approx e^{-(K^2/2M)(it + Tt^2)} \quad . \quad (140).$$

So the treatment of translation, where the main difference between liquid and solid would appear is essentially based on the assumption that translation can be considered as free, even if the translations are treated as "normal modes" applicable to a solid.

The hindered rotation is replaced by torsional vibration with a single frequency  $\omega_r$ , which was treated by Krieger (see Nelkin, 1960). The averaging over orientations in this case, as for vibrations, is done by approximating the averaging over orientation of a product of terms corresponding to different normal modes by a product of averages. The equivalent mass of the molecule for this vibration mode is taken to be 2.32 (as shown by Krieger and Nelkin, 1956).

Based on experimental evidence of a peak in the energy distribution of  $90^\circ$  scattered cold neutrons which correspond to an energy increase of 60 meV., the value  $\hbar\omega_r = 0.06 \text{ eV.}$  was used. The value of  $q_r$  used is given as

for each energy range of incident and final energies. Thus, between 0.01 and 0.15 eV. incident energy, translations are assumed to be free and only elastic vibrational transitions are exactly treated. Between 0.20 and 0.48 eV. the excitation of the 0.205 eV. vibrational level is properly treated and the approximate form of Equation (142) is used for rotations. Between 0.15 and 0.20 eV. the parameter choice for the vibrational motions depends on the final neutron energies, and above 0.48 eV. the  $q_1$  vibration is treated as free-atom motion and the excitation of the 0.48 eV. vibration level is considered.

This treatment of the scattering kernel has been used to calculate many quantities measurable by experiments. For example, the total cross section

$$\sigma_T = \sigma_a + \int \int \sigma(E_o, E, \theta) dE d\theta \quad (144)$$

is compared with experiment in Figure 14 and seen to agree very well. The Nelkin model leads to a value of  $M_2 = 91.6$  per molecule at room temperature in  $H_2O$ .

#### IX. NUMERICAL CALCULATIONS OF THE ICE DIFFUSION PARAMETERS

So far the discussion of the methods of calculation has not found direct application to the case of ice. However, in the discussion of the Nelkin kernel it was pointed out that the nature of the kernel was such that water was treated as an 'ice-like' material in that diffusive transport of the molecules was neglected, and the free-atom

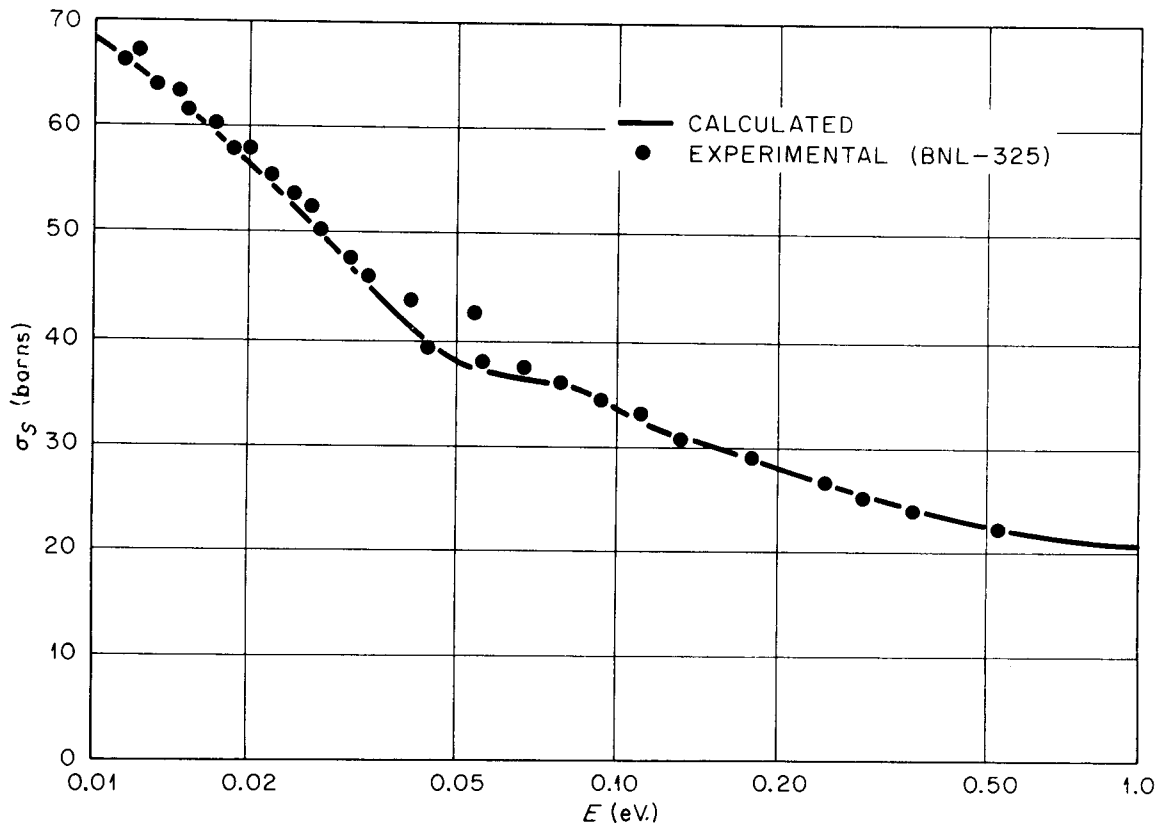


Figure 14. Comparison of total scattering cross section for  $H_2O$  as calculated by the Nelkin model and experimental values.

$$q_r = \exp [K^2/M_r] f(\omega_r, T, t) \approx \exp \left[ -\frac{K^2}{2M_r} (it + \bar{E}_r t^2) \right] \quad (141)$$

where  $\bar{E}_r = [n(\omega_r/T) + \frac{1}{2}] \omega_r = 0.036$  eV. This is based on an expansion of  $f(\omega_r, T, t)$  in powers of  $t$ , keeping only terms up to quadratic since for sufficiently large energy transfer only small collision times matter.

The vibrational energy states in the vapor are known to be 0.205 eV., 0.474 eV. and 0.488 eV. (Herzberg, 1950). The orientation averaging is again done as before, and the simplifications are made that the two higher levels are treated as degenerate and that the vibrations are not assumed to be thermally excited. This leads to

$$q_v = q_1 q_2 = \exp \left[ \frac{K^2}{6M_v \omega_1} (e^{-i\omega_1 t} - 1) \right] \exp \left[ \frac{K^2}{3M_v \omega_2} (e^{-i\omega_2 t} - 1) \right] \quad (142)$$

where  $\hbar\omega_1 = 0.205$  eV. and  $\hbar\omega_2 = 0.481$  eV. The effective mass for vibration,  $M_v = 1.95$  energy of the incident neutron the scattering approaches the free-atom scattering.

The total  $q$  is then assumed to be

$$q = q_t q_r q_v \quad (143)$$

For convenience in numerical calculations it is further assumed that the excitation of only one of the modes has to be treated properly

approximation used for the translational motions was based on a consideration of the binding in a solid, rather than taking specific liquid effects into account. It will be further shown in Chapter V. that cold water does have distinctly solid-like characteristics, and that according to Singwi and Sjölander (1960), a molecule executes, in the mean, some 10 vibrations at a "lattice position" in water before diffusively moving to another location.

According to a model by Gössman (1962), water near freezing is treated as a saturated solution of ice in liquid, with 85 per cent of the volume in ice-like states. (See Chapter V.)

Therefore, it would be expected that the Nelkin-kernel method would provide reasonable good calculations even for solid ice, as long as the temperature was not so low that the available energy-transfer modes become very restricted.

M. J. Ohanian (1963; also Ohanian and Daitsch, 1964), has solved the time-dependent thermalization problem with a discrete energy (multigroup-like) numerical method both by direct integration of the Boltzmann equation, using a Taylor expansion, and by a modal expansion of the neutron density in terms of the eigenfunctions of the Boltzmann operator. One of his objectives was to study the effect of the choice of scattering kernel on the asymptotic spectrum in both the infinite medium and finite media. As specific scattering models he used the mass-1, Wigner-Wilkins hydrogen gas model (Wigner and Wilkins, 1944) and the Nelkin model with an improvement due to Goldman and Federighi (1961), which consists of detailed consideration of the amount of

energy transferred in the scattering process. Since the kernels are too complex for analytical treatment Ohanian developed numerical methods, coded for computer use, for calculating such quantities as time-dependent, steady-state, and asymptotic spectra in finite and infinite media.

Two methods for solution are used. One is a direct integration of the time-dependent Boltzmann equation, by expanding the density in a Taylor series about  $t = t_0$ , keeping only one term since  $\delta t \ll 1$ :

$$P \chi(E, t_0 + \delta t) = \chi(E, t_0) + \delta t \left. \frac{\partial \chi(E, t)}{\partial t} \right|_{t = 0} \quad (145)$$

where  $\chi(t)$  is the symmetrized neutron density given by

$$\chi(t) = \frac{N(E, t)}{\sqrt{M(E)}} . \quad (146)$$

$N(E, t)$  is the total density of neutrons with energy  $E$  a time  $t$ . For the infinite medium problem

$$\left. \frac{\partial \chi(E, t)}{\partial t} \right|_{t = 0} = P \chi(E, t_0) + \zeta(E, t_0) \quad (147)$$

where  $P$  is the Boltzmann operator defined by:

$$P \chi(E, t) \equiv \int_0^{\infty} \{K(E' \rightarrow E) - v[\Sigma_s(E) + \Sigma_a(E)] \delta(E - E')\} \chi(E', t) dE', \quad (148)$$

$\zeta(E, t_0)$  is the symmetrized neutron source,

$$\zeta(E, t_0) = \frac{S(E, t_0)}{\sqrt{M(E)}}, \quad (149)$$

and

$$K(E' \rightarrow E) = K(E \rightarrow E') = \frac{[\Sigma_s(E' \rightarrow E) v \sqrt{M(E')}]}{\sqrt{M(E)}} \quad (150)$$

is the symmetric scattering kernel. So, if the neutron density and the source are known at time  $t_0$ , then the spectrum at later times can be obtained in successive small time steps, using the spectrum at each time point as source for the next step. If the source is a delta function in time and the flux is assumed zero for  $t < t_0$ , one obtains simply:

$$\begin{aligned} N(E, t_0 + \delta t) &= \sqrt{M(E)} \zeta(E) \delta t = S_0 \delta(E - E_0) \delta t \\ N(E, t_0 + 2\delta t) &= \sqrt{M(E)} [(1 + \delta t P) \chi(E, t_0 + \delta t)] \\ &\vdots \\ N(E, t_0 + k\delta t) &= \sqrt{M(E)} \{(1 + \delta t P) \chi[E, t_0 + (k - 1) \delta t]\} . \end{aligned} \quad (151)$$

Similarly, in a finite medium the solution for the  $k$ 'th time interval would be

$$N(E, t_0 + k\delta t) = \sqrt{M(E)} \{[1 + \delta t(P - vD(E)E^2)] \chi[E, t_0 + (k - 1) \delta t]\} \quad (152)$$

For the second solution method the symmetrized transport equation

$$\frac{\partial \chi(\mathbb{E}, t)}{\partial t} = - [\Sigma_s(\mathbb{E}) + \Sigma_a(\mathbb{E})] v \chi(\mathbb{E}, t) + \int_0^{\infty} K(\mathbb{E}' \rightarrow \mathbb{E}) \chi(\mathbb{E}', t) d\mathbb{E}' + \zeta(\mathbb{E}, t) \quad (153)$$

is used, and its homogeneous part is assumed to be expressible as:

$$\chi(\mathbb{E}, t) = \sum_{n=1}^{\infty} a_n \psi_n(\mathbb{E}) e^{-\lambda_n t} . \quad (154)$$

Putting this into the homogeneous part of Equation (152) gives, for each term:

$$P \psi_n(\mathbb{E}) = - \lambda_n \psi_n(\mathbb{E}) .$$

Ohanian shows that, as was discussed in an earlier section,  $\lambda_n(0) = [\sigma \Sigma_s(\mathbb{E})]_{\min}$  is a limit point for the spectrum of discrete eigenvalues. Therefore, the set of discrete eigenfunctions  $\psi_n(\mathbb{E})$  is not infinite, and hence not complete, and a modal expansion involving only the discrete modes, is not possible. Continuum eigenvalues must be included also:

$$\chi(\mathbb{E}, t) = \sum_{n=1} a_n^{(d)} \psi_n^{(d)}(\mathbb{E}) e^{-\lambda_n^{(d)} t} + \int_{[\nu \Sigma_s(\mathbb{E})]_{\min}}^{\infty} a_{\lambda}^{(c)} \psi_{(\mathbb{E}, \lambda)}^{(c)} e^{-\lambda^{(c)} t} d\lambda^{(c)} \quad (155)$$

Ohanian then sets up a discrete-energy model suitable for numerical integration, in which Equation (147) becomes

$$\frac{\partial}{\partial t} (\chi) = (P)(\Delta E)(\chi) + (\zeta) \quad (156)$$

where  $(\chi)$  and  $(\zeta)$  are column matrixes,  $(\Delta E)$  is a diagonal matrix, and  $(P)$  is a square matrix with diagonal elements:

$$P_{ii} = - \left[ \sum_{i \neq \ell}^J \Sigma_{s_{\ell i}} \Delta E_{\ell} + \Sigma_{a_i} \right] \frac{v_i}{\Delta E_i} \quad (157)$$

and off-diagonal elements:  $P_{ij} = K_{ij}$ . A similar equation (analogous to Equation (153)) results in the finite medium case:

$$\frac{\partial}{\partial t} (\chi) = [(P)-(L)] (\Delta E)(\chi) + (\zeta) \quad (158)$$

where  $(L)$  is a diagonal matrix with  $l_{nn} = v_n D(E_n) B^2$ .

The direct solution in the discrete-energy case proceeds as before so that

$$(\chi)_{k+1} = [(1) + \delta t(P)(\Delta E)] (\chi)_k + \delta t(\zeta)_k \quad (159)$$

where the subscripts refer to times  $(t_0 + k\delta t)$  and  $[t_0 + (k+1)\delta t]$ .

Similarly, a modal-expansion solution exists in the discrete-energy presentation.

Ohanian then develops a method for solving the finite-medium problem by a perturbation method in terms of the infinite-medium eigenfunctions. The finite medium eigenfunctions and eigenvalues are given by

$$[P - vD(E)B^2] \theta_n(E) = \gamma_n \theta_n(E) \quad (160)$$

whereas the infinite-medium case has the equation:

$$P\psi_n(E) = -\lambda_n \psi_n(E). \quad (161)$$

As expected, for  $B^2 = 0$  the two problems become identical so that  $\theta_n = \psi_n$  and  $\lambda_n = \gamma_n$ . So, expanding using the standard perturbation technique:

$$\begin{aligned} \gamma_n &= \alpha + \lambda_n^{(0)} + a_n^{(2)} B^2 + a_n^{(4)} B^4 + \dots \\ \theta_n &= \psi_n + \theta_n^{(2)} B^2 + \theta_n^{(4)} B^4 \dots \end{aligned} \quad (162)$$

assuming  $v\bar{\Sigma}_a = \alpha = \text{const.}$  Putting Equation (162) into Equation (160) and equating like powers of  $B^2$ , gives:

$$P\psi_n = -\lambda\psi_n \quad (163a)$$

$$[P + \lambda_n] \theta_n^{(2)} = -a_n^{(2)} + vD\psi_n \quad (163b)$$

$$[P + \lambda_n] \theta_n^{(4)} = -a_n^{(4)} \psi_n + vD\theta_n^{(2)} - a_n^{(2)} \theta_n^{(2)} \quad (163c)$$

Equations (163b) and (163c) represent the first and second order perturbations.

Since the  $\psi_m$  form a complete orthonormal set both  $\theta_n^{(2)}$  and  $\theta_n^{(4)}$  can be expanded in terms of them (remember that the set  $\psi_n$  may contain continuous eigenvalues):

$$\theta_n^{(2)} = \sum_{m=1}^{\infty} c_{nm} \psi_m . \quad (164)$$

$$\theta_n^{(4)} = \sum_{m=1}^{\infty} d_{nm} \psi_m . \quad (165)$$

Using Equation (164) the first-order perturbation becomes

$$-\sum_{m=1}^{\infty} c_{nm} \lambda_m \psi_m + \lambda_n \sum_{m=1}^{\infty} c_{nm} \psi_m = -a_n^{(2)} \psi_n + vD\psi_n . \quad (166)$$

Multiplying this by  $\psi_k$  and integrating over E, using the orthonormality gives:

$$c_{nk}(\lambda_n - \lambda_k) = -a_n^{(2)} \delta_{nk} + \int vD \psi_k \psi_n dE . \quad (167)$$

Considering the normalization, one obtains then:

$$\begin{aligned} \gamma_n &= \alpha + \lambda_n^{(0)} + B^2 \int vD\psi_n^2 dE \\ \theta_n &= \psi_n + B^2 \sum_{m \neq n}^{\infty} \frac{\int vD\psi_m \psi_n dE}{(\lambda_n^{(0)} - \lambda_m^{(0)})} \end{aligned} \quad (168)$$

In a similar way, the second-order perturbation is expanded in the eigenfunctions  $\psi_m$  to give:

$$\gamma_n = \alpha + \lambda_n^{(0)} + B^2 h_{mn} + B^4 \sum_{n \neq m} \frac{(h_{mn})^2}{(\lambda_n^{(0)} - \lambda_m^{(0)})} \quad (169)$$

where

$$h_{mn} = \int vD \psi_m \psi_n dE . \quad (170)$$

It should be noted that  $a_n^{(2)}$  and  $a_n^{(4)}$ , the coefficients of the  $B^2$  and  $B^4$  terms, are given exactly by the first-order and second-order perturbations, respectively. For the lowest eigenvalue (asymptotic spectrum at long times)  $\gamma_1$ , one obtains:

$$a_1^{(2)} = \int vD m dE = \bar{vD} = (vD)_0 \quad (171)$$

and

$$|a_1^{(4)}| = \sum_{m=2}^{\infty} \left[ \int vD \sqrt{M} \psi_m dE \right]^2 / \lambda_m^{(0)} = |C_D| . \quad (172)$$

Note that this solution was developed in the diffusion approximation so that a transport-theory component of  $C$ ,  $C_T$  must be added  $C = C_D + C_T$  (see Equation (128)).

Ohanian calculated  $vD$  and  $C_D$  using the discrete-energy representations of Equations (171) and (172):

$$D_o = \sum_{j=1}^J v_j D(E_j) M(E_j) \Delta E_j \quad (171a)$$

$$C_D = - \sum_{m=2}^J \left[ \sum_{j=1}^J v_j D(E_j) \sqrt{M(E_j)} \psi_m(E_j) \Delta E_j \right]^2 / |\lambda_m^{(0)}| \quad (172a)$$

$C_D$  was computed using the improved Nelkin kernel. The transport part of  $C$ ,  $C_T$ , was computed using the discrete-energy representation of Equation (128):

$$C_T = - \left[ \sum_{j=1}^J \frac{1}{3\Sigma_{tr}^2(E_j)} \left( \frac{4}{15\Sigma_s(E_j)} - \frac{(vD)_o}{v_j} M(E_j) \Delta E_j \right) \right] \sum_{j=1}^J \frac{M(E_j)}{v_j} \Delta E_j .$$

Ohanian calculated the values of  $vD$  and  $C$  for two of the temperatures used in the present experiment. The results will be given in Chapter V. and compared with the experimental results.

## CHAPTER III

### THE EXPERIMENT

#### I. THE EXPERIMENTAL ARRANGEMENT

The source of neutrons for the present work was a Cockcroft-Walton type accelerator capable of a maximum accelerating voltage of 300,000 volts.<sup>2</sup> The high voltage source was a SAMES (Société Anonyme des Machines Electrostatiques, Grenoble, France) power supply which operates on the principle of the induction generator. An insulating, hollow, rotating cylinder is spun in a high-pressure hydrogen atmosphere, and static charge is placed on its outer surface by induction at one point of the rotation, and removed at another. The control system permits operation at any intermediate voltage up to the maximum. From the power supply the voltage is led, by means of an insulated cable, to the secondary side of a 1:1 isolation transformer (made by Beta Electric Corp.) whose secondary coil is insulated both from ground and from the primary coil by sufficient oil-bath insulation to withstand a potential difference of 300,000 volts. The primary of this transformer is connected to a source of 60 cps., 115 V. current. The output of the secondary, therefore, carries the same alternating voltage, but is biased to the high voltage. Figure 15 shows the power

---

<sup>2</sup>The accelerator was designed by F. Glass and F. Duncan of the ORNL Instrumentation and Controls Division and built by the Instrument and Controls Division of ORNL. The pulsed ion source is of a type designed by King and Parker (1955).

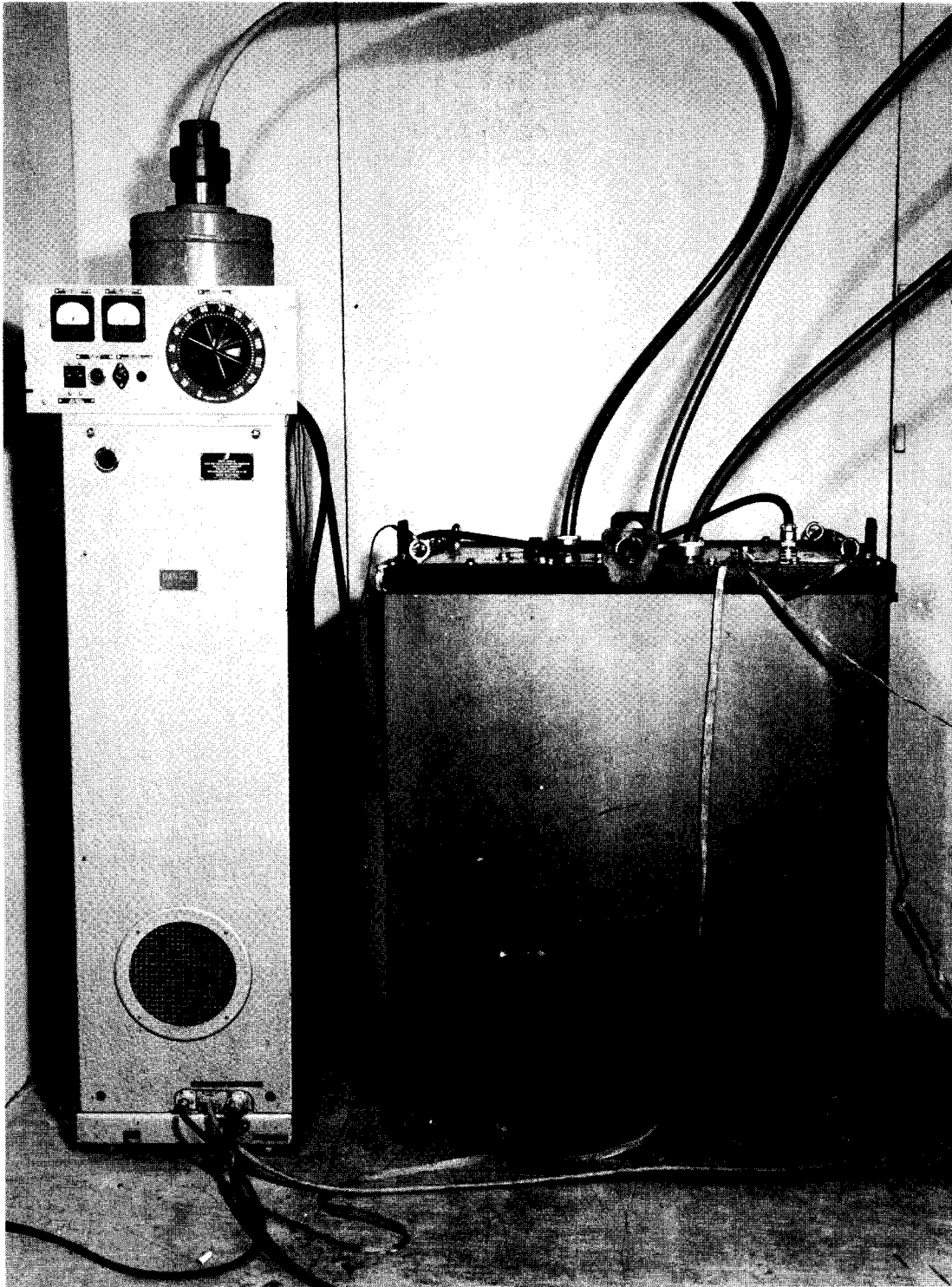


Figure 15. Isolation transformer and 300,000-volt power supply.

supply and the isolation transformer. The A.C. power supplies the various circuits in the ion source of the accelerator.

In the ion source (designed by W. N. Good and J. H. Neiler, ORNL) the particles to be accelerated, in the form of a gas, are fed into the vacuum system by means of a controllable leak (a temperature-controlled palladium plug). The gas is ionized by a radio-frequency field produced by an rf.-oscillator, and the positive ions are driven towards the target by an extraction voltage. Near the base of the glass ion-source bottle the ions are partly focused by a magnetic lens, and some of them then pass through a small aperture into the lens section. In this section the particles pass through a two-stage electrostatic lens system (the Einzel lens) powered by two Beta Electric Corp. Model 206 30-kV.-D.C. power supplies located in the ion source. At the exit from the lens system the particles constitute a well-collimated beam with an energy ranging from 1.0- to 3.0-keV. (1 keV. =  $1.0 \times 10^3$  electron volt or  $1.593 \times 10^{-9}$  erg.). The particles then pass between a pair of deflection plates and then through an aperture into the accelerating tube, which consists of a series of 16 equally spaced equipotential planes (metal discs) with central holes. By means of a series arrangement of 50-megohm resistors connecting the plates the total accelerating voltage is divided into 16 equal steps.

This arrangement of equipotential plates and resistors serves as a series of focusing lenses which keep the beam focused and aligned down the center of the accelerating tube.

In order to produce a pulsed source of neutrons the accelerator beam must be capable of being rapidly turned on and off. In this machine, the primary pulsing device consisted of the pair of deflecting plates mentioned above, located just beyond the outlet of the Einzel lens (King and Parker, 1955). One of these plates could be charged to six hundred volts from a power supply in the ion source head. When a 600 V. potential difference exists across the two plates (one is grounded, the other swings 600 V. positive) the ion beam is deflected and thus prevented from passing through the following aperture into the accelerating tube system. Thus, a square-wave signal applied to the deflection plates produces a pulsed beam, which is off when the plates are charged, and on when the plates carry no voltage.

There are in general three alternative methods to maintain the necessary synchronism between the pulsed source and the detecting equipment. For one, the accelerator can be free-running (i.e., have an internal frequency source) and one may then detect the leading edge of each particle burst and use it as a timing signal for the detector system, alternatively one may have a separate timing system which sends a signal to the accelerator to initiate each pulse at the proper time (and perhaps also to terminate each pulse) or the deflection may be made on the accelerated beam. The first system has the advantage that no communication with the high-voltage terminal is required during the experiment. However it is then necessary to have access to the ion source to change the frequency or duration of the pulses. The second system is in principle completely operable from the control station;

however it requires that the timing signal bridge the potential gap from ground to the ion source voltage. The third method suffers from background due to the deflected accelerated beam.

The second alternative was chosen for the present equipment. The timing and logic circuitry forms part of the ground-potential analyzer system. From it a pulsing signal consisting of a square-wave pulse which directs both the turning on and the turning off of the accelerator beam is transmitted across the potential gap by an X-band-radar transmitter and receiver system. Figure 16 shows the ion source and the transmitter in position.

The Palladium-leak heater voltage, the extraction voltage, the magnetic lens voltage and the two focusing lens voltages are each controllable from either of two control stations (one in the target area and one at the analyzer station behind the shield) by means of a three-component selsyn system for each. One selsyn of each triplet is mounted at the ground-plane plate of the accelerator and is directly coupled to a variac inside the ion source by means of an insulating rod. In this way the beam can be optimized and focused directly while the high voltage is on, and adjustments can be made behind the shield during operation to maintain the desired neutron production rate. The system described here was designed by F. Glass and H. Todd of the ORNL Instrumentation and Controls Division.

Figure 17 is a diagram of the relative locations of the items of equipment used in this work. The vacuum system components, consisting of a mechanical roughing pump, two stages of oil-vapor diffusion pumps,

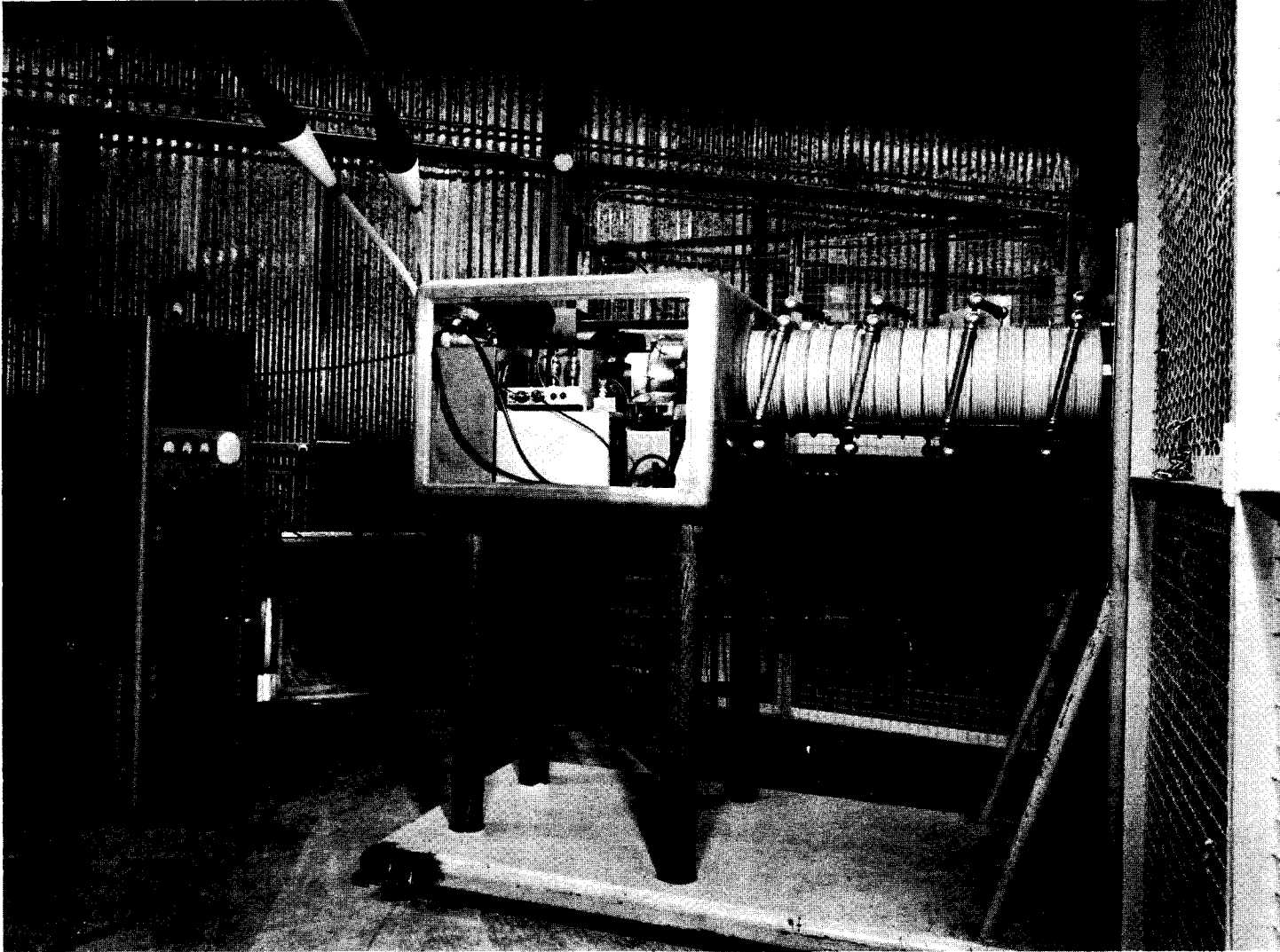


Figure 16. Accelerator ion source head and radar transmitter.

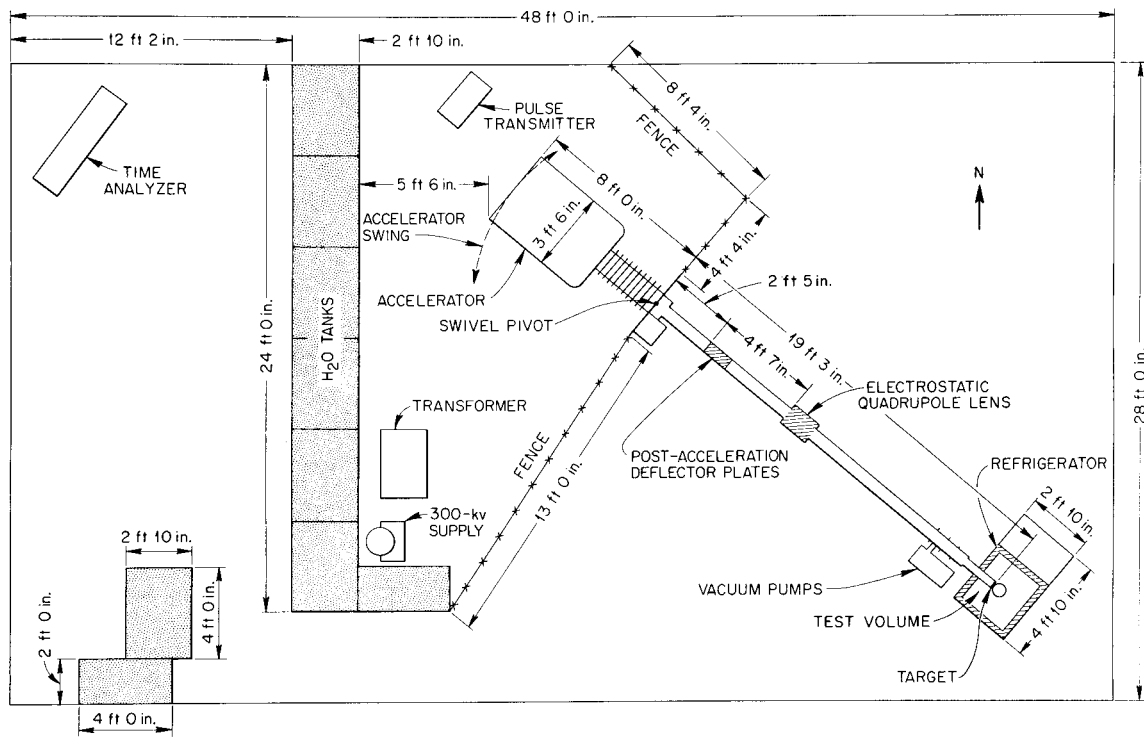


Figure 17. Experimental setup for the pulsed-neutron measurements in ice cylinders.

plus a liquid-nitrogen cold trap between the pumps and the vacuum system were located near the ground-plane. The diffusion pumps could be by-passed to rough-pump the system initially. An ion-gauge type vacuum gauge also was located at this point, and used as the main pressure determining device. After opening the system approximately one hour was required to attain the operating pressure range from  $1 \times 10^{-8}$  to  $3 \times 10^{-8}$  torr.

The beam arrangement in Figure 17 (page 105) was dictated by the need to keep space available for other experiments during the time of this work. The accelerator could be swiveled as shown and thus used for other experiments. The long drift path of the accelerated ions made it desirable to install a quadrupole electrostatic focusing lens in the beam tube in order to counteract the tendency of the beam to spread due to focusing inadequacies and space-charge effects. The impingement of the beam produces considerable outgassing, and due to the long narrow shape of the beam tube sizable pressure gradients could thus arise between the target and the vacuum pump of the system. In order to prevent excessive defocusing due to this pressure, a secondary vacuum system was located, as shown, near the target end of the drift tube.

In the following sections a number of components of the experimental system will be described in more detail, together with calculations and experiments performed to develop these items for use in the present measurements.

The time analyzer and switching circuit. The time analyzer, shown in Figure 18, was designed by F. Glass and built by the Instrument and Controls Division of the Oak Ridge National Laboratory. It consists of a control circuit and nineteen scaler circuits plus the needed power supplies. The basic timing source is a sine-wave generator capable of frequencies from 16 cps. to several megacycles. This sine-wave signal is amplified, clipped and differentiated to produce a series of evenly spaced short time-marker pulses with a repetition rate equal to the frequency,  $f$ , of the sine oscillator. These pulses are shown on line 1 of Figure 19. The frequency of the time-marker pulses was continuously monitored by a Berkley Model 5500 Universal Counter and Timer which used an internal oven-controlled Piezo crystal as an accurate clock.

This instrument was checked several times against a frequency standard over the period of the experiments and found to be stable within one part in  $10^4$  over periods of many months. With this meter it was determined that the repetition rate of the time marker pulses would drift randomly by about 0.01- to 0.03 per cent per hour depending on temperature stability of the experimental room and on voltage fluctuations of the supply voltage. However the frequency was manually adjusted within 0.01 per cent at least once in every two hours, so that the mean deviation of the frequency from the nominal value was no more than 0.02 per cent, and most usually no more than half that amount for any given run.

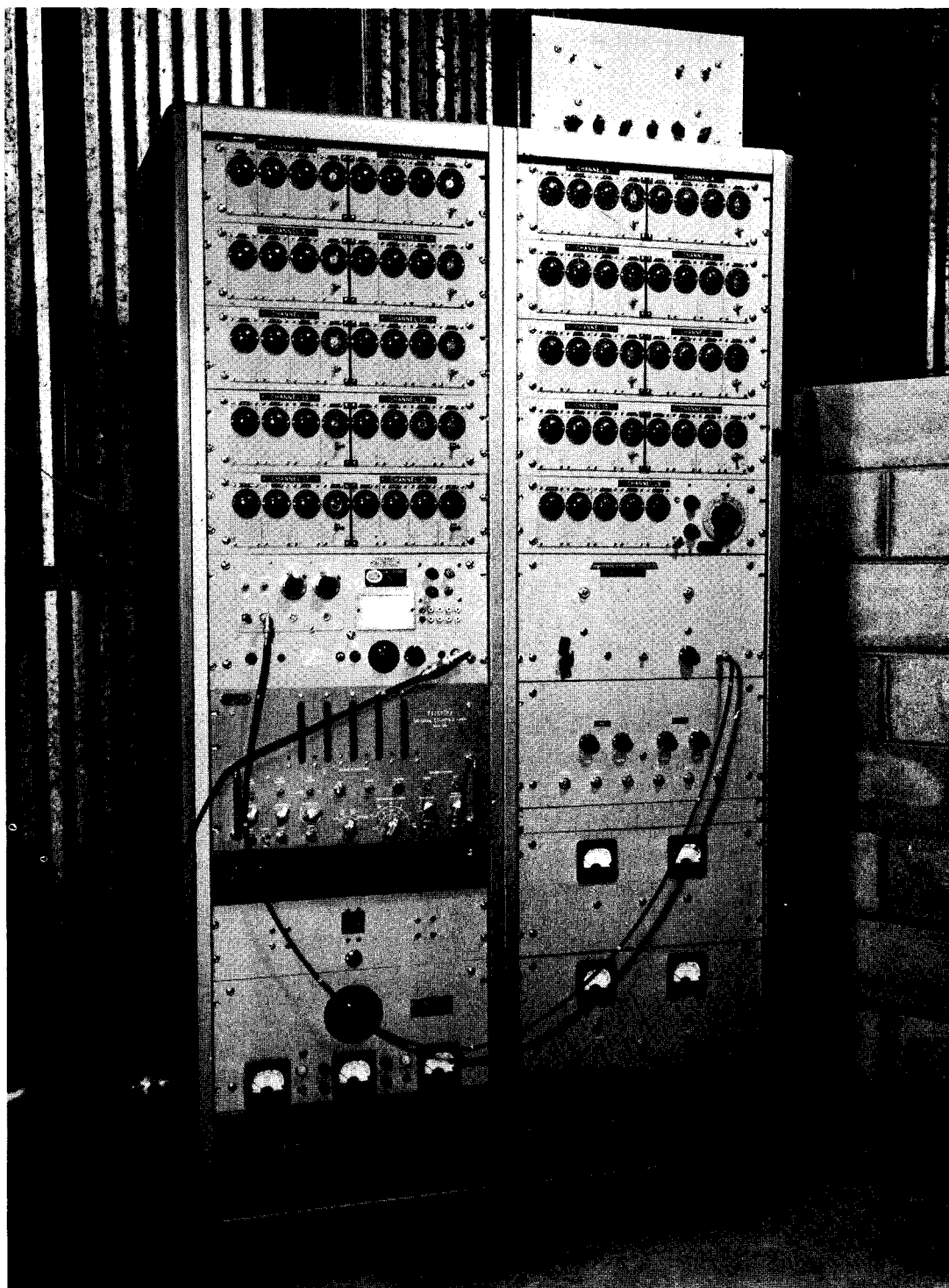


Figure 18. Time analyzer, including frequency meter, logic circuit, scalars, and DD2 amplifier.

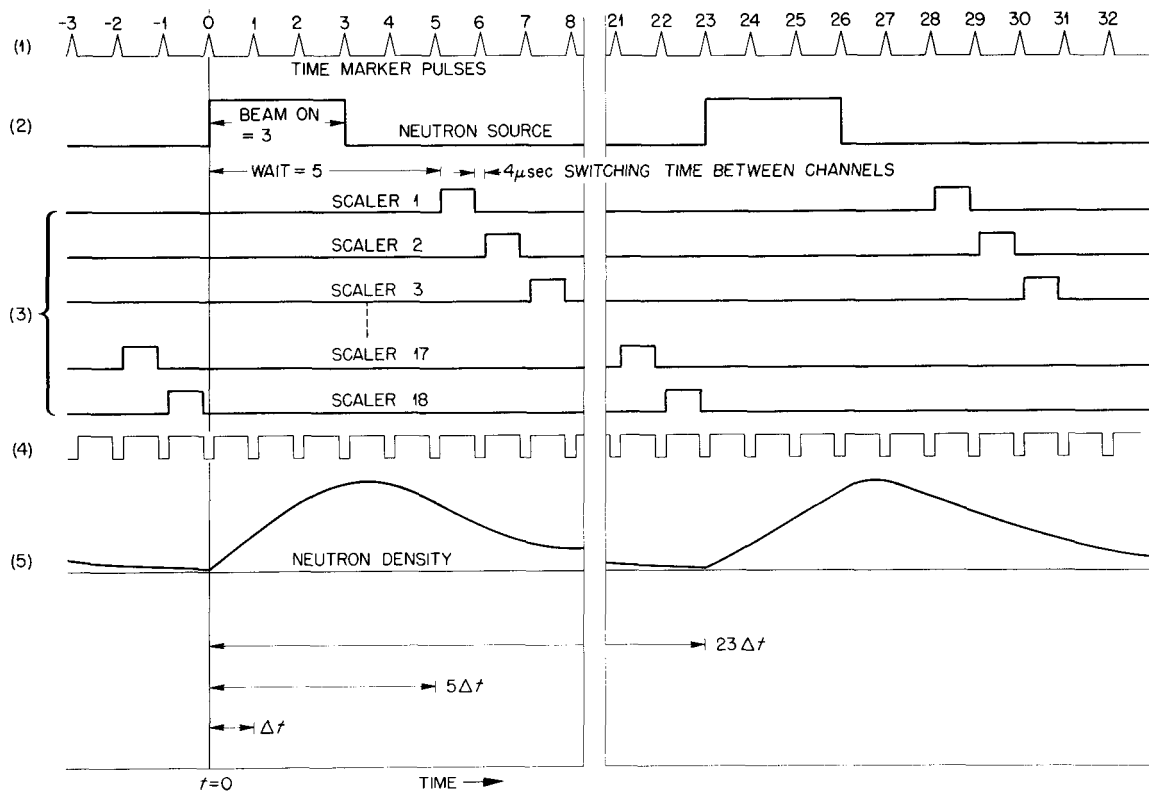


Figure 19. Time sequence of time analyzer: (1) time marker pulses, (2) beam-on time, (3) scaler-on time, (4) master gate circuit, and (5) thermal-neutron count rate in detector.

At the beginning of a run, the first time-marker pulse causes a signal to be transmitted to the accelerator turning the beam on. The beam then remains on for a period of time  $M/f = M(\Delta t)$  where  $M$  is an integer between 1 and 99 manually selected by a pair of decade switches. In Figure 19 (page 111) the neutron burst is shown for the case where  $M = 2$ . As will be seen below, in the present experiments the values of  $(\Delta t)$  were set in the vicinity of one-fourth of the decay period of the neutrons, and the beam-on-time was usually set at  $3(\Delta t)$  or  $4(\Delta t)$ . When the beam is turned on the thermal neutron density in the fundamental mode rises approximately as  $N_s(1 - e^{-\lambda t})$ , where  $\lambda$  is the thermal neutron decay frequency and  $N_s$  is the saturated neutron density in the ice cylinder that would be attained if the source were left on indefinitely with the same intensity it has during the pulse. Thus the peak neutron density in the ice block just after the end of each neutron pulse was of the order of  $(1 - e^{-1}) N_s = 0.63 N_s$ . This choice of burst width [ $M(\Delta t) \approx 1/\lambda$ ] is close to optimum since much longer pulses would yield increasingly less additional density, and for much shorter pulses the yield would be almost proportionately less. Line 4 in Figure 19 (page 111) shows the neutron density schematically.

The time analyzer and logic equipment utilized Burroughs MO-10 beam switching tubes, used in series pairs to provide eighteen time channels. With only eighteen time channels available these had to be used to best advantage in finding the asymptotic decay constants of the neutrons in each ice cylinder. It would be useless to collect data before the establishment of the fundamental-mode neutron population.

The circuit was therefore designed to allow a waiting time  $N(\Delta t)$  (where  $N$  could be selected to be any number from 1 to 99) after the initiation of the neutron pulse. After the waiting time the control circuit gates the 'channel 1' scaler open for a time approximately equal to  $(\Delta t)$  after which the channel 1 scaler is gated shut and the channel 2 scaler gates on for the same length of time. In this fashion all eighteen scalers are gated open in sequence, thus collecting data over a time interval  $18(\Delta t)$ . Immediately upon the closing of the eighteenth time channel the next neutron burst is initiated and the cycle repeats. Line 3 of Figure 19 (page 111) indicates the gating operation of the scalers.

Initially the switching of the MO-10 tubes caused the opening and closure of the scaler gates directly. The switching-over time is of the order of three microseconds. However non-uniformities in the switching-over times introduced channel width errors of the order of one  $\mu\text{sec}$ . which amounts to  $\sim 5\%$  for the shortest channel widths used. The channel widths were measured by keeping the accelerator on full time (by disabling the pulsing receiver) but cycling the time analyzer normally. Under these conditions the neutron flux in the ice cylinder is saturated, and the neutron leakage rate becomes constant in time. Therefore each channel should count the same number of counts in a given large number of sweeps except for statistical variations. Figure 20 shows a typical result for five runs, in each of which 100,000 counts per channel were collected. The observed relative counts are shown for each channel, as well as a histogram of the distribution and the Gaussian curve of the expected spread, assuming only random counting statistics to be operating.

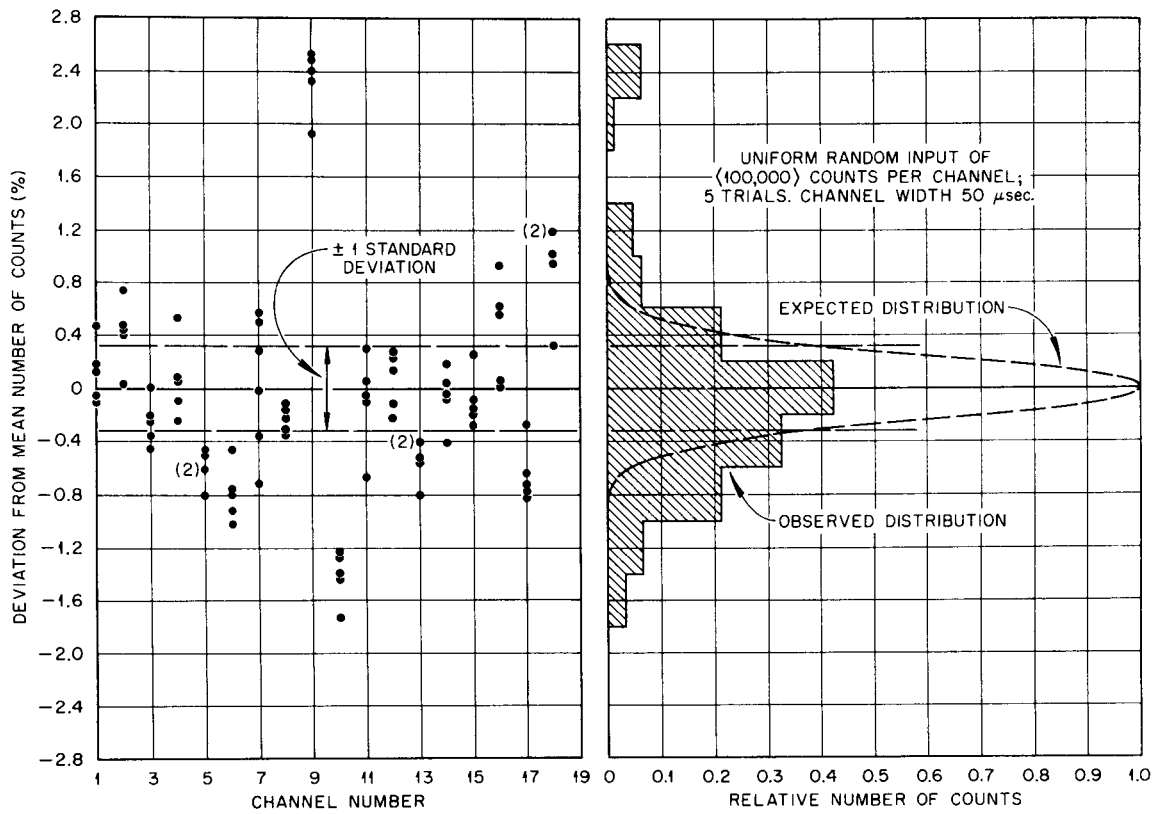


Figure 20. Distribution of number of counts collected in each channel with 100,000 counts per channel on the average. Results for five runs are shown. On the right the summed distribution is also shown together with the normal distribution curve expected for counting statistics. Data taken without master gate circuit. (See text).

It is apparent that there were systematic channel differences and the over-all spread is far greater than would be attributable to statistics alone.

To combat this problem an additional gate circuit was installed<sup>3</sup> which closes approximately one  $\mu$ sec. before the switching occurs and remains closed for 4.5- to 5- $\mu$ sec., thus blanketing the variable switch-over interval. Line 4 of Figure 19 (page 111) shows the operation of this master gate circuit schematically. Figure 21 shows the results of four test runs, collecting 100,000 counts per channel in each run, after installation of the master gate circuit. The distribution now comes much closer to the expected distribution, and most of the systematic channel width variation has been eliminated. Any remaining differences were most probably due to small differences in the dead-time of the scalers. Figures 22 and 23 show the distribution of total counts for a much more extensive series of tests using the improved circuit. No evidence of width variations appeared, so it may be concluded that the channel widths are uniform to within 1/4 per cent.

The eighteen scalers each have a display capacity of 9,999 counts plus an optional additional undisplayed decade scaler so that 99,999 counts can be collected in each.

---

<sup>3</sup>This circuit was also designed by F. Glass of the Instruments and Controls Division of Oak Ridge National Laboratory.

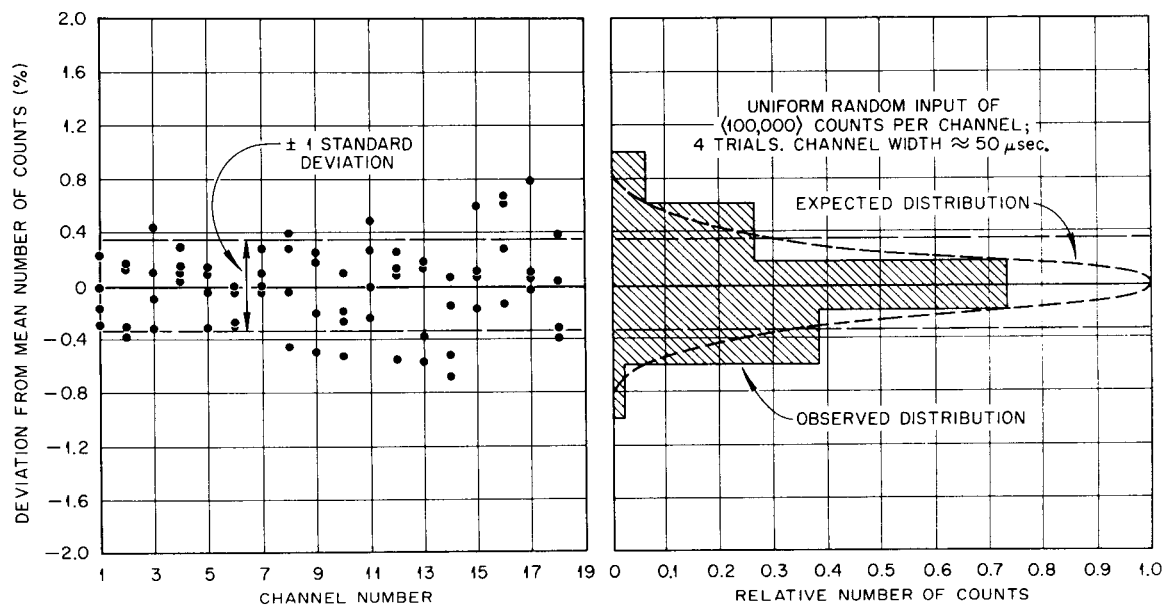


Figure 21. Distribution of number of counts collected in each channel, with 100,000 counts per channel on the average. Results for four runs are shown. On the right the summed distribution is also shown together with the normal distribution curve expected for counting statistics. Data taken with master gate circuit. (See text).

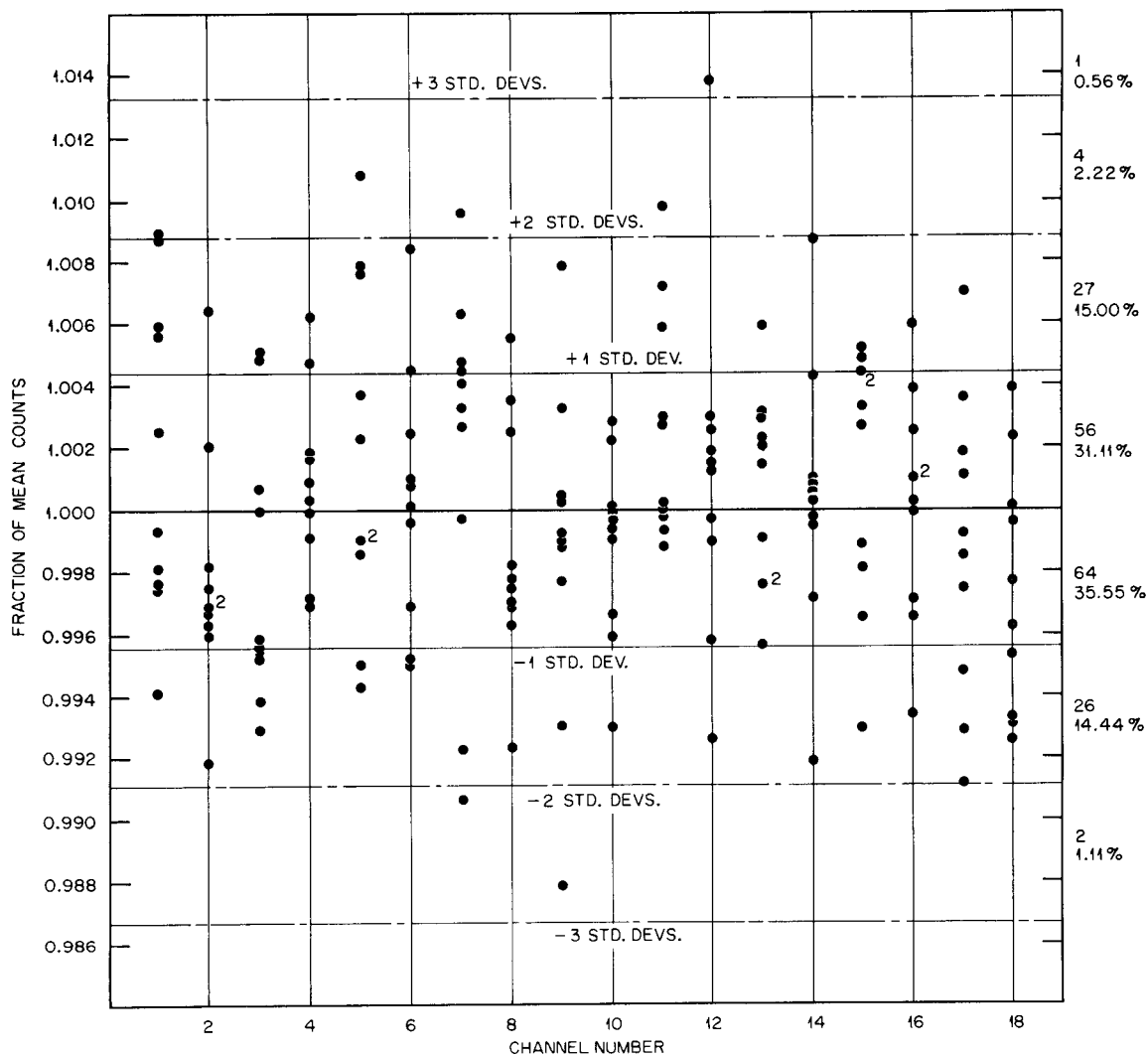


Figure 22. Observed distribution of counts in ten trials with uniform input to all eighteen channels. The average number of counts per channel each trial is 50,914. All runs normalized to the same mean number per channel. The location of the  $\pm 1$ , 2, and 3 standard deviation limits is shown, as well as the actual and per cent distribution in each band of one standard deviation. The theoretically expected per cent distribution is 34, 14, and 2 per cent.

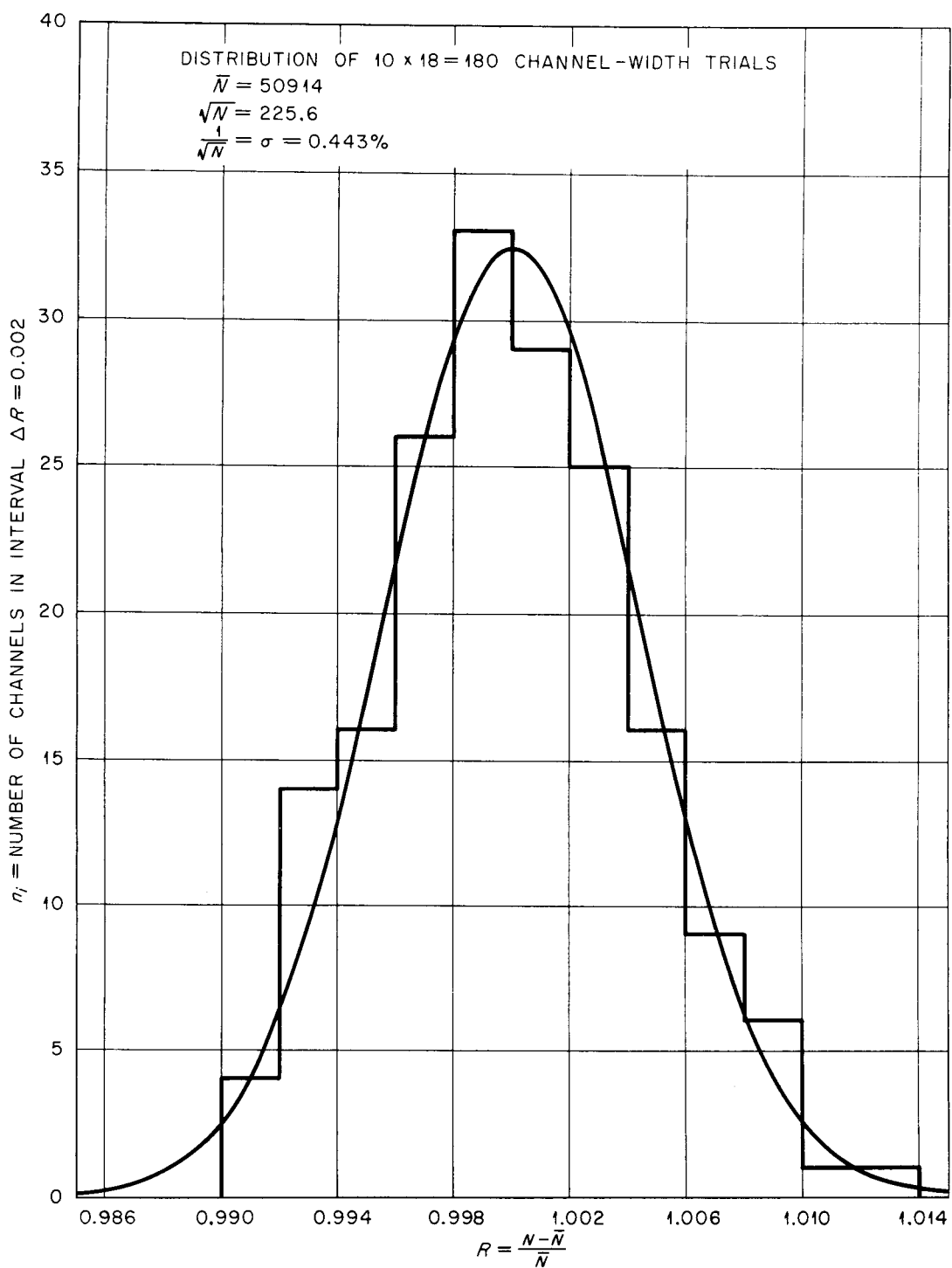


Figure 23. Histogram of observed count distribution and Gaussian expected if only counting statistics spread the distribution. The data are those shown in Figure 22.

The detector and amplifier system. Various detector types have been used in pulsed-neutron work. The first used were  $\text{BF}_3$ -filled ionization counters (Von Dardel, 1954). These have good discrimination against gamma rays and adequate sensitivity. However they are not very localized, and may therefore introduce significant counting delay errors caused by flight time of the neutrons into and in the tube (Pal, Bod, and Szatmary, 1965). Fission chambers have also been used. They are excellent for gamma discrimination but tend to have low efficiency, and may introduce errors due to thermalization of the fission neutrons. Their use has been mainly confined to multiplying systems (Meyer, 1965, and Weale et al., 1965). In the present work a  ${}^6\text{LiI(Tl)}$  crystal together with a RCA 6355 photomultiplier was used as detector. The advantages are very high efficiency and very localized detection.

Scintillation crystals tend to be sensitive to gamma rays, but by making the crystal thin (0.3 cm.) the gamma background was kept acceptably low. The  ${}^6\text{Li(I)}$  crystal functions by the reaction (Ashby and Catron, 1959)  ${}_0^1\text{n} + {}_3^6\text{Li} \rightarrow {}_2^4\alpha + {}_1^3\text{H} + 4.79 \text{ MeV}$ . The two charged particles give up their kinetic energy in the crystal producing fluorescence. The absorption cross section of  ${}^6\text{Li}$  is 945 b. which gives  $\Sigma_a(\text{LiI}) = 18.0 \text{ cm.}^{-1}$  of which  $17.2 \text{ cm.}^{-1}$  is due to  ${}^6\text{Li}$ . Thus 95.6 per cent of captures are in  ${}^6\text{Li}$  and in a 3 mm. thick crystal, assuming normal incidence, 99.4 per cent of the incident neutrons are captured. For oblique incidence the capture probability is even higher.

Most of the data collection was done with a 1.0-in.-diameter crystal. However, after a long period of use, the bonding between the aluminum cladding and the glass cover on the crystal failed due to the severe thermal stressing and cycling encountered in the present work, and the crystal was destroyed by cracking and absorption of moisture. Since higher counting rates were needed for the smallest ice cylinders the replacement crystal had a diameter of 1.75 in. The crystals were obtained from Harshaw Chemical Co. already canned in an aluminum container with one glass face. This glass face was optically bonded to the end-window of a 2-in. photomultiplier tube and then taped onto the tube with black plastic tape, both for mechanical support and for light-tightness. Using the single-channel analyzer of the amplifier (see below) a count-rate vs. pulse-height curve could be obtained for each crystal. This was done, at least roughly, at frequent intervals to find the best pulse-height discriminator level for gamma discrimination. The pulse height output of the crystal-photomultiplier combination was markedly temperature dependent, being a factor of 2.37 higher at  $-80^{\circ}\text{C}$ . than at  $-5^{\circ}\text{C}$ . Therefore the setting of the pulse-height discriminator needed to be adjusted at each temperature. Figure 24 shows two typical pulse-height spectra obtained with the 1-in. crystal. In both a large number of small pulses is seen, which is due to low-level noise and gamma rays. These rapidly decrease in number with increasing pulse-height; the dashed continuation below the peak is a rough estimate of the counting rate due to gamma rays, based on interpolation of the points above and below the peak. The distinct peak in each curve is the neutron response. The larger of

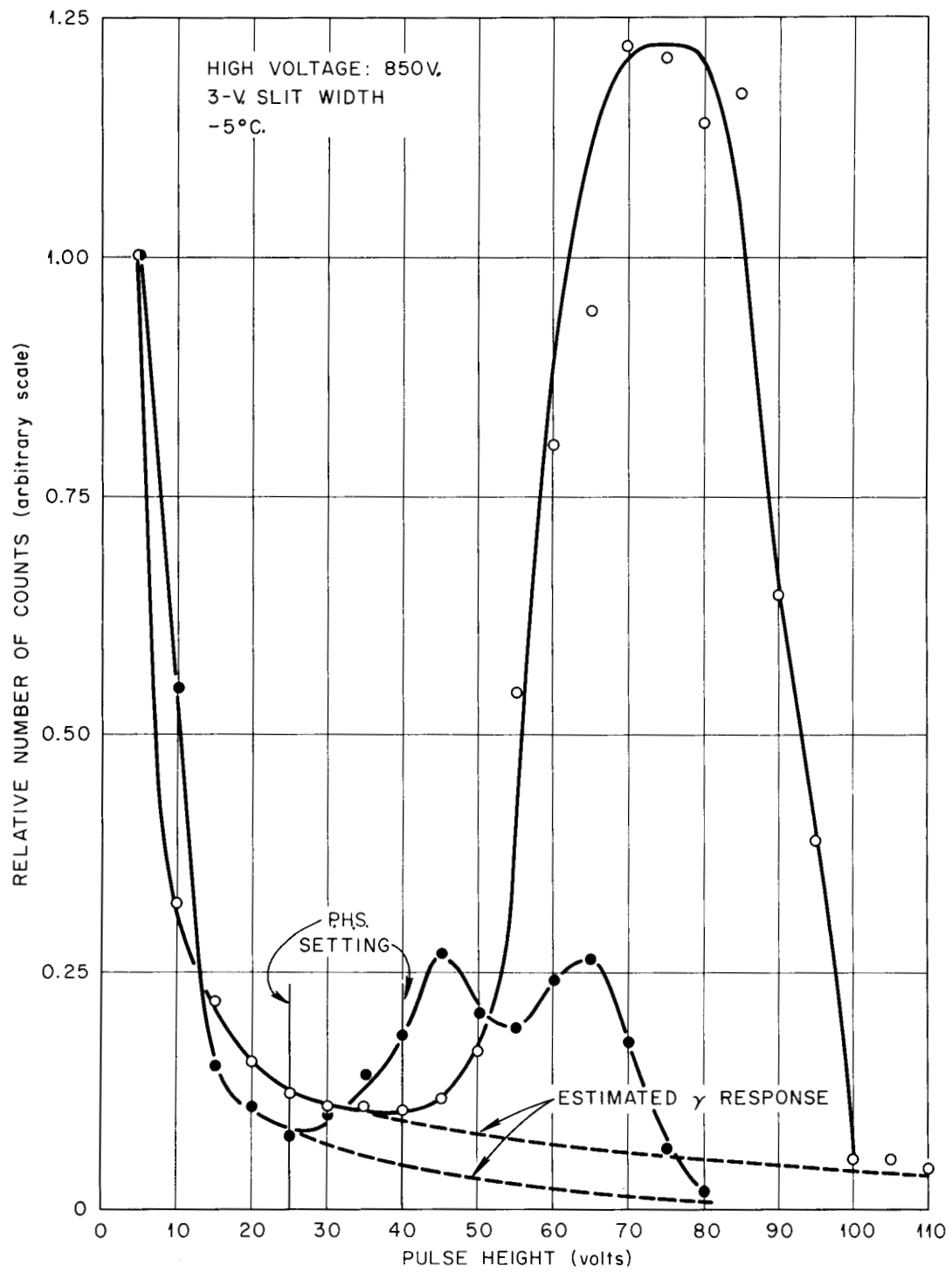


Figure 24. Pulse-height spectra obtained from 1-in.  ${}^6\text{LiI}$  crystal at  $-5^\circ\text{C}$ .

the neutron peaks in Figure 24 is seen to be somewhat irregular. This is attributed to cracking of the crystal, which caused the light output to vary from different regions of the crystal, so that the neutron response was actually split into several peaks with somewhat different positions. In the case of the one-inch crystal, by the time its use was discontinued, there were two very distinct peaks, shown in the lower curve of Figure 24. The relatively much higher number of small-amplitude pulses in the latter curve is due to the fact that this count was obtained using an Am-Be neutron source, which has a high production of low energy gamma rays. The two spectra are each normalized to unity at 5 volts pulse height. For both cases the setting of the pulse height selector chosen on the basis of these data is shown.

Figures 25 and 26 show the effect of the temperature and the voltage applied to the photomultiplier on the location of the peak of the neutron-caused pulse amplitude distribution in the pulse height spectrum. The effect of voltage on the pulse-height is quite large, so a stable power supply (Hamner Electronics, Inc. Model N 401) was used. This supply had an output voltage stable to within about 5 volts at 1000 V. over several months.

The pulses from the photomultiplier were amplified in a DD2 double-differentiating linear amplifier (Fairstein, 1962). Figure 27 reproduces oscilloscope traces showing the shape of the output pulses from the amplifier. The DD2 is equipped with a 'single channel analyzer' capable of discriminating those output pulses which lie in a 'window' whose width can be adjusted from 0 to 10 volts, and whose lower edge can

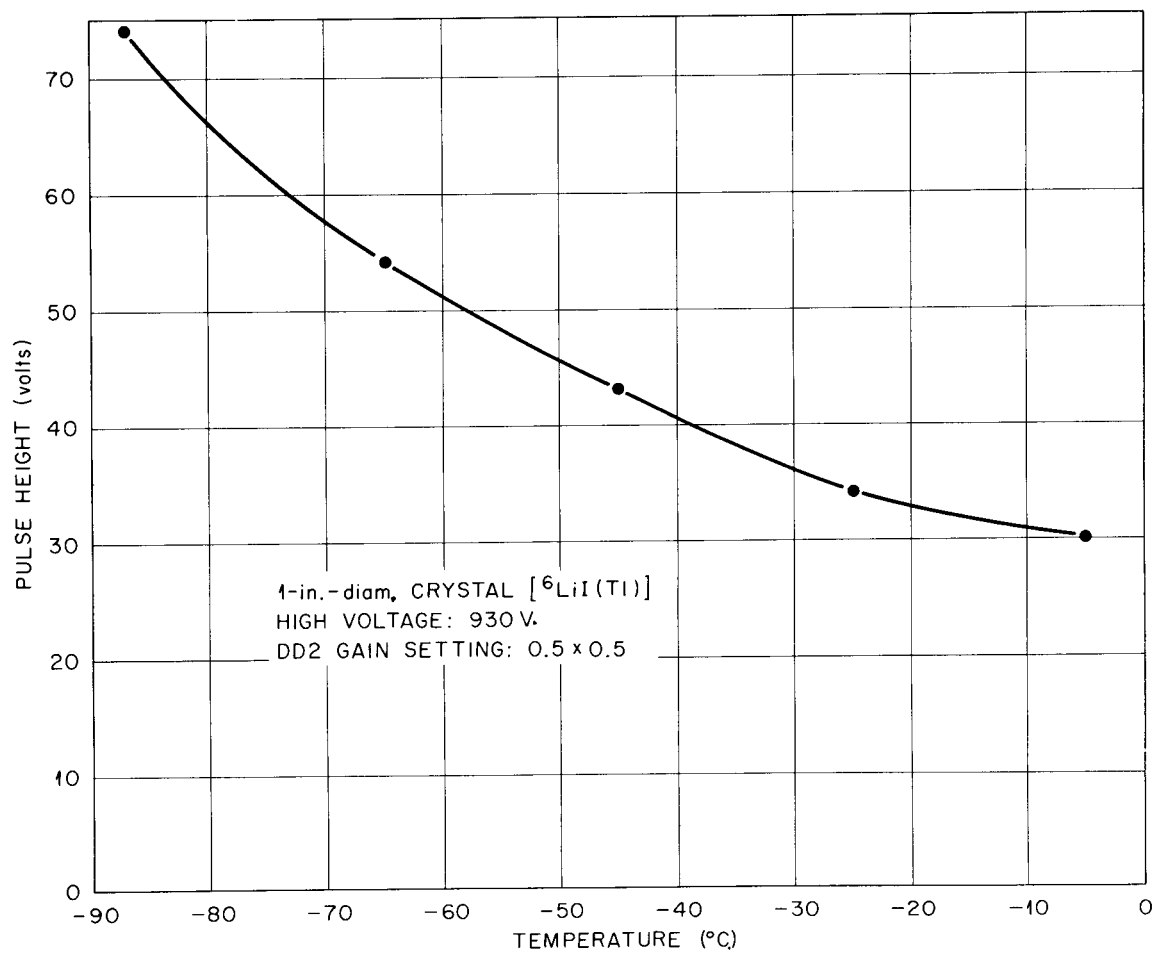


Figure 25. Location of neutron peak in pulse-height distribution as function of detector temperature.

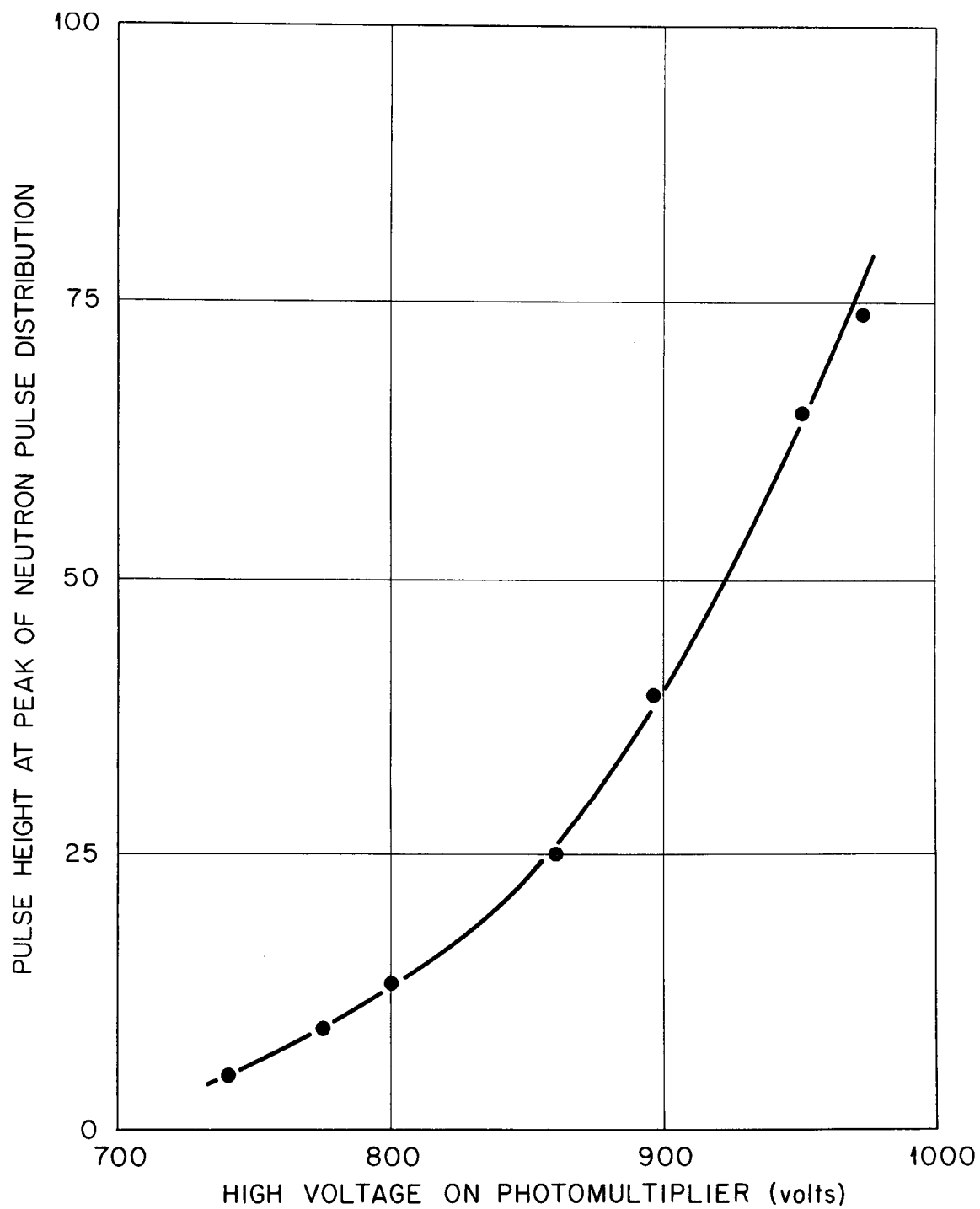


Figure 26. Location of neutron peak in pulse-height distribution as function of photomultiplier voltage.

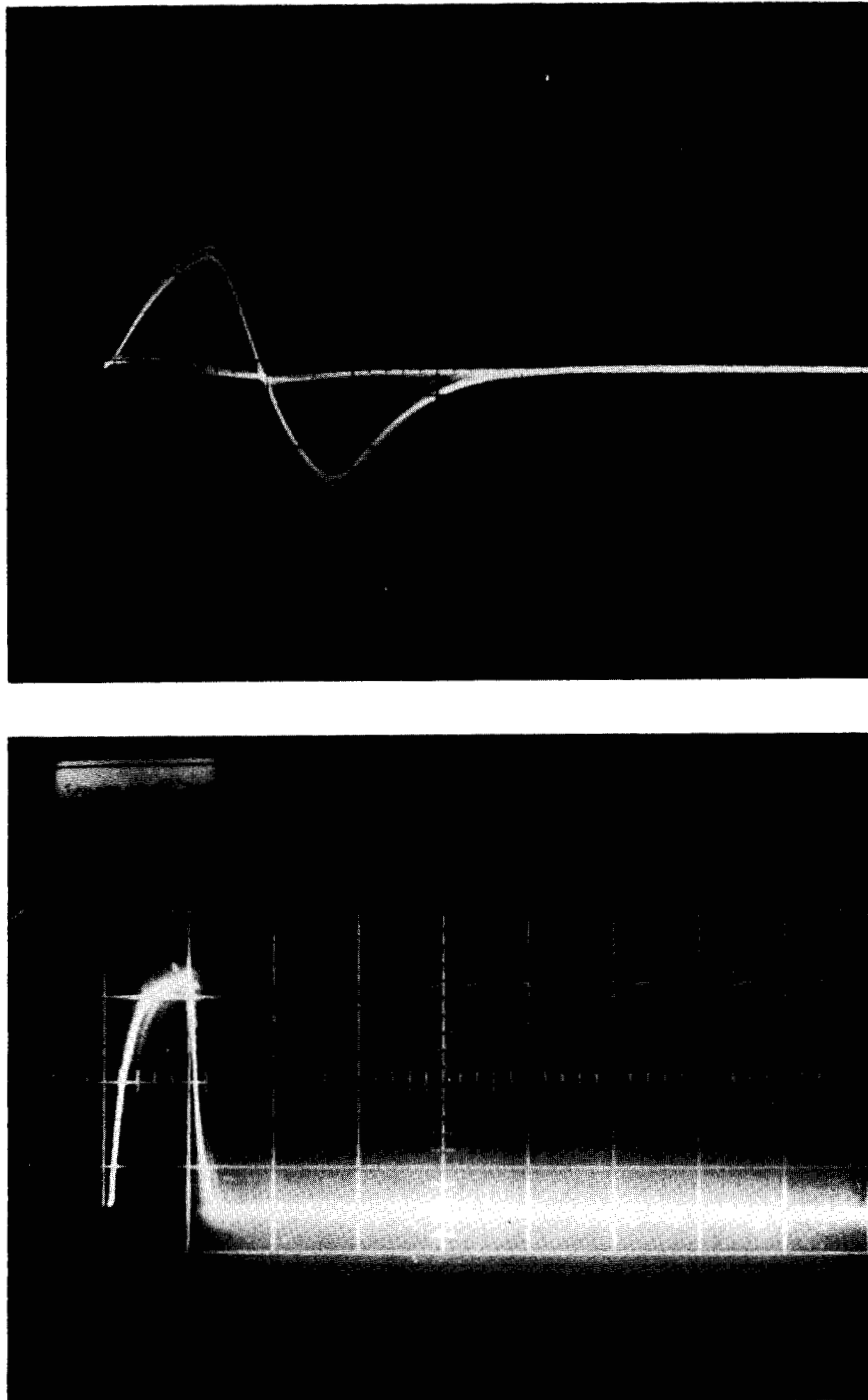


Figure 27. Oscilloscope traces. Upper trace shows the output of the DD2 amplifier. Lower trace shows the output of the PHS circuit of the DD2.

be set anywhere from 0 volts to 100 volts. For each such pulse a uniform-sized output pulse is emitted by the single-channel analyzer circuit. An alternative method of using the DD-2 discriminator circuit, the so-called integral mode, dispenses with the window, and emits a constant pulse for each input pulse larger than the magnitude  $H$  described above. The DD-2 was used in this mode to collect all the experimental decay information in the present work.

In order to establish the maximum allowable count-rate in the analyzer it was necessary to know the total dead-time losses from all sources that would occur due to pulses arriving too soon after a previous pulse to be detected. The dead-time was therefore measured in one of the 18 channels, by using two neutron sources separately and together, and measuring the count-rate. For this experiment the analyzer switching was disabled so that all counts were gated into scaler No. 3. Appendix A gives the derivation of the dead-time equation and the calculation of the result. The result was  $(6.03 \pm 3.28) \mu\text{sec}$ . This dictated the maximum allowable count rate in channel 1, the fastest-counting scaler. Since the actual counting rate in each channel is  $(18 + N)$  times as large as the observed mean counting rate, the true counting rate must be no more than 2,000 cts./sec. to keep the dead-time loss in the first channel to less than 2 per cent (Appendix A). For  $N = 10$  (it varied from 8 to 12 in the experiments), one obtains a maximum mean counting rate of 100,000 counts in 1408 sec. or 23.5 minutes. A working rule was therefore adopted by which the count rate was adjusted so that a 'full count, i.e., 100,000 counts in channel 1, was collected in not less than half an hour.

Secondary pulse deflection system. It was observed early in the use of the accelerator that during the times when the beam was nominally cut off by the ion-source deflection voltage, a certain amount of beam would nevertheless be accelerated to the target and produce neutrons. Such a background current is serious even with an off/on beam ratio of only of the order of  $1.0 \times 10^{-3}$  to  $1.0 \times 10^{-4}$  (these were the best values attainable using the primary deflector only) because the background current is 20 to 50 times more effective in producing counts than the pulse current, due to the fact that the neutron density is not saturated during the beam-on time and decays further by at least a factor of 10 before counting is even begun. The off-current neutrons, on the other hand, are in equilibrium with their source intensity and suffer no such attenuation.

Three sources of beam background were recognized. One is the true background current consisting of ions which are scattered by the residual gas in the system, or by solid surfaces in the lens area, so that they are deflected into the acceptance cone of the accelerator aperture, and of atoms of residual gas ionized by electrons accelerated back up the potential gradient. Another source, which at times consisted of large portions of the deflected beam, was due to the discharge of the deflection plate potential by excessive impinging beam current. Thus, by certain combinations of settings of the control voltages the deflected ions could be extracted in a partly focussed beam despite the action of the deflection system.

A third source of background was due to occasional failure of the pulse transmission system due to noise pick-up. To eliminate such background sources a secondary deflection system was added to deflect the accelerated beam in the drift tube. This system operated in synchronism with the primary pulser, controlled by the same signal which is transmitted by the radar transmitter to the ion-source. Figure 28 shows an end view of the deflector section with the deflection plates, which are 15 inches long. The electronic equipment was designed by R. J. Scroggs of the ORNL Instrumentation and Controls Division.

By making use of the secondary deflector system the relative background dropped by factors ranging from 5 to 20. Figure 29 shows two runs, made with the same ice cylinder, under the same conditions, except that in one case the secondary deflector was not used.

All the large-buckling cylinders (cylinders 6, 7, 8, ... 12) were measured using the secondary deflector system.

The test chamber. The experiments made use of a two-stage refrigeration unit with integral test-chamber which was manufactured by Coolley, Inc. of Cincinnati, Ohio, and rated to  $-100^{\circ}\text{C}$ . The test volume is 24 in. by 24 in. by 30 in. in size, and the walls are 5 in. thick. An internal fan and baffling plate serve to force air over the cooling coil, and circulate the air in the chamber.

The inner walls of the refrigerated chamber were lined with Boral (a dispersion of boron in aluminum) 0.25 in. thick to minimize the effects

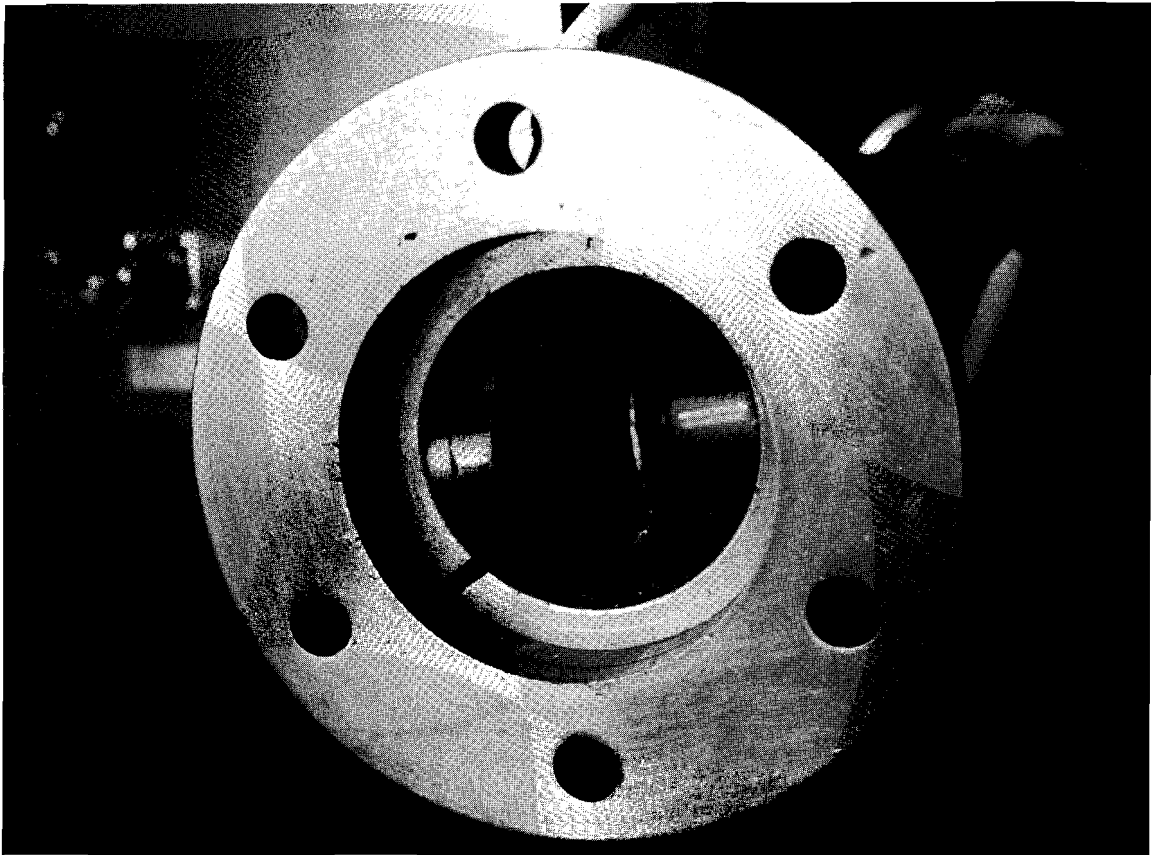


Figure 28. Secondary detector section with view of deflection plates.

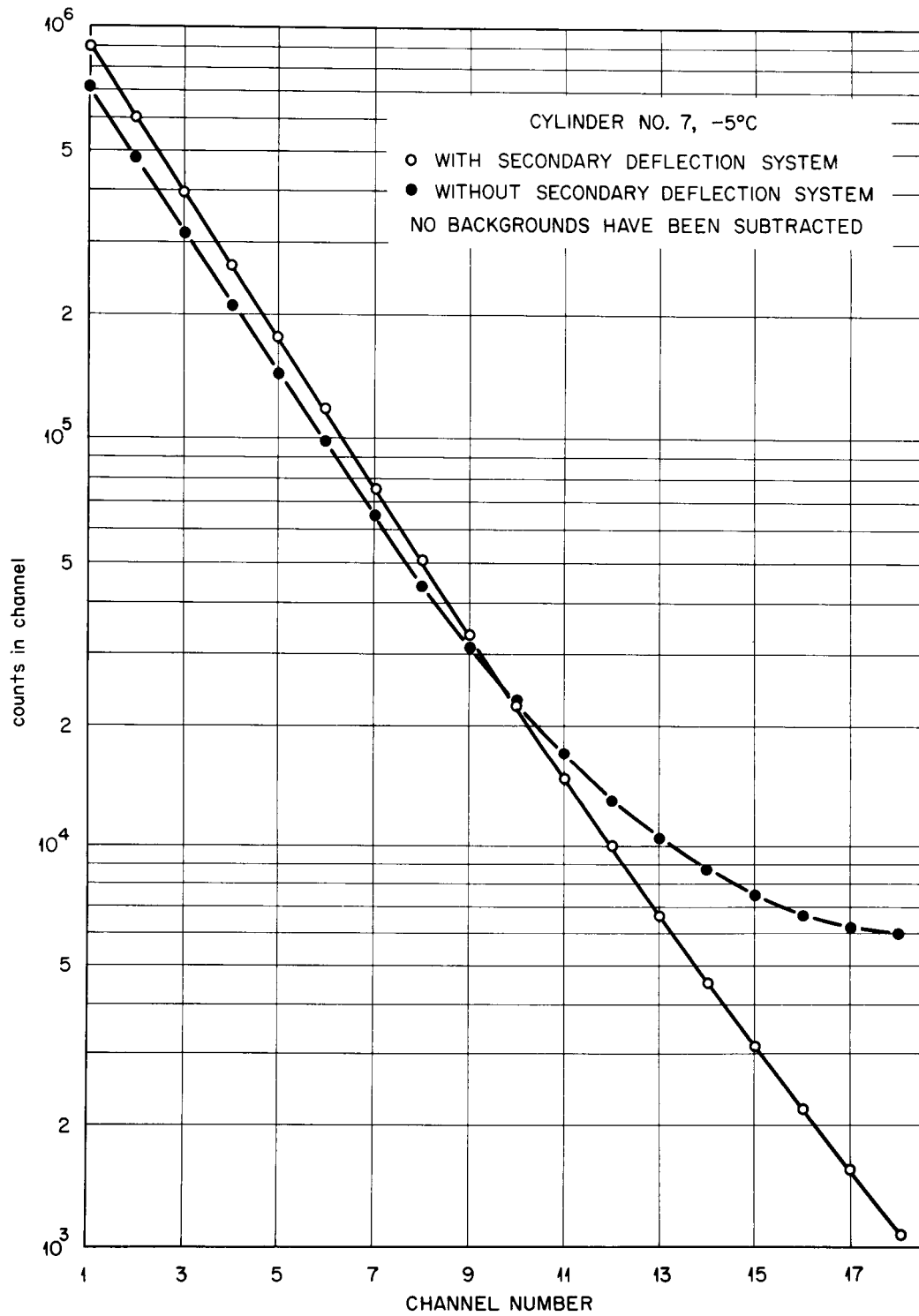


Figure 29. Effect of post-acceleration deflector on observed neutron decay in ice cylinder Number 7 at  $-5^{\circ}\text{C}$ .

of the wall. To determine the neutron reflection effect of the refrigerator walls pulsed-neutron measurements were performed on a plastic cylinder both inside and outside the refrigerator. Figure 30 shows the result. No discernible effect due to wall-scattering was noted. However, later analysis on cylinders with more rapid decay showed slight effects that may be attributable to wall scattering, but are masked in the test shown by being too close to the main decay period. The experiment in the refrigerator yielded a measured decay constant of  $(1.337 \pm 0.003) \times 10^4 \text{ sec.}^{-1}$ , and the test outside gave  $(1.334 \pm 0.005) \times 10^4 \text{ sec.}$  The temperature inside the refrigerator was  $20.5^\circ\text{C.}$ , and outside it was  $20.0^\circ\text{C.}$  Correcting the result inside for the temperature difference (assuming  $v\Sigma_a$  to be constant, and  $(vD)$  to be proportional to the temperature) gave an adjusted result inside the refrigerator of  $(1.330 \pm .006) \times 10^4 \text{ sec.}^{-1}$  which agrees very well with the result outside.

The small effect, later attributed to wall-scattering, apparently gives rise to a period of the order of  $1.0 \times 10^4$  to  $1.8 \times 10^4 \text{ sec.}^{-1}$ ; its effect was not observable in the test described here.

The temperature in the refrigerator was maintained at the desired level by means of a Copper-Constantan thermocouple exposed to the air in the test chamber in the vicinity of the ice cylinder. The signal from this couple was recorded by a Brown strip chart recorder which also served as control device. The motion of the pen carriage on signal from the balancing potentiometer actuated a relay which turned the second-stage refrigeration unit on and off as required.

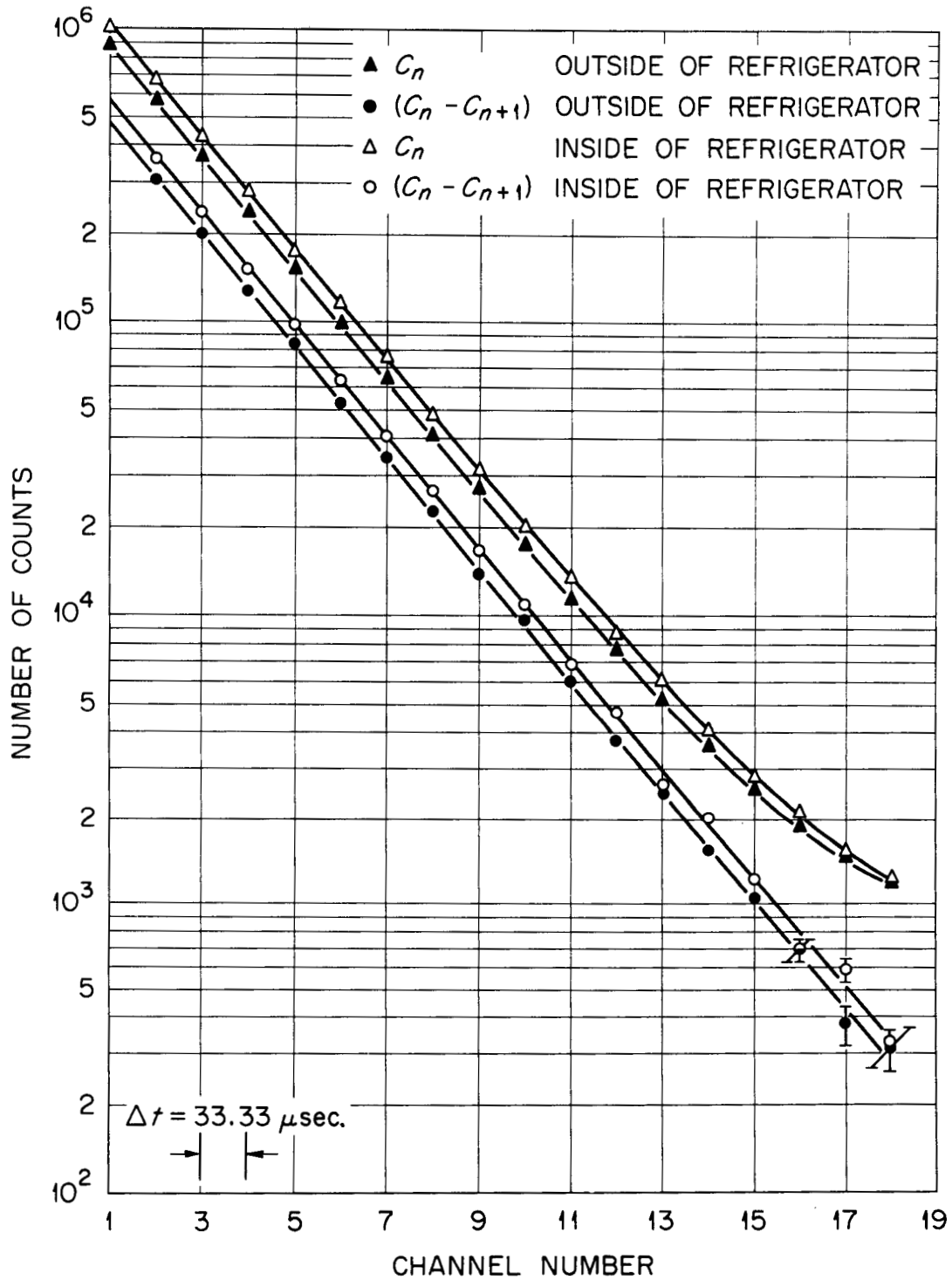


Figure 30. Observed decay of neutrons in a Teflon cylinder inside and outside the refrigerator.

The thermocouple and chart recorder were calibrated against precision thermometers on several occasions, and found not to have drifted by more than  $1.0^{\circ}\text{C}$ . over several months in the worst case. In order to be certain that the temperature in the ice cylinders was uniform throughout and in equilibrium with the air temperature in the test chamber, an experiment was performed using the largest ice cylinder (cylinder 1). A hole was drilled into the cylinder to its central point, and a second thermocouple was frozen into this location by adding water to fill the drill hole after insertion of the thermocouple. The signal of this thermocouple was recorded on a separate Brown recorder. Figure 31 shows the result obtained in a full-range test, i.e., cooling rapidly from  $-7^{\circ}\text{C}$ . to  $87^{\circ}\text{C}$ . The air temperature required 220 minutes to change, and the temperature in the center of the ice cylinder attained a temperature within  $0.5^{\circ}\text{C}$ . of the average air temperature in 420 minutes (7 hours). In the data-taking process every temperature change in an ice cylinder was made overnight, i.e., at least 10 hours before the measurement was begun. Since the temperature accommodation in the smaller cylinders would be more rapid than in the largest, it was concluded from the test that, when the fan was working, all measurements were carried out at the average temperature indicated on the air-temperature thermocouple recorder.

Since the refrigerator could not reliably attain temperatures lower than  $-90^{\circ}\text{C}$ . the temperature limit for this work was fixed at  $-85^{\circ}\text{C}$ ., which could always be reached with reasonable dispatch and maintained even in high ambient temperatures.

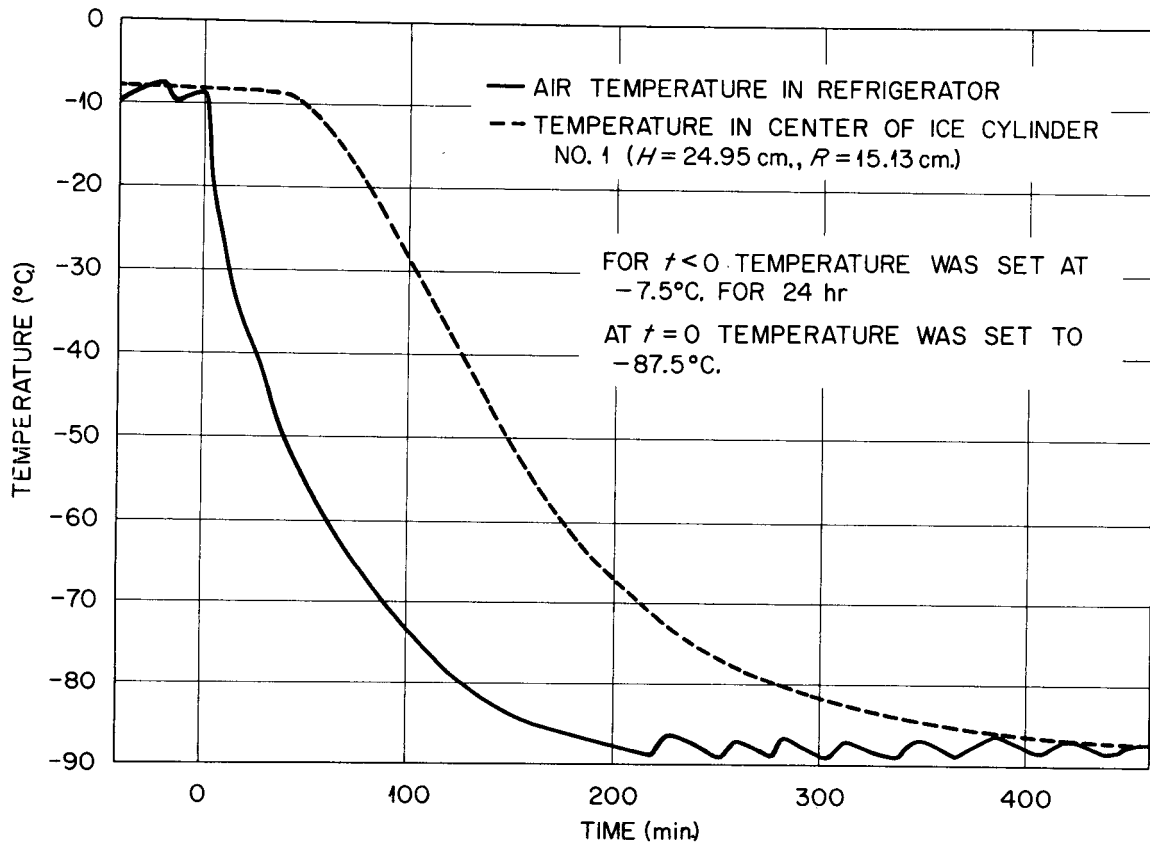


Figure 31. Temperature versus time as recorded by thermocouples in air of the test chamber and in the center of ice cylinder Number 1. At  $t = 0$  the temperature demand point was changed from  $-7^{\circ}$  to  $-87^{\circ}\text{C}$ .

The walls of the refrigerated chamber are pierced by four penetrations. Two of these are at the midpoints of the two facing side walls, and are 4 in. inside diameter each. A third, of the same dimensions, is in the center of the roof, and a much smaller penetration, intended for thermometry, was located in a side face near the bottom. The top hole was used to introduce the thermocouple and the electrical leads to the detector; one side hole was used for the beam tube, and the others were plugged. The excess area of the holes being used was plugged with wadding of thin plastic sheet, which showed good temperature insulating properties, and was not susceptible to water-logging.

Inside the test chamber the ice cylinder was placed on an aluminum plate covered with boral, which was supported by three adjustable-height 'Cenco Lab-Jacks.' These were adjusted to bring the symmetry plane of the ice cylinders to the midplane of the refrigerator, where the beam target was also located. The detector was positioned with a clamp-stand inside the volume. Figure 32 shows a typical experimental setup inside the refrigerator.

The target. With this type of accelerator the choice of useful target material is limited to either deuterium or tritium. The targets used in this work were prepared by B. J. Massey of the ORNL Isotopes Division (Massey, 1957) using silver and tungsten as backing materials. The latter has the advantage of much higher yields. Performance tests were made to determine the yields of neutrons from both types of targets. The results of these calibrations are included in Appendix B.

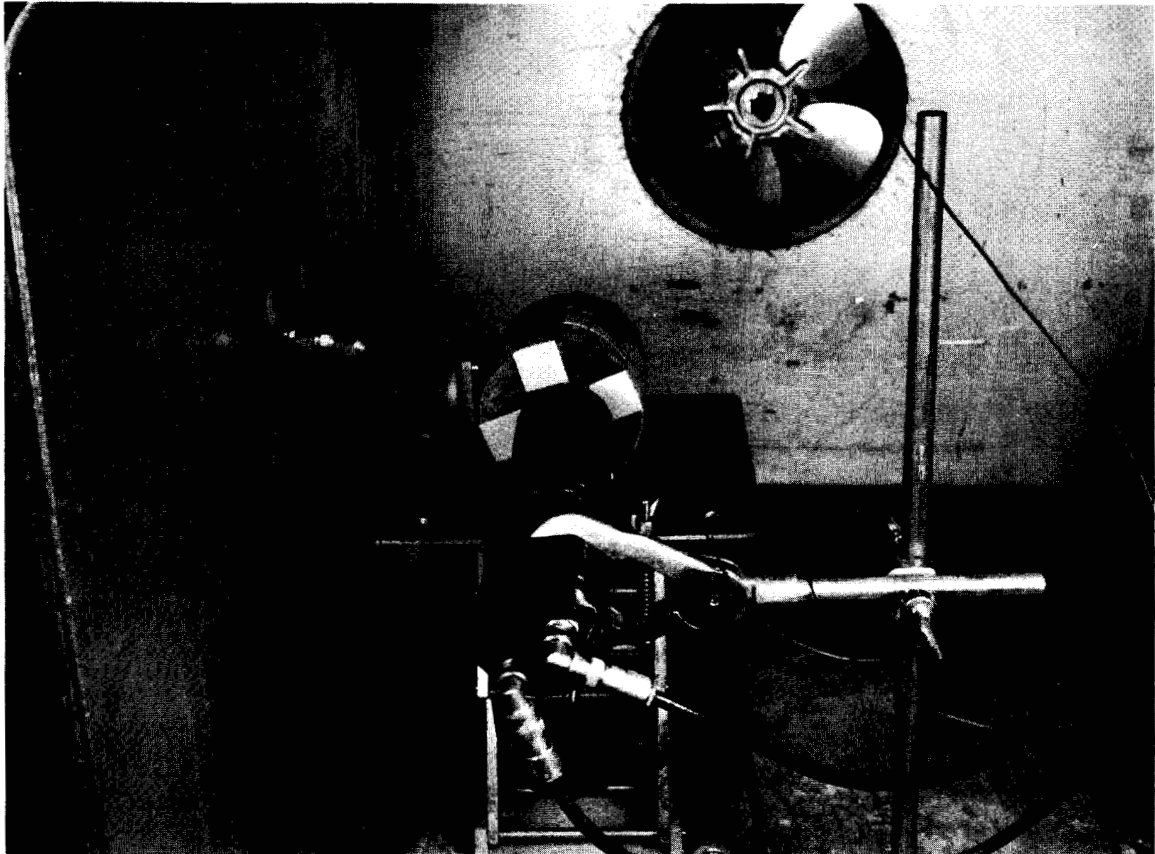
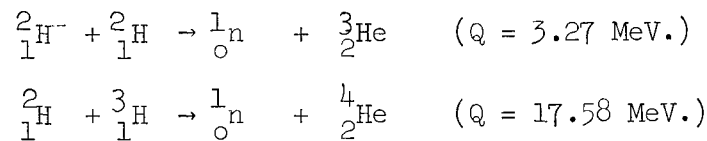


Figure 32. Interior of refrigerated test chamber with ice cylinder and detector in place.

With a tritium target containing 500  $\mu$ grams of  $^3\text{H}$ , using 300,000 eV. deuterons, the yield was about  $2.5 \times 10^7$  neutrons per second per  $\mu\text{A}$ . of beam current. With a similar deuterium target the yield was about  $2 \times 10^5$  neutrons per second per  $\mu\text{A}$ . of beam current. The reactions producing the neutrons in the two cases are (Ashby and Catron, 1959):



The reactions are isotropic in the center-of-mass system, but are somewhat forward peaked in the laboratory due to the deuteron kinetic energy. Non-relativistic calculations show that with the D-T reaction the forward fraction of neutrons is 0.524 for 0.1 MeV. deuterons and 0.541 for 0.3 MeV. deuterons. With the D-D reaction the corresponding fractions are 0.643 and 0.742.

In the course of the experiments the average beam current varied from about 10  $\mu\text{A}$ . to 150  $\mu\text{A}$ . At  $3 \times 10^5\text{V}$ . this represents a power dissipation in the target of 3 to 45 watt, on a target area of the order of 1  $\text{cm}^2$ .

To prevent overheating the target was provided with a water cooling system shown in Figure 33. Water circulating behind the foil kept the target cool enough at all operating power levels.

Due to the much higher neutron yield, the initial experiments utilized a tritium target. However, with such a target an objectionably large

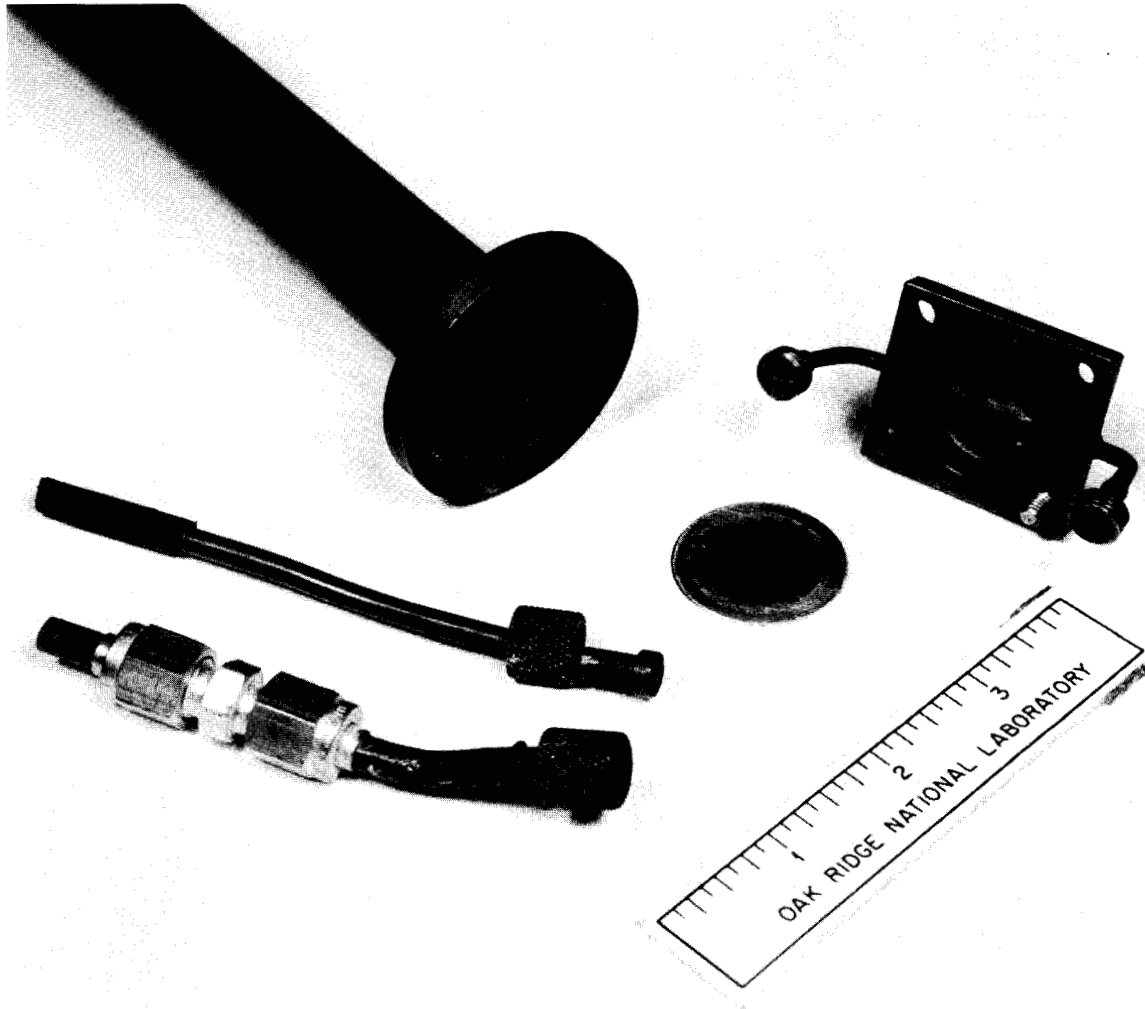


Figure 33. Target disassembled to show the water cooling provisions.

background was observed, which could be attributed neither to background beam effects nor to electronic noise sources.

A measurement of the time behavior of the background over relatively long time periods was made since it appeared to persist for several seconds after a given run was terminated. A manual set-up was devised employing two scalars both connected to the DD2 PHS output. A toggle switching arrangement was devised to gate one scalar open and the other one shut alternately. Then, after operating the accelerator for about one minute, successive 10-sec. counts were taken in alternate scalars until no further decay of the activity was observed. Figure 34 shows the result obtained from summing the data of 8 such runs. The measured decay period is  $(0.0885 \pm 0.0062) \text{ sec.}^{-1}$ , which is equivalent to a half-life of  $(7.83 \pm 0.55) \text{ sec.}$  The mechanism probably responsible for this activity is as follows: 14 MeV. neutrons react with the oxygen of the water to form  $^{16}\text{N}$  ( $^1_0\text{n} + ^{16}_8\text{O} \rightarrow ^1_1\text{p} + ^{16}_7\text{N}$ ) (Ashby and Catron, 1959).  $^{16}\text{N}$  decays with a 7.32 sec. half-life (which agrees, within the error, with the observed half-life). This reaction has a threshold at a neutron energy of 10.24 MeV., and a resonance peak in the cross section of 84 mb. at 11.8 MeV. (Stehn et al., 1964, p. 8-16-5; De Juren, Stooksberry, and Wallis, 1962). The Q of the reaction is  $-(9.603 \pm 0.013) \text{ MeV.}$  (Ashby and Catron, 1959). The decay of the  $^{16}\text{N}$  with beta and gamma emission can cause counts in two ways. One is by direct gamma pile-up in the crystal and the other is by producing neutrons by the reaction  $\gamma + ^2_1\text{H} \rightarrow ^1_1\text{H} + ^1_0\text{n}$  with the natural deuterium component of the water. This reaction has a Q value of -2.23 MeV.

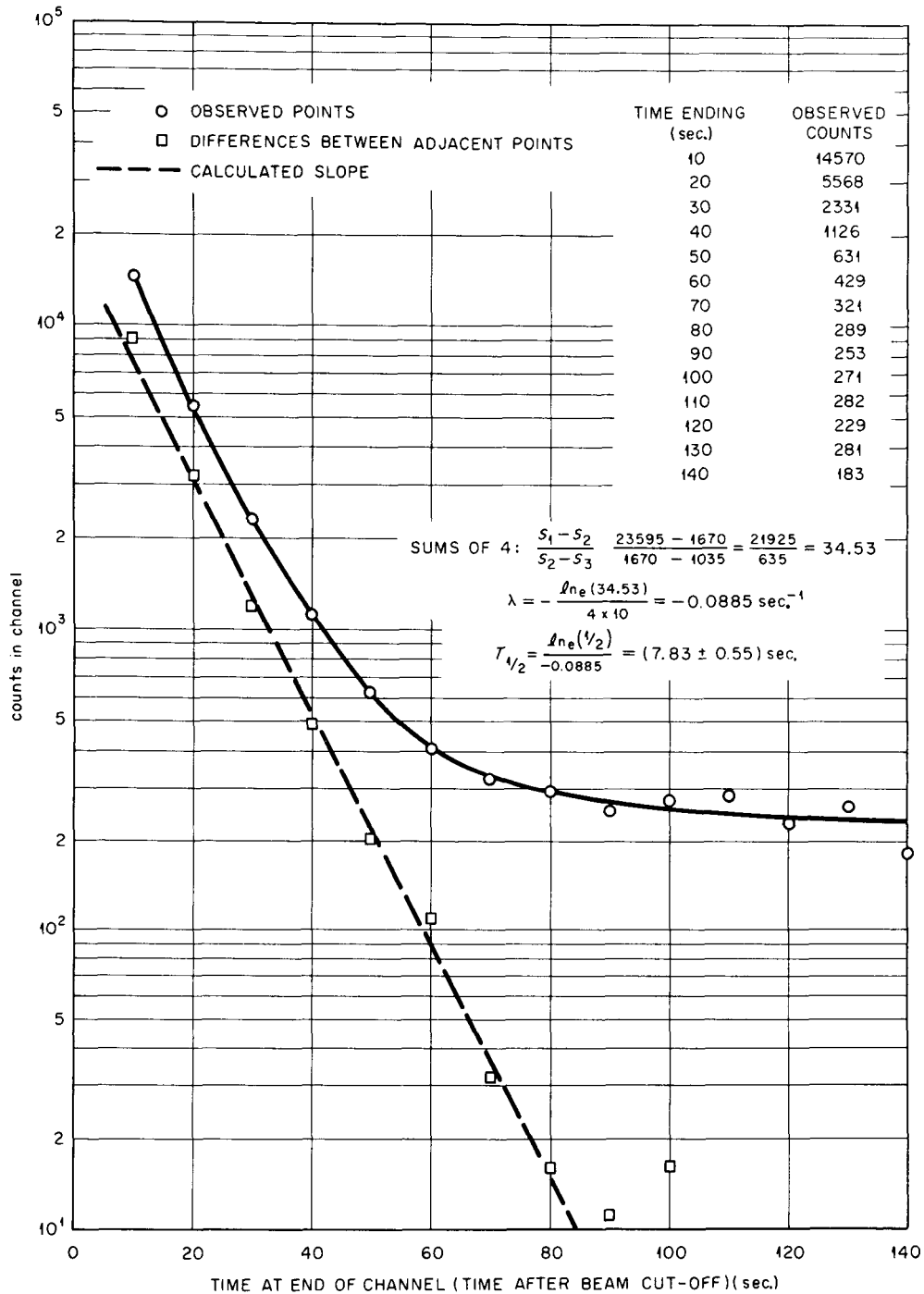


Figure 34. Measured long-lived decay observed with source of D-T neutrons in ice. The Cornell method (Cornell, 1956) was used to obtain the decay frequency shown. It corresponds to a half-life  $T_{1/2} = 7.83 \pm 0.55$  sec.

(Ashby and Catron, 1959) so it is quite accessible to the 6.13 MeV. gammas from the  $N^{16}$  decay. In order to decide which mechanism was dominant in producing this background effect the following rough calculation of the  $(\gamma, n)$  neutron yield was made. It is assumed that neutrons of 14 MeV. will be removed below the threshold for  $(n, p)$  reaction by scattering in hydrogen,  $(n, \alpha)$  reaction in oxygen,  $(n, \gamma)$  reaction in oxygen, or the  $(n, p)$  reaction. Elastic scattering in oxygen is neglected since it will not change the neutron energy much. The cross sections are as follows at 14 MeV.:

- (1) hydrogen scattering, 720 mb. per atom or 1440 mb. per  $H_2O$  molecule (Bratenahl, Peterson, and Stohring, 1958)
- (2)  $(n, \gamma)$  in oxygen, 250 mb. (Stehn et al., 1964)
- (3)  $(n, \alpha)$  in oxygen, 300 mb. (Bormann et al., 1963)
- (4)  $(n, p)$  in oxygen, 45 mb. (DeJuren, Stooksberry, and Wallis, 1962)

Thus 2.2 per cent of the neutrons make a first collision to produce the  $n, p$  reaction. Assuming a thick water medium and a neutron source intensity of  $5 \times 10^8$  neutrons per second, the production rate of  $N^{16}$  is  $1 \times 10^7$  per second. The decay rate is of the same magnitude. About 74 per cent of the decays are accompanied by gamma emission with gammas of 6.06 MeV., and 7.12 MeV. (Ajzenberg-Selove and Lauritsen, 1959). For photons of such energy the deuteron photo-disintegration cross section is about 1.5 mb. (Blatt and Weisskopf, 1952). The abundance of deuterium in water is 0.015 per cent (Sullivan, 1956). Assuming that the gammas traverse a water layer 10 cm. thick, the number of neutrons produced is of

the order of 1.5 per second. Since the observed background was much higher, it must be due mainly to gamma detection by the  ${}^6\text{LiI}$  detector.

With this mechanism in mind, it was attempted to eliminate the background by using D-D neutrons, since the energy of these neutrons (about 2.5 MeV.) is below the threshold energy for the (n,p) reaction. Indeed, when the experiment was repeated with a deuterium target the long-lived decay was completely eliminated, and the observed background dropped by a factor of about 20 in the test decay investigated.

As a result of these experiments all measurements in ice in this work were carried out with D-D neutrons, even though the available intensity was thereby seriously diminished.

Satisfactory deuterium targets can be made by merely placing a metal foil (silver is a useful material due to its high thermal conductivity) at the target position, and irradiating it with the deuteron beam. The deuterons driven into the foil by the beam then act as target nuclei for impinging deuterons. However, in the present work pre-deposited targets supplied by ORNL Isotopes Division were used (Massey, 1957). In both cases the yield, after some hundreds of hours of operation will be the same, but initially the prepared targets have an advantage of about a factor of three (after operating each about ten hours).

An undesirable corollary of this drive-on target effect is that, at the locations where the accelerated deflected beam strikes the walls of the vacuum system, or baffles placed for the purpose, a target is built up, which produces neutrons during the off-time. In the present

work this problem was not overly severe, since the ion-source deflector prevented most of the deuterons produced during the off-phase from being accelerated.

## II. ICE CYLINDER PREPARATION

The geometries suitable for use in a pulsed-neutron search for diffusion parameter values must be (1) of simple shape to permit ready calculation of geometric bucklings, and (2) of compact shape, both to minimize the volume of material required for a given buckling, and to maximize the difference between the decay constant of the fundamental mode and those of higher modes. The ideal shape from these points of view would be a sphere. However, the practical difficulties in producing accurately shaped spheres are sufficiently great to make this a very unattractive proposition. Cylindrical and near-cubical parallelepipedal shapes are next best. The latter are most frequently used where solid moderators are involved because assemblies of various bucklings can then be easily put together using smaller building blocks of parallelepipedal shape. In the present instance, however, where each test body had to be produced as a separate entity the cylindrical shape appeared most attractive. First, because the volume-to-buckling ratio is somewhat more advantageous, and second, because the cylindrical wall is less likely to suffer deformation due to internal pressures generated during freezing than would be the case with thin plane container walls in a parallelepipedal vessel. Also, the ease of producing accurately shaped cylinders on a lathe argued for this choice.

Early trials. For the purposes of this experiment it was necessary that the ice cylinders be accurately dimensioned and of uniform density. The dimensional accuracy is needed to permit accurate buckling calculations, and the density must be uniform since the diffusion parameters are sensitive to it in various degrees. The term  $v\Sigma_a$  is directly proportional to the density; the term  $(vD)$  is inversely proportional to the density and  $C$  is proportional to the inverse cube of the density. Therefore, to be able to compare results with results in water the density needs to be accurately known, and to obtain accurate parameters the density must be uniform for all cylinders.

It was found that simply placing a container of water in the test chamber was unsatisfactory because it produced ice with non-uniform density and with an irregular top surface. The non-uniformity in density was due to voids formed in the ice because of the evolution of gases dissolved in the water. Since the solubility drops as freezing takes place these gases form bubbles which are trapped in the forming ice. In order to determine the extent of the density differences the apparatus described in Appendix D was set up. The results of density measurements on ice samples are also given there. It was found that ice cylinders produced by simply freezing exhibited density inhomogeneities of the order of 10 per cent. The shape irregularities were due to expansion of the water during freezing, which caused stress cracking and surface distortions.

After extensive trials two procedures were adopted which proved satisfactory. One was used for the large cylinders, and the other for the small ones. These will now be briefly described.

Large cylinders. For each of the four large cylinder diameters a plug was constructed with a diameter 0.5 cm. smaller than the diameter of the corresponding ice cylinder. A diagram of one of these plugs is shown in Figure 35. The plugs consisted of a hollow brass cylinder about four inches high. Inside each plug was a water reservoir communicating with the water volume of the cylinder through a small tube which extended down through the center of the plug about three inches. A spiral of copper tubing was soldered to the bottom plate of the plug. This spiral was connected to the water line to permit circulation of water through the spiral during the freezing process. Each plug was fitted with three adjustable supports by which it could be levelled at the desired height in the aluminum cylinder in which the ice was to be frozen.

The water was first de-gassed by boiling for two to three hours under a layer of paraffin about two inches thick. This paraffin served both as air seal filling the space between plug and cylinder wall, and as heat barrier, to prevent excessive heat transfer from the bottom of the plug to the water. In the absence of such a layer freezing would not occur at all even at  $-50^{\circ}\text{C}$ . The plug was then lowered into the cylinder far enough to force paraffin into the crack between the wall and the plug. This caused some water to rise into the expansion volume. This water was covered with a layer of mineral oil to prevent reabsorption

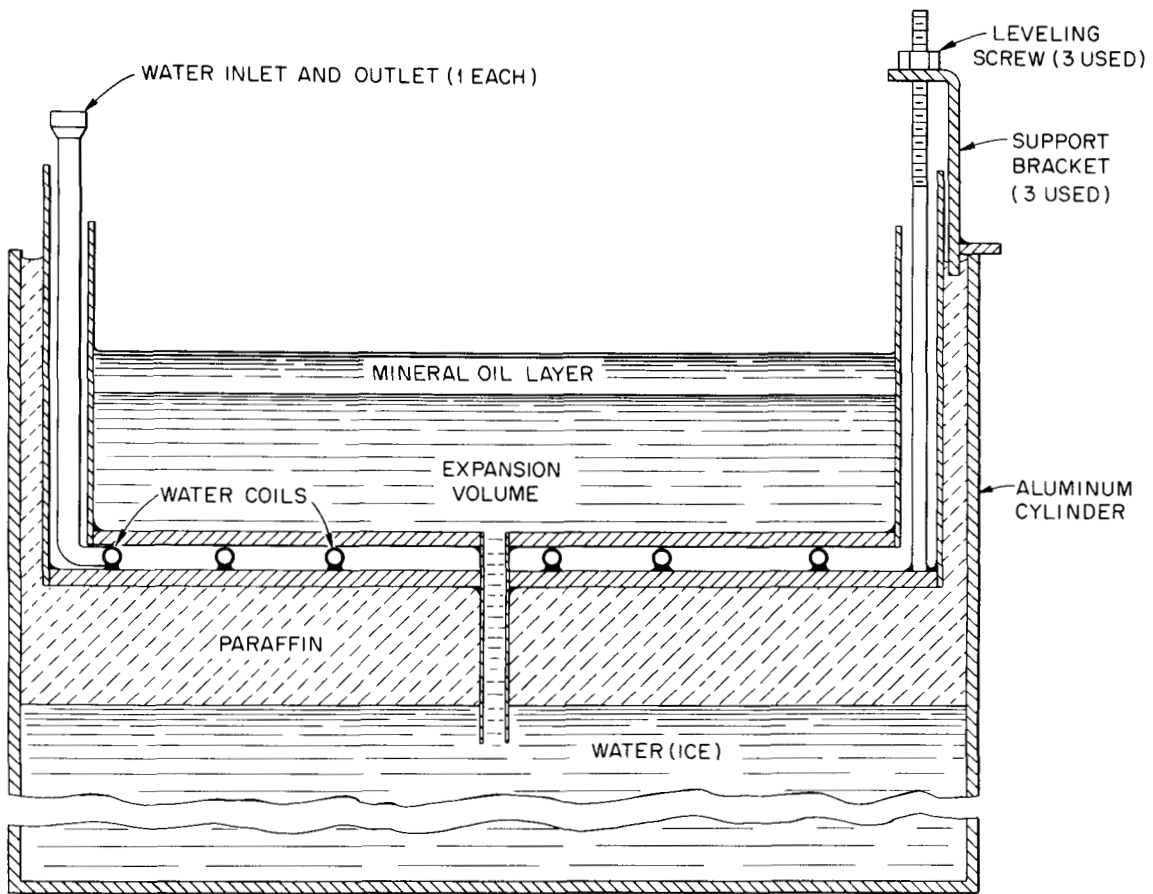


Figure 35. Plug made for freezing large ice cylinders. The plug is shown in place in the aluminum water container.

of air. The assembly was then placed in the freezer and frozen until solid. The plug was then removed, the paraffin taken off, and the small hole left by the reservoir tube filled with distilled water and refrozen. Any other small surface irregularities were also removed by adding a small layer of water to the top surface and refreezing. The surface was then covered with aluminum foil to prevent sublimation of the ice, and 0.03-in.-thick cadmium sheet was placed all around the cylinder. A hole was left in the cadmium at the center of the flat surface at the top to permit neutrons to enter the detector.

Small cylinders. Since it did not appear reasonable to make plugs as described for the small cylinders a different process was developed, which used vacuum, rather than boiling to remove dissolved gases. A diagram of the apparatus used is shown in Figure 36. These cylinders were formed in hollow, open aluminum cylinders with initial length about 10 cm. greater than the final height. The aluminum containers used for the small ice cylinders were turned on a lathe to be accurately round and thin-walled. The bottom was closed by placing the cylinder on a glass plate and pressing Apiezon "Q" Sealing Compound around the edge of the cylinder thus forming a seal between the cylinder and the plate. A flange with vacuum connection and neoprene seal was made to attach the cylinder to the vacuum system, as shown in Figure 36. On the same vacuum system were two other flasks, one containing water to approximately twice the volume required for filling the cylinder to the desired height and the other containing sufficient mineral oil to form a layer in the cylinder several centimeters thick. The system was

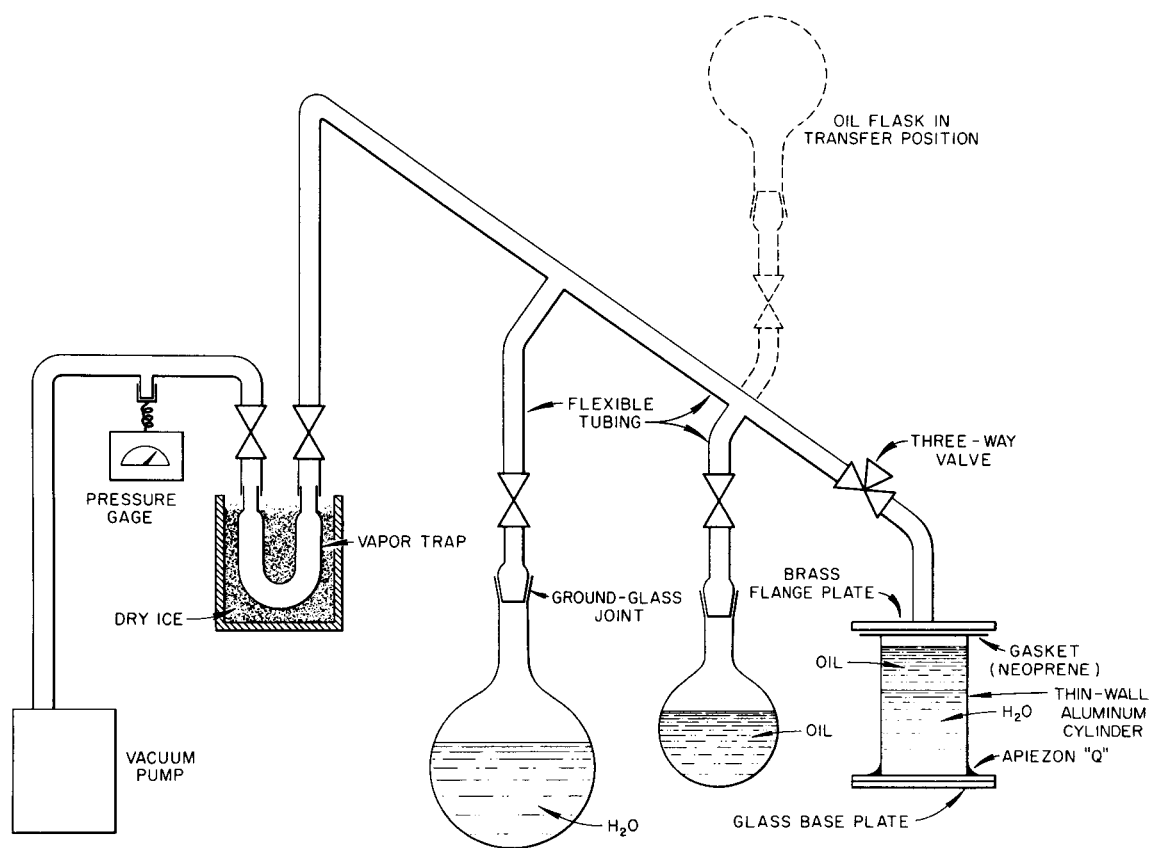


Figure 36. Vacuum system used for making small ice cylinders.

then pumped on for several hours through a cold trap consisting of a U-shaped tube immersed in a dry ice-acetone mixture. During this time approximately one third of the water in the flask would be lost to the cold trap.

After the degassing was completed water was transferred by gravity from the flask to the cylinder to a height about 2 cm. greater than desired for the final cylinder. Then oil was similarly transferred onto the top of the water to form a layer about 4 cm. thick. The cylinder was then disconnected from the vacuum and frozen at  $-5^{\circ}\text{C}$ . until solid. Then the temperature was gradually lowered to  $-80^{\circ}\text{C}$ . At this temperature the sealing material was brittle and the glass base plate could be removed by a sharp blow, leaving the bottom ice surface flat and smooth. The oil on top of the water was also virtually solid at this temperature. The cylinder was then (still at  $-80^{\circ}\text{C}$ .) sawed off at about the desired height with a band saw, thus removing the oil layer and the top ice portion including the irregular surface. The sawed-off surface was then accurately faced off on a lathe to produce a plane surface parallel to the bottom. Occasionally small ice chips were broken out of the machined face. These were easily repaired by filling with a drop or two of distilled water. The exposed end surfaces were then covered with aluminum foil which was taped to the aluminum cylinder wall, and the entire cylinder was covered with Cd, except for a hole at one end to permit neutrons to enter the detector.

A total of 12 cylinders were made by these two processes and used in the experiments. Table III gives the dimensions of these cylinders.

TABLE III  
DIMENSIONS OF THE ICE CYLINDERS  
USED IN THE EXPERIMENTS

| Cylinder<br>Number | Height<br>(cm.) | Radius<br>(cm.) |
|--------------------|-----------------|-----------------|
| 1                  | 24.95 ± 0.31    | 15.13 ± 0.17    |
| 2                  | 18.54 ± 0.20    | 12.55 ± 0.12    |
| 3                  | 25.30 ± 0.22    | 10.035 ± 0.10   |
| 4                  | 21.27 ± 0.18    | 10.035 ± 0.10   |
| 5                  | 16.51 ± 0.13    | 10.035 ± 0.10   |
| 6                  | 16.05 ± 0.12    | 7.325 ± 0.04    |
| 7                  | 10.44 ± 0.06    | 5.575 ± 0.025   |
| 8                  | 9.069 ± 0.05    | 4.190 ± 0.02    |
| 9                  | 6.400 ± 0.040   | 4.001 ± 0.015   |
| 10                 | 4.196 ± 0.040   | 5.550 ± 0.032   |
| 11                 | 7.520 ± 0.040   | 3.073 ± 0.012   |
| 12                 | 7.188 ± 0.027   | 2.858 ± 0.012   |

### III. DATA COLLECTION

The procedure adopted for collecting the experimental data will be described here. The objectives were (1) to assure alignment of the beam on the target to maximize neutron production, (2) to make certain that all the detecting and analyzing equipment was functioning properly throughout the data-collecting time, (3) to make certain that the time allowed for higher modes to decay and for spectrum adjustments to occur would be sufficient, (4) to minimize the background, (5) to adjust the count-rates for the maximum consistent with tolerable dead-time effects, and (6) to collect a sufficient amount of data for good statistics.

The procedure was as follows: Before placing a new ice cylinder in the refrigerator the beam target was temporarily replaced by a quartz viewer and the beam alignment was checked. The cylinder and detector were then positioned and the refrigerator was set at the desired temperature and left at least 10 hours to allow the temperature in the ice cylinder to stabilize at the set point. Then with the beam on continuously at low level neutrons were produced to permit testing of the detector equipment and setting of the pulse-height-discrimination level. A series of counting runs were then made with the beam still on continuously in order to check the uniformity of the channel widths. If these were uniform within 0.5 per cent the beam would be pulsed and a series of short test-runs performed to determine the optimum selection of pulsing parameters. The scheme used for this was as follows: First the waiting time between the end of the neutron pulse and the opening of scaler 1

would be set at  $3(\Delta t)$  sec. and the frequency adjusted so that the decay rate amounted to about a factor of 4 in  $4(\Delta t)$  sec. Then the beam intensity at a neutron pulse width of  $2(\Delta t)$  was increased as much as possible and the waiting time increased until the counting rate in scaler No. 1 (channel 1) was at the desired level of  $10^5$  counts in 30 to 40 minutes. Three or four "full-count runs" ( $10^5$  counts in channel 1) were then made with these settings and the total counts per channel as well as the differences between adjacent channels were plotted to verify that the decay was exponential.

The advantage of plotting channel differences lies in the fact that it not only eliminates the flat background, but also exaggerates the effects of the presence of components other than a single exponential.

Assuming that the decay consists of a single exponential term plus a flat background, one may write for the counts collected in channel  $n$  after  $P$  cycles:

$$C_n = A_0 P(\Delta t) e^{-n(\Delta t)\lambda} + B_0 P(\Delta t) \quad (173)$$

where  $A_0$  is the count-rate in counts per unit time at  $t = 0$  minus the background and  $B_0$  is the counting rate due to the background. One then has

$$C_n - C_{n+1} = \Delta C_n = PA_0(\Delta t) \left[ e^{-n\lambda(\Delta t)} - e^{-(n+1)\lambda(\Delta t)} \right] \quad (174)$$

or

$$\Delta C_n = PA_0(\Delta t) \left[ 1 - e^{-\lambda(\Delta t)} \right] e^{-n\lambda(\Delta t)} = A' e^{-n\lambda(\Delta t)} \quad (175)$$

With the parameters chosen as described  $C_2/C_1 \approx 0.75$ , so that  $(C_1 - C_2) \approx 0.25 C_1$ . So, if, due to mode or slowing-down effects,  $C_1$  is in error by  $x$  per cent, then the error relative to  $(C_1 - C_2)$  is about  $4x$  per cent.

If the plot of the difference data yielded no evidence of deviation in the first channel, then the waiting time was increased by an additional  $2(\Delta t)$  sec. beyond the last point at which a detectable error existed. For example, if the test run with a waiting time of  $7(\Delta t)$  sec. showed the first two channels to deviate from a single exponential, the waiting time was increased to  $11(\Delta t)$  sec. The burst width would then be increased to give the desired count rate in the first channel.

However, in no case was the burst width greater than  $5(\Delta t)$  sec. because with  $n = 1/4(\Delta t)$ , further increases would increase the background with relatively little additional gain in the count rate of the early channels.

A further provision was imposed. Careful tests with a small cylinder at  $-85^\circ\text{C}$ . showed that there was no detectable change in decay after a minimum of  $170 \mu\text{sec}$ . of waiting time after the burst. Therefore, no shorter waiting times than  $170 \mu\text{sec}$ . were used, even though, with the smallest cylinders, about  $120 \mu\text{sec}$ . sufficed to satisfy the other conditions.

In the case of the smallest ice cylinders it was not possible to achieve the desired count-rate, while still fulfilling the conditions imposed on the frequency, waiting time, and burst width. In these cases the lower counting rate was accepted. In the worst case it required about 70 minutes to obtain one full count.

In order to ascertain that no beam-pulsing failure occurred which would adversely affect data quality, and as a general check of the proper functioning of the system, a long-counter beam monitor located about 150 cm. from the target was used to detect fast neutrons (see Appendix C for long counter calibrations).

If, during any run, the count-rate exceeded the rate corresponding to  $10^5$  counts per 30 minutes by a factor of 1.3 or more the run was discarded. For every ice block and temperature a minimum of  $7 \times 10^5$  counts in channel 1 were thus collected. In most cases the number was between  $9 \times 10^5$  and  $1.2 \times 10^6$  counts. Thus a total of about  $4 \times 10^8$  counts were collected in this experiment.

(In the case of cylinder 9 only, the run intended to be made at  $-45^\circ\text{C}$ . was actually made at  $-50^\circ\text{C}$ . The correction of this one point to the  $-45^\circ\text{C}$ . temperature is discussed in the section on data processing.)

The most widely varying factor from run to run, other things being equal, was the relative magnitude of the background. This problem was largely solved by use of the secondary deflection system. However the earlier (large-cylinder) data do have quite variable backgrounds. The attempt to minimize this background was always made; however, the relative magnitude of the background depended in a complex nonlinear way on all the settings of the console beam-controls so that a true maximization of burst yield, together with minimization of the background was not possible.

Appendix C lists the observed counts for each cylinder and temperature, in the second column of each table.

## CHAPTER IV

### DATA REDUCTION AND ANALYSIS

#### I. EVALUATION OF DECAY FREQUENCIES FROM THE DATA

The first task to be undertaken in the data reduction process was to choose appropriate methods for analyzing the data, and for extracting the value of the decay frequency. In the previous section the methods of obtaining the raw data were described and the basis for choosing the waiting time was described. If the waiting time is sufficiently long then the data should contain only a single exponential and a background. The analysis of such data has been discussed by Peierls (1935) who gives exact calculation methods for estimating the parameters and their errors when statistical errors in the observed counts are present. However, this method is not applicable if other types of perturbations than normally distributed errors with zero mean are present.

Cornell (1956) developed a method for analyzing data consisting of combinations of exponentials. However, in this analysis each point is equally weighted, so that it applies strictly only if an infinite number of counts are collected at each point so that counting statistics becomes negligible.

Numerical methods can be used to fit data to any analytical model, with arbitrary weights for the data points, using the method of least squares. In this method the quantity

$$S^2 = \sum_j [Y_j - f(a_1, a_2, a_3, \dots, a_n, j)]^2 \quad (176)$$

is minimized. Here  $Y_j$  is the observed number of counts in the  $j$ th channel,  $f(a_1, a_2, \dots, a_n, j)$  is the calculated value of the model function for the  $j$ th channel where  $a_1, a_2, \dots, a_n$  are  $n$  parameters. The least-squares method consists of making successive modifications to a set of initial-guess parameters  $a_1^0, a_2^0, \dots, a_n^0$  so as to reduce  $S^2$ . In effect one is searching for the lowest point on the  $n$ -dimensional surface whose equation is Equation (176).

Such a procedure is generally carried out on a digital computer (in the present case on IBM-7090) since the numerical work is enormous.

Unfortunately the  $S^2$ -surface may, in general, have more than one local minimum (a local minimum is a point  $S^2(a'_1, a'_2, \dots, a'_n)$  such that any small change in one or more of the  $a'_i$  increases  $S^2$ , that is at such a minimum:

$$\frac{\partial S^2}{\partial a_i} = 0 \quad \text{for } i = 1, 2, \dots, n \quad (177)$$

$$S^2[a'_1, a'_2, \dots, (a'_i + \delta a_i), \dots, a'_n] > S^2(a'_1, a'_2, \dots, a'_n)$$

when  $\delta a_i$  is a small change in  $a_i$ ). There is no guarantee that the minimum found is the "true" minimum, i.e., the smallest one. In principle a different choice of initial parameter estimates may lead to convergence at a different one of the local minima. For the work in the present instance a general nonlinear least-squares fit program written by Busing

and Levy (1962) was used. Various tests were performed to gather information about the convergence characteristics under the conditions arising in the present work.

In the previous section the methods of obtaining the raw data were described and the basis for choosing the required waiting time was presented. Assuming that such a waiting time has been employed the data collected should contain only a single exponential decay and a flat background. The first analysis method employed to obtain the decay constants (based on this assumption) was that of Cornell (1956) fitting the data with three independent parameters. Appendix E gives the Cornell method formulas as they apply to the present case of a fit to a single exponential and a flat background. This estimation method was coded for the IBM-7090 computer, and the values of the parameters and their variances were computed for the sets of data obtained from ice cylinders Number 2, 3, 4, and 5 at each temperature. In order to determine whether the decay was indeed fitted adequately by a single exponential, each of these twenty sets of eighteen-point decay data was analyzed using five different data-point subsets. As discussed in Appendix E, the number of channels must be a number divisible by three. Therefore, the analysis was done in five ways for each set, using all eighteen, channels, and using the four fifteen-channel sets 1-15, 2-16, 3-17, and 4-18. In this way different time segments of the decay curve were analyzed in order to determine whether a consistent trend of change with time would be observed. The presence of such a trend would be evidence of the presence of another decay component. Figures 37, 38,

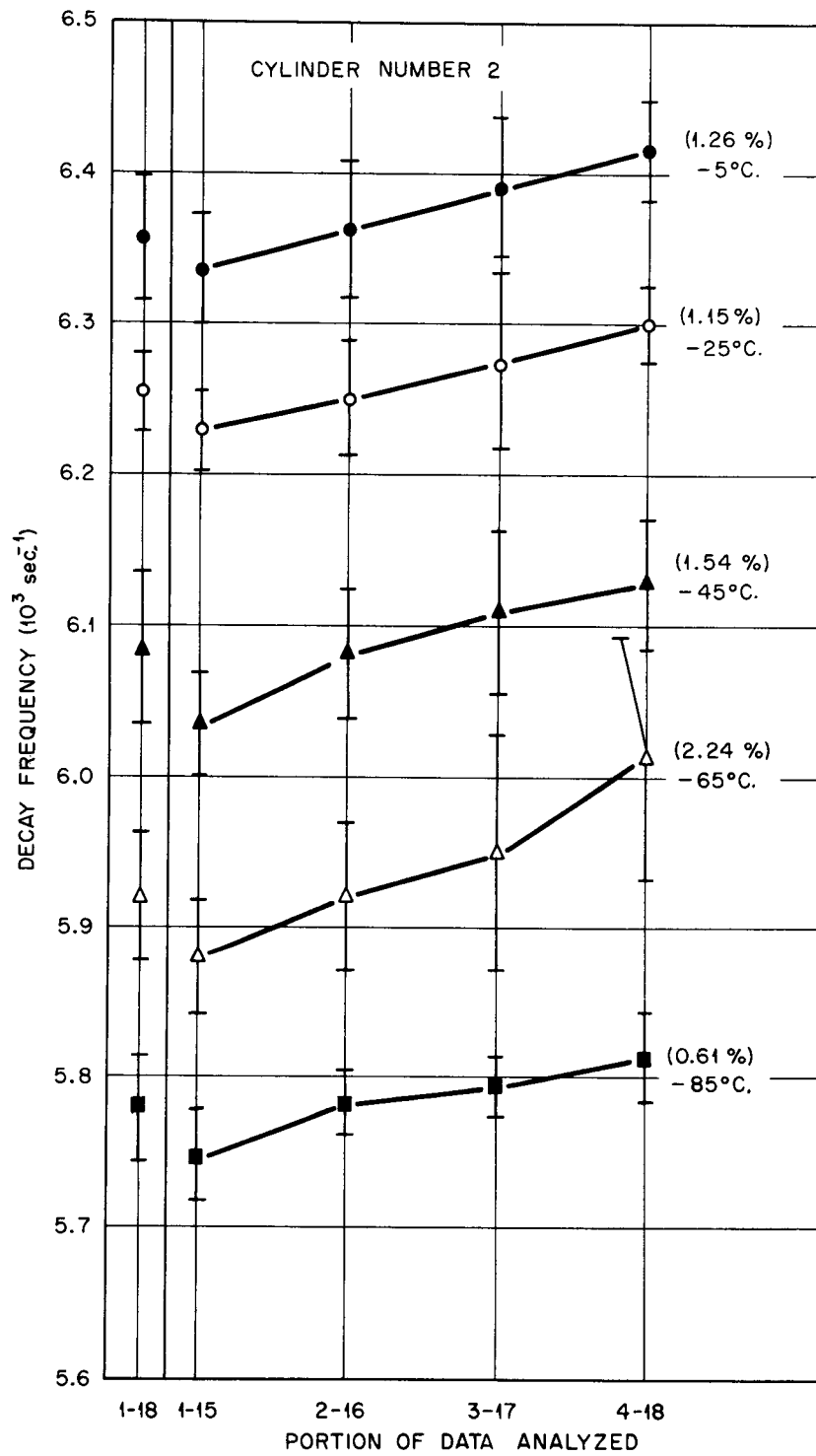


Figure 37. Results of three-parameter Cornell analyses of cylinder Number 2 as function of the portion of the decay data analyzed.

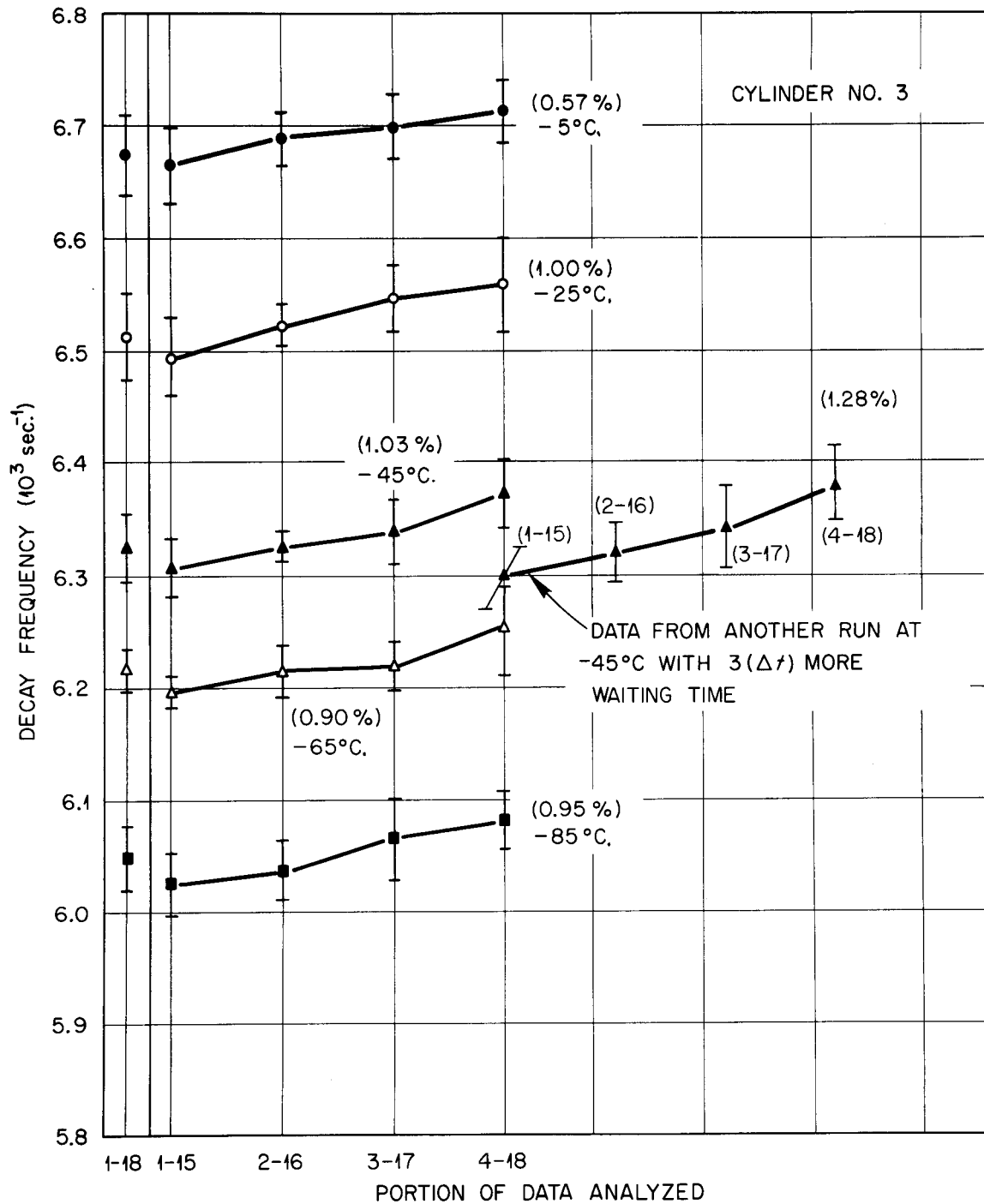


Figure 38. Results of three-parameter Cornell analyses of cylinder Number 3 as function of the portion of the decay data analyzed.

39, and 40 show the results obtained by this analysis. (The values of the decay frequency are obtained by Equation E-15 and the errors shown are the square root of the variance obtained by Equation E-23 in Appendix E.)

It is clearly seen that a consistent trend toward increasing decay frequencies with time appears when the fifteen-channel analyses beginning with Channels 1, 2, 3, and 4, respectively, are compared. In the figures the per cent increase in the decay frequency obtained from the analysis of Channels 4-18 compared with the value obtained from the analysis of Channels 1-5 is shown in parentheses. The mean change is 0.89 per cent, which is smaller than the error bars, but which by its consistent appearance suggests a systematic cause. It is significant that in the two instances where a given cylinder at a particular temperature was measured with two different waiting times (Cylinder 3 at  $-45^{\circ}\text{C}$ . and Cylinder 5 at  $-85^{\circ}\text{C}$ .) the increase is observed in each run but does not continue over the pair of runs. In Cylinder 3 the mean values of the decay frequency in the two runs are  $6.336 \times 10^3 \text{ sec.}^{-1}$  and  $6.337 \times 10^3 \text{ sec.}^{-1}$ , respectively, and in the case of Cylinder 5 the respective mean values are  $6.480 \times 10^3 \text{ sec.}^{-1}$  and  $6.491 \times 10^3 \text{ sec.}^{-1}$ . The mean change in the averages for the two cases is thus only 0.09 per cent which is quite small compared to the difference observed between the first and last analyses taken from one set of decay data. This suggests strongly that the effect is caused by some aspect of the data collection or analysis, and is not a reflection of a true change in the neutron decay with time. If such a change were really taking

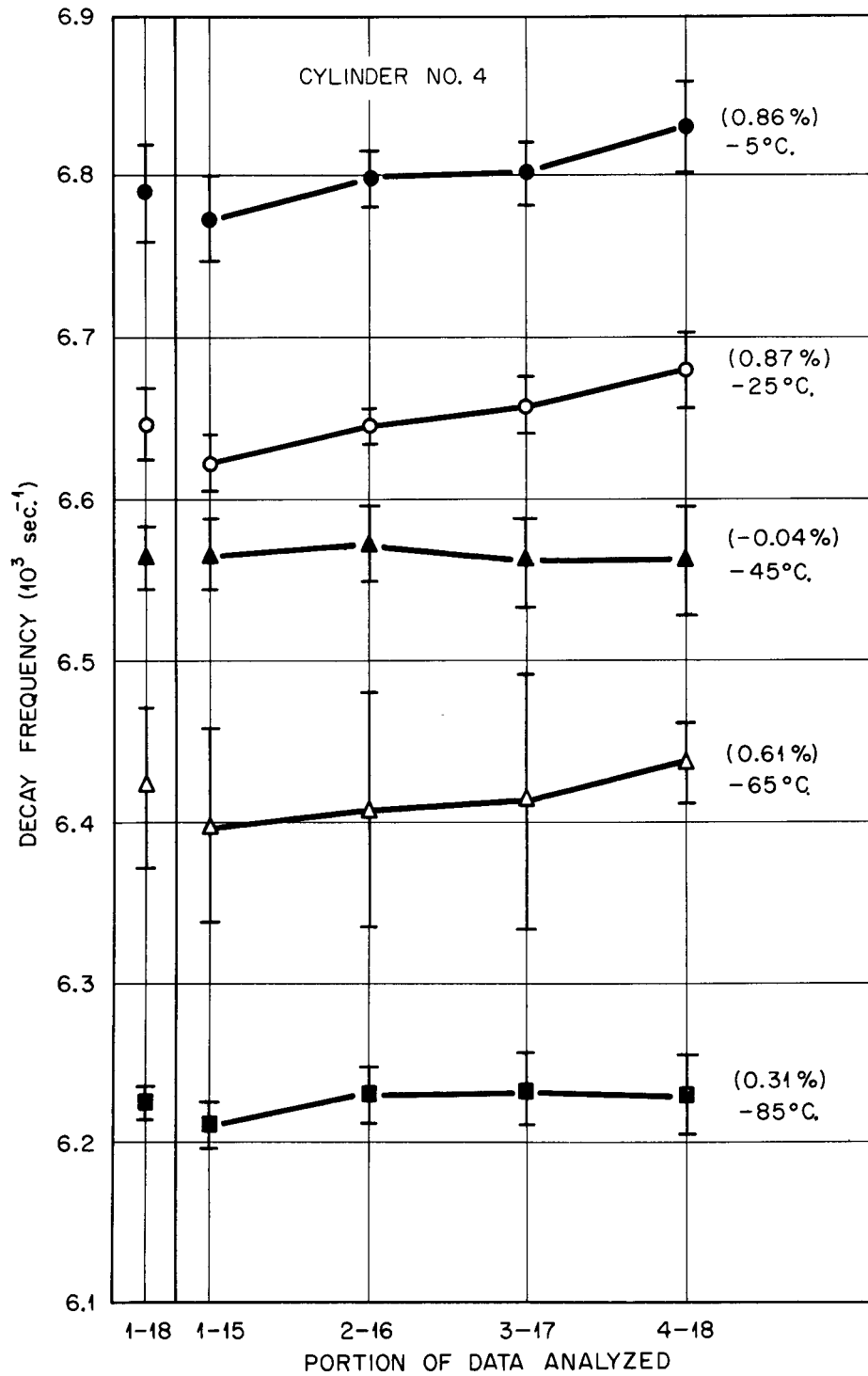


Figure 39. Results of three-parameter Cornell analyses of cylinder Number 4 as function of the portion of the decay data analyzed.

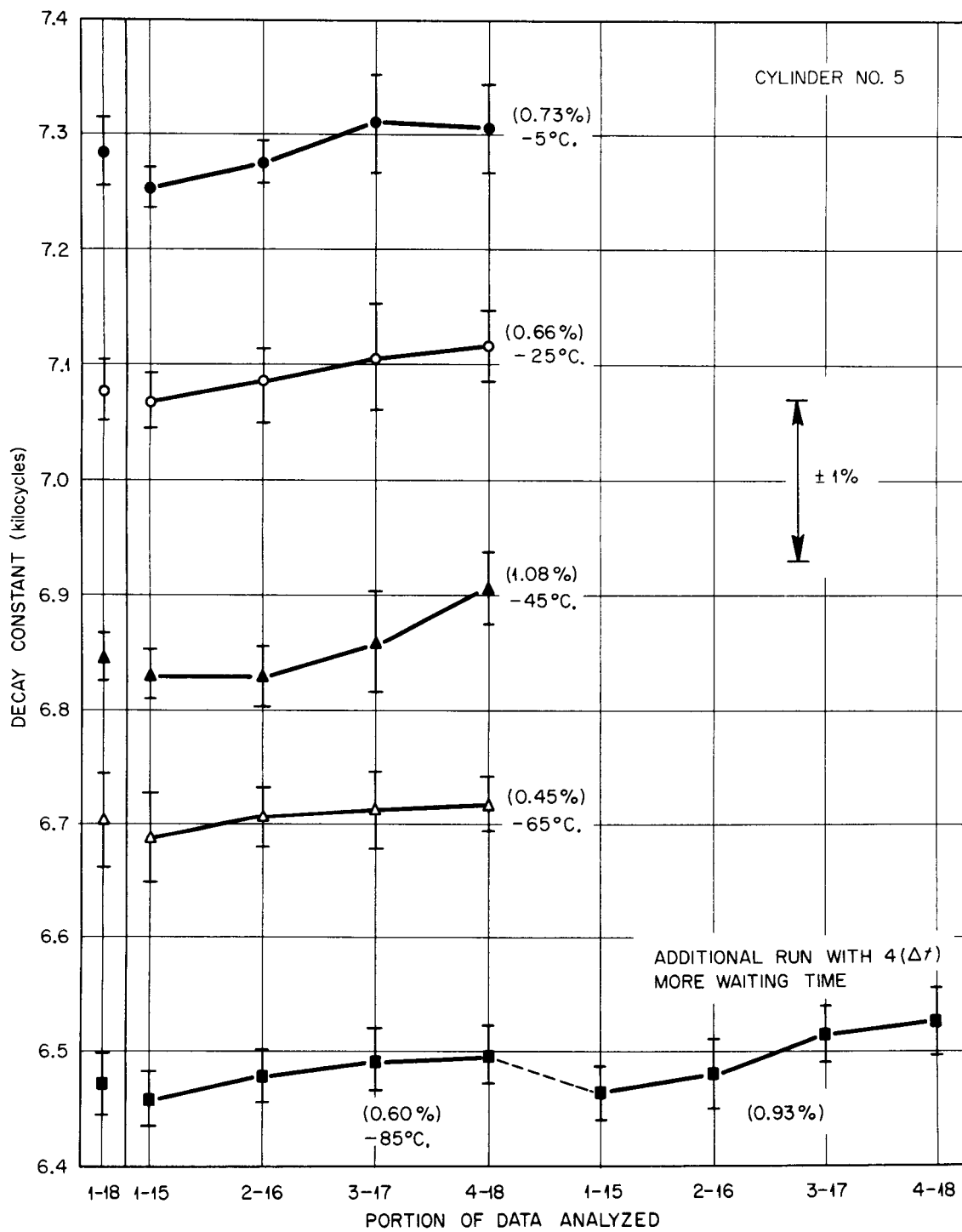


Figure 40. Results of three-parameter Cornell analyses of cylinder Number 5 as function of the portion of the decay data analyzed.

place, then one would expect that the results for a run with longer waiting time would be still larger than the last result obtained from the run with shorter waiting time.

It is also interesting to observe that the effect represents a steepening of the slope with time. If this effect were due to the existence of several spectral groups (as was the case in beryllium) (Silver, 1962), the most persistent mode would become more dominant, leading to a decrease in decay frequency with time.

It is readily seen that no combination of exponential components of positive amplitude will result in a steepening slope. In such a case the relative contribution of the slower-decaying components will continue to increase with time, leading always to a decreasing slope. The only possible way of arriving at a steepening slope is by means of a component with negative amplitude, or if the decay is nonexponential.

In view of these observations, considering the direction of change, the effect of waiting time, and the temperature-independence of the magnitude of the effect, the following explanation was proposed.

If there are counting losses due to dead-time effects, then the number of counts lost per unit time is given by Equation A-14 of Appendix A as:

$$\text{Counts lost per unit time} \cong \tau R^2 . \quad (178)$$

So the number of counts observed in the  $n$ th channel is given by

$$C_n \approx \alpha_0(\Delta t) + \alpha_1(\Delta t)e^{-n\beta(\Delta t)} - \tau \left[ \alpha_0(\Delta t) + \alpha_1(\Delta t)e^{-n\beta(\Delta t)} \right]^2 . \quad (179)$$

Now, assuming that  $\alpha_0(\Delta t) \ll \alpha_1(\Delta t)e^{-n\beta(\Delta t)}$  (which is valid for the cases under discussion), we may write

$$C_n \approx \alpha_0(\Delta t) + \alpha_1(\Delta t)e^{-n\beta(\Delta t)} - \tau[\alpha_1(\Delta t)]^2 e^{-2n\beta(\Delta t)}. \quad (180)$$

So the effect of dead-time is to introduce a negative-amplitude mode with twice the decay frequency as that of the fundamental.

To determine the effect that such a higher mode has on the observed decay, the following considerations are useful.

Let the normalized neutron density equation be given by:

$$N(t) = e^{-\lambda t} - ae^{-c\lambda t} \quad (181)$$

where  $a$  is the ratio of the amplitude of the higher mode component of the decay relative to that of the fundamental decay at  $t = 0$ ,  $\lambda$  is the fundamental mode decay constant,  $c$  is the ratio of the two decay constants, and the background is considered negligible. (If the higher mode is due to dead-time then  $c = 2$  as shown above.) In the absence of the higher mode the slope of the decay is given by

$$S = \frac{d}{dt} [\ln N(t)] = -\lambda. \quad (182)$$

If the higher mode is present then we have

$$S(t) = \frac{d}{dt} [\ln N(t)] = \frac{-\lambda + ac\lambda e^{(1-c)\lambda t}}{1 - ae^{(1-c)\lambda t}} \quad (183)$$

or

$$\begin{aligned}
 S(t) &= \lambda \left[ 1 - ace^{-(1-c)\lambda t} \right] \sum_{n=0}^{\infty} a^n e^{n(1-c)\lambda t} \\
 &= \lambda \left[ 1 + (1-c) \sum_{n=1}^{\infty} a^n e^{n(1-c)\lambda t} \right]. \quad (184)
 \end{aligned}$$

So

$$S(0) = -\lambda \frac{1 - ac}{1 - a}. \quad (185)$$

With the condition that  $a \ll 1$  (experimentally it is found to range from 0.005 to 0.04) we may drop higher terms and write

$$S(t) \approx -\lambda \left[ 1 + (1-c)ae^{(1-c)\lambda t} \right]. \quad (186)$$

The difference in waiting time for an analysis beginning with Channel 1 and one beginning with Channel 4 is of the order of  $1/\lambda$  sec. So a useful measure of the rate of change of the slope is given by

$$R = \frac{S(1/\lambda)}{S(0)} = \frac{1 - a}{1 - ac} \left[ 1 + (1-c)ae^{(1-c)} \right]. \quad (187)$$

Figure 41 shows a plot of  $(R - 1)$  as function of  $a$  for various values of  $c$ . It is seen that for  $a = 0.01$  and  $C = 2$  a 0.6 per cent change of slope over four channels would result. Figure 42 shows a plot of the Cornell method decay frequencies obtained with an artificial set of data without any statistical errors, which consisted of a fundamental mode and a double-frequency negative term with 0.03 initial

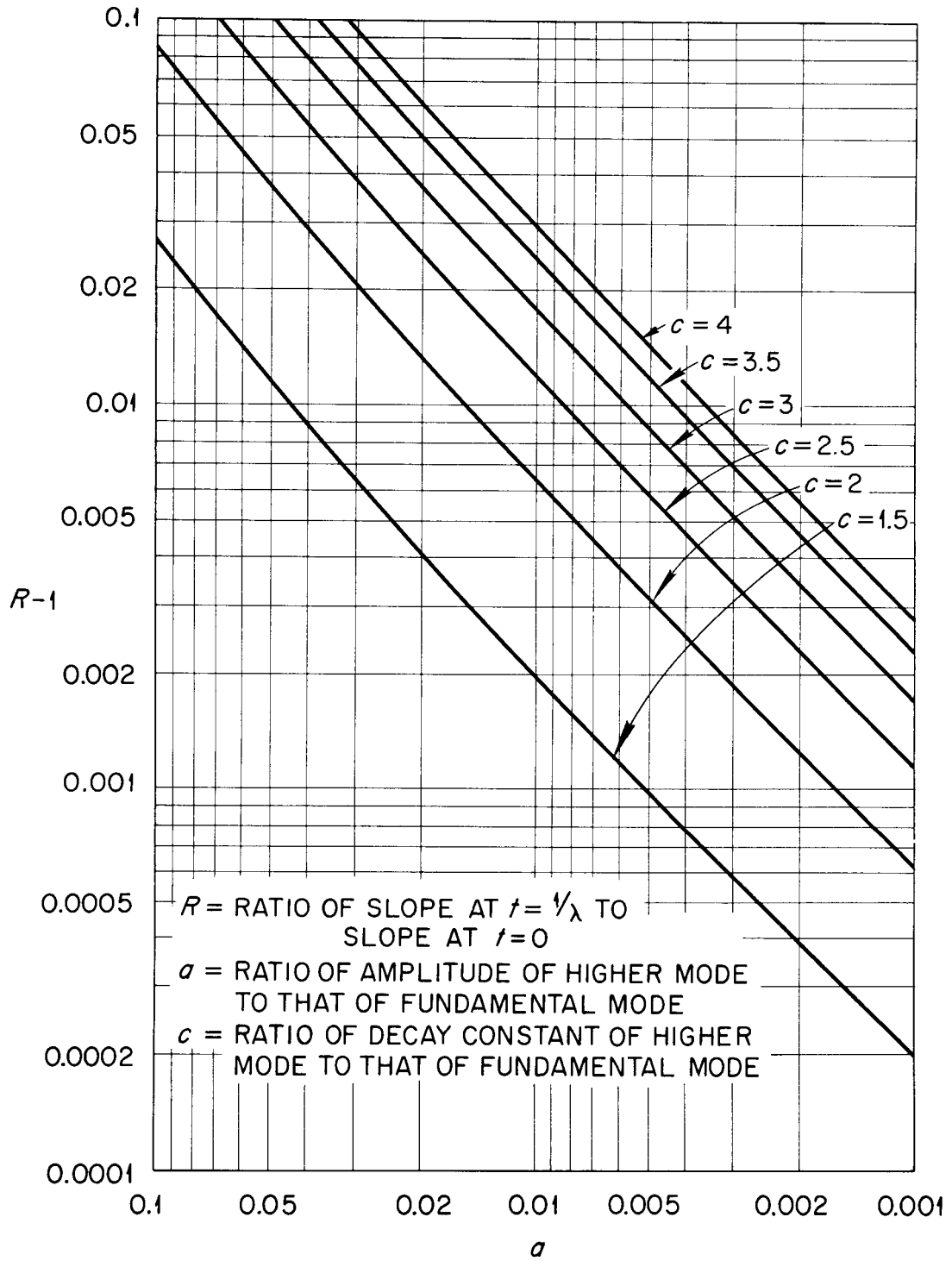


Figure 41. Plot of  $(R-1)$  versus  $a$  for various values of  $c$ , where  $R$ ,  $a$ , and  $c$  have the definitions shown in the figure.

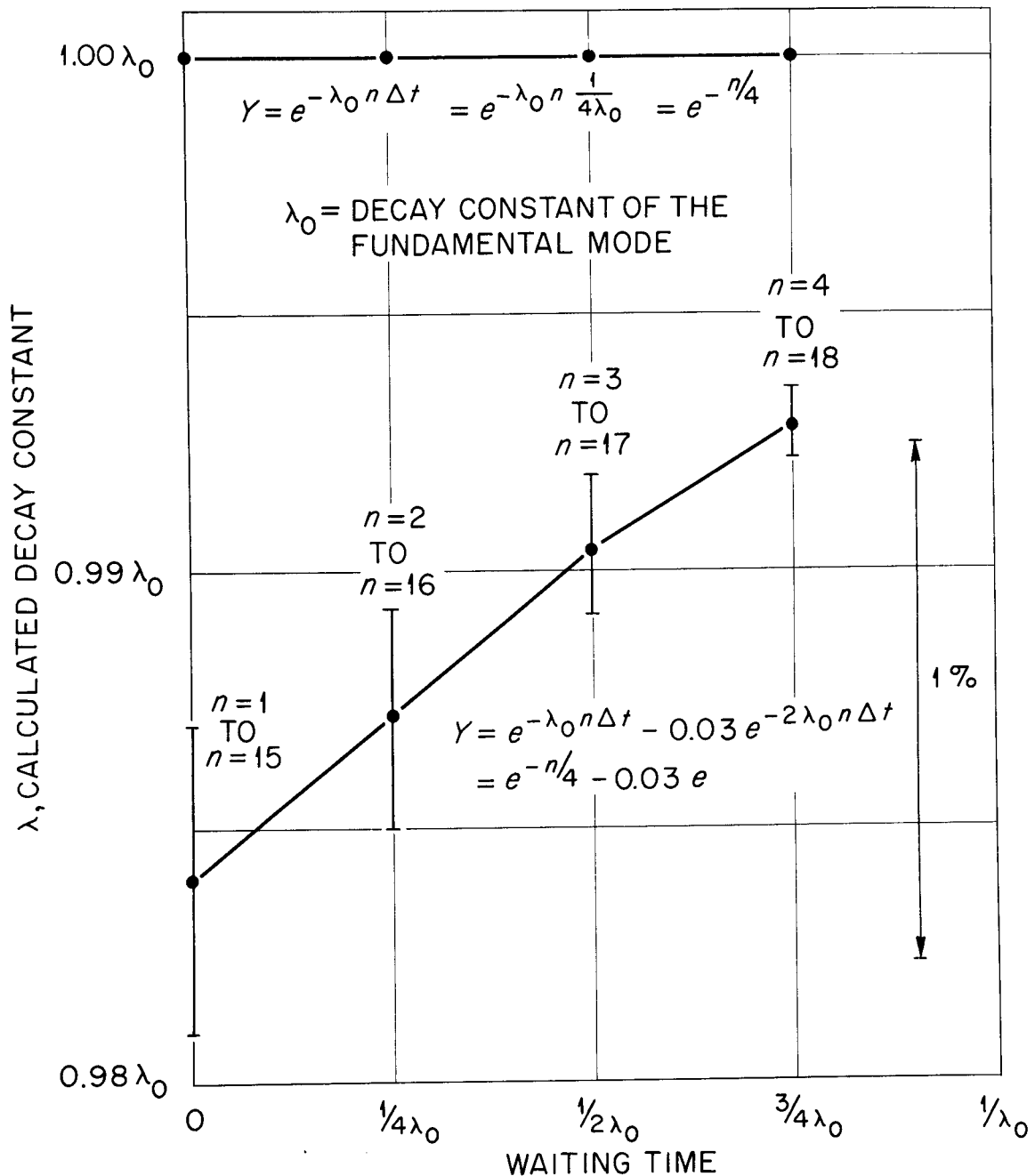


Figure 42. Results of Cornell-method analysis on an artificial set of decay data, without statistical variance, constructed from the equation  $N(t) = e^{-\lambda_0 t} - 0.03 e^{-2\lambda_0 t}$ . The "channel widths" are  $1/(4\lambda_0)$  sec. wide, and each analysis extends over fifteen channels. The decay constant of the pure fundamental mode is shown for comparison.

relative amplitude. The channels were taken to be  $(1/4 \lambda_0)$  sec. wide. It is seen that the result is just the sort of small increase in apparent decay constant which was observed in the analyses of the experiment by the three-parameter Cornell method. In this instance the Cornell method analysis using eighteen data points gave a result of  $0.988 \lambda_0$ , and the mean of the four fifteen-channel analysis results is  $0.989 \lambda_0$ . So in this case an error of the order of one per cent would be made by ignoring the presence of the faster-decaying component. Thus, the results with the test data are in good agreement with the hypothesis proposed for the observed effect.

In order to analyze the experimental results in accordance with these considerations, the Cornell method was abandoned and a nonlinear least-squares fitting method was used instead (Busing and Levy, 1962). The model used was of the form

$$C_n = P_1 + P_2 e^{-P_3 n(\Delta t)} + P_4 e^{-c P_3 n(\Delta t)}, \quad (188)$$

where  $C_n$  is the number of counts in the  $n$ th channel. In the cases at hand there were four parameters to be fitted; the background,  $P_1$ , the two amplitudes of the decay terms,  $P_2$  and  $P_4$ , and the fundamental mode decay frequency,  $P_3$ . The ratio,  $c$ , of the two decay frequencies was taken to be 2.0. The weights of the data were assumed to be solely due to counting statistics.

The results of the three-parameter Cornell analysis were used as input parameters. In order to be sure that the choice of the initial

guess would not affect the final values a test was performed in which a case was run with sets of input parameters in which one parameter was taken to range from 0.1 to 10 times the correct value, keeping the other three input guesses at about the correct value. In each case the code "pulled in" to the correct value over the entire range of input parameter guesses, except for parameter  $P_3$ , the decay frequency parameter. In this case correct convergence was obtained in the range  $0.3 (P_3^{\text{true}})$  to  $5.0 (P_3^{\text{true}})$ . Outside this range the code did not converge at all within the small (9) number of cycles allowed for convergence. In no case did convergence to a wrong value occur. Since in all actual cases the converged values were within only a few per cent of the input parameters it was concluded that error in input parameter choice of a single parameter could not lead to false convergence. A somewhat more limited test was also performed to assess the effect of simultaneous erroneous choices of several input parameters. Again it was found that no combination of wrong choices of parameter  $P_1$ ,  $P_2$ , and  $P_4$  would lead to wrong convergence. And the limits of convergence of parameter  $P_3$  were about the same as above, even with other parameters erroneous by a factor of ten.

Each set of decay data was then analyzed with this code and this four-parameter model: (1) using all eighteen channels, (2) using the four partial sets 1-15, 2-16, 3-17, and 4-18, and (3) using only even-numbered or odd-numbered channels. In each case the variation of the value of  $P_3$ , the decay frequency, was examined for evidence of consistent change. Table IV gives a sampling of the results obtained by

TABLE IV  
 RESULTS OF FOUR-PARAMETER ANALYSIS ASSUMING DOUBLE  
 DECAY FREQUENCY FOR THE SECOND DECAY COMPONENT

|            | -5°C. | -25°C. | -45°C. | -65°C. | -85°C. |
|------------|-------|--------|--------|--------|--------|
| Cylinder 1 |       |        |        |        |        |
| 1-18       | 5.886 | 5.724  | 5.635  | 5.579  | 5.443  |
| 1-15       | 5.900 | 5.729  | 5.642  | 5.582  | 5.460  |
| 2-16       | 5.890 | 5.722  | 5.652  | 5.586  | 5.429  |
| 3-17       | 5.883 | 5.732  | 5.639  | 5.560  | 5.432  |
| 4-18       | 5.885 | 5.721  | 5.618  | 5.584  | 5.417  |
| Cylinder 3 |       |        |        |        |        |
| 1-18       | 6.745 | 6.585  | 6.413  | 6.266  | 6.096  |
| 1-15       | 6.754 | 6.610  | 6.391  | 6.264  | 6.096  |
| 2-16       | 6.748 | 6.578  | 6.420  | 6.280  | 6.074  |
| 3-17       | 6.765 | 6.576  | 6.431  | 6.241  | 6.143  |
| 4-18       | 6.726 | 6.604  | 6.422  | 6.263  | 6.104  |
| Cylinder 5 |       |        |        |        |        |
| 1-18       | 7.321 | 7.121  | 6.888  | 6.825  | 6.493  |
| 1-15       | 7.306 | 7.134  | 6.847  | 6.823  | 6.551  |
| 2-16       | 7.317 | 7.132  | 6.910  | 6.782  | 6.546  |
| 3-17       | 7.342 | 7.155  | 6.987  | 6.850  | 6.478  |
| 4-18       | 7.369 | 7.109  | 6.961  | 6.802  | 6.493  |
| Cylinder 6 |       |        |        |        |        |
| 1-18       | 8.829 | 8.468  | 8.214  | 8.052  | 7.593  |
| 1-15       | 8.829 | 8.474  | 8.217  | 8.054  | 7.566  |
| 2-16       | 8.826 | 8.479  | 8.220  | 8.037  | 7.579  |
| 3-17       | 8.869 | 8.464  | 8.233  | 8.052  | 7.672  |
| 4-18       | 8.791 | 8.461  | 8.179  | 8.057  | 7.650  |

TABLE IV (continued)

|             | -5°C.  | -25°C. | -45°C. | -65°C. | -85°C. |
|-------------|--------|--------|--------|--------|--------|
| Cylinder 8  |        |        |        |        |        |
| 1-18        | 16.668 | 15.899 | 14.915 | 14.341 | 13.310 |
| 1-15        | 16.723 | 16.001 | 14.952 | 14.383 | 13.319 |
| 2-16        | 16.628 | 16.345 | 14.921 | 14.300 | 13.232 |
| 3-17        | 16.583 | 15.707 | 14.856 | 14.375 | 13.318 |
| 4-18        | 16.662 | 15.652 | 14.860 | 14.307 | 13.311 |
| Cylinder 11 |        |        |        |        |        |
| 1-18        | 23.401 | 22.335 | 21.118 | 20.299 | 18.297 |
| 1-15        | 23.520 | 22.487 | 21.248 | 20.460 | 18.443 |
| 2-16        | 23.270 | 22.348 | 21.092 | 20.197 | 18.282 |
| 3-17        | 23.098 | 22.214 | 20.925 | 20.078 | 18.096 |
| 4-18        | 22.764 | 21.843 | 20.476 | 19.903 | 17.875 |
| Cylinder 12 |        |        |        |        |        |
| 1-18        | 25.107 | 23.788 | 22.441 | 21.715 | 19.866 |
| 1-15        | 25.603 | 24.098 | 22.602 | 21.913 | 19.960 |
| 2-16        | 24.902 | 23.723 | 22.181 | 21.677 | 19.760 |
| 3-17        | 24.012 | 23.395 | 21.994 | 21.396 | 19.603 |
| 4-18        | 22.377 | 22.390 | 21.639 | 20.063 | 19.420 |

this method, and Figures 43 and 44 show some plots of the decay frequency as a function of the channel number with which the analysis is begun.

For the cases of the large cylinders (Number 1 through about Number 8) the method of correcting by use of a second period with twice the frequency of the fundamental mode works very well. The variations are only of the order of the uncertainties, and there is, more important, no consistent trend toward either increasing or decreasing period with increasing waiting time. It may, therefore, be concluded that the dominant perturbing effect is indeed due to a period of about twice the fundamental, and the hypothesis that this is a dead-time effect appears to fit the observed facts. The mean ratio of  $|P_4/P_2|$  for the twenty-five cases representing the five largest cylinders at each of the five temperatures was  $0.019 \pm 0.006$ . This is in good agreement for the estimate of two per cent dead-time loss in Channel 1 at the counting rate selected for the experiments, described in Chapter III. It may be pointed out here that "normal" dead-time corrections would have been difficult to apply in this work because the counting rates for each channel are different, and often also varied significantly during the data collection time.

In the smallest cylinders, however, particularly with Cylinders Number 10, 11, and 12, the situation was far less satisfactory. There appeared to be a relatively large change in  $P_3$  in going from analysis of Channels 1-15 to the analysis of Channels 4-18, which became worse when a second period of twice the fundamental frequency was fitted to the data than with only a single exponential. The effect here is a

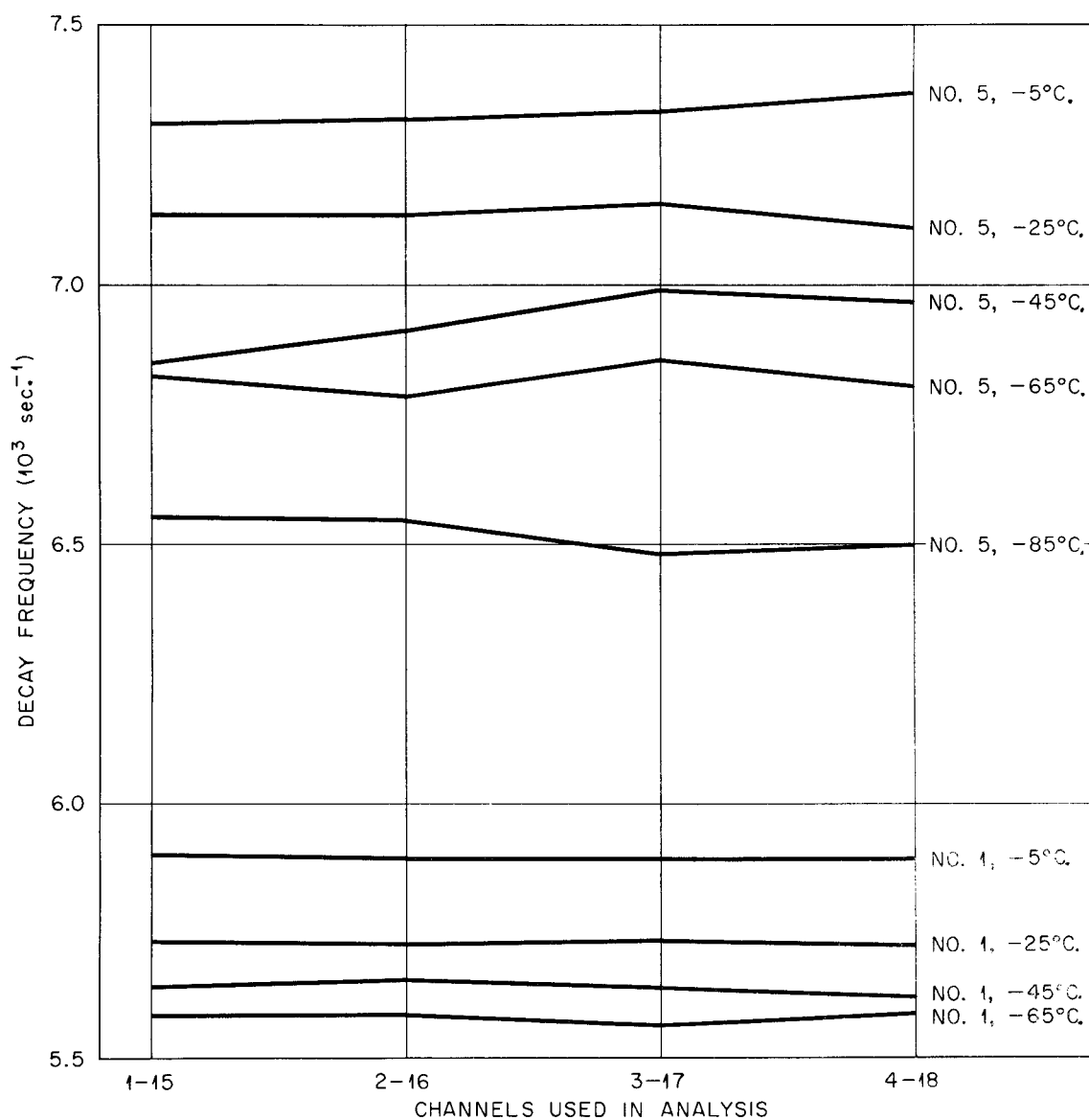


Figure 43. Calculated decay frequency versus channels used in the analysis for cylinders Number 1 and 5, based on four-parameter least-squares analyses assuming a negative-amplitude second decay component with twice the decay frequency of the main decay.

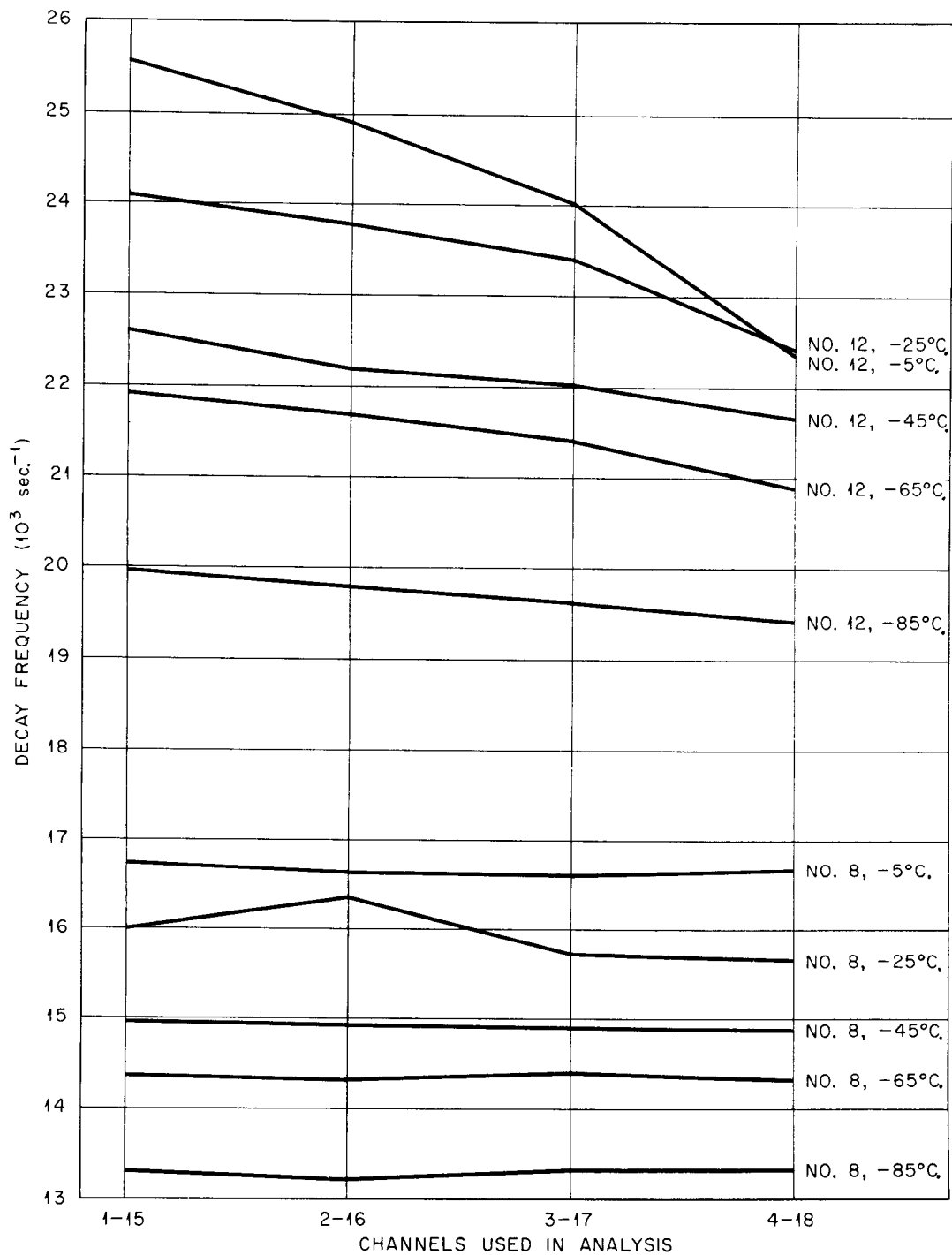


Figure 44. Calculated decay frequency versus channels used in the analysis for cylinders Number 8 and 12, based on four-parameter least-squares analyses assuming a negative-amplitude second decay component with twice the decay frequency of the main decay.

decrease of decay frequency with time, rather than an increase. Of great interest is the fact that for a given buckling the effect is largest at the highest temperature as may be seen in Table V, which shows the per cent decrease in the measured fundamental mode decay frequency (obtained by use of the four-parameter model with double frequency for the second component) in going from analysis of channels 1-15 to analysis of channels 4-18.

It will be seen that the effect is serious for Cylinders 11 and 12 and the more so at high temperatures. It was, therefore, necessary to understand the cause and find a rational method for determining the best value of the decay frequency.

The fact that the effect is most apparent at high temperature, i.e., when the decay frequency is highest, points to a perturbing component which has a longer persistence than the dominant "fundamental" decay. This is also consistent with the observation that the apparent change is made worse by attempting to fit these data with a second component of higher frequency, and hence shorter persistence; and is also supported by the fact that the change is an apparent decrease of the measured decay frequency.

If such a lower-frequency mode is present which is independent of the temperature, then one would expect that the higher the frequency of the main decay, the sooner the small lower-frequency "background" becomes relatively important, and hence the more apparent it becomes at a given time after the neutron burst. In Cylinders 11 and 12 the data at each temperature were measured with the same waiting time, and

TABLE V  
PERCENT DECREASE IN CALCULATED DECAY PERIOD  
FOR ANALYSES OF CHANNELS 4-18, RELATIVE  
TO ANALYSES OF CHANNELS 1-15

| $^{\circ}\text{C}.$ | Cylinder<br>9 | Cylinder<br>11 | Cylinder<br>12 |
|---------------------|---------------|----------------|----------------|
| -5                  | 0.9%          | 3.8%           | 12.8%          |
| -25                 | 0.0%          | 2.9%           | 7.1%           |
| -45                 | 1.2%          | 3.8%           | 4.3%           |
| -65                 | 0.1%          | 2.7%           | 3.9%           |
| -85                 | 0.2%          | 3.1%           | 2.8%           |

precisely this effect was observed. To test this hypothesis artificial decay curves were constructed, without statistics or higher modes. Figure 45 shows the decay curves that were obtained this way between 150 and 550  $\mu\text{sec.}$  after  $t = 0$  for five decays of 12, 18, 21, 24, and  $27 \times 10^3 \text{ sec.}^{-1}$ , respectively, adding to each a component with  $6.0 \times 10^3 \text{ sec.}^{-1}$  frequency and an initial amplitude of 0.2 per cent of the amplitude of the main decay, plus a flat background of 0.02% of the initial amplitude of the main decay. Table VI shows the values for the decay frequency obtained by a Cornell analysis over the time intervals 150 to 400  $\mu\text{sec.}$ , 200 to 450  $\mu\text{sec.}$ , 250 to 500  $\mu\text{sec.}$ , and 300 to 550  $\mu\text{sec.}$  These time intervals and frequencies correspond closely to those that were used in the measurement of the smallest cylinders. In these actual cases the analysis extended from 140  $\mu\text{sec.}$  after the pulse to 520  $\mu\text{sec.}$  after the pulse, and the frequencies of the main decay are just in the range chosen for the artificial data.

The results in Table VI correspond precisely to the effect observed with the real data. As long as the main decay frequency is less than about  $22 \times 10^3 \text{ sec.}^{-1}$  no significant change in the calculated decay frequency is observed with increasing waiting time, but above that the change rapidly becomes very large. The explanation is that, if the main decay is rapid enough, then the slower "background decay" becomes dominant in the last channels even though its initial amplitude is very small. As may be seen from Figure 45 the curvature introduced by the presence of the extra decay frequency is very small, and virtually undetectable by inspection despite the absence of statistics even

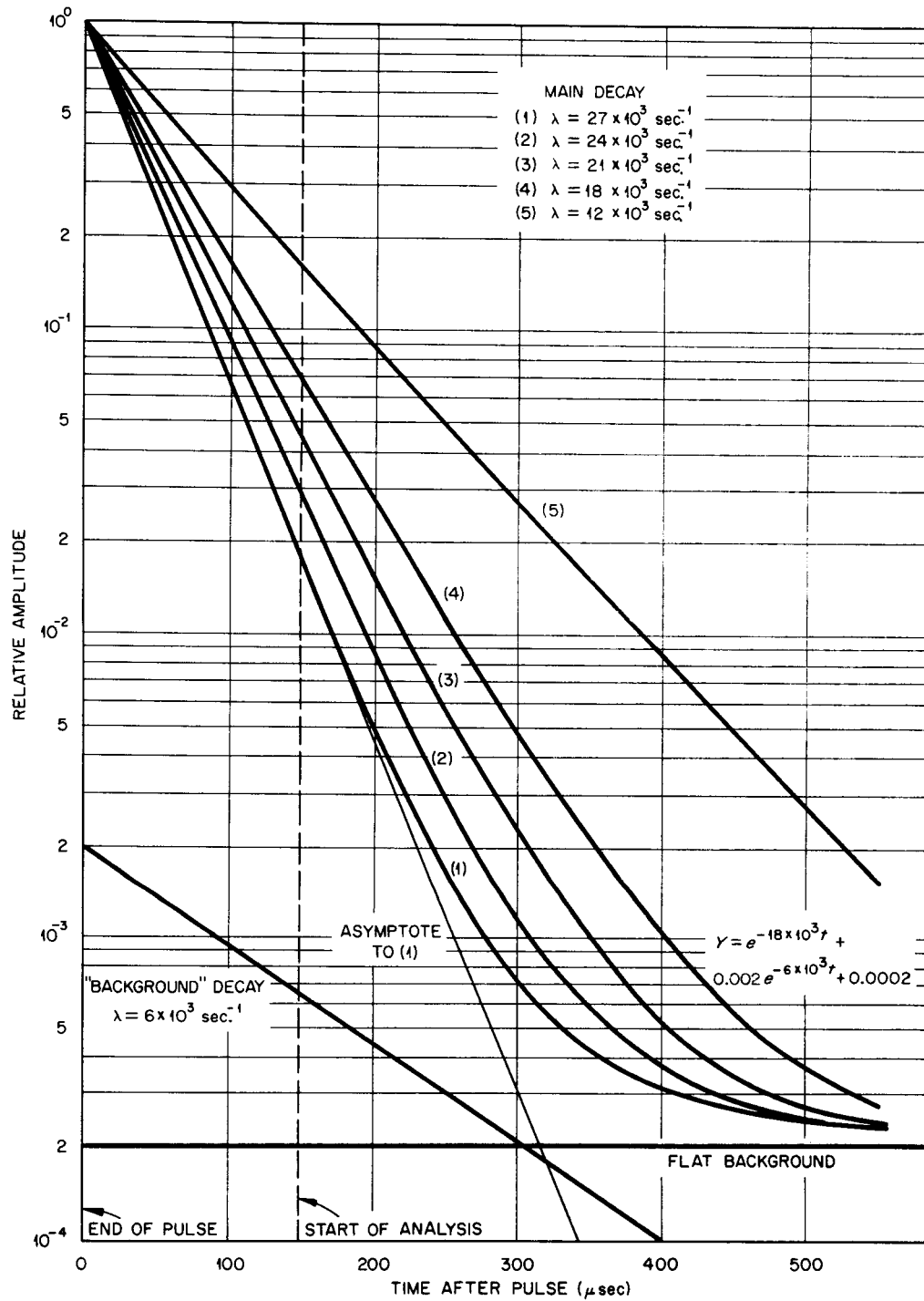


Figure 45. Theoretical decay curves for various main decay frequencies, in the presence of a "background decay" and a flat background.

TABLE VI

EFFECT OF A SMALL DECAY COMPONENT WITH LOW FREQUENCY ON MEASURED DECAY  
FREQUENCY IN THE PRESENCE OF BACKGROUND. TEST WITH ARTIFICIAL DATA

| Analysis Interval     | Main Decay Frequency |               |               |                |                |
|-----------------------|----------------------|---------------|---------------|----------------|----------------|
|                       | 12 $\mu$ sec.        | 18 $\mu$ sec. | 21 $\mu$ sec. | 24 $\mu$ sec.  | 27 $\mu$ sec.  |
| 150 to 400 $\mu$ sec. | 11.99                | 17.80         | 20.67         | 23.27          | 25.51          |
| 200 to 450 $\mu$ sec. | 11.99<br>0%          | 17.75<br>0.3% | 20.40<br>1.3% | 22.47<br>3.4%  | 23.52<br>7.8%  |
| 250 to 500 $\mu$ sec. | 11.97<br>0.2%        | 17.61<br>1.1% | 19.88<br>3.8% | 20.90<br>10.2% | 20.07<br>21.3% |
| 300 to 550 $\mu$ sec. | 11.96<br>0.2%        | 17.40<br>2.2% | 19.09<br>7.6% | 18.59<br>20.1% | 15.04<br>41.0% |

The upper figure of each entry is the value obtained for  $\lambda$  by a three-parameter Cornell Analysis of the artificial data shown in Figure V. The lower figure is the per cent decrease relative to the value found in the first time interval.

where the effect on the calculated slope is of the order of 50 per cent. This is due to the presence of flat background which masks the effect of the added frequency.

However, by the method of plotting the differences between adjacent channels, it was possible to perform a graphical separation of the extra decay in a few cases where the waiting time was long enough. Figure 46 shows the data, including the difference curves, for cylinder 10 at  $-65^{\circ}\text{C}$ . The lower curve shows the differences in the counts in adjacent channels. By extending the asymptotic slope of the difference curve (obtained from the early channels) it appears that the last difference points lie systematically above the asymptote. Plotting this deviation in the last few channels the points shown near the top of the figure were obtained. The best straight line through these points (only subjectively determined) yields a slope corresponding to  $(9.2 \pm 2) \times 10^3 \text{ sec.}^{-1}$  for this background decay frequency. Figure 47 shows the same analysis for the case of cylinder 10 at  $-45^{\circ}\text{C}$ . In this case a slope of  $(8.6 \pm 1.5) \times 10^3 \text{ sec.}^{-1}$  was obtained.

It appears, in view of the investigations described here, that a very small amplitude mode (with initial relative amplitude  $\leq 0.0025$ ) is present in the data, which is neither detectable, nor has an appreciable effect on the decay frequency of the large and intermediate-size ice cylinders, but which needs to be corrected for in the case of those cylinders whose decay frequencies are above about  $20 \times 10^3 \text{ sec.}^{-1}$ .

Thus, a method was needed for extracting the main decay from the experimental data for these cases.

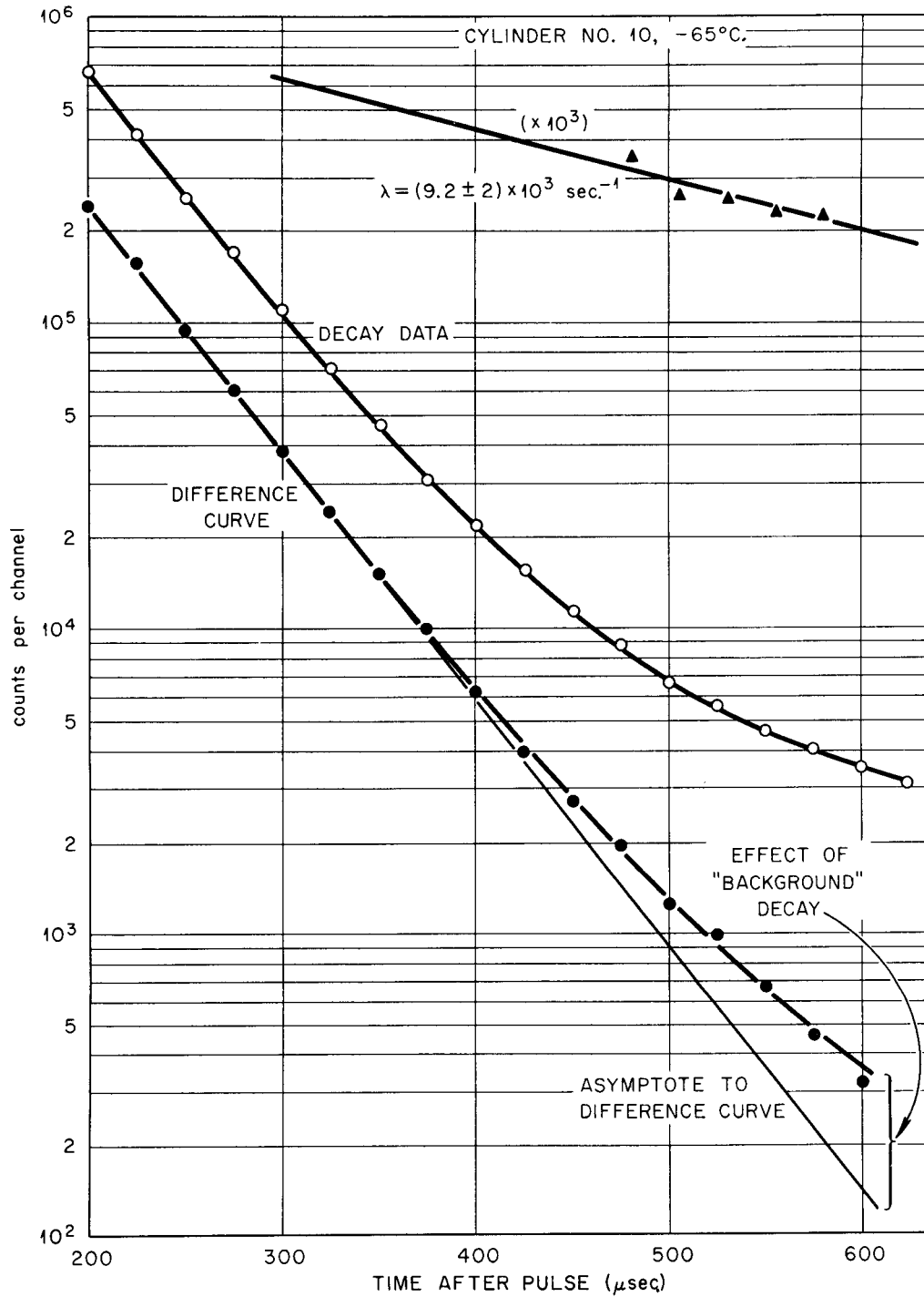


Figure 46. Experimental decay data for cylinder Number 10 at  $-65^{\circ}\text{C.}$ , showing also the difference curve and the "background decay" obtained from it.

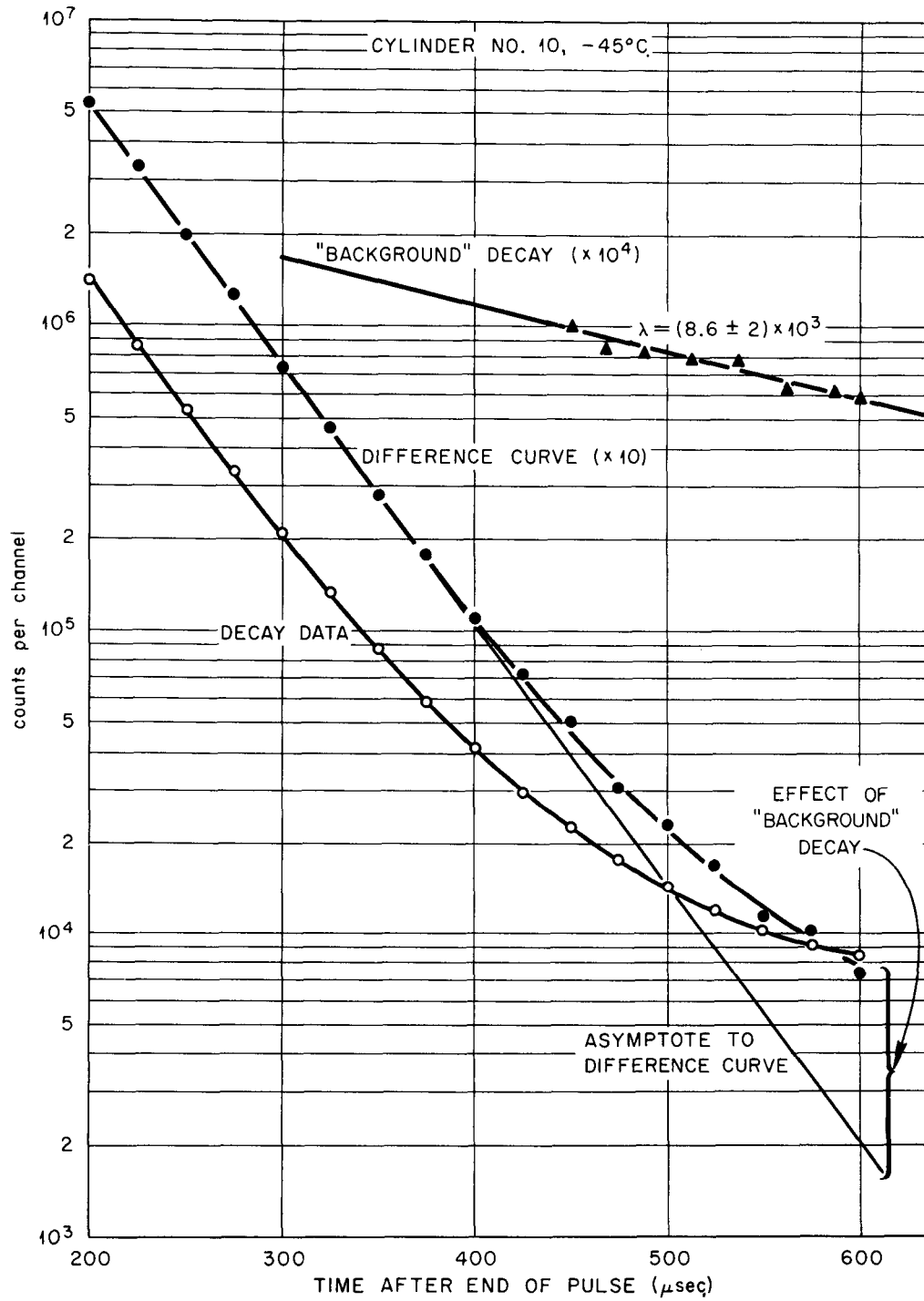


Figure 47. Experimental decay data for cylinder Number 10 at  $-45^\circ\text{C}$ ., showing also the difference curve and the "background decay" obtained from it.

Since the Busing least-squares code is quite general it seemed quite natural to use this code to determine directly the amplitude and frequency of the "background mode" by fitting the experimental data to a model of the form:

$$C_n = P_1 + P_2 e^{-P_3 n(\Delta t)} + P_4 e^{-P_5 n(\Delta t)} \quad (189)$$

Accordingly the data from the smallest cylinders were fitted to this five-parameter model with the Busing code. The results initially were very disappointing because in most instances the code failed to converge at all. In a few cases convergence was obtained after very large numbers of iterations (between 40 and 100), but in most instances, even after 100 iterations, the code failed to converge.

Since it was not certain whether the convergence difficulty could be ascribed to the nature of the model or whether it was due to the presence in the data of an unsuspected component of different shape, a set of artificial data consisting of two exponentials, and including normally distributed random counting errors was constructed. Appendix F gives the details and results of that test. It is clear that, even in the absence of any other factors, such as other modes or non-normal counting variations, it is difficult to fit the data to five parameters simultaneously. The results with the actual experimental data were even more discouraging than those with the artificial data since convergence was obtained in only about 40 per cent of the cases attempted, and usually only for those attempts with the longest waiting time, in which most of the data collected were not used, and in which,

therefore, the accuracy obtained for the main decay frequency was relatively poor.

However, it was found, both with the real data and the artificial data, that holding one of the five parameters, in particular  $P_5$ , fixed resulted in rapid convergence of all cases, and reasonable error assignments for the determination of  $P_3$ . It may be well to define here again the following symbols:  $P_1$ ,  $P_2$ ,  $P_3$ ,  $P_4$ , and  $P_5$  are the coefficients of the fitting model

$$C_n = P_1 + P_2 e^{-P_3 n(\Delta t)} + P_4 e^{-P_5 n(\Delta t)}, \quad (18)$$

where  $C_n$  is the number of counts in the  $n$ th channel.  $\Sigma^2$  is the sum of the squares of the differences between the observed and calculated counts in the channels for any given analysis.

The procedure adopted for the analysis of the small-cylinder data was, therefore, based on this method. For each set of data a series of four-parameter analyses were performed over a range of fixed values of the parameter  $P_5$ . The case which resulted in the minimum value of the sum of the squares of the residuals was taken to be the best fit, and the value of  $P_3$  corresponding to this case was used as the correct value of the decay frequency.

In all the analyses of the two smallest cylinders (11 and 12) the parameter  $\Sigma^2$  possessed a well-defined though often broad minimum and the choice of the best value of  $P_3$  was, therefore, unequivocal. However, for the larger cylinders the result was sometimes that the minimum value of  $\Sigma^2$  occurred for  $P_5 = P_3$ , i.e., the best fit occurred

if the two decays were of the same slope, so that in effect only one exponential parameter was found. And in several cases the minimum of  $\Sigma^2$  occurred at values of  $P_5$  close to zero or even slightly negative. When  $P_5$  is close to zero the "decay term"  $P_4 e^{-P_5 n(\Delta t)}$  becomes essentially a flat background term.

Indeed, when  $P_5$  was  $< 1 \times 10^3 \text{ sec.}^{-1}$  the values of  $P_4$  and  $P_1$  were usually large, but of opposite sign and such magnitude that the sum corresponds to the flat background.

Since, from the results for those cases where  $\Sigma^2$  had a proper minimum, a mean value of  $P_5$  was obtainable, the decay data for Cylinders 8 and 9, as well as some of the data sets for Cylinder 10 were analyzed by specifying for the value of  $P_5$  the mean value obtained from the small-cylinder analyses. It was found, however, that in these intermediate-size cases the amplitude  $P_4$  that resulted was very small, and the effect on  $P_3$  of making this correction was negligible, amounting to, at most, 0.21 per cent in the worse case.

Table VII lists the values obtained for  $P_5$  in Cylinders 10, 11, and 12 by the minimum- $\Sigma^2$  method described above. The variations are seen to be large, and the errors associated with the individual values are also relatively large, since the minima are broad, and difficult to determine accurately. However, the effect of an error in  $P_5$  on  $P_3$  is very small, so that the values of  $P_3$  are not dependent on an accurate value of  $P_5$ . Figure 48 shows the variation of  $P_3$  as a function of  $P_5$ , and also the variation of  $\Sigma^2$  with  $P_5$  for Cylinder 12 at  $-25^\circ\text{C}$ . The method appears, from the figure, to give an extremely sensitive

TABLE VII  
 VALUE OF  $P_5$  CORRESPONDING TO MINIMUM  
 SQUARE SUM OF RESIDUALS

|   | Units of $10^3 \text{ sec.}^{-1}$ |                |                |
|---|-----------------------------------|----------------|----------------|
|   | Cylinder<br>10                    | Cylinder<br>11 | Cylinder<br>12 |
| $-5^\circ\text{C.}$                             | 3.5                               | 7.9            | 4.0            |
| $-25^\circ\text{C.}$                            | 4.0                               | 5.5            | 6.0            |
| $-45^\circ\text{C.}$                            | 9.5                               | 10.0           | 8.5            |
| $-65^\circ\text{C.}$                            | 8.3                               | 8.0            | 4.5            |
| $-85^\circ\text{C.}$                            | 5.8                               | 4.0            | 12.0           |
| Mean Value $6.77 \times 10^3 \text{ sec.}^{-1}$ |                                   |                |                |

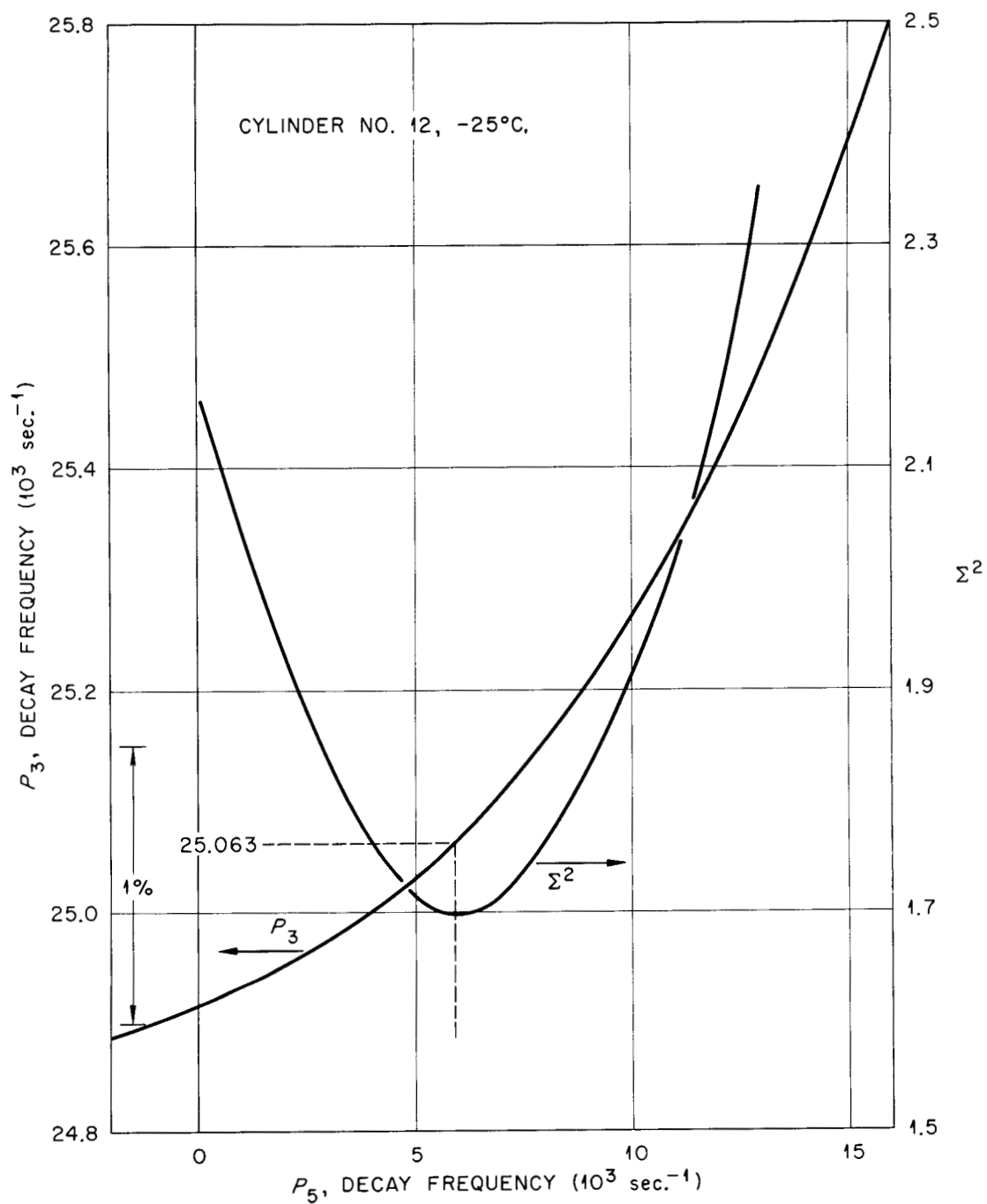


Figure 48.  $P_3$ , the decay frequency, and  $\Sigma^2$ , the square sum of residuals, versus  $P_5$ , the "background" decay frequency obtained by four-parameter least-squares analyses of the decay data in cylinder Number 12, at  $-25^\circ\text{C}$ .

criterion for choosing the best value of  $P_3$ . However this is somewhat spurious. Very small shifts in the values of the counts of the last few channels have a relatively large effect on the location of the minimum. A test was performed by varying the value of  $C_{18}$  the number of counts in Channel 18 for this case by  $\pm\sqrt{C_{18}}$  and  $\pm 3\sqrt{C_{18}}$ . In each case the curve of  $P_3$  versus  $P_5$  was shifted only very slightly, but the location of the minimum of the  $\Sigma^2$  curve shifted significantly. The results are shown in Table VIII. This accounts for the large variations in the location of the minima seen in Table VII (page 186).

For the purpose of checking results this method of analysis was also extended to some of the large ice cylinders. The results supported the conclusion that a small component of negative amplitude and about twice the frequency was present. For example, Figure 49 shows the result obtained for cylinder 1 at  $-5^\circ\text{C}$ . The minimum in  $\Sigma^2$  occurs for  $P_5 = 15.5 \times 10^3 \text{ sec.}^{-1}$ , and the value of  $P_3$  corresponding to the minimum is  $5.856 \times 10^3 \text{ sec.}^{-1}$ . The amplitude,  $P_4$ , of the second component is negative, and amounts to 1.54 per cent of the amplitude of the main component at  $t = 0$ . Note that the value of  $P_3$  corresponding to  $P_5 = 2P_3$  is  $P_3 = 5.89 \times 10^3 \text{ sec.}^{-1}$  which is in very good agreement with the value of  $P_3 = 5.886 \times 10^3 \text{ sec.}^{-1}$  obtained by the earlier method.

In many cases the analysis of the large-cylinder data by this method failed, due to the reasons already described. In most cases where the analysis succeeded the results for  $P_3$  agreed within the limits of error with those obtained by the methods described earlier. Therefore, the large-cylinder decay constants were taken to be those

TABLE VIII  
 EFFECT OF CHANGING THE NUMBER OF COUNTS IN CHANNEL 18  
 OF CYLINDER NUMBER 12 AT  $-25^{\circ}\text{C}$ . ON THE VALUES OF  
 $P_3$  AND  $P_5$  CORRESPONDING TO MINIMUM  $\Sigma^2$

| $C_{18}$                         | Best Value of $P_3$                    | Value of $P_5$ at<br>Location of $\Sigma^2$ Minimum |
|----------------------------------|--|---|
| $C_{18} - 3\sqrt{C_{18}} = 1408$ | $24.890 \times 10^3 \text{ sec.}^{-1}$ | $3.3 \times 10^3 \text{ sec.}^{-1}$                 |
| $C_{18} - \sqrt{C_{18}} = 1486$  | $25.042 \times 10^3 \text{ sec.}^{-1}$ | $5.2 \times 10^3 \text{ sec.}^{-1}$                 |
| $C_{18} = 1525$                  | $25.063 \times 10^3 \text{ sec.}^{-1}$ | $5.9 \times 10^3 \text{ sec.}^{-1}$                 |
| $C_{18} + \sqrt{C_{18}} = 1564$  | $25.086 \times 10^3 \text{ sec.}^{-1}$ | $6.8 \times 10^3 \text{ sec.}^{-1}$                 |
| $C_{18} + 3\sqrt{C_{18}} = 1642$ | $25.124 \times 10^3 \text{ sec.}^{-1}$ | $8.0 \times 10^3 \text{ sec.}^{-1}$                 |

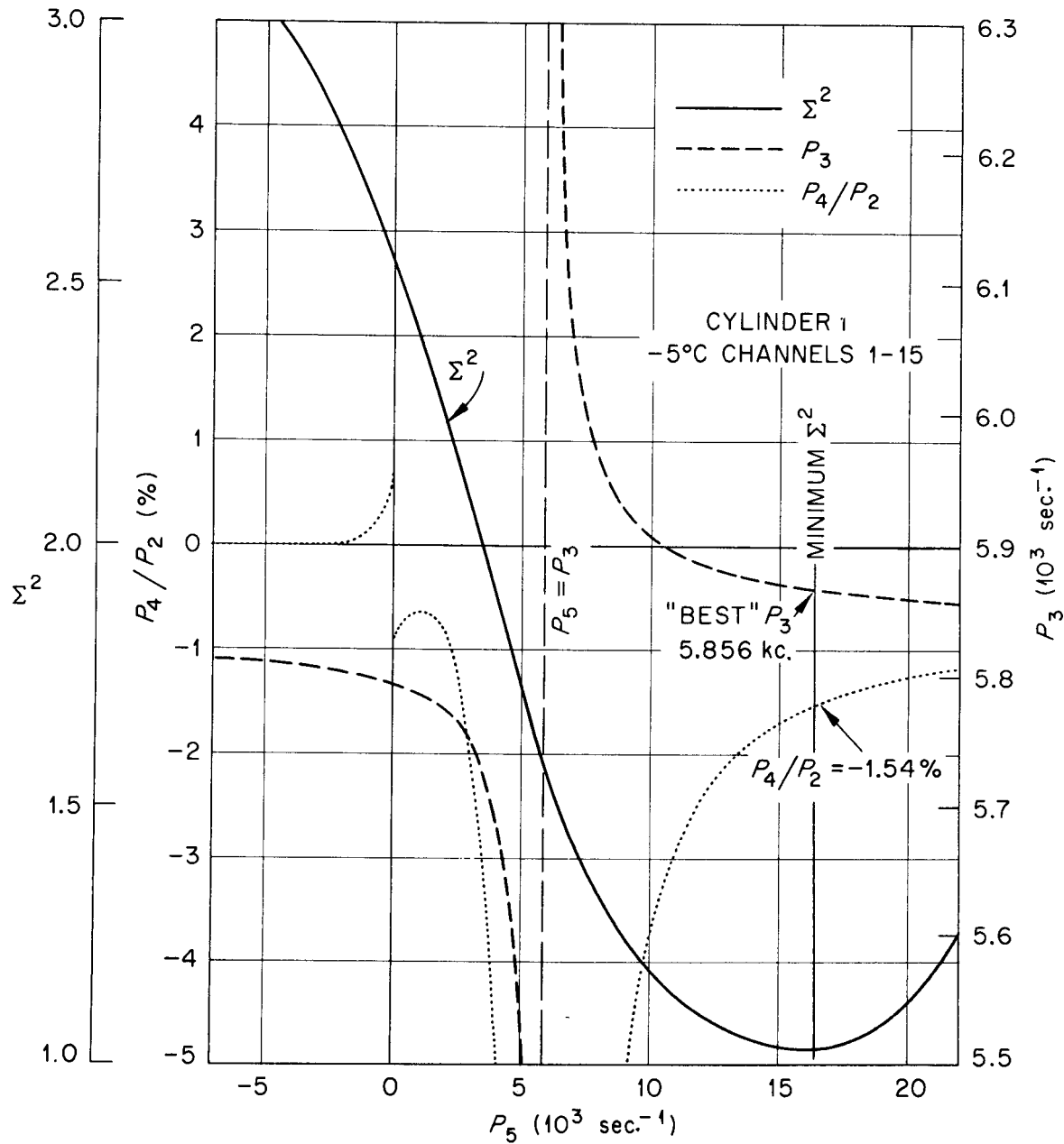


Figure 49. The weighted sum of residuals squared,  $\Sigma^2$ , the parameter  $P_3$ , and the ratio  $P_4/P_2$ , as a function of  $P_5$  for cylinder Number 1 at  $-5^\circ\text{C}$ . The data shown resulted from a series of fixed- $P_5$  fits of the neutron decay data.

obtained by the four-parameter analysis described before.

To summarize briefly, the methods used for obtaining the decay frequencies from the data were the following:

1. Data for Cylinders 1, 2, ..., 6 were analyzed on the assumption that the only significant source of error was the presence of a negative-amplitude mode of double the fundamental frequency. This was checked in some cases by a five-parameter analysis and found to be valid.
2. The data for Cylinders 7, 8, and 9 were analyzed by assuming that a "background" decay with  $P_5 = 6.77 \times 10^3 \text{ sec.}^{-1}$ , (as determined from the small-cylinder data) was present. However, the effect of including this correction was small, and in most cases the results agreed, within the errors, with the values obtained by the large-cylinder analysis method. In these cylinders the effects of the additional decay were almost always smaller than the uncertainties due to the statistics.
3. The three smallest cylinders (10, 11, and 12) were analyzed by a five-parameter model, performing a series of calculations with a range of fixed values for  $P_5$ . In these cylinders, particularly in the last two at high temperatures, the effect of the "background mode" was clearly evident, and was accounted for as described.

It may be appropriate to digress briefly here to consider the cause of the "background decay" observed in the small-cylinder data. Two possible sources suggest themselves. One is back-scattering from

the refrigerator walls and ground; the other is the accelerator itself. Although back-scattering of thermal neutrons was largely reduced by use of cadmium covering on the ice cylinders and the boral inner liner on the test chamber, a very small effect due to epi-cadmium neutrons is not eliminated.

A second possibility is that the accelerator itself might cause such an effect if a very small "tail" were present at the trailing edge of the pulses. Such a tail would have to have an amplitude of only 0.0002-0.0006 at beam cutoff relative to the beam current in the pulse to produce the observed effect. Such a tail would be very difficult to observe directly.

As has already been mentioned, a test was performed inside the test chamber and out without finding any effect attributable to wall scattering. However, the decay frequency of the test cylinder was too low to permit observing such an effect if it were present. In sum, the problem of the origin of this "background" decay is not resolved. However, the amplitude is very low and the effect of this decay component was adequately correctable.

## II. ASSIGNMENT OF DECAY FREQUENCY ERRORS

There are two sources of uncertainty in the values of the decay frequencies,  $P_3$ . One is due to the counting statistics, and the other is due to systematic errors such as the presence of other decay modes, timing errors, channel-width errors, and room-return effects.

The error assignments applied to the data consisted of three parts, which were combined by the usual rule

$$E(P_3) = (E_c^2 + E_t^2 + E_\Delta^2)^{1/2}, \quad (190)$$

where  $E_c$  is the counting error, or statistical error,  $E_t$  is the timing error, and  $E_\Delta$  is the systematic error.

The errors  $E_c$  were obtained directly from the least-squares fit analyses. The weight assigned to each input channel-count was based on the counting statistics only. That is, with  $C_n$  counts observed in the  $n$ th channel the weight assigned to this number is  $(C_n)^{-1}$ . The variance for each output parameter is calculated based on the propagation of the input weights.

The systematic errors,  $E_\Delta$ , would be absent if the data were a perfect fit to the model, within the statistics. However, it is clear from the discussions above, that this is not the case. Two types of perturbations have been discussed in detail, and one or the other has been accounted for in the model applied to each set of decay data. But, while one of these is dominant in any one case, they must both be present, so that neglecting the other must give some source of systematic error. In addition, the effects of channel-width nonuniformities have not been included, though, at least for the early data taken without the use of the master gate circuit (see Chapter III) such errors may be significant.

As a test of the presence of errors other than statistics the distribution of residuals was tested. A FORTRAN Code was written to process the input data as follows. For each set of decay data a

back-calculation was performed, using the final set of five parameters, to obtain the set of values  $Y_{k,\ell,n}$  where  $k$  designates the twelve cylinder numbers,  $\ell$  designates the five temperatures, and  $n$  designates the eighteen channel numbers. The ratio

$$(Y_{k,\ell,n} - C_{k,\ell,n}) / [(C_{k,\ell,n})^{1/2}] \quad (191)$$

was then obtained for each of the 1080 channel counts. This ratio is the residual between the observed and calculated value of the channel count, in units of the standard deviation. The distribution of the absolute values of this ratio was then computed. Appendix G includes the flow sheet and listing of this FORTRAN program, which was also used to generate the Table of Results of Appendix C.

Figure 50 shows the distribution obtained, and the expected distribution assuming only statistical errors in the data.

It is apparent that the spread of the data is significantly wider than would be expected on the basis of counting statistics alone. Examination of the residuals listed in Appendix C shows that most of this spread is due to the small cylinders. To take these error sources into account, the following procedure was used.

The noncounting-statistic errors are of two types. One is due to random channel counting errors, beyond those due to counting statistics. In order to evaluate these, without the effects of nonrandom errors such as other modes and room return, each set of data was divided into two sets. One consisted of Channels 1, 3, 5, ..., 17,

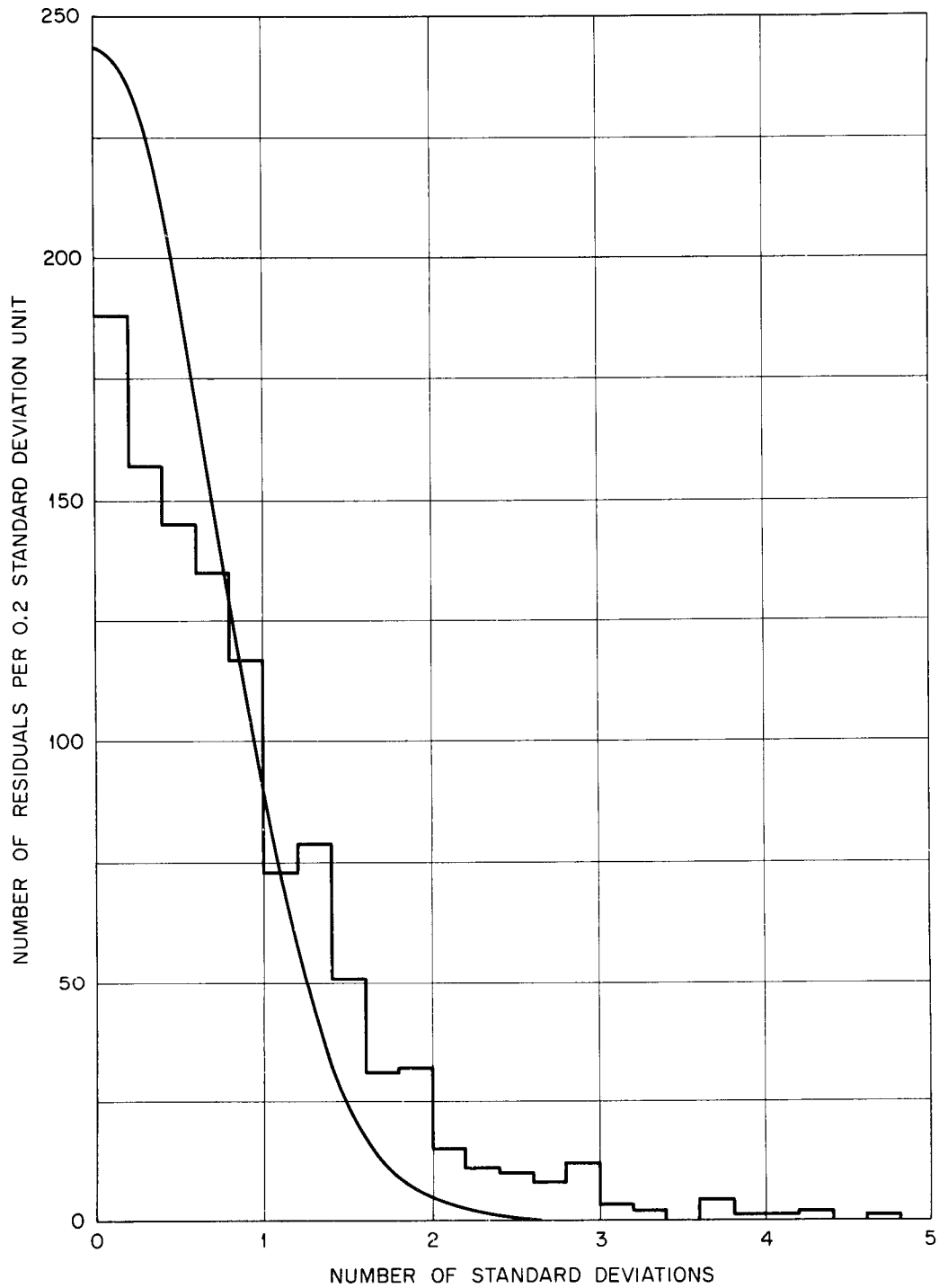


Figure 50. Distribution of absolute values of residuals between the observed and calculated channel counts. The normal distribution curve assuming only counting-statistical errors is shown for comparison.

and the other of Channels 2, 4, 6, ..., 18.

It was found that the results of these two analyses often differed by more than the error ascribable to the statistics. In order to estimate the random error not due to statistics the mean of the absolute values of the differences (averaged over the five temperatures for each cylinder) was taken as a measure of the total random error, and the counting statistics was then subtracted to get the estimate of the error due to other random sources. The equation used was

$$E_{k,l} = \left\{ \left[ \frac{1}{5} \sum_{l=1}^5 |P_{3(k,l)}^{\text{odd}} - P_{3(k,l)}^{\text{even}}| \right]^2 - \left( \frac{V_{k,l}^{\text{odd}} + V_{k,l}^{\text{even}}}{2} \right)^{1/2} \right\}, \quad (192)$$

where  $P_{3(k,l)}^{\text{odd}}$  and  $P_{3(k,l)}^{\text{even}}$  are the values of the parameter  $P_3$  obtained using the odd-numbered and even-numbered channels respectively, and  $V^{\text{odd}}$  and  $V^{\text{even}}$  are the corresponding variances obtained for parameter  $P_3$  by the least-squares calculation. If

$$\frac{1}{5} \sum_{l=1}^5 |P_{3(k,l)}^{\text{odd}} - P_{3(k,l)}^{\text{even}}| \leq \frac{1}{2} (V_{k,l}^{\text{odd}} + V_{k,l}^{\text{even}}) \quad (193)$$

then  $E_{k,l}^{(r)}$  was set equal to zero.

The contribution to the error due to the nonrandom factors such as room-return and higher modes was obtained by considering the mean difference between the analysis of Channels 1-15 and 4-18, averaged over the five temperatures for each cylinder. If no systematic effects are present, the mean value should be zero. Since it is unlikely that

the mean value of only five cases would be really zero, this method yields a conservative estimate of the error. However, in the majority of cases (eight out of twelve) at least four of the five differences had the same sign, so that it is probable that a real source of error existed in these cases. Again, the effect of counting statistics was subtracted by use of the equation

$$E_{k, \ell}^{(p)} = \left\{ \frac{1}{5} \sum_{\ell=1} \left[ P_{\bar{3}}(k, \ell) (1-15) - P_{\bar{3}}(k, \ell) (4-18) \right] \right\}^2 - \left\{ \frac{V(1-15) + V(4-18)}{2} \right\}^{1/2}, \quad (194)$$

where  $P_{\bar{3}}(k, \ell) (1-15)$  and  $P_{\bar{3}}(k, \ell) (4-18)$  are the values of  $P_{\bar{3}}$  obtained from analysis of channels 1-15 and 4-18 respectively, and where  $V_{k, \ell} (1-15)$  and  $V_{k, \ell} (4-18)$  are the variances of these parameters. In cases where the difference in Equation (194) was  $\leq 0$  the value of  $E_{k, \ell}^{(p)}$  was taken to be zero. The error  $E_{k, \ell}^{(\Delta)}$  due to systematic sources, is then given by

$$E_{k, \ell}^{(\Delta)} = \left\{ \left[ E_{k, \ell}^{(r)} \right]^2 + \left[ E_{k, \ell}^{(p)} \right]^2 \right\}^{1/2}. \quad (195)$$

The timing error  $E_t$  is not directly detectable in the data, but enters the results directly since  $P_{\bar{3}}$  is proportional to frequency of the timing oscillator. The magnitude of the time drifts was discussed in Chapter III, and was no more than 0.02 per cent over a time of eight hours, which is the time interval for collection of the data for

one cylinder at one temperature. To this must be added the uncertainty in the time calibration of the frequency meter. The frequency standard used as primary time source was certified to be accurate within 0.005 per cent, and the maximum long-term drift of the local frequency meter was found not to exceed 0.015 per cent. A total timing error of 0.03 per cent was, therefore, taken as a conservative estimate, i.e.,  $E_t$  was calculated by:

$$E_t = 0.0003 P_3 . \quad (196)$$

All the error calculations were made by the IBM-7090 computer, using a FORTRAN code called CALER written for this purpose. The flow-sheet and code are shown in Appendix G.

For the large cylinders the counting statistics, i.e.,  $E_c$ , was the dominant error, and in many instances either  $E_r$  or  $E_p$  became zero. However, for the smaller cylinders the sources of error other than  $E_c$  became dominant, amounting to most of the error (60 to 80 per cent) for the smallest cylinders.

The range of errors extends from 0.35 per cent (Cylinder 3,  $-65^\circ\text{C}.$ ) to 1.80 per cent (Cylinder 11,  $-85^\circ\text{C}.$ ).

Table IX lists the final results for the decay parameters and their associated errors. Figures 51, 52, and 53 are plots of the decay parameter as a function of temperature for each of the twelve cylinders. The variation with temperature is close to linear in all cases, with the maximum deviation from a linear fit of the order of 4 per cent.

TABLE IX  
MEASURED DECAY FREQUENCIES IN ICE CYLINDERS

| Cylinder<br>Number | Temperature (°C.) |                |                             |                |                |
|--------------------|-------------------|----------------|-----------------------------|----------------|----------------|
|                    | -5                | -25            | -45                         | -65            | -85            |
| 1                  | 5.886 ± 0.075     | 5.724 ± 0.040  | 5.630 ± 0.052               | 5.579 ± 0.059  | 5.443 ± 0.035  |
| 2                  | 6.478 ± 0.060     | 6.387 ± 0.034  | 6.207 ± 0.038               | 6.031 ± 0.035  | 5.890 ± 0.061  |
| 3                  | 6.745 ± 0.061     | 6.584 ± 0.048  | 6.413 ± 0.066               | 6.266 ± 0.022  | 6.096 ± 0.053  |
| 4                  | 6.864 ± 0.067     | 6.699 ± 0.039  | 6.584 ± 0.070               | 6.455 ± 0.038  | 6.226 ± 0.066  |
| 5                  | 7.321 ± 0.047     | 7.121 ± 0.051  | 6.888 ± 0.049               | 6.825 ± 0.076  | 6.493 ± 0.072  |
| 6                  | 8.829 ± 0.040     | 8.468 ± 0.060  | 8.214 ± 0.070               | 8.052 ± 0.073  | 7.593 ± 0.072  |
| 7                  | 12.476 ± 0.043    | 12.112 ± 0.079 | 11.493 ± 0.087              | 10.997 ± 0.076 | 10.272 ± 0.082 |
| 8                  | 16.668 ± 0.053    | 15.899 ± 0.101 | 14.915 ± 0.073              | 14.341 ± 0.065 | 13.310 ± 0.100 |
| 9                  | 20.390 ± 0.133    | 19.258 ± 0.110 | 18.083 ± 0.127 <sup>a</sup> | 17.307 ± 0.132 | 16.055 ± 0.129 |
| 10                 | 22.829 ± 0.240    | 21.409 ± 0.172 | 20.349 ± 0.245              | 19.292 ± 0.295 | 17.772 ± 0.189 |
| 11                 | 24.309 ± 0.378    | 22.841 ± 0.228 | 21.669 ± 0.258              | 21.226 ± 0.195 | 19.073 ± 0.344 |
| 12                 | 26.771 ± 0.383    | 25.063 ± 0.241 | 23.662 ± 0.229              | 22.555 ± 0.198 | 20.808 ± 0.236 |

<sup>a</sup>Interpolated. Measured value at -50°C. 17.874 ± 0.127.

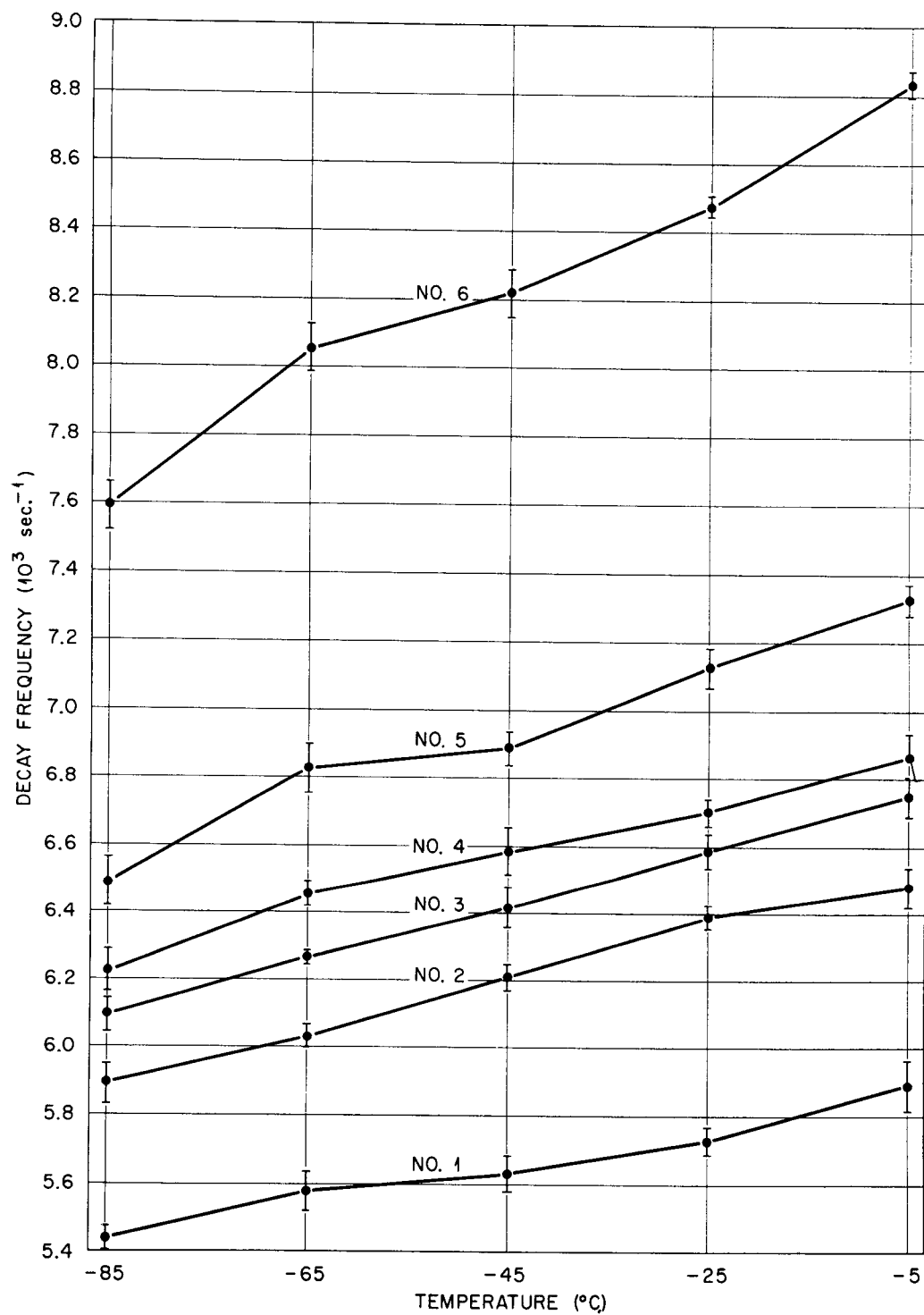


Figure 51. Decay frequencies versus temperature for cylinders Number 1, 2, 3, 4, 5, and 6.

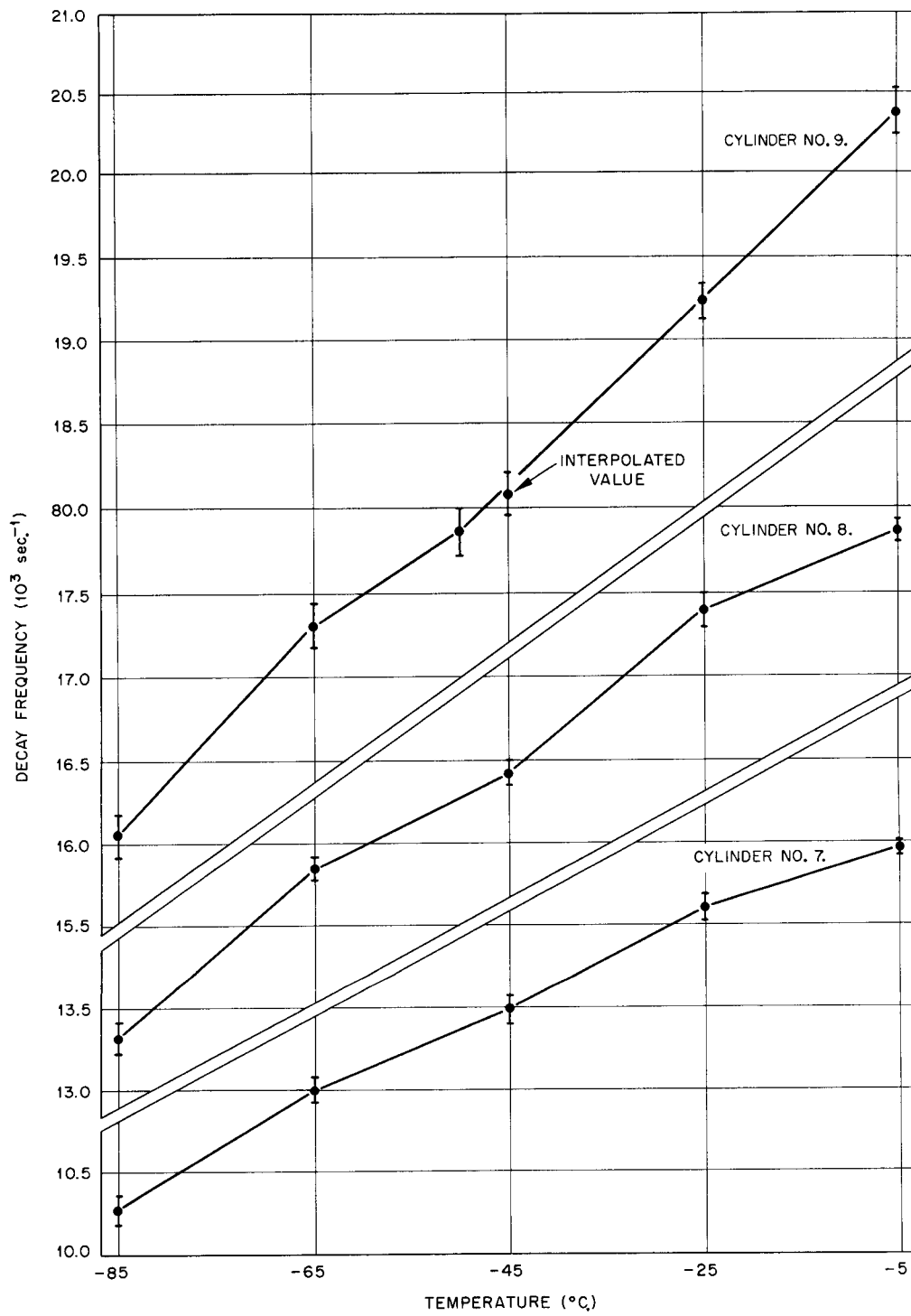


Figure 52. Decay frequencies versus temperature for cylinders Number 7, 8, and 9.

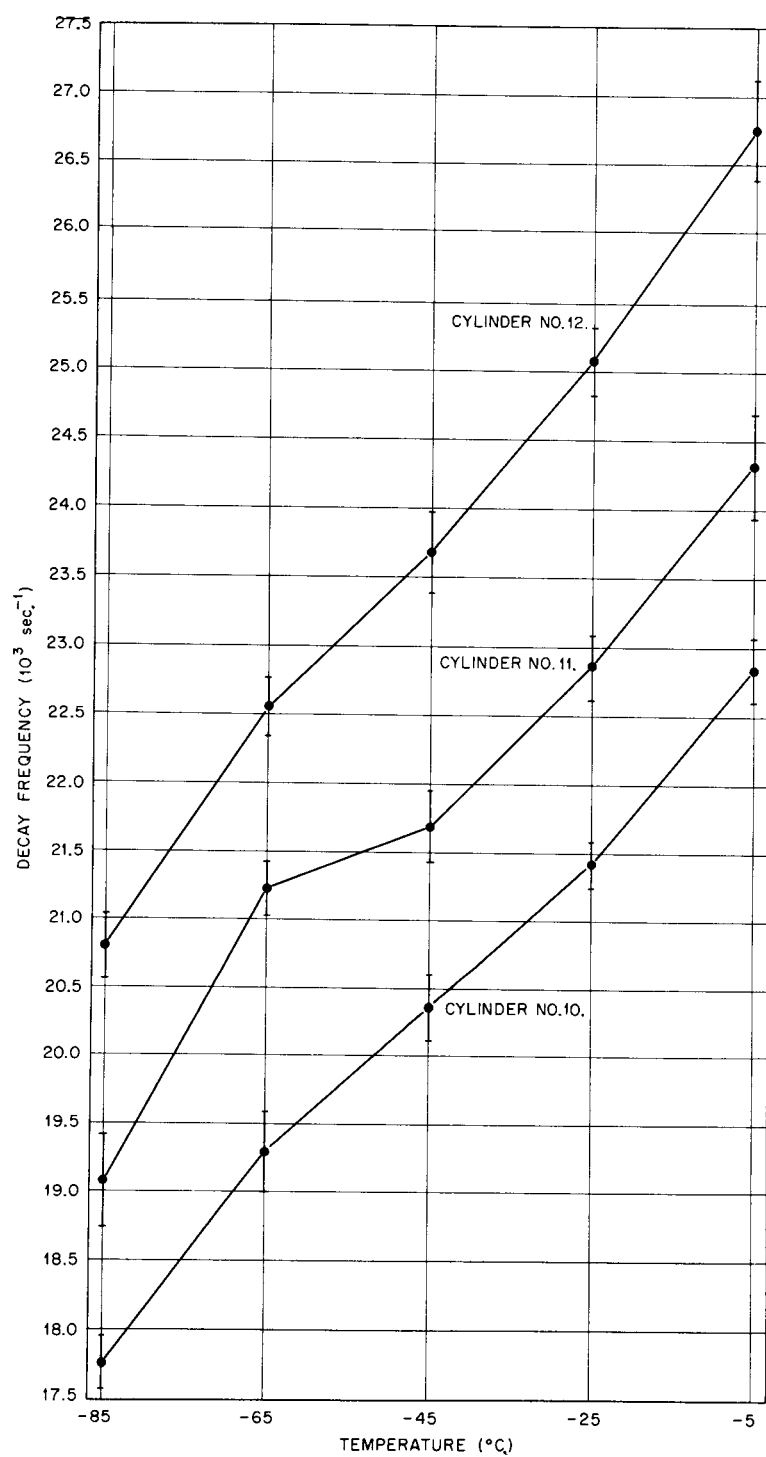


Figure 53. Decay frequencies versus temperature for cylinders Number 10, 11, and 12.

### III. CALCULATION OF THE DIFFUSION PARAMETERS

The final step in the data reduction, having obtained the decay frequencies and knowing the cylinder dimensions, is to obtain the diffusion parameters.

There are two inter-related steps to this procedure. First, a buckling must be assigned to each cylinder, and then the values of the decay frequencies (henceforth termed  $\lambda$ ) are fitted to a power-series expansion in powers of the buckling to obtain the diffusion parameters. The two steps are inter-related because the buckling is a function (because of the extrapolation distance) of the linear coefficient of the power series in the buckling.

The buckling of a cylinder of dimensions H cm. high and R cm. in diameter is given by

$$B^2 = \frac{\pi^2}{[H + e(H)]^2} + \frac{\nu_0^2}{[R + e(R)]^2} . \quad (197)$$

The extrapolation distances  $e(H)$  and  $e(R)$  have the form:

$$e(H) = 2F_e(3D)P \quad (198)$$

$$e(R) = F_e(3D)Q \quad , \quad (199)$$

where  $F_e = 0.704$  is the extrapolation-distance factor obtained for flat vacuum boundaries by one-velocity transport theory (Weinberg and Wigner, 1958) assuming pure scattering, i.e., no absorption, D is the diffusion coefficient, and P and Q are the correction factors (Chapter II).

The coefficient of the linear term in the expansion

$$\lambda = a_0 + a_1 B^2 + a_2 (B^2)^2 + \dots = \sum_{k=0}^n a_k (B^2)^k \quad (200)$$

is identified as:

$$a_1 = (vD)_0 = \frac{2v_0}{\sqrt{\pi}} \left( \frac{T}{T_0} \right)^{1/2} D \quad (201)$$

Therefore,

$$D = \frac{a_1 \sqrt{\pi T_0}}{2v_0 \sqrt{T}} = (6.902 \times 10^{-5}) \frac{a_1}{\sqrt{T}} \quad (202)$$

Equation (202) is the connecting link between the buckling and the diffusion coefficient.

In order to solve for the implicit dependence on D an iterative procedure was devised as follows:

First an estimate of D for the given temperature is made and the buckling for each cylinder is calculated by Equation (197) at this temperature.

Then the twelve value-pairs  $(\lambda_i, B_i^2)$  are used to perform a linear least-squares fit to Equation (185) to the desired order in  $B^2$ . The coefficient  $a_1$  is then used to recalculate D by Equation (202), and the bucklings are recalculated using this new value of D. The least-squares fitting procedure is then repeated with the new buckling values. This iterative process is repeated until the values obtained for D agree

within some predetermined error limit. The convergence criterion used in the present work was

$$\left| \frac{D_n - D_{n+1}}{D_n} \right| \leq 1 \times 10^{-4} . \quad (203)$$

The fitting procedure described here was coded for the computer and the code (BIFIT LEAST SQUARES) is given in Appendix G.

This fitting was done by means of a code BIFIT, which has provisions for explicit inclusion of errors in both parameters. The errors in the  $\lambda$  values were obtained as described in Chapter IV and the errors in  $B^2$  are obtained from the dimension uncertainties:

$$\begin{aligned} \delta B^2 &= \left[ \left( \frac{\partial B^2}{\partial H} \right)^2 (\delta H)^2 + \left( \frac{\partial B^2}{\partial R} \right)^2 (\delta R)^2 \right]^{1/2} \\ &= \left\{ \frac{4\pi^4}{[H + e(H)]^6} (\delta H)^2 + \frac{4\nu_o^4}{[R + e(R)]^6} (\delta R)^2 \right\}^{1/2} . \quad (204) \end{aligned}$$

The code solves this equation at each  $B^2$  computation and this  $\delta B^2$  value is used in the least-squares fitting procedure.

This calculation was applied at each of the five temperatures, and values of the parameters were obtained for linear quadratic, third-power and fourth-power fits of  $\lambda$  versus  $(B^2)$ , i.e., with  $n$  [Equation (200)] equal to 1, 2, 3, and 4. Table X shows the values obtained for the coefficients in each of the four fits performed at each temperature.

It was necessary at this point to decide how many terms in the

TABLE X  
 PARAMETERS OBTAINED BY FITTING  $\lambda$  VERSUS  $B^2$  DATA TO VARIOUS ORDERS OF THE SERIES  $\lambda = \sum_{k=0}^n a_k (B^2)^k$

| Temperature<br>(°C.) | Parameter | Order of Fitting                |                                  |                                  |                                  |
|----------------------|-----------|---------------------------------|----------------------------------|----------------------------------|----------------------------------|
|                      |           | n = 1                           | n = 2                            | n = 3                            | n = 4                            |
| -5                   | $a_0$     | $(4.655 \pm 0.036) \times 10^3$ | $(4.485 \pm 0.058) \times 10^3$  | $(4.494 \pm 0.094) \times 10^3$  | $(4.610 \pm 0.149) \times 10^3$  |
|                      | $a_1$     | $(3.062 \pm 0.020) \times 10^4$ | $(3.298 \pm 0.063) \times 10^4$  | $(3.279 \pm 0.150) \times 10^4$  | $(2.996 \pm 0.311) \times 10^4$  |
|                      | $a_2$     |                                 | $-(3.734 \pm 1.113) \times 10^3$ | $-(3.090 \pm 5.641) \times 10^3$ | $(13.62 \pm 18.64) \times 10^3$  |
|                      | $a_3$     |                                 |                                  | $-(0.693 \pm 5.742) \times 10^3$ | $-(39.87 \pm 40.88) \times 10^3$ |
|                      | $a_4$     |                                 |                                  |                                  | $(28.36 \pm 29.05) \times 10^3$  |
| -25                  | $a_0$     | $(4.650 \pm 0.027) \times 10^3$ | $(4.445 \pm 0.047) \times 10^3$  | $(4.483 \pm 0.079) \times 10^3$  | $(4.680 \pm 0.118) \times 10^3$  |
|                      | $a_1$     | $(2.806 \pm 0.017) \times 10^4$ | $(3.137 \pm 0.061) \times 10^4$  | $(3.056 \pm 0.140) \times 10^4$  | $(2.540 \pm 0.265) \times 10^4$  |
|                      | $a_2$     |                                 | $-(4.729 \pm 0.986) \times 10^3$ | $-(1.831 \pm 5.071) \times 10^3$ | $(29.53 \pm 16.02) \times 10^3$  |
|                      | $a_3$     |                                 |                                  | $-(2.967 \pm 4.926) \times 10^3$ | $-(74.82 \pm 34.31) \times 10^3$ |
|                      | $a_4$     |                                 |                                  |                                  | $(50.35 \pm 23.51) \times 10^3$  |
| -45                  | $a_0$     | $(4.638 \pm 0.031) \times 10^3$ | $(4.484 \pm 0.050) \times 10^3$  | $(4.442 \pm 0.086) \times 10^3$  | $(4.522 \pm 0.132) \times 10^3$  |
|                      | $a_1$     | $(2.579 \pm 0.017) \times 10^4$ | $(2.819 \pm 0.060) \times 10^4$  | $(2.905 \pm 0.150) \times 10^4$  | $(2.694 \pm 0.292) \times 10^4$  |
|                      | $a_2$     |                                 | $-(3.432 \pm 0.972) \times 10^3$ | $-(6.334 \pm 5.327) \times 10^3$ | $(6.557 \pm 17.47) \times 10^3$  |
|                      | $a_3$     |                                 |                                  | $(2.869 \pm 5.034) \times 10^3$  | $-(27.04 \pm 37.7) \times 10^3$  |
|                      | $a_4$     |                                 |                                  |                                  | $(21.15 \pm 26.61) \times 10^3$  |
| -65                  | $a_0$     | $(4.590 \pm 0.026) \times 10^3$ | $(4.463 \pm 0.044) \times 10^3$  | $(4.395 \pm 0.085) \times 10^3$  | $(4.305 \pm 0.142) \times 10^3$  |
|                      | $a_1$     | $(2.448 \pm 0.016) \times 10^4$ | $(2.648 \pm 0.055) \times 10^4$  | $(2.784 \pm 0.150) \times 10^4$  | $(3.011 \pm 0.313) \times 10^4$  |
|                      | $a_2$     |                                 | $-(2.824 \pm 0.877) \times 10^3$ | $-(7.384 \pm 5.307) \times 10^3$ | $-(20.79 \pm 18.57) \times 10^3$ |
|                      | $a_3$     |                                 |                                  | $(4.443 \pm 4.953) \times 10^3$  | $(35.47 \pm 40.32) \times 10^3$  |
|                      | $a_4$     |                                 |                                  |                                  | $-(22.17 \pm 28.37) \times 10^3$ |
| -85                  | $a_0$     | $(4.597 \pm 0.022) \times 10^3$ | $(4.499 \pm 0.046) \times 10^3$  | $(4.504 \pm 0.073) \times 10^3$  | $(4.584 \pm 0.110) \times 10^3$  |
|                      | $a_1$     | $(2.160 \pm 0.017) \times 10^4$ | $(2.320 \pm 0.057) \times 10^4$  | $(2.309 \pm 0.132) \times 10^4$  | $(2.089 \pm 0.257) \times 10^4$  |
|                      | $a_2$     |                                 | $-(2.316 \pm 0.920) \times 10^3$ | $-(1.916 \pm 4.754) \times 10^3$ | $(11.75 \pm 15.56) \times 10^3$  |
|                      | $a_3$     |                                 |                                  | $(0.405 \pm 4.504) \times 10^3$  | $-(31.59 \pm 33.25) \times 10^3$ |
|                      | $a_4$     |                                 |                                  |                                  | $(21.60 \pm 22.62) \times 10^3$  |

series to use. Hobson, Calame, and Daitch (1963) performed a "computer experiment" (which is free of the problems of errors and statistics) based on a fairly simple model of neutron transport in water. They used a Nelkin isotropic energy-exchange kernel and a Goertzel-Selengut-Nelkin P-1 kernel in diffusion theory and included transport corrections for the diffusion cooling coefficient. They point out that since the parameters change as more terms are added, the correct value is the asymptotic value as the number of terms becomes infinite. However, when they repeated their calculations with artificial random errors normally distributed, with mean-square deviations of one half and one per cent, they found that the accuracy of the coefficients diminishes rapidly as coefficients are added, and they conclude that one should fit to only a quadratic in  $B^2$ .

The present data bear out this conclusion very well. Figure 54 shows the effect on the coefficients  $a_0$  and  $a_1$  as the number of terms is increased, for the data at  $-25^\circ\text{C}$ . The same behavior is noted at the other temperatures. There is a real change in these two parameters in going from  $n = 1$  to  $n = 2$ . Thereafter the increase in errors is rapid, and the errors become so large that the values for  $a_0$  and  $a_1$  found with  $n = 3$  and  $n = 4$  are consistent with those found using  $n = 2$ . This is indicated by the dotted lines in Figure 54 which is a level line at the value of the parameter at  $n = 2$ . Further, the trend is not monotonic with increasing  $n$  in this case, though it is for some other temperatures. However, in most cases, the values of  $a_0$  and  $a_1$  obtained with  $n = 2$  are consistent with those obtained with larger  $n$  within the errors.

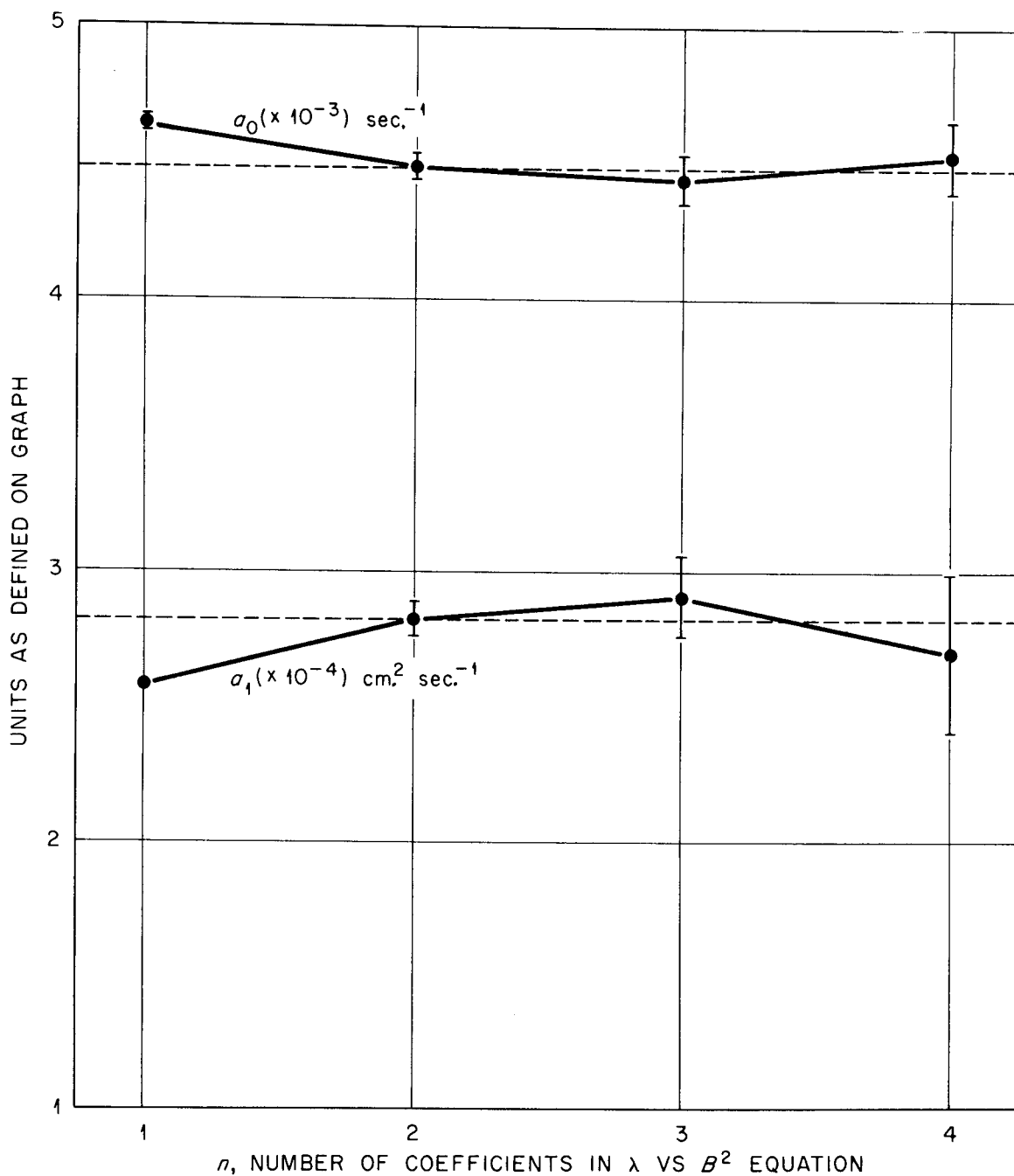


Figure 54. Parameters  $a_0$  and  $a_1$  obtained by fitting the decay frequencies at  $-45^\circ\text{C}$ . to the equation  $\lambda = \sum_{k=0}^n a_k (B^2)^k$ , as function of  $n$ . Dotted lines are at the values for  $n = 2$ .

Figure 55 shows the effect of  $n$  on  $a_2$  and  $a_3$ . As far as  $a_2$  is concerned, the value obtained with  $n = 3$  is consistent with that for  $n = 2$ , though the size of the error on the  $n = 3$  value makes this of little significance. With  $n = 4$  the error in  $a_2$  is much larger than the value, so no significance can be attached to this value, although, again, it is consistent with the value found using  $n = 2$ .

Both the values for  $a_4$  have errors much larger than the value, so that no information about the existence of such a term can be inferred, particularly since the two values have opposite signs. A value of zero is quite consistent with the data. The same holds true for the single value obtained for  $a_5$  by fitting to  $B^8$  terms: its error is greater than the value, so that no significance can be attached to it.

These results, as well as the calculations by Hobson, Calame, and Daitch (1963), thus agree that the most suitable choice of a model to fit the decay data is

$$\lambda = a_0 + a_1 B^2 + a_2 B^4 . \quad (205)$$

The column for  $n = 2$  in Table X (page 206) thus lists the final data from the present experiments. The interpretation of these results will be treated in the next Chapter.

Figures 56, 57, 58, and 59 are plots of  $\lambda$  versus  $B^2$  with  $n = 1, 2, 3,$  and  $4$  at  $-45^\circ\text{C}$ . Figures 60, 61, 62, and 63 are plots of the curves of  $\lambda$  versus  $B^2$  at  $-5^\circ\text{C}$ .,  $-25^\circ\text{C}$ .,  $-65^\circ\text{C}$ ., and  $-85^\circ\text{C}$ ., respectively with  $n = 2$ . In each of these figures the data points and the fitted curve as well as the asymptote to the curve at  $B^2 = 0$  are shown. The

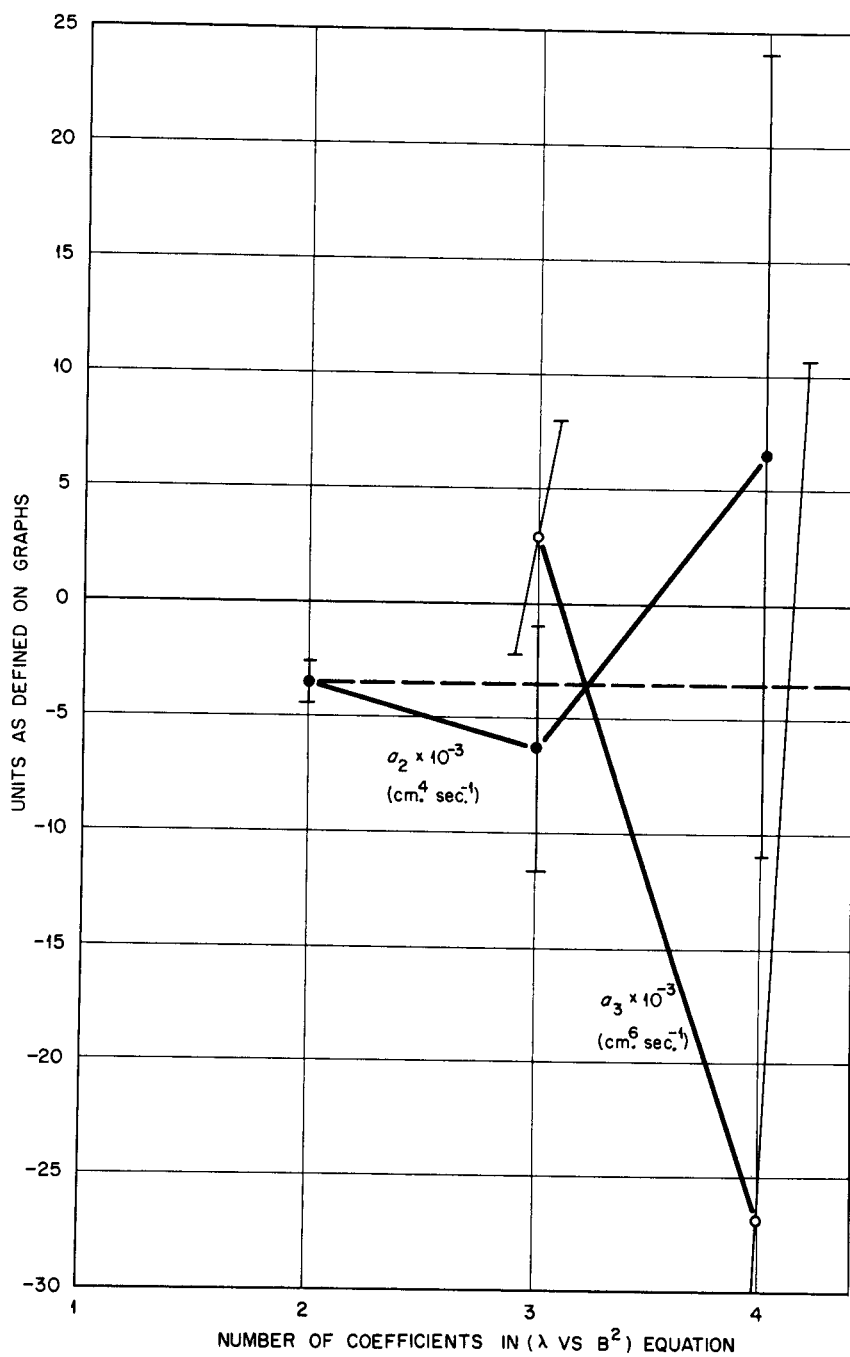


Figure 55. Parameters  $a_2$  and  $a_3$  obtained by fitting the decay frequencies at  $-45^\circ\text{C}$ . to the equation  $\lambda = \sum_{k=0}^n a_k (B^2)^k$ , as function of  $n$ . Dotted lines are at the value for  $n = 2$ .

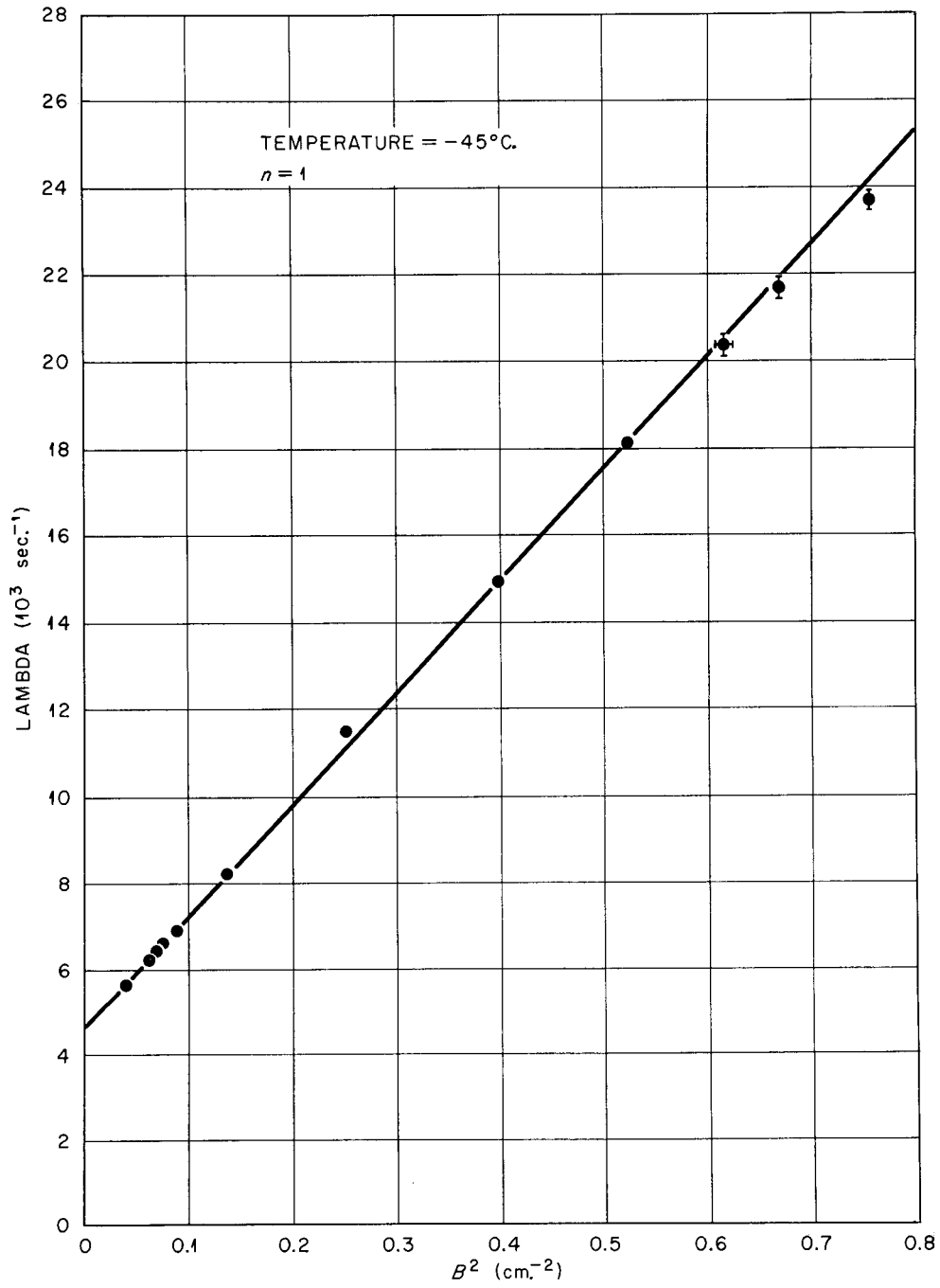


Figure 56.  $\lambda$  versus  $B^2$  for data at  $-45^\circ\text{C}$ . The data are fitted to the equation  $\lambda = \sum_{k=0}^n a_k (B^2)^k$  for  $n = 1$ .

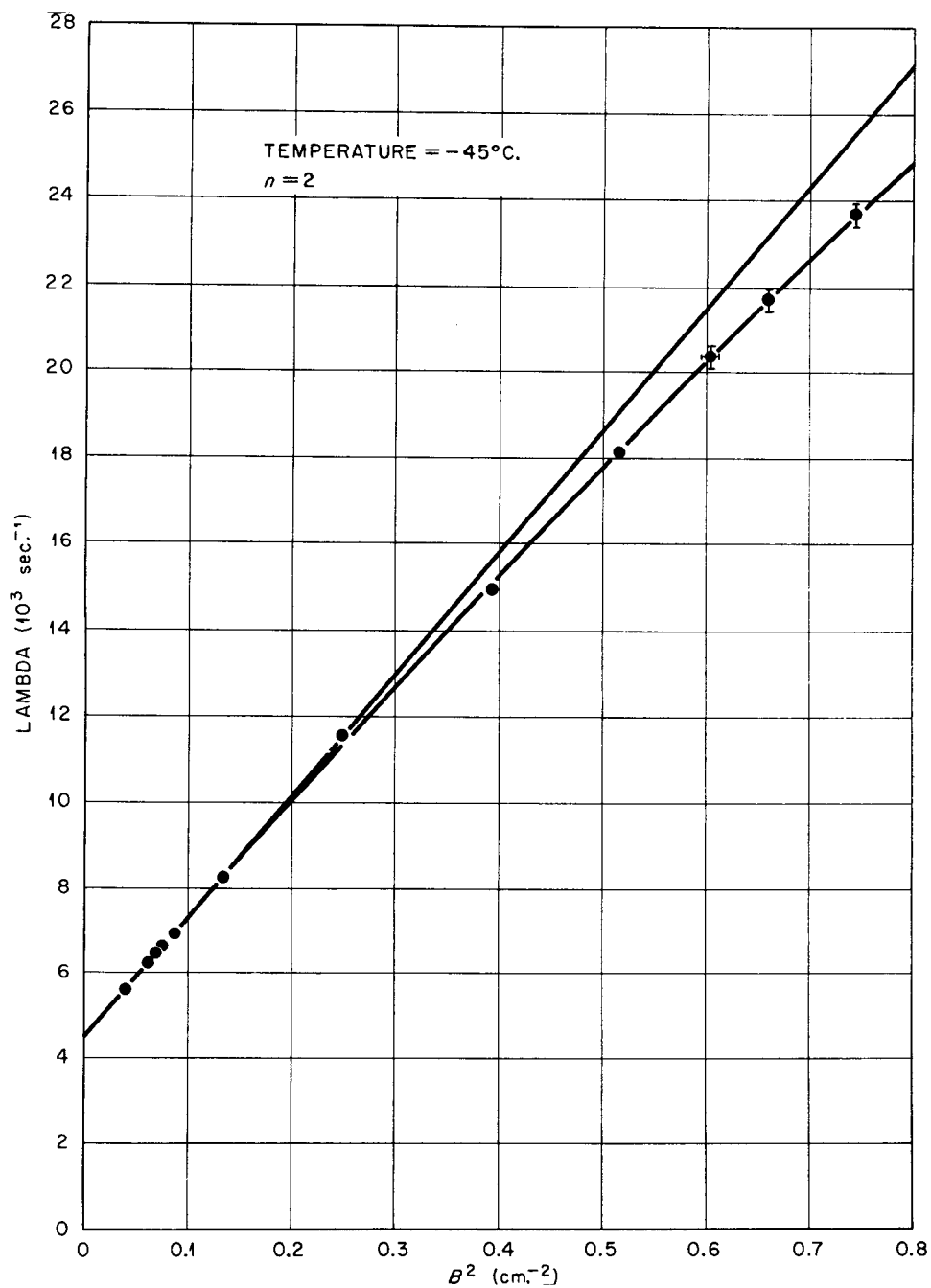


Figure 57.  $\lambda$  versus  $B^2$  for data at  $-45^\circ\text{C}$ . The data are fitted to the equation  $\lambda = \sum_{k=0}^n a_k (B^2)^k$  for  $n = 2$ . The straight line shows the slope of the curve at  $B^2 = 0$ .

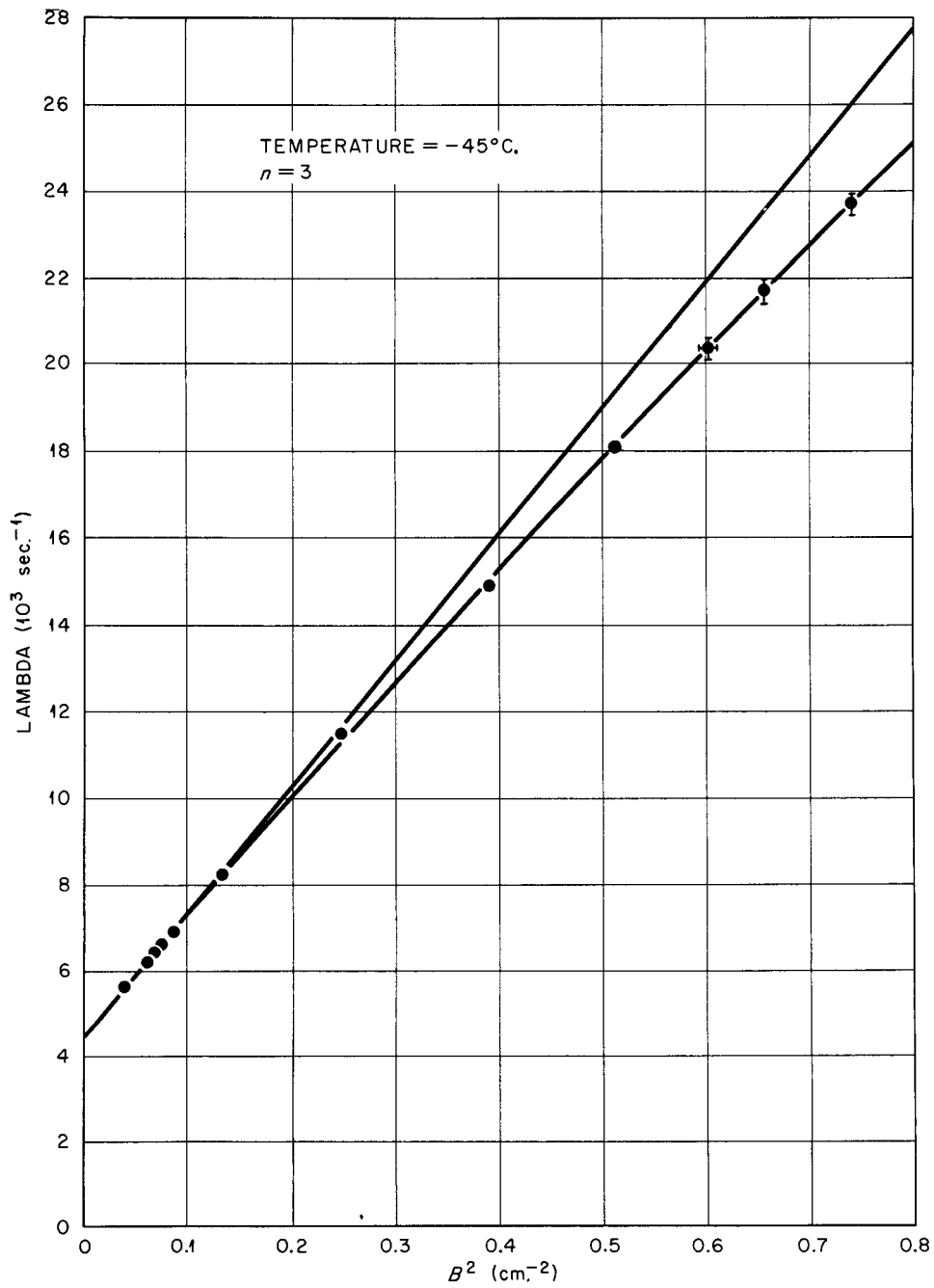


Figure 58.  $\lambda$  versus  $B^2$  for data at  $-45^\circ\text{C}$ . The data are fitted to the equation  $\lambda = \sum_{k=0}^n a_k (B^2)^k$  for  $n = 3$ . The straight line shows the slope of the curve at  $B^2 = 0$ .

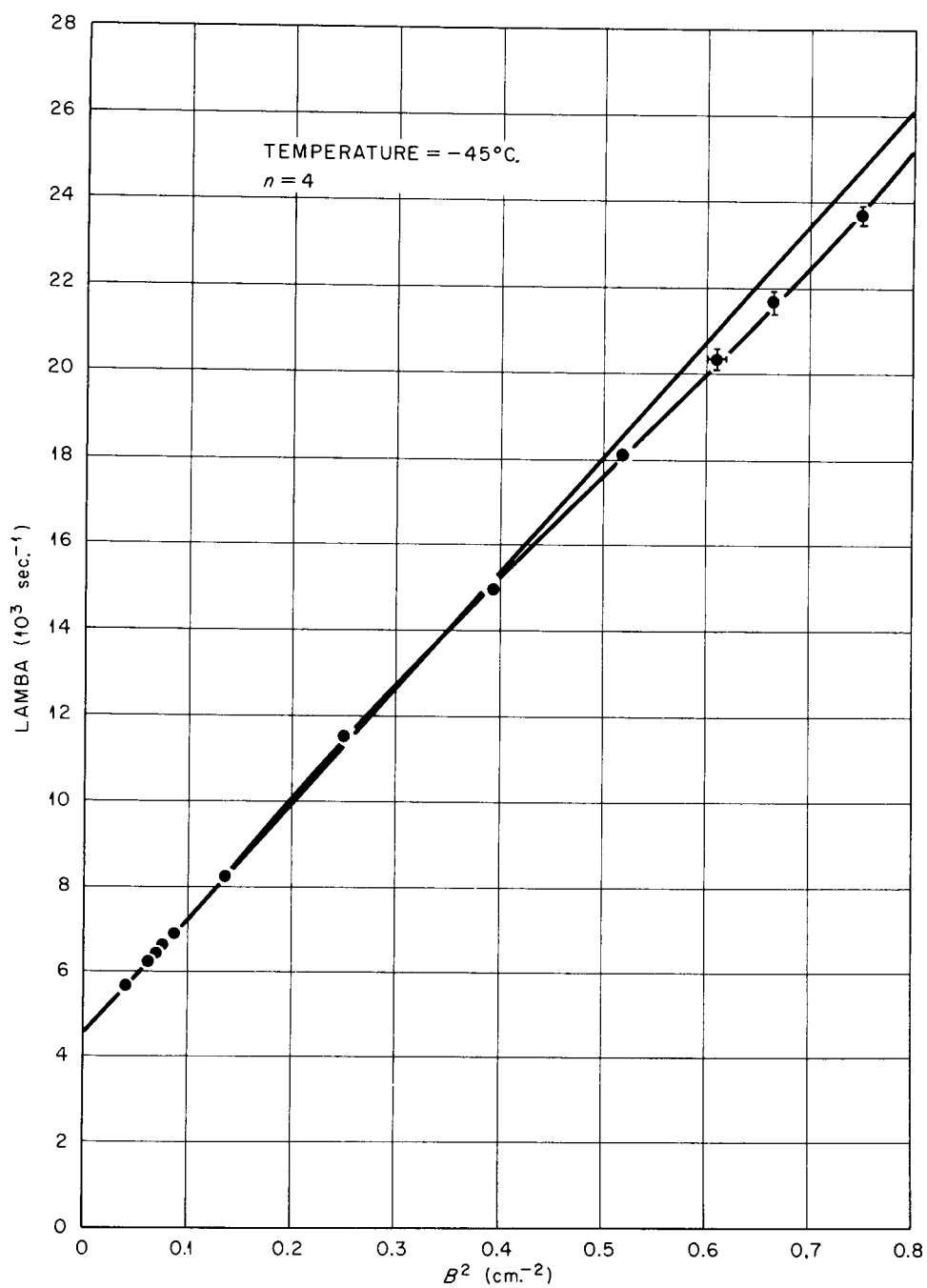


Figure 59.  $\lambda$  versus  $B^2$  for data at  $-45^\circ\text{C}$ . The data are fitted to the equation  $\lambda = \sum_{k=0}^n a_k (B^2)^k$  for  $n = 4$ . The straight line shows the slope of the curve at  $B^2 = 0$ .

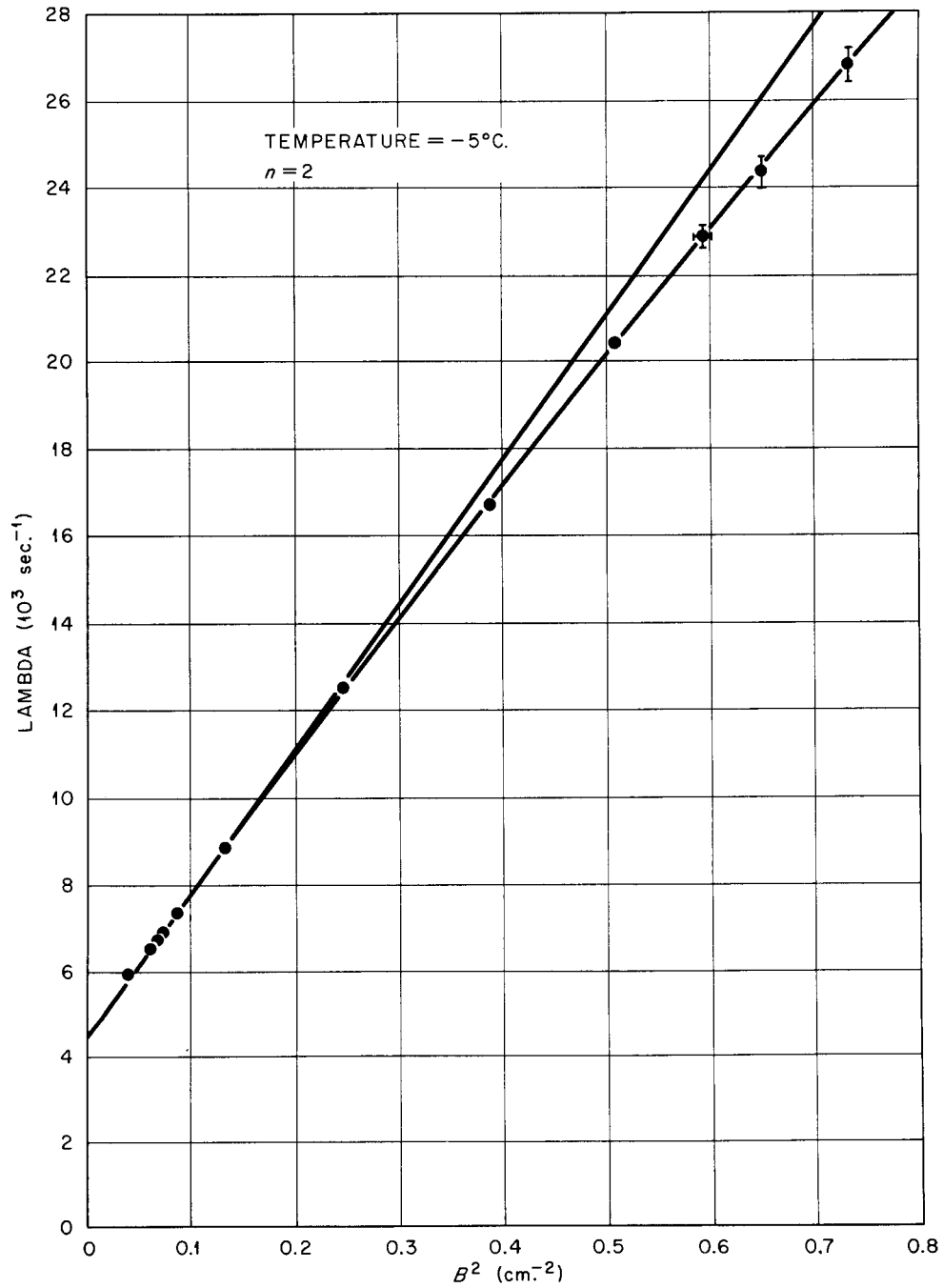


Figure 60.  $\lambda$  versus  $B^2$  for data at  $-5^{\circ}\text{C}$ . The data are fitted to the equation  $\lambda = a_0 + a_1 B^2 + a_2 B^4$ . The straight line shows the slope at  $B^2 = 0$ .

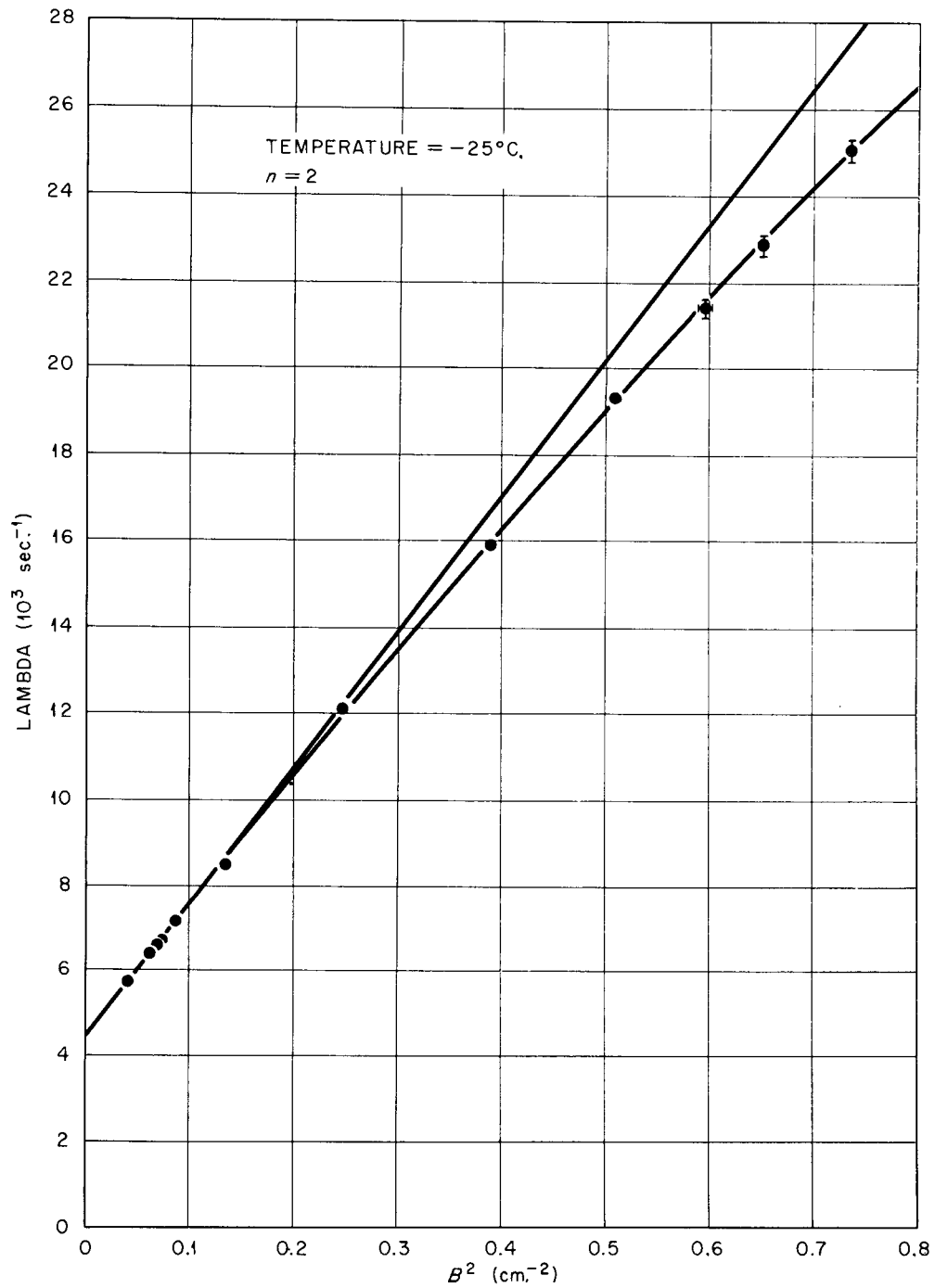


Figure 61.  $\lambda$  versus  $B^2$  for data at  $-25^{\circ}\text{C}$ . The data are fitted to the equation  $\lambda = a_0 + a_1 B^2 + a_2 B^4$ . The straight line shows the slope at  $B^2 = 0$ .

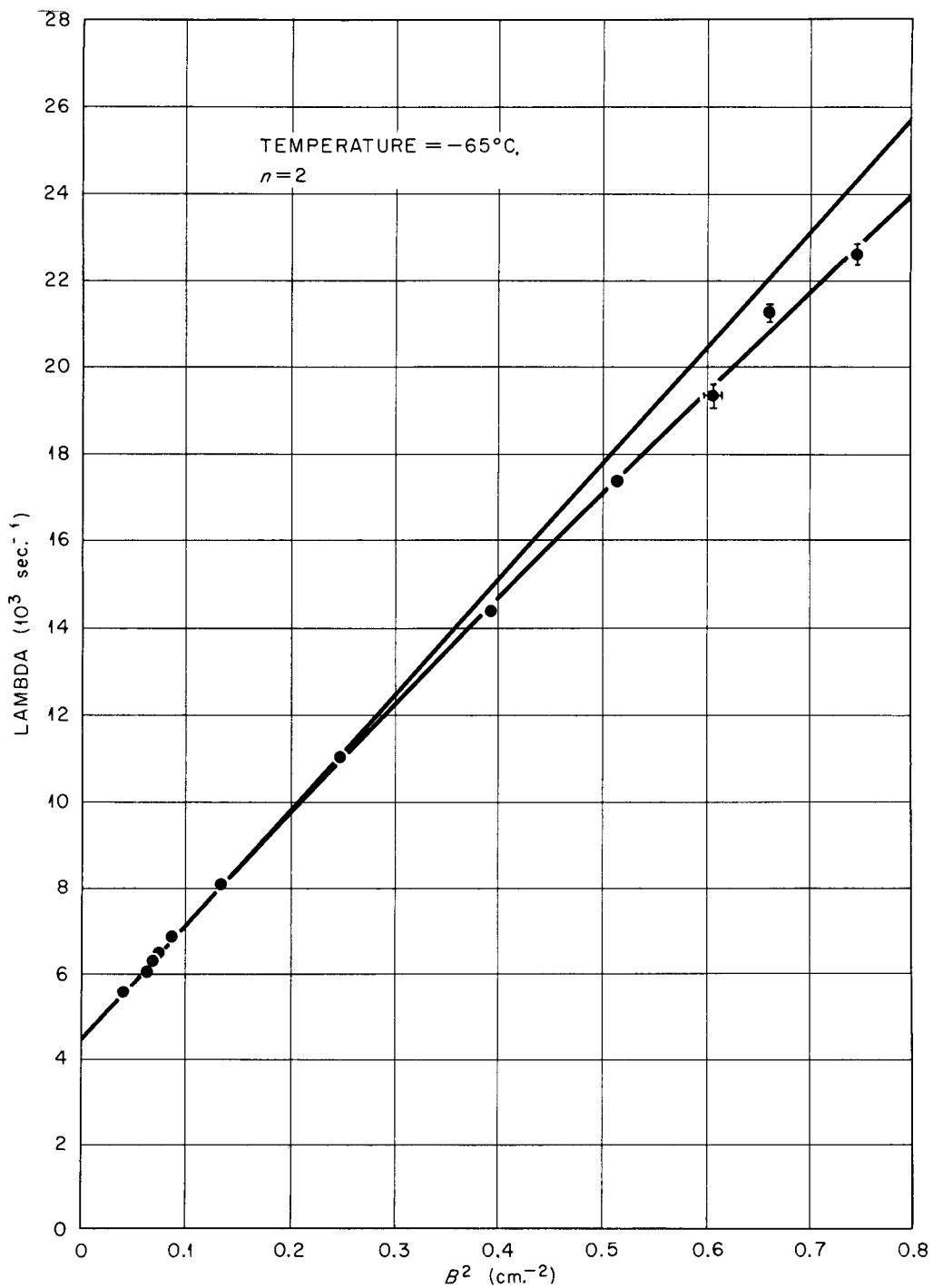


Figure 62.  $\lambda$  versus  $B^2$  for data at  $-65^\circ\text{C}$ . The data are fitted to the equation  $\lambda = a_0 + a_1 B^2 + a_2 B^4$ . The straight line shows the slope at  $B^2 = 0$ .

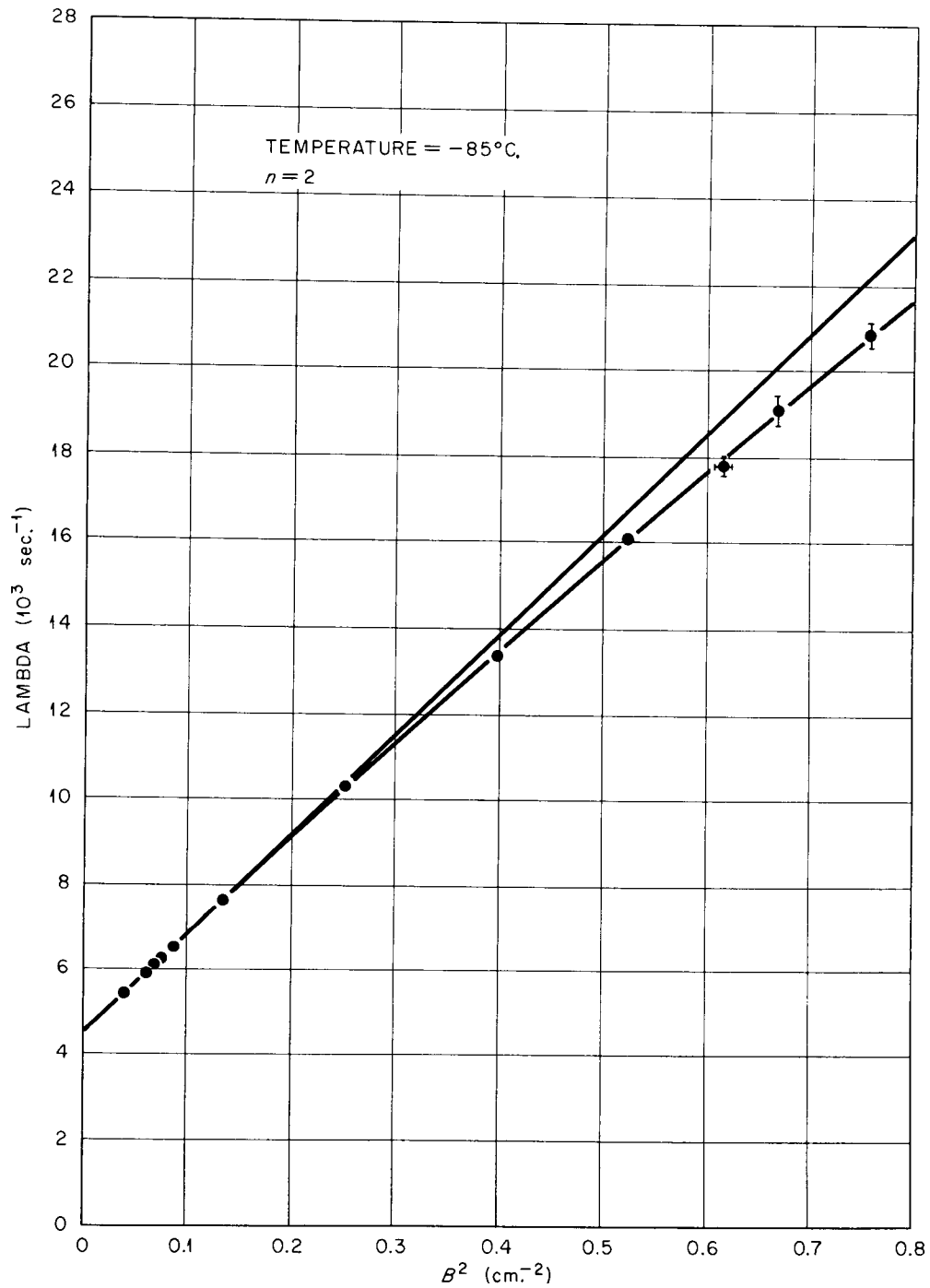


Figure 63.  $\lambda$  versus  $B^2$  for data at  $-85^{\circ}\text{C}$ . The data are fitted to the equation  $\lambda = a_0 + a_1 B^2 + a_2 B^4$ . The straight line shows the slope at  $B^2 = 0$ .

cross-bars on each data point, both vertically and horizontally, represent the uncertainties in  $B^2$  and  $\lambda$  respectively.

The bucklings are temperature dependent through Equations (199) and (202) because of the fact that the diffusion coefficient is temperature dependent, which affects the extrapolation distance. Table XI gives the bucklings for each cylinder and temperature. The values are those obtained by the iterative procedure with  $n = 2$ .

TABLE XI

VALUES OF BUCKLING FOR EACH ICE CYLINDER AT EACH TEMPERATURE

| Cylinder<br>Number | -5°C.           | -25°C.          | -45°C.          | -65°C.          | -85°C.          |
|--------------------|-----------------|-----------------|-----------------|-----------------|-----------------|
| 1                  | 0.0393 ± 0.0010 | 0.0393 ± 0.0010 | 0.0394 ± 0.0010 | 0.0395 ± 0.0010 | 0.0396 ± 0.0010 |
| 2                  | 0.0618 ± 0.0008 | 0.0618 ± 0.0008 | 0.0621 ± 0.0008 | 0.0621 ± 0.0008 | 0.0624 ± 0.0009 |
| 3                  | 0.0686 ± 0.0011 | 0.0687 ± 0.0011 | 0.0689 ± 0.0011 | 0.0690 ± 0.0011 | 0.0693 ± 0.0011 |
| 4                  | 0.0745 ± 0.0011 | 0.0746 ± 0.0011 | 0.0748 ± 0.0011 | 0.0749 ± 0.0011 | 0.0752 ± 0.0011 |
| 5                  | 0.0875 ± 0.0013 | 0.0876 ± 0.0013 | 0.0880 ± 0.0013 | 0.0881 ± 0.0013 | 0.0885 ± 0.0013 |
| 6                  | 0.1344 ± 0.0012 | 0.1346 ± 0.0012 | 0.1352 ± 0.0012 | 0.1354 ± 0.0012 | 0.1362 ± 0.0012 |
| 7                  | 0.2469 ± 0.0016 | 0.2473 ± 0.0016 | 0.2490 ± 0.0017 | 0.2494 ± 0.0017 | 0.2514 ± 0.0017 |
| 8                  | 0.3892 ± 0.0028 | 0.3899 ± 0.0028 | 0.3933 ± 0.0029 | 0.3941 ± 0.0029 | 0.3981 ± 0.0029 |
| 9                  | 0.5101 ± 0.0031 | 0.5110 ± 0.0031 | 0.5161 ± 0.0032 | 0.5174 ± 0.0032 | 0.5233 ± 0.0033 |
| 10                 | 0.5964 ± 0.0074 | 0.5978 ± 0.0074 | 0.6058 ± 0.0076 | 0.6078 ± 0.0076 | 0.6172 ± 0.0078 |
| 11                 | 0.6519 ± 0.0038 | 0.6532 ± 0.0038 | 0.6606 ± 0.0039 | 0.6624 ± 0.0039 | 0.6710 ± 0.0040 |
| 12                 | 0.7356 ± 0.0045 | 0.7371 ± 0.0045 | 0.7460 ± 0.0046 | 0.7482 ± 0.0046 | 0.7586 ± 0.0047 |

## CHAPTER V

### RESULTS AND DISCUSSION

The objectives of the experiments described in this work were (1) to establish whether an asymptotic spectrum evidenced by constant decay frequency could be established in ice over the temperature range available and (2) to measure the diffusion parameters in ice as function of temperature.

#### I. ATTAINMENT OF ASYMPTOTIC DECAY

With respect to the former objective, the establishment of an asymptotic spectrum would be evidenced by an unvarying decay frequency as the waiting time after the neutron injection is increased. If a "trapping" effect, like that observed in beryllium were present then the measured decay frequencies would continue to decrease with time. As has already been discussed, the analysis of the data for cylinders Number 1 through 8 showed no such effect, rather a somewhat opposite result attributed to dead-time effects. In the smallest cylinders there was evidence for a small component with lower decay frequency, which appeared not to depend on buckling or temperature within the rather wide limits of error with which it could be determined. Since the time range available for analyses within one set of eighteen-channel data was rather short, a series of measurements covering several temperatures and bucklings were performed with extended waiting times, in order to check on the constancy of the decay frequency. In each case the shorter waiting time

is the standard waiting time established as described in Chapter III, and the result is that already quoted for the case at hand. The data obtained with longer waiting time involved much higher relative backgrounds, and fewer counts, both due to the effects of the longer waiting time.

The results shown in Table XII confirm the results of the analyses of the regular data. No effect of changing spectrum is observed. However, a small slower component which was ascribed to room return or similar effects has already been subtracted from the small-cylinder data in the process of the analysis. A trapping effect would also appear as a small slower decay component, though its magnitude should be sensitive to temperature. While such a temperature effect was not observed, errors in the parameters of the second decay mode are large enough so that it might be possible for a temperature effect on the relative amplitude of the second component to be masked by the fluctuations. In the cylinders of intermediate size, such as Number 7 and Number 8, no persistent-decay effect was observed at any temperature, whereas, if a trapping effect were present it might be expected to appear at low temperatures in even intermediate-sized cylinders.

In summary, the data supports the conclusion that there is no trapping effect, and all the data collected can be understood without recourse to such an effect. However, because of the presence of the effect ascribed to "room-return" with the associated very large uncertainties in the amplitude and frequency of the second decay component fitted to the data, the possibility of the presence of a small trapping effect is not absolute eliminated.

TABLE XII  
EFFECT OF EXTENDED WAITING TIME  
ON MEASURED DECAY FREQUENCIES

| Cylinder Number | Temperature (°C.) | Waiting Time (μsec.) | Decay Constant (10 <sup>3</sup> sec. <sup>-1</sup> ) |
|-----------------|-------------------|----------------------|--|
| 3               | -65               | 280                  | 6.266 ± 0.022  |
|                 |                   | 440                  | 6.250 ± 0.050  |
| 6               | -65               | 280                  | 8.052 ± 0.073  |
|                 |                   | 400                  | 7.988 ± 0.082  |
| 8               | -5                | 175                  | 16.668 ± 0.053                                       |
|                 |                   | 250                  | 16.642 ± 0.088                                       |
| 8               | -85               | 175                  | 13.310 ± 0.100                                       |
|                 |                   | 275                  | 13.357 ± 0.121                                       |
| 9               | -50               | 180                  | 16.085 ± 0.129                                       |
|                 |                   | 220                  | 16.177 ± 0.220                                       |
| 11              | -85               | 140                  | 19.073 ± 0.344                                       |
|                 |                   | 220                  | 18.827 ± 0.444                                       |
| 12              | -5                | 140                  | 26.771 ± 0.383                                       |
|                 |                   | 220                  | 26.801 ± 0.543                                       |
| 12              | -85               | 140                  | 20.808 ± 0.236                                       |
|                 |                   | 220                  | 21.107 ± 0.355                                       |

II. DIFFUSION PARAMETERS - COMPARISON WITH  
OTHER EXPERIMENTAL RESULTS

It has been shown, at the end of the previous section, that the decay data do not support assignment of nonzero values to coefficients in powers of  $B^2$  greater than two. Accordingly, the data was fitted to a quadratic function in  $B^2$  and three parameters obtained which are identified as  $a_0 = \overline{(v\Sigma_a)}$ ,  $a_1 = \overline{(vD)}_{T_0}$ , and  $a_2 = C$ . Each will be discussed in turn and its values compared with calculated and experimental values obtained by others.

The absorption term,  $v\Sigma_a$ . It has been frequently stated that the absorption cross section of hydrogen for thermal neutrons is proportional to  $(1/v)$ . If this is the case then  $\sigma_a(v) = \sigma_a(v_0)(v_0/v)$ , and

$$\overline{\sigma_a} = \frac{\sigma_a(v_0) \cdot v_0 \int_0^{\infty} n(v)(1/v) dv}{\int_0^{\infty} n(v) dv} = \frac{\sigma_a(v_0) \cdot v_0 \int_0^{\infty} v e^{-v^2/v_0^2} dv}{\int_0^{\infty} v^2 e^{-v^2/v_0^2} dv} = \frac{2}{\sqrt{\pi}} \overline{\sigma_{a_0}}. \quad (206)$$

As a standard,  $v_0$  is taken to be  $2.2 \times 10^5$  cm./sec. which is very close to the most probable velocity at  $20^\circ\text{C}$ . ( $2.198 \times 10^5$  cm./sec.).

Figure 64 shows the results obtained at each of the five temperatures. The left-hand ordinates show the values of  $(v\Sigma_a)$  and the right-

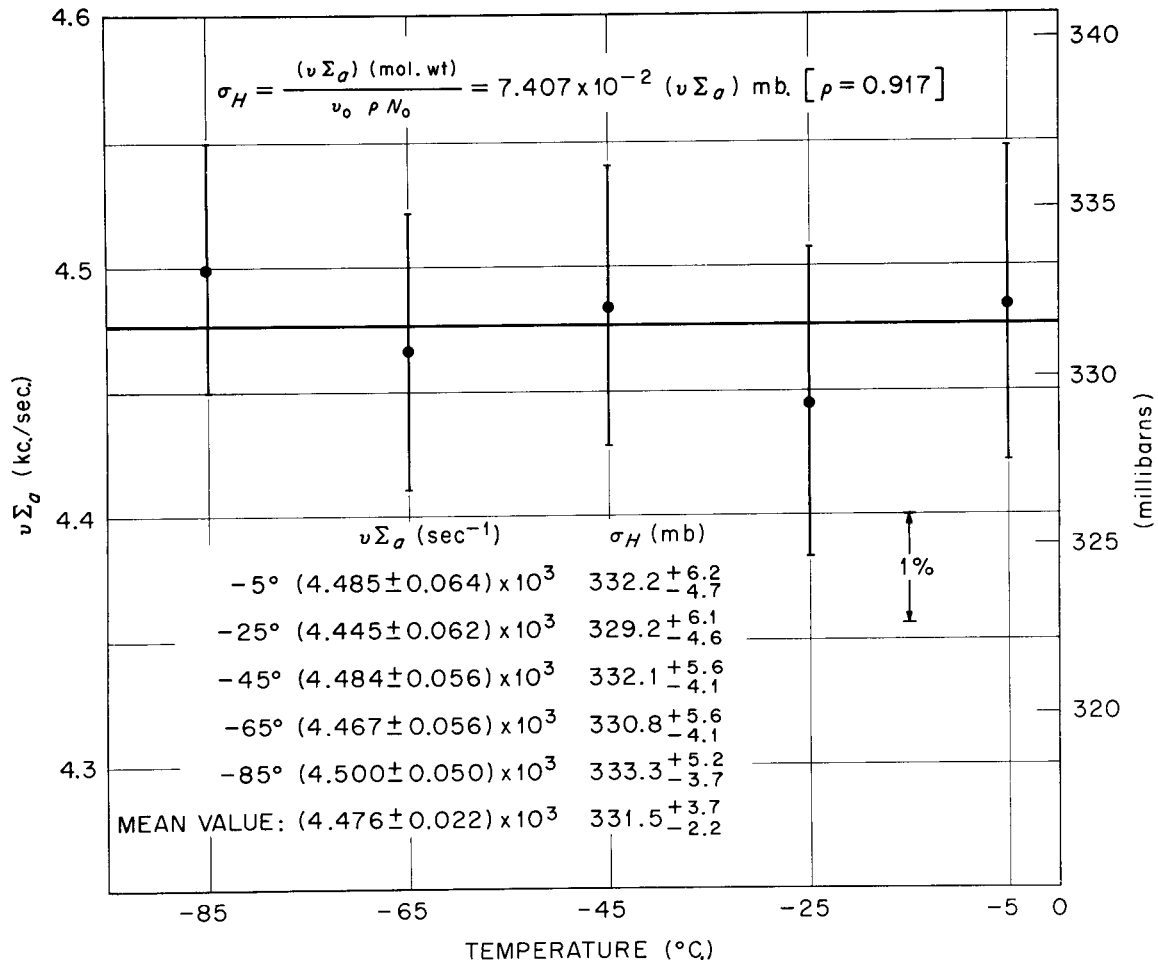


Figure 64. Measured values of  $v\Sigma_a$  as function of ice temperature. The values of  $\sigma_a$  are indicated on the right-hand ordinate scale in the table.

hand ordinates are the microscopic "2,200 m.sec." cross-section values calculated from them. The errors in the microscopic cross section include a contribution for the ice density uncertainty. In accordance with the experimental data the ice density was taken as the theoretical density. Therefore, allowance was made for an error only in the direction of decreased density. The error bars in the figure are for the errors in  $a_0$  only. If the absorption cross section did not vary as  $1/v$  then the value of  $a_0$  would vary with temperature. Within the limits of error of the experiment no such variation is observed, confirming the  $1/v$  nature of this cross section.

In the present work care was taken to use pure water and the measurements were extended to small bucklings in order to obtain a precise value of  $(v\Sigma_a)$ . Indeed, the error limits obtained are of the same order of magnitude as those of the other best measurements of  $\sigma_a(H)$ .

Care was, therefore, taken in computing the error limits. The sources of error considered were: the errors due to the uncertainties in the decay constants, the errors due to the uncertainties in the cylinder dimensions, and the error in the ice density.

The errors in the decay frequencies are independent for each of the five values obtained, but the errors due to the ice density and the dimension uncertainties are not. The error contribution due to the dimension uncertainties was obtained by performing a fit of the  $\lambda$  versus  $B^2$  equation with the BIFIT LEAST SQUARES code, assigning zero errors to the dimensions. The remaining uncertainty in the value of  $(v\Sigma_a)$ , which amounted to about 80 per cent of the total uncertainty was ascribed to

the uncertainty in the decay frequencies. Thus, the error in the mean value of  $\sigma_a$  was computed by

$$(\Delta_D) = \frac{1}{5} \sum_{n=1}^5 \left\{ \left[ \Delta_T^{(n)} \right]^2 - \left[ \Delta_{P_0}^{(n)} \right]^2 \right\}^{1/2} \quad (207)$$

$$\Delta = \left\{ \left[ \Delta_D \right]^2 + \frac{1}{25} \sum_{n=1}^5 \left[ \Delta_{P_0}^{(n)} \right]^2 \right\}^{1/2} \quad (208)$$

where  $\left[ \Delta_T^{(n)} \right]$  is the total error in the value of  $(v\Sigma_a)$  obtained at temperature  $T_n$ ,  $\left[ \Delta_{P_0}^{(n)} \right]$  is the error in  $(v\Sigma_a)$  at temperature  $T_n$ , assuming the dimension errors to be zero,  $(\Delta_D)$  is the mean error due to the dimension uncertainties, and  $\Delta$  is the final mean error in the value of  $(v\Sigma_a)$ . The error in the mean value of  $\sigma_a(H)$  was then obtained by

$$\epsilon = \frac{(\Delta)(\text{Mol. Wt.})}{v_0 P N_0} \frac{+\Delta p}{-0} = (7.407 \times 10^{-2})(\Delta) \frac{+\Delta p}{-0}$$

where  $\epsilon$  is the error in  $\sigma_a$ ,  $v_0 = 2.198 \times 10^5$  cm./sec.,  $P = 0.917$  g./cm.<sup>3</sup>,  $N_0$  is Avogadro's Number, and (Mol. Wt.) is the molecular weight per hydrogen atom equal to 9.0.

The value of  $\sigma_a(H)$  obtained is

$$\sigma_a(H)_{2,200 \text{ m./sec.}} = (331.5 \begin{smallmatrix} +3.7 \\ -2.2 \end{smallmatrix}) \times 10^{-3} \text{ barns .}$$

The error limits for this parameter are of the same order of magnitude as those quoted for this cross section in the literature, so this experiment can be considered as an independent additional measurement of  $\sigma_a(H)$ . The "Barn Book" (Stehn et al., 1964) lists a number of measurements, and gives a recommended value of  $(332 \pm 2) \times 10^{-3}$  barns, in excellent agreement with the present results. Some other recent measurements include the work of Kay and Harris (1964), who obtained  $(328 \pm 4) \times 10^{-3}$  barns, Wynchank and Cox (1963), who found  $(334.7 \pm 0.8)$  barns, Meadows and Whalen (1961), who measured  $(335 \pm 5) \times 10^{-3}$  barns, all using measurements of the neutron lifetime in water, and Cummins (1957), who used a pile oscillator and found  $(329 \pm 2) \times 10^{-3}$  barns. Many other measurements are reported, with generally consistent results. As early as 1936 Amaldi and Fermi reported a magnitude of 0.31 barn and in 1942 Manley, Haworth, and Luebke found a value of  $(330 \pm 20) \times 10^{-3}$  barns by a neutron lifetime measurement.

The diffusion coefficient, (vD). Figure 65 shows the values obtained for (vD), as well as the values in ice obtained by other workers. Results in water useful for extrapolating to 0°C. are also shown. In order to make direct comparison possible the data in liquid water have been scaled to the density of ice by the relationship  $D_w/D_{w(i)} = \rho_i/\rho_w$  where w, i, and w(i) refer respectively to water, ice, and water of the artificial density of ice (0.917 g./cm.<sup>3</sup>) in all the discussion following. The values of (vD) are consistent with a linear temperature dependence within the errors and the line shown in the figure is the result of weighted linear

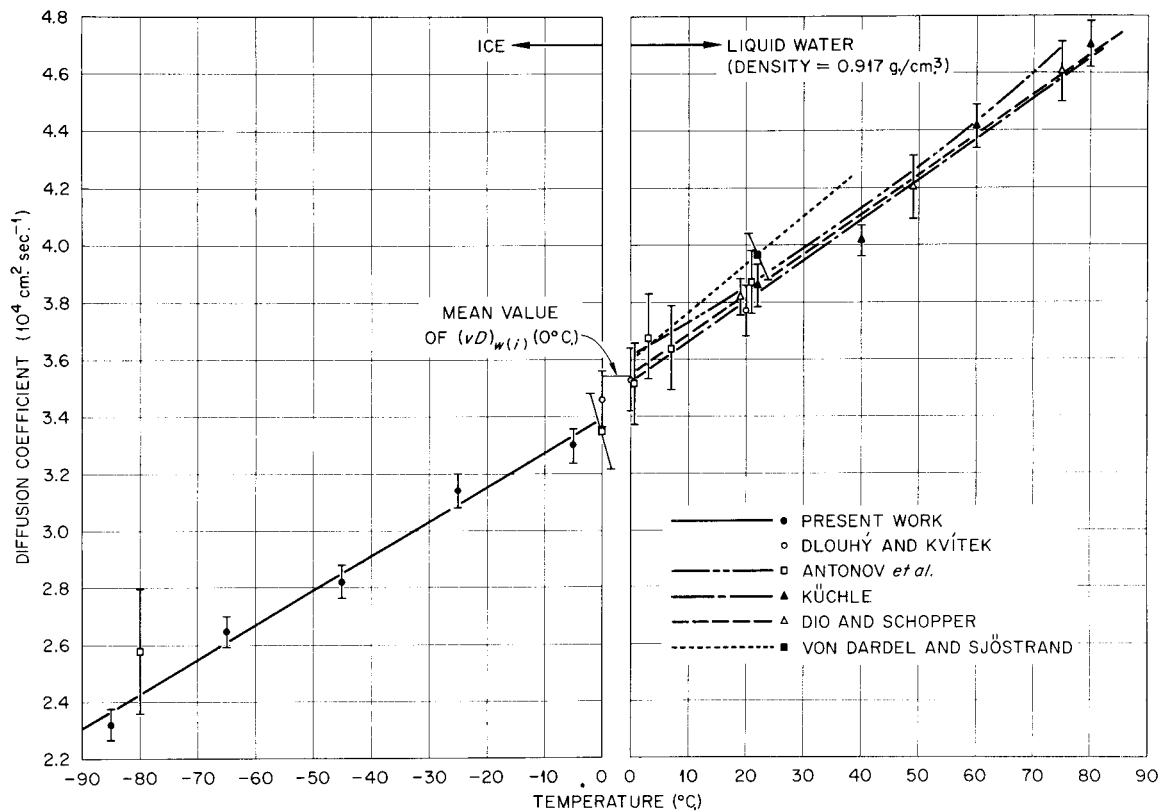


Figure 65. Measured values of  $(vD)$  in ice as function of temperature. Results of other measurements in ice are also shown. The results of others in liquid  $\text{H}_2\text{O}$ , which could be extrapolated to find  $(vD)$  ( $0^\circ\text{C}.$ ) are also shown. The values above  $0^\circ\text{C}.$  have been scaled by 1.0905 to correspond to the same density as that of ice.

least squares fit about the temperature  $-45^{\circ}\text{C}$ . (the center of the range of measured values). The result is:

$$\begin{aligned}
 (vD)(T^{\circ}\text{C.}) = & [(28.46 \pm 0.28) \times 10^3 \\
 & + (T^{\circ}\text{C.} + 45)(1.22 \pm 0.10) \times 10^2] \text{ cm.}^2 \text{ sec.}^{-1} \quad (209)
 \end{aligned}$$

The only other measured values of  $(vD)$  in ice are those of Antonov et al. (1960, 1962) and Dlouhý and Kvítek (1962). The values of  $(vD)$  of Antonov et al. must be obtained by combining results from two separate papers. In one (Antonov et al., 1960) Antonov published values of the ratio of values of  $(vD)$  and  $C$  obtained in water at  $0^{\circ}\text{C}$ . to values in ice at  $0^{\circ}\text{C}$ .,  $-80^{\circ}\text{C}$ ., and  $-196^{\circ}\text{C}$ .. The ratios for  $D$  found by Antonov are:

$$(vD)_i(0^{\circ}\text{C.}) / (vD)_w(0^{\circ}\text{C.}) = (1.04 \pm 0.02)$$

$$(vD)_i(-80^{\circ}\text{C.}) / (vD)_w(0^{\circ}\text{C.}) = (0.80 \pm 0.06)$$

$$(vD)_i(-196^{\circ}\text{C.}) / (vD)_w(0^{\circ}\text{C.}) = (0.32 \pm 0.06).$$

The numerical values of the ratio at  $0^{\circ}\text{C}$ . are given, but the ratios at  $-80^{\circ}\text{C}$ . and  $-196^{\circ}\text{C}$ . are presented only in graphical form and were extracted from the figure. In order to permit direct comparison with the present data, these ratios were converted to absolute values by reference to Antonov et al. (1962) in which a measured value of  $(vD)(21^{\circ}\text{C.})$  is given, together with a quadratic formula for values at other temperatures, based on measurements of thirteen temperature points ranging from  $0.5^{\circ}\text{C}$ . to  $286^{\circ}\text{C}$ .. The equation is:

$$\frac{(vD)(T^{\circ}\text{C.})}{(vD)(21^{\circ}\text{C.})} = (0.934 \pm 0.028) + (0.289 \pm 0.009) \times 10^{-2}T + (0.106 \pm 0.003) \times 10^{-4}T^2 \quad (210)$$

and the value at  $21^{\circ}\text{C.}$  is  $(0.355 \pm 0.010) \times 10^5 \text{ cm.}^2/\text{sec.}$  Combining this number with the ratio values, one arrives at a result of  $(vD)_w(0^{\circ}\text{C.}) = (33.157 \pm 1.36) \times 10^3 \text{ cm.}^2 \text{ sec.}^{-1}$ . This leads to:

$$(vD)_i(0^{\circ}\text{C.}) = (34.48 \pm 1.57) \times 10^3 \text{ cm.}^2 \text{ sec.}^{-1}$$

$$(vD)_i(-80^{\circ}\text{C.}) = (26.52 \pm 2.27) \times 10^3 \text{ cm.}^2 \text{ sec.}^{-1}$$

$$(vD)_i(-196^{\circ}\text{C.}) = (10.62 \pm 2.32) \times 10^3 \text{ cm.}^2 \text{ sec.}^{-1}$$

However, in the same paper there is also a quoted value of  $(vD)_w(0.5^{\circ}\text{C.})/ (vD)_w(21^{\circ}\text{C.}) = (0.91 \pm 0.03)$  Using this ratio a value of  $(vD)_w(0^{\circ}\text{C.}) = (32.22 \pm 1.26) \times 10^3 \text{ cm.}^2 \text{ sec.}^{-1}$  is obtained, which leads to:

$$(vD)_i(0^{\circ}\text{C.}) = (33.51 \pm 1.35) \times 10^3 \text{ cm.}^2 \text{ sec.}^{-1}$$

$$(vD)_i(-80^{\circ}\text{C.}) = (25.77 \pm 2.20) \times 10^3 \text{ cm.}^2 \text{ sec.}^{-1}$$

$$(vD)_i(-196^{\circ}\text{C.}) = (10.31 \pm 2.19) \times 10^3 \text{ cm.}^2 \text{ sec.}^{-1}$$

Since the latter set of values is based on an experimental point very close to  $0^{\circ}\text{C.}$  and since it leads to smaller errors in the computed  $(vD)$  values in ice, these values are taken to be the best available from the work of Antonov et al. and are plotted in the figure.

Dlouhý and Kvítek (1962) reported values of  $(vD)$  and  $C.$  at  $20^{\circ}\text{C.}$ , and  $0^{\circ}\text{C.}$  in water, and at  $0^{\circ}\text{C.}$  in ice. Their value of  $(vD)$  in ice is:

$(vD)_i(0^\circ\text{C.}) = (3.46 \pm 1.0) \times 10^3 \text{ cm.}^2 \text{ sec.}^{-1}$ . The two values found by Antonov et al. and the value found by Dlouhý and Kvítek in ice all agree, within the error limits, with the values obtained in the present work.

Considering the behavior of  $(vD)$  across the phase transition, both Antonov et al. and Dlouhý and Kvítek found a discontinuity in  $(vD)$  at  $0^\circ\text{C.}$  Antonov et al. reported

$$(vD)_i(0^\circ\text{C.})/(vD)_{w(i)}(0^\circ\text{C.}) = (0.95 \pm 0.02)$$

and Dlouhý and Kvítek report a value for water of  $(vD)_w(0^\circ\text{C.}) = (32.4 \pm 1.0) \times 10^3 \text{ cm.}^2 \text{ sec.}^{-1}$  which leads to a ratio of:

$$(vD)_i(0^\circ\text{C.})/(vD)_{w(i)}(0^\circ\text{C.}) = (0.98 \pm 0.04).$$

A large number of measurements of the diffusion parameters in water are in the literature, and these are summarized in Table XIII. Several of these include values of  $(vD)$  over a range of temperatures, so that the value of  $(vD)_w(0^\circ\text{C.})$  can be obtained by extrapolation. Specifically Kúchle (1960), Dio and Schopper (1958), and Von Dardel and Sjöstrand (1954) have made measurements from which the value of  $(vD)_w(0^\circ\text{C.})$  was obtained by extrapolation. Kúchle reports measurements at  $22^\circ\text{C.}$ ,  $40^\circ\text{C.}$ ,  $60^\circ\text{C.}$ , and  $80^\circ\text{C.}$  A linear fit was made with his values of  $(vD)$  (shown in Figure 65, p. 229); it leads to a value of  $(vD)(0^\circ\text{C.}) = (35.20 \pm 0.9) \times 10^3 \text{ cm.}^2 \text{ sec.}^{-1}$ . Dio and Schopper report results at  $19^\circ\text{C.}$ ,  $49^\circ\text{C.}$ , and  $75^\circ\text{C.}$  A linear extrapolation using their points yields a value of:  $(35.50 \pm 1.4) \times 10^3 \text{ cm.}^2 \text{ sec.}^{-1}$  for  $(vD)_{w(i)}(0^\circ\text{C.})$ . This fit is also shown in Figure 65.

TABLE XIII

MEASURED DIFFUSION PARAMETERS IN H<sub>2</sub>O AND IN H<sub>2</sub>O OF ICE-EQUIVALENT DENSITY

| Experimenter and Year <sup>a</sup> | Method                 | Temperature<br>(°C.) | (vD)<br>(cm. <sup>2</sup> sec. <sup>-1</sup> ) | -C<br>(cm. <sup>4</sup> sec. <sup>-1</sup> ) | (vD) (Ice Density)<br>(cm. <sup>2</sup> sec. <sup>-1</sup> ) | -C (Ice Density)<br>(cm. <sup>4</sup> sec. <sup>-1</sup> ) |
|------------------------------------|------------------------|----------------------|--|--|--|--|
| Scott, Thomson, and Wright (1954)  | Pulsed Neutron         | room                 | $(38.5 \pm 0.8) \times 10^3$                   |  | $(42.0 \pm 0.9) \times 10^3$                                 |  |
| VonDardel and Sjöstrand (1954)     | Pulsed Neutron         | 22                   | $(36.34 \pm 0.75) \times 10^3$                 | $(7.3 \pm 1.5) \times 10^3$                  | $(39.63 \pm 0.82) \times 10^3$                               | $(9.5 \pm 1.9) \times 10^3$                                |
| Antonov <i>et al.</i> (1955)       | Pulsed Neutron         | 22                   | $(35.0 \pm 1.0) \times 10^3$                   | $(4.0 \pm 1.0) \times 10^3$                  | $(38.2 \pm 1.1) \times 10^3$                                 | $(5.2 \pm 1.3) \times 10^3$                                |
| Bracci and Coceva (1956)           | Pulsed Neutron         | 22                   | $(34.85 \pm 1.10) \times 10^3$                 | $(3.0 \pm 1.0) \times 10^3$                  | $(38.00 \pm 1.2) \times 10^3$                                | $(3.9 \pm 1.3) \times 10^3$                                |
| Campbell and Stelson (1956)        | Pulsed Neutron         | room                 | $34.8 \times 10^3$                             | 0  | $37.9 \times 10^3$   | 0  |
| Beckurts and Klüber (1958)         | Poisoning              | 20                   | $(35.3 \pm 1.1) \times 10^3$                   |  | $(38.5 \pm 1.2) \times 10^3$                                 |  |
| Dio (1958)                         | Pulsed Neutron         | 19                   | $(35.05 \pm 0.60) \times 10^3$                 | $(3.6 \pm 0.7) \times 10^3$                  | $(38.22 \pm 0.65) \times 10^3$                               | $(4.7 \pm 0.9) \times 10^3$                                |
| Dio and Schopper (1958)            | Pulsed Neutron         | 49                   | $(38.55 \pm 1.00) \times 10^3$                 | $(5.2 \pm 1.5) \times 10^3$                  | $(42.04 \pm 1.1) \times 10^3$                                | $(6.7 \pm 1.9) \times 10^3$                                |
| "                                  | "                      | 75                   | $(42.25 \pm 1.00) \times 10^3$                 | $(5.6 \pm 1.5) \times 10^3$                  | $(46.07 \pm 1.1) \times 10^3$                                | $(7.3 \pm 1.9) \times 10^3$                                |
| Küchle (1960)                      | Pulsed Neutron         | 22                   | $(35.40 \pm 0.70) \times 10^3$                 | $(4.2 \pm 0.8) \times 10^3$                  | $(38.60 \pm 0.76) \times 10^3$                               | $(5.4 \pm 1.0) \times 10^3$                                |
| "                                  | "                      | 40                   | $(36.80 \pm 0.50) \times 10^3$                 | $(3.3 \pm 0.6) \times 10^3$                  | $(40.13 \pm 0.55) \times 10^3$                               | $(4.3 \pm 0.8) \times 10^3$                                |
| "                                  | "                      | 60                   | $(40.50 \pm 0.70) \times 10^3$                 | $(5.5 \pm 0.8) \times 10^3$                  | $(44.16 \pm 0.76) \times 10^3$                               | $(7.1 \pm 1.0) \times 10^3$                                |
| "                                  | "                      | 80                   | $(43.10 \pm 1.70) \times 10^3$                 | $(5.8 \pm 2.0) \times 10^3$                  | $(47.00 \pm 0.76) \times 10^3$                               | $(7.5 \pm 2.6) \times 10^3$                                |
| Antonov <i>et al.</i> (1961)       | Pulsed Neutron (ratio) | 0.5                  | $D/D_{21} = 0.91 \pm 0.03$                     | $C/C_{21} = 1.0 \pm 0.4$                     |  |  |
| "                                  | "                      | 3                    | $D/D_{21} = 0.95 \pm 0.03$                     | $C/C_{21} = 1.1 \pm 0.4$                     |  |  |
| "                                  | "                      | 7                    | $D/D_{21} = 0.94 \pm 0.03$                     | $C/C_{21} = 0.9 \pm 0.3$                     |  |  |
| "                                  | Pulsed Neutron         | 21                   | $(35.5 \pm 1.0) \times 10^3$                   | $(4.0 \pm 1.0) \times 10^3$                  | $(38.71 \pm 1.1) \times 10^3$                                | $(5.2 \pm 1.3) \times 10^3$                                |
| "                                  | Pulsed Neutron (ratio) | 71                   | $D/D_{21} = 1.22 \pm 0.04$                     | $C/C_{21} = 1.2 \pm 0.4$                     |  |  |
| "                                  | "                      | 98                   | $D/D_{21} = 1.34 \pm 0.04$                     | $C/C_{21} = 1.8 \pm 0.6$                     |  |  |
| Antonov <i>et al.</i> (1962)       | Pulsed Neutron (ratio) | 0(i)                 | $D_i/D_w(0^\circ) = 1.04 \pm 0.02$             | $C_i/C_w(0^\circ) = 2.5 \pm 0.4$             |  |  |
| Lopez and Beyster (1962)           | Pulsed Neutron         | 26.7                 | $(37.503 \pm 0.366) \times 10^3$               | $(5.116 \pm 0.776) \times 10^3$              | $(40.90 \pm 0.399) \times 10^3$                              | $(6.63 \pm 0.47) \times 10^3$                              |
| Bretscher (1962)                   | Pulsed Neutron         | 26                   | $(36.98 \pm 1.63) \times 10^3$                 | $(5.02 \pm 2.49) \times 10^3$                | $(40.33 \pm 1.78) \times 10^3$                               | $(6.5 \pm 3.2) \times 10^3$                                |
| Starr and Koppel (1962)            | Poisoning              | 21                   | $(35.85 \pm 1.0) \times 10^3$                  | $(2.9 \pm 0.35) \times 10^3$                 | $(39.09 \pm 1.1) \times 10^3$                                | $(3.8 \pm 0.5) \times 10^3$                                |
| Dlouhý and Kvítek (1962)           | Pulsed Neutron         | 20                   | $(34.60 \pm 0.80) \times 10^3$                 | $(4.00 \pm 0.8) \times 10^3$                 | $(37.7 \pm 0.9) \times 10^3$                                 | $(5.2 \pm 1.0) \times 10^3$                                |
| "                                  | "                      | 0(w)                 | $(32.4 \pm 1.0) \times 10^3$                   | $(4.20 \pm 1.0) \times 10^3$                 | $(35.3 \pm 1.1) \times 10^3$                                 | $(5.4 \pm 1.3) \times 10^3$                                |
| "                                  | "                      | 0(i)                 | $(34.6 \pm 1.0) \times 10^3$                   | $(8.30 \pm 2.0) \times 10^3$                 | $(34.6 \pm 1.1) \times 10^3$                                 | $(8.30 \pm 2.0) \times 10^3$                               |
| Antonov <i>et al.</i> (1962)       | Pulsed Neutron         | -196                 | $(9.5 \pm 0.4) \times 10^3$                    | $(2.0 \pm 1.0) \times 10^3$                  | $(9.5 \pm 0.4) \times 10^3$                                  | $(2.0 \pm 1.0) \times 10^3$                                |
| Springer <i>et al.</i> (1964)      | Single Scattering      | 20                   | $(35.30 \pm 0.5) \times 10^3$                  |  | $(38.41 \pm 0.3) \times 10^3$                                |  |
| Pál, Bod, and Szatmáry (1965)      | Pulsed Neutron         | 22                   | $(36.533 \pm 1.36) \times 10^3$                | $(5.939 \pm 3.148) \times 10^3$              | $(39.84 \pm 1.48) \times 10^3$                               | $(7.70 \pm 4.08) \times 10^3$                              |
| DeJuren (1965)                     | Pulsed Neutron         | 23                   | $(36.110 \pm 0.15) \times 10^3$                |  | $(39.38 \pm 0.16) \times 10^3$                               |  |
| Present Work (1965)                | Pulsed Neutron         | -5                   | $(32.98 \pm 0.62) \times 10^3$                 | $(3.73 \pm 1.13) \times 10^3$                | $(32.98 \pm 0.63) \times 10^3$                               | $(3.73 \pm 1.13) \times 10^3$                              |
| "                                  | "                      | -25                  | $(31.38 \pm 0.61) \times 10^3$                 | $(4.73 \pm 0.99) \times 10^3$                | $(31.38 \pm 0.61) \times 10^3$                               | $(4.73 \pm 0.99) \times 10^3$                              |
| "                                  | "                      | -45                  | $(28.19 \pm 0.60) \times 10^3$                 | $(3.43 \pm 0.97) \times 10^3$                | $(28.19 \pm 0.60) \times 10^3$                               | $(3.43 \pm 0.97) \times 10^3$                              |
| "                                  | "                      | -65                  | $(26.48 \pm 0.55) \times 10^3$                 | $(2.82 \pm 0.88) \times 10^3$                | $(26.48 \pm 0.55) \times 10^3$                               | $(2.82 \pm 0.88) \times 10^3$                              |
| "                                  | "                      | -85                  | $(23.20 \pm 0.57) \times 10^3$                 | $(2.32 \pm 0.92) \times 10^3$                | $(23.20 \pm 0.57) \times 10^3$                               | $(2.32 \pm 0.92) \times 10^3$                              |

a. References will be found in the Bibliography.

VonDardel and Sjöstrand report a value at 22°C., and a temperature dependence of  $(0.0042 \pm 0.0004)$  per °C. This yields:

$$(\nu D)_{w(i)}(0^\circ\text{C.}) = (35.97 \pm 0.90) \times 10^3 \text{ cm.}^2 \text{ sec.}^{-1}.$$

Combining these extrapolated results with the two values from Antonov et al. and Dlouhý and Kvítek one obtains a mean value of:

$$(\nu D)_{w(i)}(0^\circ\text{C.}) = (35.42 \pm 0.71) \times 10^3 \text{ cm.}^2 \text{ sec.}^{-1}.$$

With this value and the present result of  $(\nu D)_i(0^\circ\text{C.}) = 33.95 \pm 0.73) \times 10^3 \text{ cm.}^2 \text{ sec.}^{-1}$ , the ratio of  $(\nu D)$  in ice and ice-equivalent water at 0°C. is:

$$(\nu D)_i(0^\circ\text{C.})/(\nu D)_{w(i)}(0^\circ\text{C.}) = (0.96 \pm 0.03),$$

which agrees, within the errors, with the ratios of Antonov et al. and of Dlouhý and Kvítek.

It is, therefore, concluded that a real discontinuity in the value of  $(\nu D)$  exists across the water-ice phase transition, independent of the density change. The result of Dlouhý and Kvítek would also be consistent with the opposite conclusion, but since all three independent experiments find a discontinuity in the same sense with magnitudes consistent within the errors, the reality of this phenomenon seems to be well established. The mean results, combining the three ratio values is

$$(\nu D)_i(0^\circ\text{C.})/(\nu D)_{w(i)}(0^\circ\text{C.}) = (0.96 \pm 0.02).$$

The diffusion cooling coefficient, C. The results of the present work for the diffusion cooling coefficient are shown in Figure 66, together with the results of other experiments in ice and water.

The same sources reporting values of  $(vD)$  in ice also supply measurements of  $C$ , namely those of Antonov et al. and of Dlouhý and Kvitek. Dlouhý and Kvitek obtained a value of  $C_i(0^\circ\text{C.}) = -(8.30 \pm 2.0) \times 10^3 \text{ cm.}^4 \text{ sec.}^{-1}$ . The results obtained by Antonov et al. must, again, be inferred from reported ratio values, relative to the value in water at  $0^\circ\text{C.}$  and the latter in turn must be obtained by making use of a result reported by Antonov et al. at  $21^\circ\text{C.}$  and ratio values at other water temperatures.

Discussing the latter procedure first, Antonov and co-workers published (Antonov et al., 1961) a value of  $C$  in water at  $21^\circ\text{C.}$  of:

$$C_w(21^\circ\text{C.}) = -(4.0 \pm 1.0) \times 10^3 \text{ cm.}^4 \text{ sec.}^{-1} .$$

The same paper lists values of the ratio of  $C$  to the value at  $21^\circ\text{C.}$  for a number of temperatures ranging from  $0.5^\circ\text{C.}$  to  $286^\circ\text{C.}$  Using these ratio values a linear least-squares fit was performed to obtain the best value for  $0^\circ\text{C.}$ , with the result:

$$C_w(0^\circ\text{C.}) = -(3.7 \pm 1.0) \times 10^3 \text{ cm.}^4 \text{ sec.}^{-1} .$$

In (Antonov et al., 1960) ratios are given for the values of  $C$  in ice at  $0^\circ\text{C.}$ ,  $-80^\circ\text{C.}$ , and  $-196^\circ\text{C.}$ , relative to water at  $0^\circ\text{C.}$  The

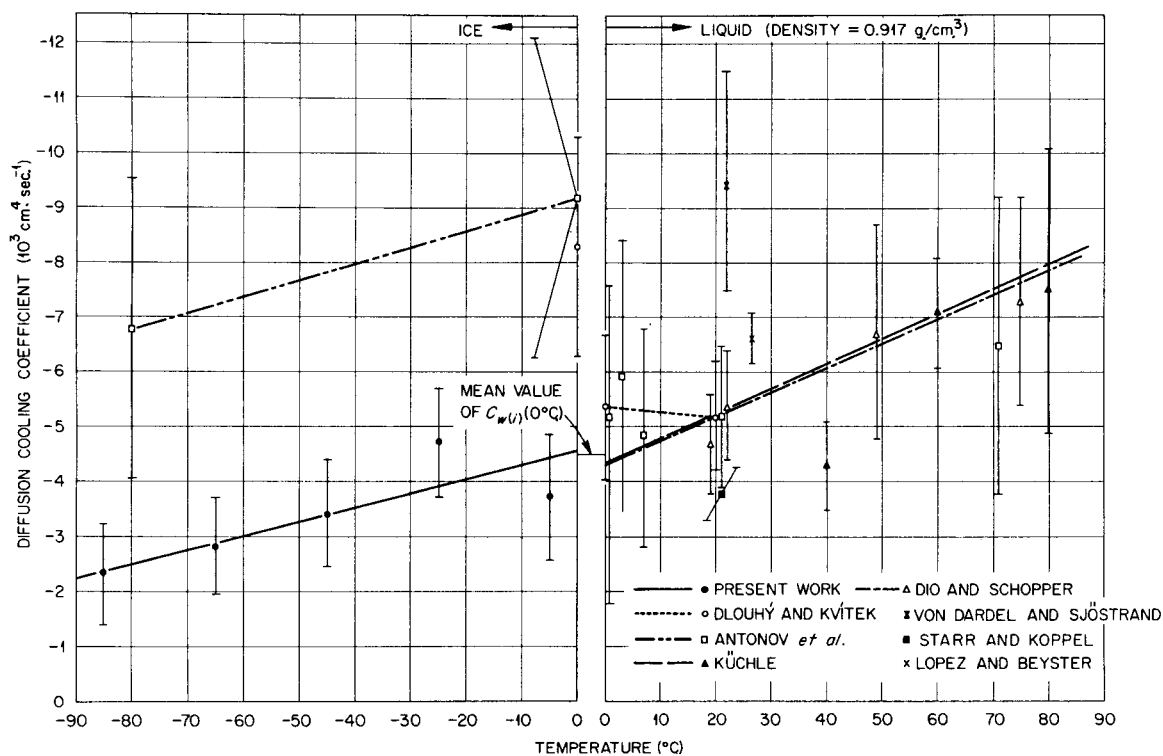


Figure 66. Measured value of  $C$ , the diffusion cooling coefficient, in ice as function of temperature. Results of other measurements in ice are also shown, including results in liquid  $\text{H}_2\text{O}$ , which could be extrapolated to find  $C$  ( $0^{\circ}\text{C}$ ). The values above  $0^{\circ}\text{C}$ . have been scaled by  $1.0905^3$  to correspond to the same density as that of ice.

latter two are reported only in graphical form from which numerical values were obtained. For ice at 0°C. the ratio measured by Antonov et al. is:

$$c_i(0^\circ\text{C.})/c_w(0^\circ\text{C.}) = (2.5 \pm 0.4) .$$

Combining this with the value in water at 0°C. discussed above one obtains a value in ice of:

$$c_i(0^\circ\text{C.}) = -(9.2 \pm 2.9) \times 10^3 \text{ cm.}^4 \text{ sec.}^{-1} .$$

The ratio values obtained from the graph are:

$$c_i(-80^\circ\text{C.})/c_w(0^\circ\text{C.}) = (1.65 \pm 0.25) ,$$

$$c_i(-196^\circ\text{C.})/c_w(0^\circ\text{C.}) = (0.7 \pm 0.25) ,$$

which gives values of

$$c_i(-80^\circ\text{C.}) = -(6.0 \pm 4.4) \times 10^3 \text{ cm.}^4 \text{ sec.}^{-1}$$

$$c_i(-196^\circ\text{C.}) = -(2.6 \pm 1.1) \times 10^3 \text{ cm.}^4 \text{ sec.}^{-1} .$$

There are also, in addition to the results of Antonov et al. just discussed, several other measurements of C for water in the literature. Again, in order to facilitate comparison with the ice data, the results in water are scaled to compensate for the density difference. In this case, since the dimensions of C are  $(\text{cm.}^4 \text{ sec.}^{-1}) = (\text{cm.}^3 \times \text{velocity})$ , the values of C are proportional to the inverse cube of the density. Therefore, all the water values are scaled by:

$$C_{w(i)}/C_w = (0.917)^{-3} = 1.297 .$$

The only other workers reporting values of C for several temperatures, thus permitting extrapolation to 0°C., are Dio and Schopper (1958), and Kùchle (1960). In addition, Dlouhý and Kvítek reported a direct measurement in water at 0°C.

A weighted linear fit using the three values reported by Dio at 19°C., 49°C., and 75°C., gave  $C_{w(i)}(0^\circ\text{C.}) = -(3.8 \pm 2.5) \times 10^3 \text{ cm.}^4 \text{ sec.}^{-1}$ . Fitting the four values of Kùchle, at 22°C., 40°C., 60°C., and 80°C. to a linear model also led to the identical extrapolated value of  $C_{w(i)}(0^\circ\text{C.}) = -(3.8 \pm 2.3) \times 10^3 \text{ cm.}^4 \text{ sec.}^{-1}$ , which, in view of the large errors must be considered fortuitous. The value of Dlouhý and Kvítek at the same temperature is  $-(5.4 \pm 1.3) \times 10^3 \text{ cm.}^4 \text{ sec.}^{-1}$ . Combining the four values (those of Antonov et al., Dlouhý and Kvítek, Dio and Schopper, and Kùchle) a mean value of C at the freezing point in ice-equivalent water is found to be:

$$C_{w(i)}(0^\circ\text{C.}) = -(4.5 \pm 1.1) \times 10^3 \text{ cm.}^4 \text{ sec.}^{-1}.$$

The results of the present work can be fitted to a linear dependence on the temperature, within the limits of error. The result is

$$C_i(T^\circ\text{C.}) = -[(3.43 \pm 0.32) \times 10^3 + (T + 45)(2.55 \pm 1.16) \times 10] \text{ cm.}^4 \text{ sec.}^{-1}, \quad (211)$$

which then gives a value at 0°C. of

$$C_i(0^\circ\text{C.}) = -(4.58 \pm 0.84) \times 10^3 \text{ cm.}^4 \text{ sec.}^{-1}.$$

It is clear that the present results do not agree, even within the large limits on the errors, with the values reported by Antonov et al. and Dlouhý and Kvítek. The present results, when compared with the average value of the parameter C in ice-equivalent water at 0°C. show only an insignificant discontinuity across the phase transition of

$$C_i(0^\circ\text{C.})/C_{w(i)}(0^\circ\text{C.}) = (1.02 \pm 0.31).$$

The large uncertainty does not permit the preclusion of a discontinuity of either sign. However, the very large factor of 1.93 found by Antonov et al. or of 1.53 found by Dlouhý and Kvítek does not appear to be consistent with the present results. Although a linear fit is capable of representing the variation of C with temperature within the limits of error, there are theoretical reasons for preferring a different fitting model. This will be discussed further below.

### III. DISCUSSION OF RESULTS

The result of the present experiments with respect to the absorption cross section require no further discussion. The  $1/v$  dependence of the cross section and its magnitude have long been well established, and the values found here agree with those of previous measurements.

Diffusion coefficient. With regard to the results of the diffusion coefficient, there are several aspects which warrant discussion. First, there is the fact that the diffusion coefficient,  $(vD)$ , diminishes monotonically and, within the limits of accuracy of the experiment, linearly, with temperature. If the linear fitting is extrapolated to  $0^\circ\text{K}$ . then  $D(0^\circ\text{K.}) = (0.47 \pm 2.02) \times 10^3 \text{ cm.}^2 \text{ sec.}^{-1}$ . Thus the extrapolated diffusion coefficient approaches zero, within the limits of accuracy, as the temperature drops to  $0^\circ\text{K}$ . Since  $v$  approaches zero also, this is to be expected unless  $D$  becomes very large. The reduction of  $(vD)$  with temperature has two components, the change in  $v$  and the change in  $D$ . Separating out the change in  $v$ , the variation of  $D$  with temperature is shown in Figure 67. Within the limits of error, this curve fits a straight line also. Clearly it is not possible for both  $D$  and  $(vD)$  to vary linearly with temperature (since  $v$  is proportional to  $\sqrt{T}$ ), but the deviations are small enough over the limited temperature range covered and the uncertainties are of such magnitude that it is not possible to determine which, if either, is exactly proportional to  $(v)^{1/2}$ , that is, proportional to the temperature.

The second interesting question concerns the discontinuity at the water-ice phase transition. Since  $D = 1/3N\sigma_s(1 - \bar{\mu})$  this effect is due to either a change in  $\sigma_s$ , or a change in  $(1 - \bar{\mu})$  or both. There is some experimental evidence available concerning the change in both the cross section and the mean scattering angle. Whittemore and McReynolds (1961) measured the total scattering cross section in water at  $5^\circ\text{C}$ . and in ice

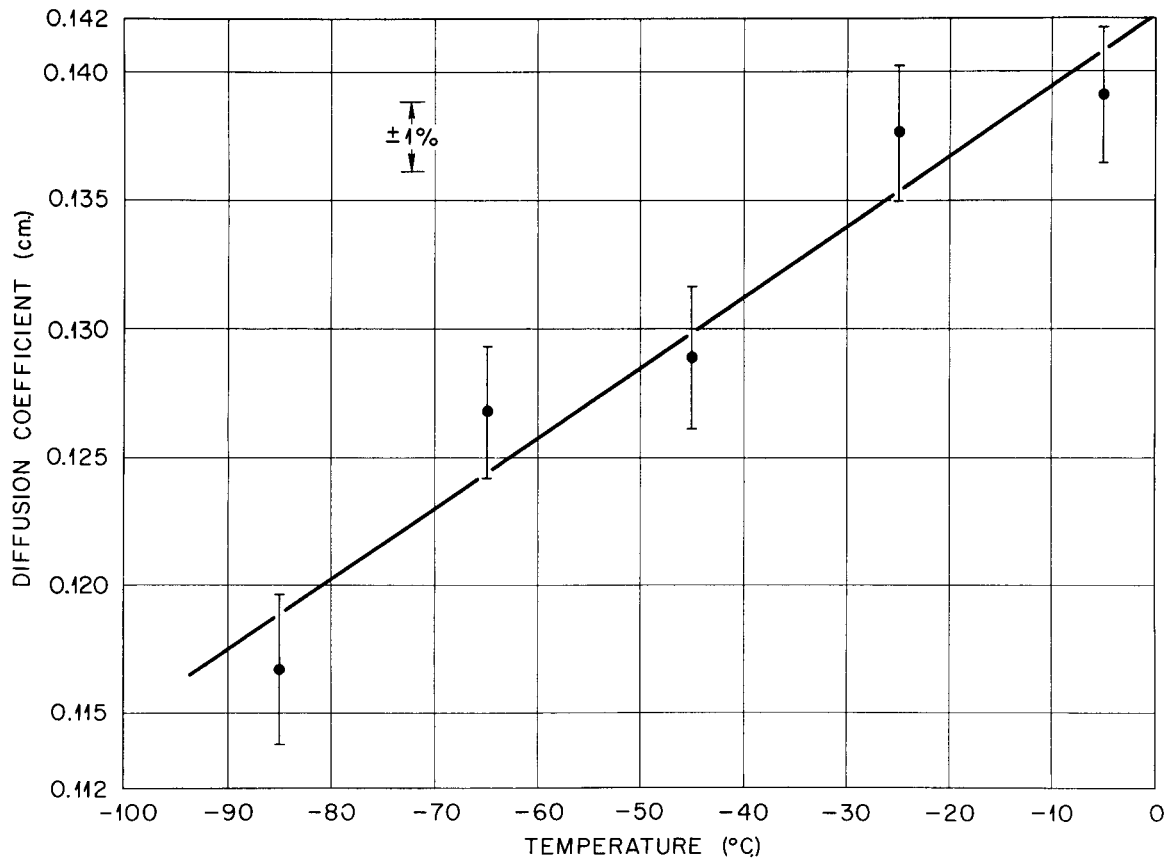


Figure 67. Measured diffusion coefficient,  $D$ , as function of temperature.

at  $-5^{\circ}\text{C}$ . as a function of neutron energy using a LINAC neutron source with time-of-flight methods. Figure 68 shows the results obtained. In addition to the large effect for very low temperature there is a significant difference of opposite sign between the ice and water cross sections in the region where the spectrum has its maximum, amounting to about 5.5 to 8 per cent in the energy region from 0.01 to 0.028 eV., in which about 65 per cent of the neutrons are, assuming a Maxwellian spectrum. A graphical solution of the equation,

$$\frac{\sigma_s^{(\text{ice})}}{\sigma_s^{(\text{water})}} = \frac{\int M(E) \sigma_s^{(\text{ice})}(E) dE}{\int M(E) \sigma_s^{(\text{water})}(E) dE} = \frac{\sum_k M_k \sigma_{sk}^{(\text{ice})} (\Delta E)_k}{\sum_k M_k \sigma_{sk}^{(\text{water})} (\Delta E)_k} = 1.034 \pm 0.018 \quad (212)$$

was performed by making use of Figure 68, with the result shown. It is interesting to observe that for very low incident neutron energies the scattering cross section in water is larger than that in ice. This is also borne out by a result obtained by Heinloth and Springer (1961), who measured the total cross section per  $\text{H}_2\text{O}$  molecule over a wide temperature range, including the water-ice transition for several incident neutron energies from  $0.018 \times 10^{-3}$  to 0.036 eV. The results are shown in Figure 69 and the appropriate values are entered in Figure 68. Oddly enough, these workers did not observe the region of higher ice cross section because, as Figure 68 makes clear, their measured initial energies skip the energy domain between 0.0027 and 0.036 eV., which is just the

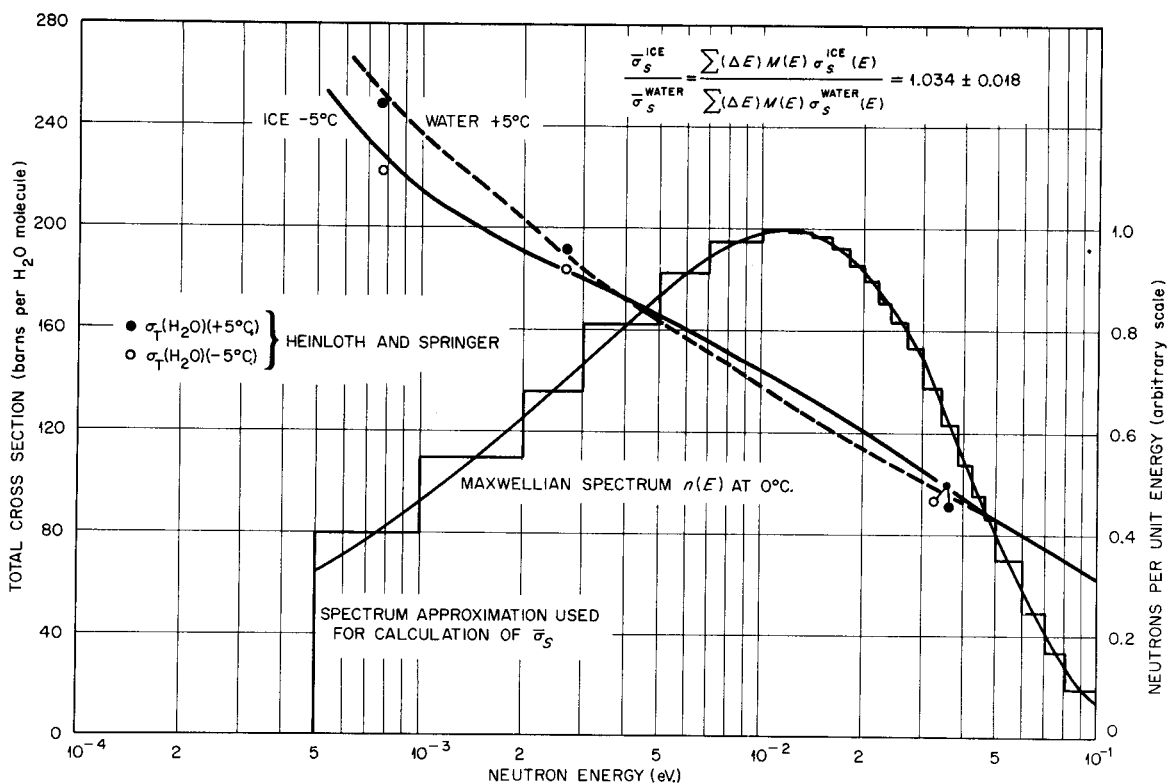


Figure 68. Measured total cross section per H<sub>2</sub>O molecule as function of neutron energy, measured by Whittemore and McReynolds (1962). A Maxwellian spectrum at 0°C. is also shown, together with an approximation to the spectrum used to calculate the ratio of the mean scattering cross section. The experimental points represent results reported by Heinloth and Springer (1961).

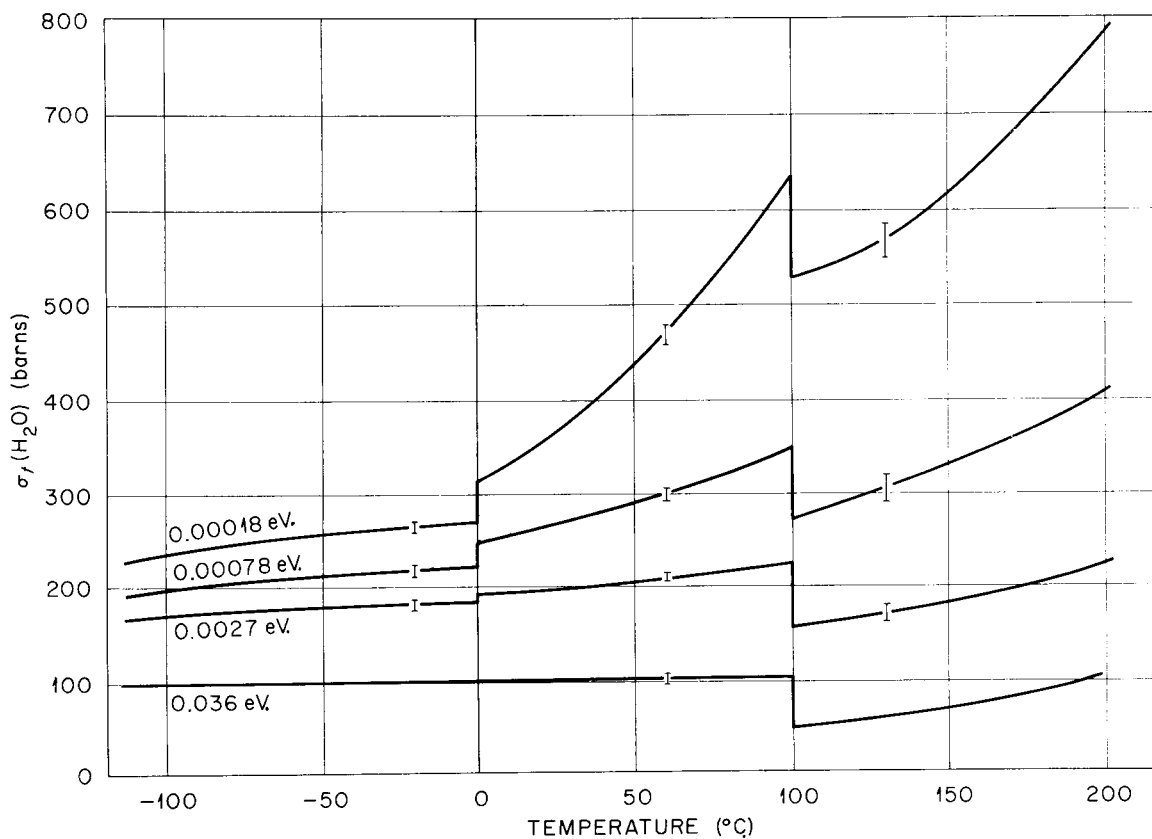


Figure 69. Total cross section per water molecule for incident neutrons of 0.00018, 0.00078, and 0.036 eV. Over the temperature range from  $-120^{\circ}$  to  $200^{\circ}\text{C}$ ., measured by Heinloth and Springer (1961).

energy region where most of the neutrons are, and also the energy region where the significant difference between ice and water scattering cross sections is to be found.

With regard to the effect of the phase transition on the parameter  $(1 - \bar{\mu})$ , Reinsch and Springer (1961) have measured the "single-differential" scattering cross section

$$\sigma(\theta) = \int_0^{\infty} dE' \sigma(E \rightarrow E', \theta, T) \quad (213)$$

for neutrons of initial energies 0.039 and 0.078 eV. in water at 21°C., and in ice at -15°C, -55°C, and -160°C. Figure 70 shows their result. The most significant aspect of this is that the angular distribution is almost completely independent of the phase of the material, except for a small oscillatory region at small angles which appears in ice and not in water. This small effect is due to the coherent scattering, which is seen to have little effect, as was expected. Reinsch and Springer have calculated the mean cosine of the scattering angle,  $\bar{\mu}$ , obtained from these measurements and give the following results for  $\bar{\mu}$ :

| <u>Neutron Energy</u> | <u>Temperature</u> |             |
|-----------------------|--------------------|-------------|
|                       | -15°C.             | +21°C.      |
| 0.039 eV.             | 0.21 ± 0.02        | 0.22 ± 0.01 |
| 0.078 eV.             | 0.28 ± 0.01        | 0.27 ± 0.01 |

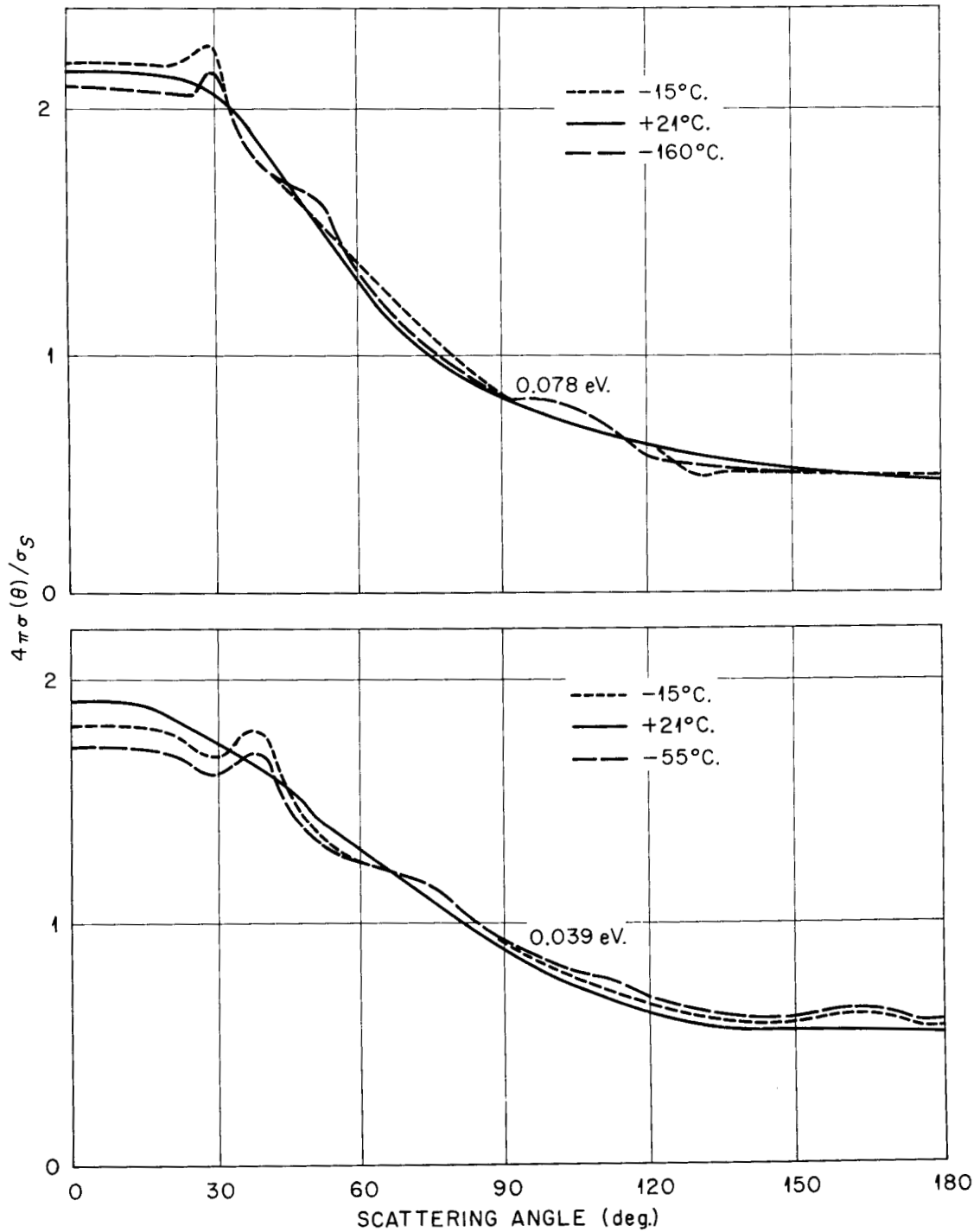


Figure 70. Differential scattering cross section,  $4\pi\sigma(\theta)/\sigma_s$  for neutrons of initial energies 0.078 and 0.039 eV. at temperatures  $-55^\circ$ ,  $-15^\circ$ , and  $+20^\circ\text{C}$ . Measured by Reinsch and Springer (1961).

Thus, the mean scattering angle at each neutron energy is the same whether the  $H_2O$  is in the solid or liquid state.

The implication of these results by Heinloth and Springer, and Whittemore and McReynolds is clear. The data give support to the conclusion that the observed discontinuity in  $(vD)$  is real, and that it must be almost completely due to the change in the total cross section rather than to changes in the angular distribution; first, because no change in  $(1 - \bar{\mu})$  was observed and, second, because within the error limits the measured change in  $\bar{\sigma}_s$  is of the right size to explain the observed discontinuity. Also, the fact that the coherence effects are observable, but are small and have no effect on the mean scattering angle, confirms the supposition that these effects are negligible for the present experiments.

The following reason for the somewhat surprising lack of effect of the ice bonding on the angular distributions is suggested by Reinsch and Springer: The scattering cross section  $\sigma(\theta)$  consists of a coherent and an incoherent part, of which the incoherent part is seen to predominate strongly. The incoherent part can be divided into an elastic and an inelastic component. The elastic component is proportional to the Debye-Waller factor

$$W(e,T) = e^{-2W} \quad (214)$$

where

$$2W = \frac{6kT}{M(k\Theta)^2} (E + E' - 2\sqrt{EE'} \cos\theta) \left(1 + \frac{\Theta^2}{36T^2} - \dots\right)$$

$$\approx 16 \pi^2 u^2 \sin^2 \frac{\theta}{2} / \lambda^2 . \quad (215)$$

In this equation  $\Theta$  is the Debye temperature which is  $\approx 250^\circ\text{K}$ . in ice and  $\approx 120^\circ\text{K}$ . in water near freezing,  $u$  is the mean amplitude of the displacements (in which the translational part is dominant) and  $\lambda$  is the neutron wavelength.

The elastic component thus decreases more rapidly with angle in water than in ice due to the change in the Debye temperature. However, the inelastic component of the incoherent scattering, which has a rather broad, flat maximum at about  $60^\circ$ , is larger in water than in ice, because more levels can be excited (to give inelastic processes) as the Debye temperature drops. These two effects, Springer and Reinsch suggest, largely cancel each other and account for the observed fact that the scattering curves are almost identical in ice and water. This result also confirms the fact that the additional hindering effect on the translational motion of the molecules caused by freezing is not important.

It is worth emphasizing here again that the apparent similarity between water and ice is due to the fact that the liquid water molecule behaves largely as though it were bound in a "quasi-crystal." A model for water based on this viewpoint was developed by Singwi and Sjolander (1960), and this view also underlies the Nelkin model, which treats translational motions in water molecules as normal modes of vibration

about lattice positions. (Nelkin finds that despite such "binding" in liquid water the translations can be treated as free.) This quasi-crystal model is experimentally verifiable by scattering experiments; for example, Brockhouse (1959) observed an elastic peak in the scattered neutron spectrum from water. The main part of the low-energy cross section comes from translational modes of vibration with periods of the order of  $5 \times 10^{-13}$  sec., whereas according to Singwi and Sjölander the mean time a molecule spends at a 'lattice position' is of the order of  $5 \times 10^{-12}$  sec., so that on the average a molecule will execute some ten vibrations about a lattice position before jumping to another lattice-like position.

An interesting model for considering this effect is discussed by Gössman (1962), who speaks of a "Schollenmodell" or "ice-floe" model. The water is treated as a saturated solution of ice-like domains or floes. Gössman finds that in water at 0°C. some 85 per cent of the water must be treated as being in ice-like clumps to account for the observed scattering of cold neutrons with 0.00018 eV. initial energy.

Diffusion cooling coefficient. The temperature dependence of the diffusion cooling coefficient, C, may be considered to be due to the combined action of two mechanisms. In the theoretical discussion of C the relation was derived

$$C = - \frac{(vD)^2}{2NM_2} \left[ 1 + 2 \frac{d(\ln \bar{D})}{d(\ln T)} \right]^2. \quad (100)$$

(The minus sign here arises because in this work the  $B^4$  term has been defined as  $+CB^4$ .)

Nelkin (1958), using a variational calculation and assuming that  $\lambda_{tr} = KE^\alpha$ , obtained the relation

$$C = - \frac{(\alpha + 1/2)^2 \sqrt{\pi}}{v_T N M_2} (vD)^2 \quad (216)$$

where  $N$  is the atomic density and  $v_T = (2kT/m)^{1/2}$ .  $C$  therefore will change with temperature as  $(1/v)(vD)^2$  (neglecting density changes) and also inversely with  $M_2$ .

Now  $\lambda_{tr} \propto 1/\sigma_{tr} = 1/(1 - \bar{\mu}) \sigma_s$ . Beyster, Young, Neill, and Mowry (1965) have published measured values of  $\bar{\mu}(E)$  in water. Combining this information with the scattering cross section data of Whittemore and McReynolds (1961) shown in Figure 68 (page 243) a curve for  $\lambda_{tr}$  as function of energy is obtained. This curve is shown in Figure 71. Curves of  $\lambda_{tr}$  vs. neutron energy calculated on the model  $\lambda_{tr} = k E^\alpha$  are also shown, fitted to agree with the experimental curve at 0.02 eV., which is near the maximum in the neutron energy distribution. The experimental shape is not in complete agreement with the exponential model, but for  $\alpha = 0.5$  the fit is reasonably good in the most important energy range from 0.01 to 0.08 eV. It will therefore be assumed that  $\alpha$  does not change with temperature and may be taken to have the value of 0.5.

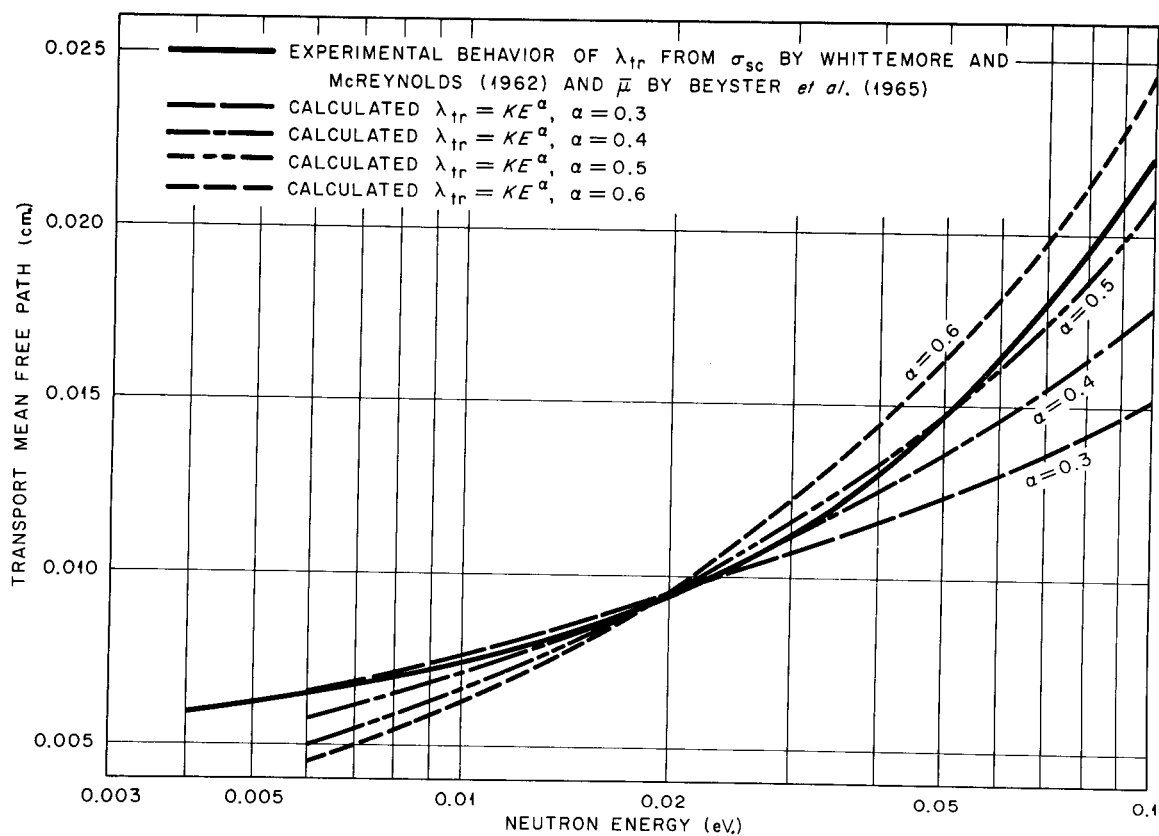


Figure 71. Comparison of the measured energy dependence of  $\sigma_T(E)$  at  $-5^\circ\text{C}$ . with the model  $\sigma_s = (136)(0.013)^\alpha E^{-\alpha}$  b. for  $\alpha = 0.2$ ,  $0.3$ , and  $0.5$ .

The Nelkin expression for C can be made to fit any one experimental value of C by treating  $M_2$  as a free parameter. This was done using the point at  $-45^\circ\text{C}$ . which is in the center of the measured temperature range and where there is a close correspondence between the measured value and the value of the straight line fit:

$$\begin{aligned} M_2(-45^\circ\text{C.}) &= \frac{(\alpha + 1/2)^2 \sqrt{\pi} [(vD)(-45^\circ\text{C.})]^2}{v_T(-45^\circ\text{C.}) C(-45^\circ\text{C.}) N} \\ &= (35.1 \pm 3.3)b. \end{aligned} \quad (217)$$

To determine the change of  $M_2$  with temperature, the value of C was calculated assuming a temperature-independent value of  $M_2 = 35.1 b.$  and taking  $\alpha = 0.5$ . Figure 72 shows a plot of  $C(T)$  calculated in this way together with the experimental values of C over the measured temperature range. The curve for C calculated with the assumption of a constant value of  $M_2$  is seen to agree quite well with the experimental results. The calculated curve of C vs. T is not linear, since, assuming that  $(vD)$  is proportional to T, one has

$$- C(T) \propto \frac{(vD)^2}{v_T} \propto \frac{T^2}{\sqrt{T}} \propto T^{1.5} \quad (218)$$

and therefore,

$$- \frac{dC(T)}{dT} \propto \sqrt{T} \quad (219)$$

However, the nonlinearity causes a change of only 16 per cent in the

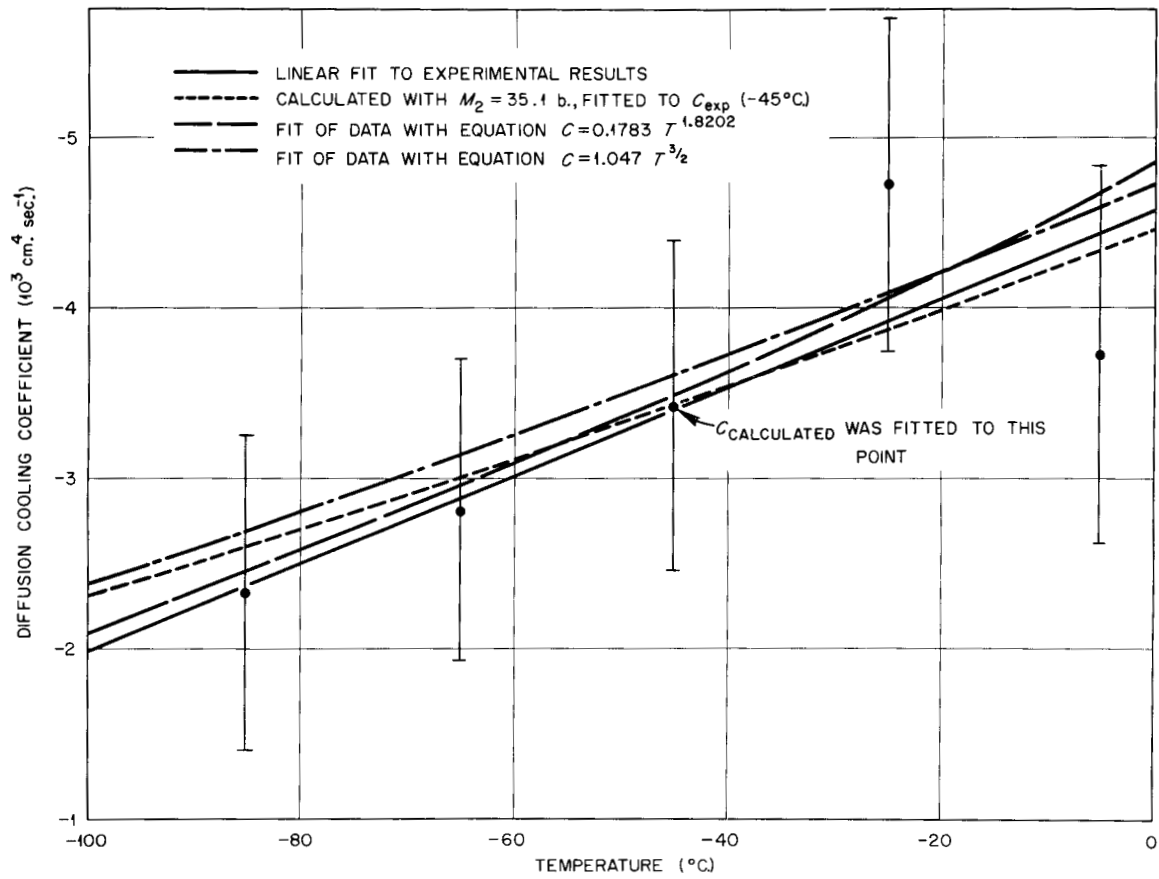


Figure 72. Experimental values of  $C$ , together with the fitted curves based on two models.  $C$  calculated assuming  $M_2$  to be a constant is also shown.

slope from  $-5^{\circ}\text{C.}$  to  $-85^{\circ}\text{C.}$  Thus, within the limits of error, the results support the conclusion that  $M_2$  is unchanged with temperature over the range measured, and has the value of  $(35.1 \pm 3.3)$  b. obtained above. It should be pointed out that the slope of the calculated curve does not depend on the choice of  $\alpha$  but only on the temperature variation of  $(1/v)(vD)^2$ . However, the value of  $M_2$  does depend on this choice. Figure 73 shows the effect on  $M_2$  ( $-45^{\circ}\text{C.}$ ) of the choice of  $\alpha$ .

In view of the large errors in  $C$  it is not certain what form of model is the most reasonable to assume in fitting to the data. A theoretical consideration of the behavior of the parameter  $C$  can, however, give information on the best choice of model. With  $(vD)$  fitted to a linear temperature dependence in  $^{\circ}\text{K.}$  the result is:

$$(vD)(T^{\circ}\text{K.}) = [(0.047 \pm 0.202) + (0.01225 \pm 0.0087) \cdot (T^{\circ}\text{K.})] \times 10^4 \text{ cm.}^2 \text{ sec.}^{-1}. \quad (220)$$

Since  $(vD)(0^{\circ}\text{K.})$  is zero within the limits of error the assumption that  $(vD)$  is proportional to  $T$  appears valid and one may write

$$(vD)(T^{\circ}\text{K.}) = \kappa T \quad (221)$$

where  $\kappa = 122.5 \text{ cm.}^2 \text{ sec.}^{-1}/(^{\circ}\text{K.})$ . With this temperature dependence of  $(vD)$  one may write:

$$C(T) = - \frac{k'(vD)^2}{(T)^{1/2}} \cdot \frac{1}{M_2(T)} = - \frac{k' \kappa^2 T^{3/2}}{M_2(T)} \text{ cm.}^4 \text{ sec.}^{-1}, \quad (222)$$

where  $k' = (\alpha + 1/2)^2 \sqrt{\pi T_0} / N v_0 = 2.248 \times 10^{-27}$  with  $\alpha = 0.5$ . Then

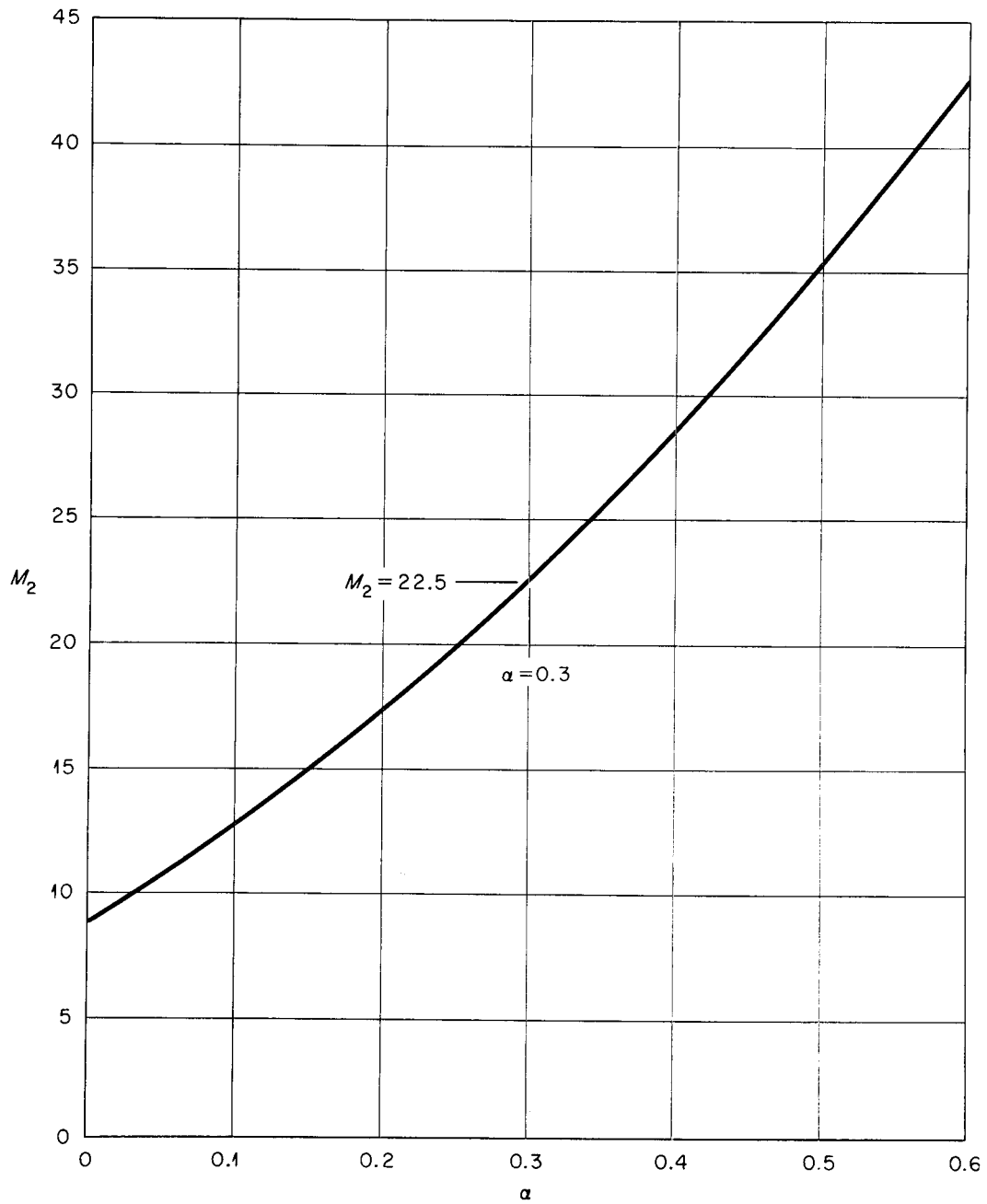


Figure 73. The effect of the value chosen for  $\alpha$  on the value of  $M_2$  calculated by Nelkin's equation (Nelkin, 1958);

$$M_2 = \frac{(\alpha + 1/2)^2 \sqrt{\pi} (vD)^2}{v_T C} .$$

$$M(T) = \frac{k'' T^{3/2}}{C(T)}$$

where  $k'' = k' \kappa^2 = 33.74 \times 10^{-24} \text{ cm.}^6 \text{ sec.}^{-1} (\text{°K.})^{-3/2}$ , and

$$\frac{dM(T)}{dT} = \frac{(3/2) k'' T^{1/2} C(T) - k'' T^{3/2} [dC(T)/dT]}{[C(T)]^2} . \quad (223)$$

Note first that, if  $[dC(T)/dT] = (3/2T)C(T)$  then  $M_2(T)$  is independent of temperature. Thus, the slope of  $C(T)$  at  $0^\circ\text{C.}$  which would result from a temperature-independent value of  $M_2$  is calculated to be:

$$\left. \frac{dC(T)}{dT} \right|_{T=0^\circ\text{C.}} = (3/2) \frac{4.58 \times 10^3}{273} = 25.2 \text{ cm.}^4 \text{ sec.}^{-1}/(\text{°K.})$$

and at  $-85^\circ\text{C.}$ :

$$\left. \frac{dC(T)}{dT} \right|_{T=-85^\circ\text{C.}} = (3/2) \frac{2.37 \times 10^3}{188} = 18.9 \text{ cm.}^4 \text{ sec.}^{-1}/(\text{°K.})$$

The measured value, from the linear fit to  $C(T)$ , is

$$\left. \frac{dC(T)}{dT} \right|_{\text{exp.}} = 25.5 \pm 11.6 \text{ cm.}^4 \text{ sec.}^{-1}/\text{°C.}$$

Within the error limits, therefore, the conclusion that  $M_2$  is independent of energy is justified. However  $M_2$  represents the energy-exchange cross section between the neutron and the crystal lattice, and, therefore, as the temperature approaches  $0^\circ\text{K.}$ ,  $M_2$  should also decrease, since more and

more of the inelastic processes by which energy exchange occurs become unavailable as the temperature decreases. The linear fit of  $C$ , however, would result in increasing values of  $M_2$  as the temperature drops, because of the positive intercept of  $C(T)$ .

The ratio of two values of  $M_2$  can be written as

$$\frac{M_2(T_1)}{M_2(T_2)} = \frac{V_2}{V_1} \frac{(vD)_1^2}{(vD)_2^2} \frac{C(T_2)}{C(T_1)} = \left(\frac{T_1}{T_2}\right)^{3/2} \frac{C(T_2)}{C(T_1)} = \left(\frac{T_1}{T_2}\right)^{3/2} \frac{a - bT_1}{a - bT_2} \quad (224)$$

where  $a$  and  $b$  are the coefficients of the linear fit for  $C$ . Then, using the linear fit to  $C$  in absolute temperature units

$$C(T^{\circ}\text{K.}) = [(2.45 \pm 2.65) - (0.0258 \pm 0.0117) \cdot (T^{\circ}\text{K.})] \times 10^3 \text{ cm.}^4 \text{ sec.}^{-1}, \quad (225)$$

one has

$$\frac{M_2(188^{\circ}\text{K.})}{M_2(268^{\circ}\text{K.})} = 1.13.$$

In fact, at  $T = a/b = 95^{\circ}\text{K.}$ ,  $M_2$  would become infinite, and below that  $M_2$  would be negative. To avoid such a catastrophe to  $M_2$ , with the minimum change in the fitting model, it will be assumed that  $C$  goes to zero at  $0^{\circ}\text{K.}$  It will, therefore, be attempted to fit the observed values of  $C$  to a model of the form

$$C(T) = - aT^b. \quad (226)$$

With this assumption  $M_2(T)$  becomes

$$M_2(T) = \frac{kT^{3/2}}{aT^b} = (k/a) T^{(3/2-b)} \quad (227)$$

The requirement that  $M_2$  should not decrease as temperature increases leads to the bounding condition  $b \leq 3/2$ ; the requirement that  $C(T)$  increase with temperature implies the bound  $b \geq 0$ . The linearized equation

$$\ln |C(T)| = \ln a + b \ln T \quad (228)$$

was used to find the optimum parameters  $a$  and  $b$  from the experimental data. The result was  $C(T) = -(0.1783 \pm 0.101) T^{(1.82 \pm 0.89)} \text{ cm.}^4 \text{ sec.}^{-1}$ . The curve is shown in Figure 72 (page 253). The value of  $b$  is outside the permitted range, though its uncertainty extends well into the allowed domain. Taking the closest allowed value  $b = 3/2$ , a fit was made to optimize  $a$ . The result was:

$$C(T) = (1.047 \pm 0.173) T^{3/2} \quad (229)$$

This curve also is shown in Figure 72. Using this  $(3/2)$  power model  $M_2$  becomes constant with temperature and its value is

$$M_2 = \frac{k'' T^{3/2}}{1.047 T^{3/2}} = (32.2 \pm 6.6)b \quad .$$

If the optimum fit is used then the formula for  $M_2$  would be

$$M_2 = \frac{k'' T^{3/2}}{0.1783 T^{1.820}} = 189.2 T^{-.320} \text{ b} , ,$$

with the results:  $M_2(-5^\circ\text{C.}) = 31.4 \text{ b.}$ ,  $M_2(-45^\circ\text{C.}) = 33.3 \text{ b.}$ , and  $M_2(-85^\circ\text{C.}) = 35.5 \text{ b.}$  The small increase in  $M_2$  as the temperature is lowered results, of course, from the too-large exponent on  $T$ .

To summarize, the analysis of the temperature dependence of the diffusion cooling parameter  $C$  on the basis of the Nelkin formula suggests that in the domain measured  $M_2$  is independent of energy and has a value of  $34 \pm 4 \text{ b.}$  This value agrees, within the error limits, with the values obtained by a linear fit to  $C(T)$ , and also by the two exponential fits which were chosen to give proper low-temperature behavior of  $M_2$ . This value may be compared with that obtained by Kuchle (1960), who found  $(31 + 6) \text{ b.}$ , using  $\alpha = 0.4$ . Converting this result to  $\alpha = 0.5$  this becomes  $(39 + 7) \text{ b.}$   $M_2$  thus decreases slightly upon freezing as would be expected. However, with the uncertainties considered, an unchanged value would also be consistent with the results. Since the total scattering cross section changes very little between cold water and ice, any decrease in inelastic scattering, which would be expected from the somewhat tighter bonding in ice, is at least partly offset by an increase in elastic scattering. This supposition is in accord with the conclusions of Heinloth and Springer discussed above.

So, within the error limits, these values support the conclusion that, contrary to the findings of Antonov et al. and Dlouhý and Kvítek, no large discontinuity in  $C$  exists across the phase transition, if correction is made for the density effect.

## IV. COMPARISON WITH OHANIAN CALCULATIONS

By use of the numerical method described in Chapter II Ohanian<sup>1</sup> has calculated the diffusion coefficient and the diffusion cooling coefficient in water at 20°C. and in ice at -5°C. and at -45°C. The results at 20°C. were

$$(vD)_{w(20^{\circ}\text{C.})} = 3.47 \times 10^4 \text{ cm.}^2 \text{ sec.}^{-1}$$

$$(C)_{w(20^{\circ}\text{C.})} = 2.99 \times 10^3 \text{ cm.}^4 \text{ sec.}^{-1} .$$

Converting to ice-equivalent density these values become:

$$(vD)_{w(i)(20^{\circ}\text{C.})} = 3.78 \times 10^4 \text{ cm.}^2 \text{ sec.}^{-1}$$

$$(C)_{w(i)(20^{\circ}\text{C.})} = 3.87 \times 10^3 \text{ cm.}^4 \text{ sec.}^{-1} .$$

These results are both in reasonable agreement with experimental results obtained by various workers, as listed in Table XIII (page 233). The results may also be compared with those of a rather similar calculation by Honeck (1962) described in Chapter II, which yielded

$$(vD)_{w(20^{\circ}\text{C.})} = 3.75 \times 10^4 \text{ cm.}^2 \text{ sec.}^{-1}$$

$$(C)_{w(20^{\circ}\text{C.})} = 2.88 \times 10^3 \text{ cm.}^4 \text{ sec.}^{-1} .$$

---

<sup>1</sup>The results to be discussed in this section are unpublished data transmitted to the author in a private communication from M. J. Ohanian, and are to be regarded as preliminary values at the time of this writing (July, 1965).

The results obtained by Ohanian in ice are as follows:

|                        | $(vD)_i$   | $(C)_i$  |
|------------------------|--|--|
| $-5^{\circ}\text{C.}$  | $3.52 \times 10^4 \text{ cm.}^2 \text{ sec.}^{-1}$ | $3.75 \times 10^3 \text{ cm.}^4 \text{ sec.}^{-1}$ |
| $-25^{\circ}\text{C.}$ | $3.12 \times 10^4 \text{ cm.}^2 \text{ sec.}^{-1}$ | $3.57 \times 10^3 \text{ cm.}^4 \text{ sec.}^{-1}$ |

It is found that for both  $(vD)$  and  $C$  the three values calculated by Ohanian are exactly collinear after the values in water are compensated for the density difference by the correction factors previously described. The equations are:

$$(vD) = [8.40 + 0.10 (T^{\circ}\text{K.})] \times 10^3 \text{ cm.}^2 \text{ sec.}^{-1} \quad (230)$$

and

$$(C) = [2.54 + 0.0045 (T^{\circ}\text{K.})] \times 10^3 \text{ cm.}^4 \text{ sec.}^{-1} \quad (231)$$

From Equation (230) one may obtain the value  $(vD)_{w(i)}(0^{\circ}\text{C.}) = 35.7 \times 10^3 \text{ cm.}^2 \text{ sec.}^{-1}$  which agrees well with measured values of  $(vD)_w(0^{\circ}\text{C.})$  but is quite high compared to the ice values obtained in the present work. However, the model used by Ohanian does not include any effects which might produce changes at the phase transition, other than the change in density which has been compensated for. Thus the observed discontinuity does not appear. If the Ohanian results in ice are adjusted to include this discontinuity (a change of  $-1.47 \times 10^3 \text{ cm.}^2 \text{ sec.}^{-1}$ ) the values become:

$$(vD)_i'(-5^{\circ}\text{C.}) = 33.7 \times 10^3 \text{ cm.}^2 \text{ sec.}^{-1}$$

$$(vD)_i'(-45^{\circ}\text{C.}) = 29.7 \times 10^3 \text{ cm.}^2 \text{ sec.}^{-1}$$

where the primes denote values adjusted as described. These values are in good agreement with the result of the present work at  $-5^{\circ}\text{C}$ . and in fair agreement with the value at  $-45^{\circ}\text{C}$ . (The differences amount to 1.04 per cent and 4.04 per cent respectively.) Since the calculated temperature dependence of  $(vD)$  is smaller than that found by the experiments the two values tend to diverge as the temperature decreases. However even at  $-85^{\circ}\text{C}$ . the calculated value is  $(vD)_i(-85^{\circ}\text{C}) = 27.2 \times 10^3 \text{ cm.}^2 \text{ sec.}^{-1}$  using the linear fit to the Ohanian values directly, or  $(vD)'_i(-85^{\circ}\text{C}) = 25.7 \times 10^3 \text{ cm.}^2 \text{ sec.}^{-1}$  if the adjusted value is used. This compares with the value of  $23.7 \times 10^3 \text{ cm.}^2 \text{ sec.}^{-1}$  obtained by the linear fit to the experimental results of the present work. So even in this worst case the disagreement amounts to 7.8 per cent, if the adjusted value of the computed result is used.

The values for  $C$  agree at both temperatures with the measured values, within the error limits, and the agreement is in fact excellent at both points. However this excellent agreement is somewhat fortuitous. The slopes of both  $(vD)$  and  $C$  with temperature as calculated by Ohanian are rather different from those obtained by the present experiments, and the agreement is due to the fact that

1. The cross-over point for the two curves lies at about  $-40^{\circ}\text{C}$ . accounting for the excellent agreement at  $-45^{\circ}\text{C}$ ., and
2. The experimental result at  $-5^{\circ}\text{C}$ . lies well below the fitted curve, accounting for the good agreement there.

At  $-25^{\circ}\text{C}$ . where the experimental value lies above the fitted curve the two results disagree by a little more than the error limits assigned to

the experimental value. The results for the values of  $(-C)$ , in units of  $10^3 \text{ cm.}^4 \text{ sec.}^{-1}$  are:

| Temperature          | Experimental Value | Calculated Value | Difference |
|----------------------|--------------------|------------------|------------|
| $-5^\circ\text{C.}$  | $3.73 \pm 1.11$    | 3.75             | 0.02       |
| $-25^\circ\text{C.}$ | $4.73 \pm 0.99$    | 3.66             | 1.07       |
| $-45^\circ\text{C.}$ | $3.43 \pm 0.97$    | 3.57             | 0.14       |
| $-65^\circ\text{C.}$ | $2.82 \pm 0.88$    | 3.48             | 0.66       |
| $-85^\circ\text{C.}$ | $2.32 \pm 0.92$    | 3.39             | 1.07       |

The two calculated values at  $-65^\circ\text{C.}$  and at  $-85^\circ\text{C.}$  were obtained by linear extrapolation of the Ohanian results, and show that, because of the much smaller slope the results tend to diverge as the temperature drops. However, in the range covered by the measurements the agreement is nowhere seriously outside the error limits assigned to the experimental values. Although precise error estimates for the calculated values are not available, Ohanian estimates these to be of the order of five per cent.

It is interesting to consider the change in  $M_2$  to be inferred from the Ohanian results. Although the rate of change of both  $(vD)$  and  $C$  with temperature is substantially less than that observed in the present experiments, the two differences tend to compensate, so that the behavior of  $M_2$  is not very much unlike that deduced from the experimental results. Applying Equation (224):

$$\frac{M_2(T_1)}{M_2(T_2)} = \left(\frac{T_2}{T_1}\right)^{1/2} \left[\frac{(vD)(T_1)}{(vD)(T_2)}\right]^2 \left[\frac{C(T_2)}{C(T_1)}\right] \quad (224)$$

one obtains

$$\frac{M_2(-45^\circ\text{C.})}{M_2(-5^\circ\text{C.})} = 0.89; \quad \frac{M_2(-85^\circ\text{C.})}{M_2(0^\circ\text{C.})} = 0.78$$

Thus the calculated results imply that  $M_2$  decreases as the temperature drops, although the decrease is not very rapid. Since both  $(-C)$  and  $(vD)$  as calculated by Ohanian have positive intercepts at  $0^\circ\text{K.}$  while  $v_T$  vanishes at this point, it is apparent that  $M_2$  would increase without limit as the temperature approaches absolute zero. In fact the linear models for  $(vD)$  and  $(-C)$  lead to a minimum value of  $M_2$  at about  $30^\circ\text{K.}$  However there is no reason to believe that the linear model should be applicable at such low temperatures, since the assumptions underlying the Nelkin model certainly do not hold in this region.

BIBLIOGRAPHY

## BIBLIOGRAPHY

- Ajzenberg-Selove, F., and T. Lauritsen, Nucl. Phys. 11, 1 (1959).
- Amaldi, E., and E. Fermi, Ric. Sci. Anno 7, I, 454 (1936).
- Andrews, W. M., Measurement of the Temperature Dependence of Neutron Diffusion Properties in Beryllium Using a Pulsed Neutron Technique (UCRL-6803, 1960).
- Antonov, A. V., A. I. Isakoff, I. D. Murin, B. A. Neupocoyev, I. M. Frank, F. L. Shapiro, and I. V. Shtranich, Proc. Intern. Conf. Peaceful Uses At. Energy, Geneva, 1955 2, 3 (1955).
- Antonov, A. V., B. V. Granatkin, and Ch. K. Smolik, page 377 in Proceedings of the International Atomic Energy Agency Symposium on Inelastic Scattering of Neutrons in Solids and Liquids, Vienna, October 11-14, 1960 (IAEA, Vienna, 1961).
- Antonov, A. V., B. V. Granatkin, Yu. A. Merkul'ev, V. V. Pusanov, and Ch. K. Smolik, At. Energ. (USSR) 13, No. 4, 373 (1962).
- Antonov, A. V., B. V. Granatkin, Yu. A. Merkul'ev, Ch. K. Smolik, At. Energ. (USSR) 12, No. 1, 22 (1962).
- Ashby, V. J., and H. C. Catron, Tables of Nuclear Reaction Q Values (UCRL-5419, 1959).
- Baker, C. P., and R. F. Bacher, Phys. Rev. 59, 332 (1941).
- Beckurts, K. H., Z. Naturforsch. 16a, 611 (1961).
- Beckurts, K. H., Nucl. Sci. Eng. 2, No. 4, 516-522 (1957).
- Beckurts, K. H., and D. Klüber, Z. Naturforsch. 13a, No. 10, 822 (1958).
- Beckurts, K. H., and K. Wirtz, Neutron Physics (Springer Verlag, New York, 1964).
- Berthelot, A., R. Cohen, and H. Reel, Compt. Rend. 225, 406 (1947).
- Beyster, J. R., J. C. Young, J. M. Neill, and W. R. Mowry, Differential Neutron Scattering from Hydrogenous Moderators (International Atomic Energy Agency Symposium on Pulsed Neutron Research, Karlsruhe, Germany, May 10-14, 1965, paper SM 62/64; proceedings to be published).
- Bhandari, R. C., J. Nucl. Energy 6, 104 (1958).

- Blatt, J. M., and V. F. Weisskopf, Theoretical Nuclear Physics (J. Wiley and Sons, New York, 1952).
- Bohl, H., E. Gelbard, P. Bürger, and G. Culpepper, SLOP-1, A Thermal Multigroup Program for the IBM-704 (WAPD-TM-188, 1960).
- Bomoto, T. T., and F. Kloverstrom, Trans. Am. Nucl. Soc. 1, No. 1, 94 (1958).
- Bormann, M., S. Cierjacks, E. Fretwurst, K.-J. Giesecke, H. Neuert, and H. Pollehn, Z. Physik 174, 1 (1963).
- Bracci, A., and C. Coceva, Nuovo Cimento 4, No. 1, 59 (1956).
- Bratenahl, A., J. M. Peterson, and J. P. Störing, Phys. Rev. 110, 927 (1958).
- Bretschler, M. M., Proc. Indiana Acad. Sci. 72, 249 (1962).
- Brockhouse, B. N., Phys. Rev. Letters 2, 287 (1959).
- Busing, W. R., and H. A. Levy, OR GLS, A General FORTRAN Least Squares Program (ORNL-TM-271, 1962).
- Campbell, E. C., and P. H. Stelson, page 32 in Physics Division Semi-annual Progress Report for Period Ending March 10, 1956 (ORNL-2076, 1956).
- Cornell, R. G., A New Estimation Procedure for Linear Combinations of Exponentials (ORNL-2120, 1956).
- Cummins, J. D., Some Pile Oscillator Cross Section Measurements Made in the DIMPLE Thermal Pit (AERE R/R 2333, 1957).
- Daughtry, J. W., and A. W. Waltner, The Diffusion Parameters of Heavy Water (International Atomic Energy Agency Symposium on Pulsed Neutron Research, Karlsruhe, Germany, May 10-14, 1965, paper SM 62/62; proceedings to be published).
- Davisson, B., Neutron Transport Theory (Oxford University Press, Oxford, 1957).
- De Juren, J. A., R. W. Stooksberry, and M. Wallis, Phys. Rev. 127, 1229 (1962).
- de Saussure, G., and E. G. Silver, page 119 in Applied Nuclear Physics Division Annual Progress Report for Period Ending September 1, 1957 (ORNL-2389, 1957).

- de Saussure, G., and E. G. Silver, page 59 in Neutron Physics Division Annual Progress Report for Period Ending September 1, 1958 (ORNL-2609, 1958).
- de Saussure, G., and E. G. Silver, Nucl. Sci. Eng. 6, No. 2, 159 (1959).
- de Saussure, G., page 1158 in Proceedings of the Brookhaven Conference on Neutron Thermalization, Vol. IV (BNL-719, 1962).
- Dio, W. H., Nukleonik 1, 13 (1958/59).
- Dio, W. H., and E. Schapper, Nucl. Phys. 6, 175 (1958).
- Dixon, W. J., and F. J. Massey, Jr., Introduction to Statistical Analysis (McGraw-Hill Book Co., New York, 1957).
- Dlouhý, Z., and J. Kuítek, Reactor Sci. Technol. 16, 376 (1962).
- Droulers, Y., J. Lacour, and V. Raievski, J. Nucl. Energy 7, No. 3, 210 (1958).
- Duggal, V. P., and J. Martelly, Proc. Intern. Conf. Peaceful Uses At. Energy, Geneva, 1955 5, 28 (1955).
- Fairstein, E., Pulse Amplifier Manual (ORNL-3348, 1962).
- Fermi, E., Neutron Physics: A Course of Lectures by E. Fermi (AECD-2664).
- Fick, A., Poggendorff's Annalen 94, 59 (1855).
- Fowler, K., and A. Brolley, Rev. Mod. Phys. 28, 2 (1956).
- Gaerttner, E. R., P. B. Daitch, and R. R. Fullwood, Effects of Coherent Scattering on the Thermalization of Neutrons in Beryllium (International Atomic Energy Agency Symposium on Pulsed Neutron Research, Karlsruhe, Germany, May 10-14, 1965, paper SM 62/52; proceedings to be published).
- Ganguly, N. K., F. C. Cobb, and A. W. Waltner, Nucl. Sci. Eng. 17, 223 (1963).
- Gelbard, E. M., and J. A. Davis, Nucl. Sci. Eng. 13, 237 (1962).
- Gerasava, L. A., A. V. Kamayev, A. K. Krasin, and I. C. Morosov, Proc. Intern. Conf. Peaceful Uses At. Energy, Geneva, 1955 5, 13 (1955).
- Glass, F., page 22 in Instrumentation and Controls Division Annual Progress Report for Period Ending July 1, 1957 (ORNL-2480, 1957).

- Glasstone, S., and M. C. Edlund, The Elements of Nuclear Reactor Theory (D. Van Nostrand Co., Inc., Princeton, N. J., 1952).
- Goldman, D. T., and F. D. Federighi, Trans. Am. Nucl. Soc. 4, 135 (1961).
- Gössman, G., Nukleonik 4, No. 3, 110 (1962).
- Häfele, W., and L. W. Dresner, Nucl. Sci. Eng. 7, 304 (1960).
- Hanson, A. O., and J. L. McKibben, Phys. Rev. 72, 673 (1947).
- Heinloth, K., and T. Springer, page 323 in Proceedings of the International Atomic Energy Agency Symposium on Inelastic Scattering of Neutrons in Solids and Liquids, Vienna, October 11-14, 1960 (IAEA, Vienna, 1961).
- Hertzberg, G., Molecular Spectra and Molecular Structure, 2nd ed., Vol. II (D. Van Nostrand Co., Inc., Princeton, N. J., 1950).
- Hobson, R. L., G. P. Calame, and P. B. Daitch, Trans. Am. Nucl. Soc. 6, No. 1, 58 (1963).
- Hodgman, C. D., editor, Handbook of Chemistry and Physics, 32nd ed., page 1853 (Chemical Rubber Publishing Co., Cleveland, 1950-1951).
- Honeck, H., page 1186 in Proceedings of the Brookhaven Conference on Neutron Thermalization, Vol. IV (BNL-719, 1962).
- Hughes, D. J., Pile Neutron Research (Addison-Wesley Publishing Co., Cambridge, Mass., 1953).
- Hughes, D. J., and R. B. Schwartz, Neutron Cross Sections, Vol. 2 (BNL-325, 1958).
- Jahnke, E., and F. Emde, Tables of Functions with Formulae and Curves, 4th ed. (Dover Publications, New York, 1945).
- Jha, S. A., J. Nucl. Energy, Part A: Reactor Sci. 12, 89 (1960).
- Joshi, B. V., V. R. Nargundkar, and K. Subbaro, Diffusion Parameters of BeO by Pulsed Neutron Method (International Atomic Energy Agency Symposium on Pulsed Neutron Research, Karlsruhe, Germany, May 10-14, 1965, paper SM 62/39; proceedings to be published).
- Kay, R. E., and M. J. Harris, private communication; cited by Stehn et al. in BNL-325, 2nd ed., Supplement 2.
- King, R. F., and V. E. Parker, page 65 in Physics Division Semiannual Progress Report for Period Ending September 10, 1955 (ORNL-1975, 1955).
- Krieger, T. J., and M. S. Nelkin, The Scattering of Slow Neutrons by Hydrogenous Moderators (KAPL-1597, 1956).

- Küchle, M., Nukleonik 2, No. 4, 131 (1960).
- Küchle, M., Nucl. Sci. Eng. 8, No. 1, 88 (1960).
- Küchle, M., and K. H. Beckurts, J. Nucl. Energy, Part A: Reactor Sci. 10, 157 (1959).
- Küsmaul, G., and H. Meister, Reactor Sci. Technol. 17, 411 (1963).
- Livingston, M. S., and H. A. Bethe, Rev. Mod. Phys. 9, No. 3, 339 (1937).
- Lopez, W. M., and J. R. Beyster, Measurement of the Diffusion Parameters of Water by the Pulsed Neutron Method (GA-1584, Rev., 1961).
- Macklin, R. L., Oak Ridge National Laboratory, private communication, 1963.
- Manley, J. H., L. J. Haworth, and E. A. Luebke, Phys. Rev. 61, 152 (1942).
- Massey, B. J., Preparation of Thin Tritium-Zirconium Targets (ORNL-2237, 1957).
- Meadows, J. W., and J. F. Whalen, Nucl. Sci. Eng. 9, 139 (1961).
- Meadows, J. W., and J. F. Whalen, Nucl. Sci. Eng. 13, 230 (1962).
- Meyer, P., An Experimental Study of the (k<sub>B</sub>/l) Pulsed Neutron Source Technique in Light Water Assemblies (International Atomic Energy Agency Symposium on Pulsed Neutron Research, Karlsruhe, Germany, May 10-14, 1965, paper SM 62/60; proceedings to be published).
- Nelkin, M., J. Nucl. Energy 8, 48 (1958).
- Nelkin, M. S., Phys. Rev. 119, 741 (1960).
- Nelkin, M., Nucl. Sci. Eng. 7, 552 (1960).
- Nelkin, M., Nucl. Sci. Eng. 7, 210 (1960).
- Nelkin, M., Physica 29, 261 (1963).
- Ohanian, M. J., Eigenfunction Analysis of Hydrogenous Neutron Spectra, Ph.D. thesis, Rensselaer Polytechnic Institute, Troy, N. Y., 1963.
- Ohanian, M. J., and P. B. Daitch, Nucl. Sci. Eng. 19, 343 (1964).
- Pál, L., L. Bod, and Z. Szatmáry, Data Evaluation Problems in the Pulsed-Neutron Source Method (International Atomic Energy Agency Symposium on Pulsed Neutron Research, Karlsruhe, Germany, May 10-14, 1965, paper SM 62/98; proceedings to be published).

- Peierls, R., Proc. Roy. Soc. (London) Ser. A 149, 467 (1935).
- Perez, R. B., and R. E. Uhrig, Nucl. Sci. Eng. 17, 1 (1963).
- Present, R. D., Kinetic Theory of Gases (McGraw-Hill Book Co., Inc., New York, 1958).
- Purohit, S. N., Nucl. Sci. Eng. 9, 157 (1961).
- Radkowsky, A., page 89 in Physics Division Quarterly Report for April, May, and June 1950 (ANL-4476, 1950).
- Raievski, V., and J. Horowitz, Proc. Intern. Conf. Peaceful Uses At. Energy, Geneva, 1955 5, 42 (1955).
- Rainwater, J., and W. W. Havens, Phys. Rev. 70, 136 (1946).
- Ramanna, R., G. S. Mani, P. K. Iyengar, S. B. D. Iyengar, and B. V. Joshi, Proc. Intern. Conf. Peaceful Uses At. Energy, Geneva, 1955 5, 24 (1955).
- Reier, M., and J. A. De Juren, J. Nucl. Energy 14, No. 1, 18 (1961).
- Reinsch, C., and T. Springer, Z. Naturforsch. 16a, 1 (1961).
- Richey, C. R., and E. Z. Block, Graphite Diffusion Length Measurements at Hanford (HW-45035, 1956).
- Rockey, K. S., and W. Skolnik, Nucl. Sci. Eng. 8, No. 1, 62 (1960).
- Schull, C. G., E. O. Wollan, G. A. Morton, and L. W. Davidson, Phys. Rev. 73, 842 (1948).
- Scott, F. R., D. B. Thomson, and W. Wright, Phys. Rev. 95, 582 (1954).
- Silver, E. G., page 981 in Proceedings of the Brookhaven Conference on Neutron Thermalization, Vol. III (BNL-719, 1962).
- Singwi, K. S., and A. Sjölander, Phys. Rev. 119, 863 (1960).
- Sjöstrand, N. G., Arkiv Fysik 15, 145 (1959).
- Sjöstrand, N. G., J. Mednis, and T. Nilsson, Arkiv Fysik 15, 471 (1959).
- Springer, T., Ch. Hofmeyr, S. Kornbickler, and H. D. Lemmel, On the Determination of the Diffusion Constants of H<sub>2</sub>O, Phenyls, and D<sub>2</sub>O by Neutron Single-Scattering Experiments (JUL-160-NP, Kernforschungsanlage, Jülich, West Germany, 1964).

- Starr, E., and J. Koppel, Nucl. Sci. Eng. 14, 224 (1962).
- Stehn, J. R., M. D. Goldberg, B. A. Magurno, and R. Wiener-Chasman, Neutron Cross Sections. Z = 1 to 20, Vol. 1, 2nd ed., Supplement 2 (BNL-325, 1964).
- Sutton, R. B., T. Hall, E. E. Anderson, H. S. Bridge, J. W. De Wire, L. S. Lavatelli, E. A. Long, T. Snyder, and R. W. Williams, Phys. Rev. 72, 1147 (1947).
- Takahashi, H., page 1299 in Proceedings of the Brookhaven Conference on Neutron Thermalization, Vol. IV (BNL-719, 1962).
- Von Dardel, G. F., Kungl. Tekniska Högskolans Handlingar, Stockholm, Sweden, No. 75 (1954).
- Von Dardel, G., and A. W. Waltner, Phys. Rev. 91, 1284 (1953).
- Von Dardel, G. F., and N. G. Sjöstrand, Phys. Rev. 96, 1245 (1954).
- Weale, J. W., W. J. Paterson, H. Goodfellow, and M. H. McTaggart, Measurement of the Prompt Neutron Decay Constant of the VERA Reactor Using the Pulsed Source Method (International Atomic Energy Agency Symposium on Pulsed Neutron Research, Karlsruhe, Germany, May 10-14, 1965, paper SM 62/26; proceedings to be published).
- Weinberg, A. M., and E. P. Wigner, Physical Theory of Neutron Chain Reactions, chapter 9 (University of Chicago Press, Chicago, 1958).
- Whittemore, W. L., and A. W. McReynolds, page 511 in Proceedings of the International Atomic Energy Agency Symposium on Inelastic Scattering of Neutrons in Solids and Liquids, Vienna, October 11-14, 1960 (IAEA, Vienna, 1961).
- Wigner, E. P., and J. E. Wilkins, Jr., Effect of the Temperature of the Moderator on the Velocity Distribution of Neutrons with Numerical Calculation for H as Moderator (AECD-2275, 1944).
- Wilson, V. C., E. W. Bragdon, and H. Kanner, The Temperature Coefficient of the Diffusion Length for Thermal Neutrons in Water (CP-2306, 1944).
- Wynchank, S. A. R., and A. E. Cox, unpublished paper given at Conference on Low and Medium Energy Nuclear Physics at Manchester, England, 1963; cited by Stehn et al. in BNL-325, 2nd ed., Supplement 2.

## APPENDIX A

APPENDICES

## APPENDIX A

### DEAD-TIME CALCULATION AND EXPERIMENT

Assuming that a second pulse arriving during the dead time of the first does not extend the dead time one has

$$R_T = \frac{R}{1 - \tau R} \quad , \quad (A-1)$$

where  $R_T$  and  $R$  are the true and observed count rates, respectively, and  $\tau$  is the dead time. With two noninteracting sources (i.e., neutrons from source one cannot scatter from source two into the detector, and vice versa) one has

$$R_{T(1+2)} = R_{T(1)} + R_{T(2)} = \frac{R_1}{1 - \tau R_1} + \frac{R_2}{1 - \tau R_2} = \frac{R_{(1+2)}}{1 - \tau R_{(1+2)}} \quad , \quad (A-2)$$

or

$$\left[ 1 - \tau R_{(1+2)} \right] (R_1 - \tau R_1 R_2 + R_2 - \tau R_1 R_2) = R_{(1+2)} (1 - \tau R_1 - \tau R_2 + \tau^2 R_1 R_2) \quad (A-3)$$

which becomes, collecting terms in powers of  $\tau$ :

$$\tau^2 \left[ R_1 R_2 R_{(1+2)} \right] + \tau (-2R_1 R_2) + \left[ R_1 + R_2 - R_{(1+2)} \right] = 0 \quad . \quad (A-4)$$

Solving for  $\tau$ :

$$\tau = \frac{1}{R_{(1+2)}} \pm \left\{ \left[ \frac{1}{R_{(1+2)}} \right]^2 - \frac{R_1 + R_2 - R_{(1+2)}}{R_1 R_2 R_{(1+2)}} \right\}^{1/2} . \quad (\text{A-5})$$

Therefore the "-" sign must be used to reduce Equation (A-5) to:

$$\frac{1}{R_{(1+2)}} - \frac{1}{R_{(1+2)}} = 0 \quad (\text{A-6})$$

for  $\tau = 0$  and  $R_{(1+2)} = R_1 + R_2$ . In an experiment performed with two Am-Be sources (see Appendix B) the following values were obtained by gating all counts into channel number 3:

$$R_1 = 3241.0 \pm 17.8 \text{ cts./sec.}$$

$$R_2 = 2478.7 \pm 14.3 \text{ cts./sec.} \quad (\text{A-7})$$

$$R_{(1+2)} = 5624.4 \pm 45.8 \text{ cts./sec.}$$

The error associated with  $R_{(1+2)}$  includes a one-half percent contribution estimated as the possible interaction effect of the two source containers.

Substituting into Equation (A-5) one obtains

$$\tau = 6.03 \text{ } \mu\text{sec} .$$

The uncertainty associated with this value can be calculated by the relation

$$\delta\tau = \left\{ \left( \frac{\partial\tau}{\partial R_1} \right)^2 (\delta R_1)^2 + \left( \frac{\partial\tau}{\partial R_2} \right)^2 (\delta R_2)^2 + \left[ \frac{\partial\tau}{\partial R_{(1+2)}} \right]^2 \left[ \delta R_{(1+2)} \right]^2 \right\}^{1/2} .$$

(A-8)

To simplify the notation define

$$x = R_1$$

$$y = R_2$$

$$z = R_{(1+2)}$$

$$U = \sqrt{1 - \frac{R_{(1+2)}}{R_1} - \frac{R_{(1+2)}}{R_2} + \frac{R_{(1+2)}^2}{R_1 R_2}} = .9658 .$$

Then, using Equation (A-5), differentiating and squaring one obtains

$$\left( \frac{\partial\tau}{\partial R_1} \right)^2 \equiv \left( \frac{\partial\tau}{\partial x} \right)^2 = \frac{(y - z)^2}{4x^2 y^2 z^2 \left( \frac{1}{z^2} - \frac{1}{xz} - \frac{1}{yz} + \frac{1}{xy} \right)} ,$$

(A-9)

and

$$\left( \frac{\partial\tau}{\partial R_2} \right)^2 \equiv \left( \frac{\partial\tau}{\partial y} \right)^2 = \frac{(x - z)^2}{4x^2 y^2 z^2 \left( \frac{1}{z^2} - \frac{1}{xz} - \frac{1}{yz} + \frac{1}{xy} \right)}$$

(A-10)

Also

$$\left[ \frac{\partial \tau}{\partial R(1+2)} \right]^2 \equiv \left( \frac{\partial \tau}{\partial z} \right)^2 = \frac{1}{z^4} \left\{ \left[ \frac{z^2 - \frac{z}{y} - \frac{z}{x}}{2u} \right] - 1 \right\}^2 . \quad (\text{A-11})$$

Substituting Equations (A-9), (A-10), and (A-11) into Equation (A-8) one obtains  $\partial \tau = 3.28 \text{ sec}$ .

A simplification results by rewriting Equation (A-5) as follows:

$$\tau = \frac{1}{z} - \left( \frac{1}{z^2} - \frac{x+y-z}{xyz} \right)^{1/2} = \frac{1}{z} \left[ 1 - \sqrt{1 - \frac{z}{xy} (x+y-z)} \right] , \quad (\text{A-12})$$

and observing that the second term under the radical has the value  $(z/xy)(x+y-z) = 0.0667$  which is small compared to one. So expanding the square root and keeping only the first-order term one gets:

$$\sqrt{1 - \frac{z}{xy} (x+y-z)} \approx 1 - \frac{z}{2xy} (x+y-z) . \quad (\text{A-13})$$

Substituting this expression in Equation (A-5) gives:

$$\tau \approx \frac{1}{z} \left[ 1 - 1 + \frac{z}{2xy} (x+y-z) \right] \quad (\text{A-14})$$

or

$$\tau = \frac{x+y-z}{2xy} . \quad (\text{A-15})$$

This formulation yields the result  $\tau = 5.93 \mu\text{sec}$  which agrees quite well with the exact result. Using Equation (A-12)

$$\delta\tau = \left[ \left( \frac{z-y}{2x^2y} \right)^2 (\delta x)^2 + \left( \frac{z-x}{2xy^2} \right)^2 (\delta y)^2 + \left( \frac{1}{2xy} \right)^2 (\delta z)^2 \right]^{1/2},$$

(A-16)

which gives

$$\delta\tau = 3.16 \text{ } \mu\text{sec} \text{ ,}$$

so

$$\tau = (5.93 \pm 3.16) \text{ } \mu\text{sec} \text{ ,}$$

by the first-order calculation or

$$\tau = (6.03 \pm 3.28) \text{ } \mu\text{sec}$$

with the exact calculation. Figure 74 shows the resulting calculated percent loss in counts as a function of counting rates. The maximum count rates used in the experiment were of the order of 3,000 c./sec. At such a rate the dead-time loss is  $1.84 \pm 0.98$  percent. Therefore, the error made in assuming the dead-time to be nonextending is negligible. For, if the dead-time were fully extending, i.e., if a count arriving during the dead-time following a previous pulse, extended the dead-time to  $\tau$  sec. after the second pulse, then the  $R(1 - \tau R)$  counts arriving during the fraction  $(1 - \tau R)$  of the total time cause a dead-time of  $\tau$  sec. each, while the  $R(\tau R)$  counts arriving during the fraction of time  $\tau R$  cause an average loss of  $3/2 \tau$  sec. each. The total time lost is, therefore, to first order (neglecting higher than triple count clusters)

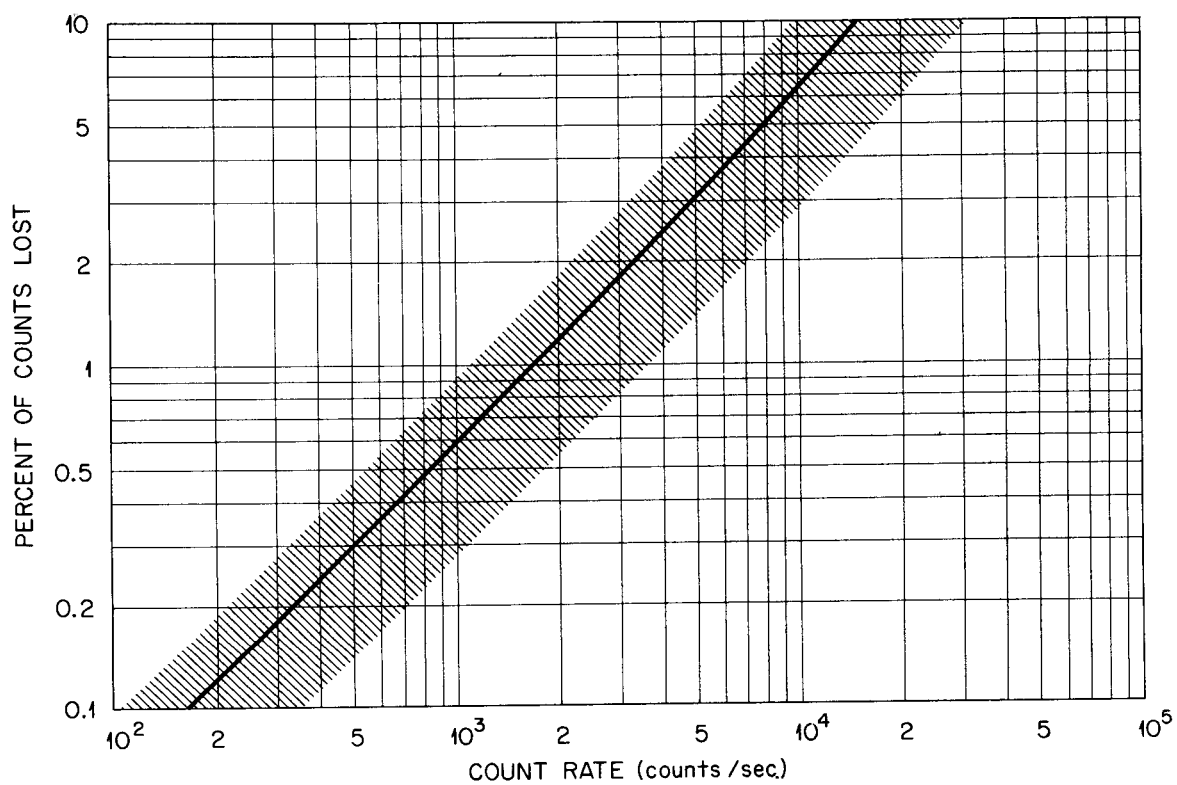


Figure 74. Calculated per cent counting loss as function of counting rate. The error limits due to dead-time uncertainty are also shown.

$$R(1 - \tau R)\tau + R(\tau R) \frac{3}{2} \tau = \tau R \left(1 + \frac{1}{2} \tau R\right) \quad (\text{A-17})$$

as compared to  $\tau R$  in the nonextending case, which for 3,000 c./sec. would make the loss  $(1.009)\tau R$  and increase the fraction of counts lost from 1.84 percent to 1.85 percent, an entirely negligible change.

The number of counts lost due to dead-time per second is given by:

$$\begin{aligned} R_T - R_o &= \frac{R_o}{1 - \tau R_o} - R_o = \frac{\tau R_o^2}{1 - \tau R_o} \\ &\approx \tau R_o^2 . \end{aligned} \quad (\text{A-13})$$

APPENDIX B

## APPENDIX B

### CALIBRATIONS OF NEUTRON YIELDS AND MONITOR RESPONSE

For the purpose of determining the neutron yield from the accelerator and the response of the long counters used as beam monitors a series of calibrations, based on use of an Am-Be neutron source of known intensity (calibrated by the National Bureau of Standards), was performed.

#### I. EXPERIMENTAL ARRANGEMENT

A small source holder was attached to the accelerator target holder which permitted placing the Am-Be sources as close as possible to the target foil of the accelerator. The holder was made of lead,  $3/32$ -in. thick, so arranged that both the Am-Be neutrons and the accelerator neutrons would pass through it to reach the long counters. The purpose of the lead was to attenuate the copious low-energy gamma radiation from the Am-Be sources.

Two similar long counters were used, one directly beneath the target position with its front surface 76.2 cm. from the center of the target foil, the other on a mobile stand, also at right angles to the accelerator beam direction at a standard distance of 265 cm. from the center of the target. The former counter was kept fixed at all times during the experiment and used as a monitor for those runs in which the location or orientation of the other counter was varied as parameter. The two counters are called, respectively, Channel I and Channel II.

Two types of detectors were used in the experiments with the long counters. The first is the original type of  $\text{BF}_3$  counter, 1.43 cm. in diameter, surrounded by a 1-cm.-thick cylinder of Ceresin wax according to the Hanson-McKibben, (1947), design, and the second is a replacement type supplied by the ORNL Instrumentation and Controls Division, intended for standard use in the future. The latter is a  $\text{BF}_3$ -filled tube, 2.54 cm. in diameter, surrounded by a Teflon cylinder 0.52-cm. thick. The total boron content of the new type of detector is the same as that in the original type. In Channel I a new type detector was used throughout the measurements, whereas in Channel II measurements were made with both types of detectors to determine the relative response rate. Assuming that the energy response function of the two detector types is the same, the new (larger diameter)  $\text{BF}_3$  tube was found to count  $1.33 \pm 0.03$  times as fast as the old-style detector exposed to the same flux in the same long counter body.

## II. DEAD-TIME MEASUREMENTS AND CALCULATIONS

The dead times of both long-counter systems were measured using two Am-Be sources, Nos. 9955 and 21. The dead time was assumed to be non-extending, which leads to the equation (see APPENDIX A):

$$\tau = \frac{1}{N_{12}} \left[ 1 - \left( 1 - \frac{N_{12}}{N_1} - \frac{N_{12}}{N_2} + \frac{N_{12}^2}{N_1 N_2} \right)^{1/2} \right], \quad (\text{B-1})$$

where  $\tau$  is the dead time and  $N_1$ ,  $N_2$ , and  $N_{12}$  are, respectively, the counting rates with one source, the other source, and both sources present.

The mean value of  $\tau$  averaged over both detectors was found to be  $(4.18 \pm 0.83) \times 10^{-5}$  sec. Assuming the dead-time equation to be

$$R_t = \frac{R_o}{(1 - R_o \tau)} \quad , \quad (\text{B-2})$$

where  $R_t$  is the true counting rate and  $R_o$  the observed rate, it follows that

$$\delta R_t = \left[ \frac{(\delta R_o)^2}{(1 - R_o \tau)^4} + \frac{R_o^4 (\delta \tau)^2}{(1 - R_o \tau)^4} \right]^{1/2} = \left[ F(R_o) (\delta R_o)^2 + G(R_o) \right]^{1/2} \quad ,$$

where  $F(R_o) = (1 - \tau R_o)^{-4}$  and  $G(R_o) = R_o^4 (\delta \tau)^2 / (1 - R_o \tau)^4$ . Figure 75 is a plot of  $R_t$  vs  $R_o$ , Figure 76 shows  $F(R_o)$  as a function of  $R_o$ , and Figure 77 shows  $G(R_o)$  as a function of  $R_o$ . These graphs were used to obtain the value of  $R_t$  and the errors associated with it.

### III. SOURCE CALIBRATIONS

The source strength of Am-Be source No. 21 was measured by comparison with Am-Be source No. 9955. Both sources were repeatedly measured in the target location by both counters in various orientations with respect to the counters. The relative count rate,  $R_{9955}/R_{21}$ , was found to be  $(0.567 \pm 0.0027)$ .

The National Bureau of Standards calibrated the Am-Be source No. 9955 and reported the value  $(4.16 \pm 0.11) \times 10^6$  neutrons/sec. as the intensity of this source. This yields the result that the source strength of source No. 21 is:

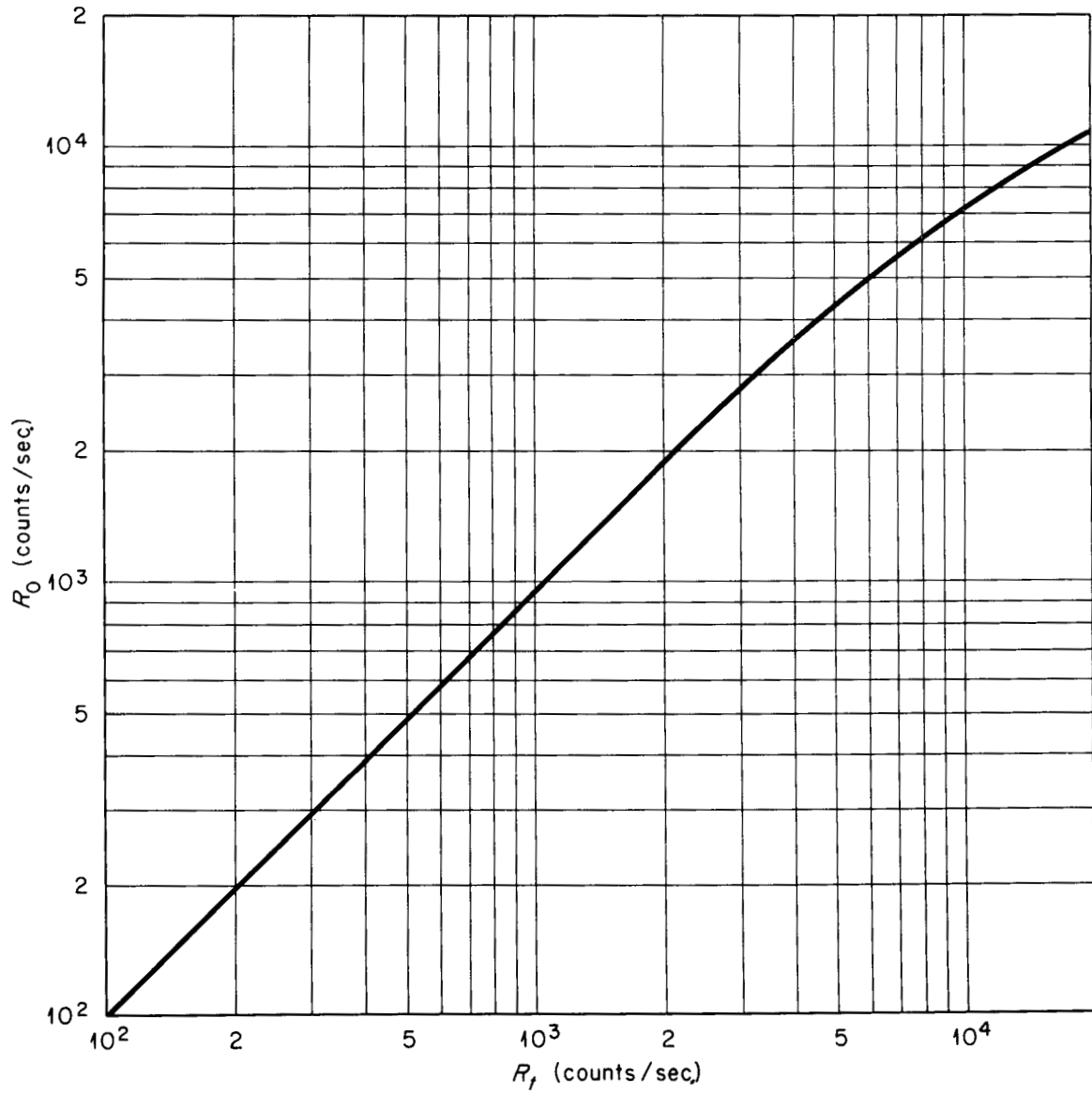


Figure 75. Plot of the function  $R_0 = R_t / (1 + \tau R_t)$  versus  $R_t$ , where  $\tau = 4.18 \times 10^{-5}$  sec.

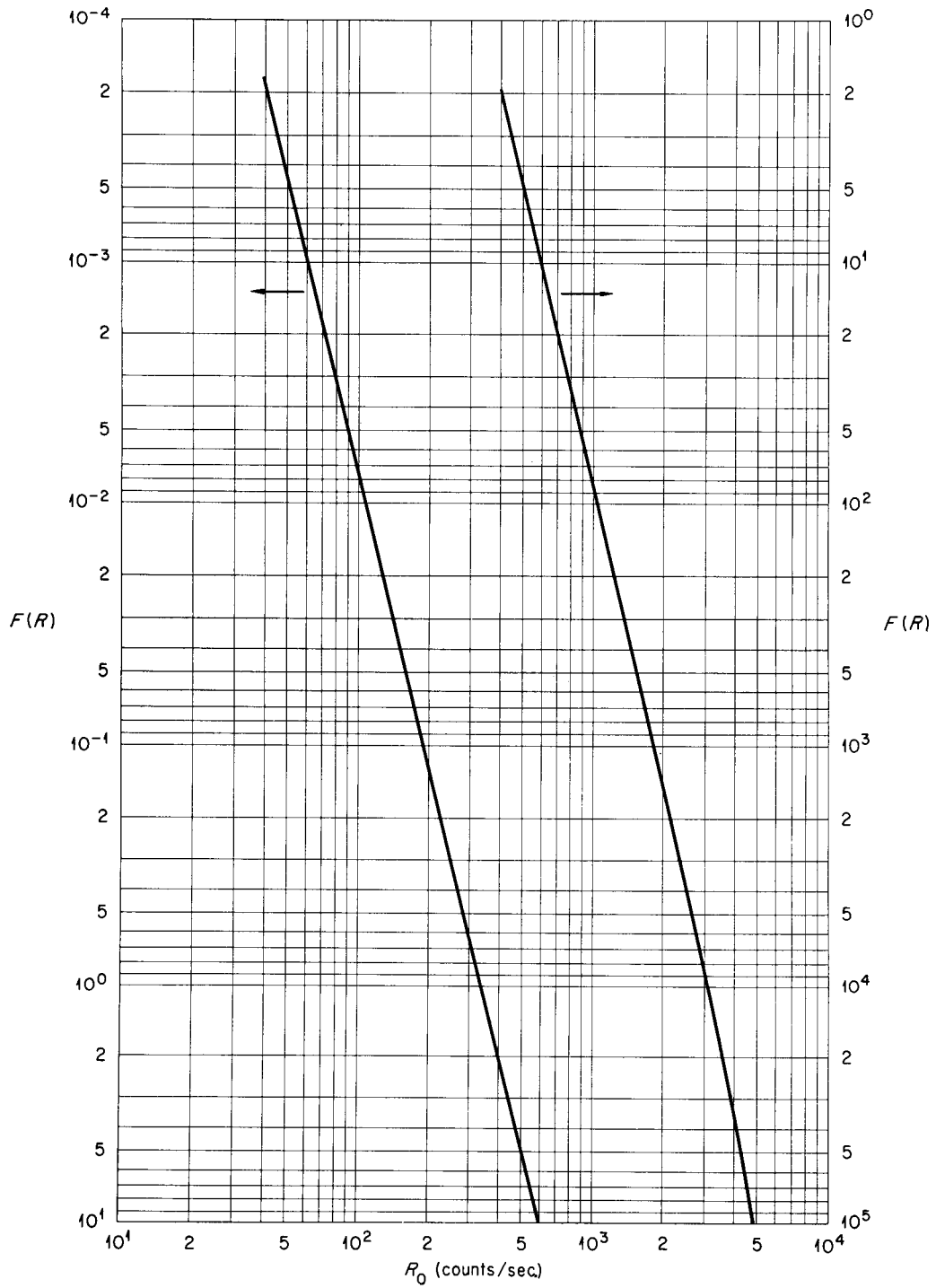


Figure 76. Plot of the function  $F(R_0) = 1/(1 - \tau R_0)^4$  versus  $R_0$ , where  $\tau = 4.18 \times 10^{-5}$  sec.

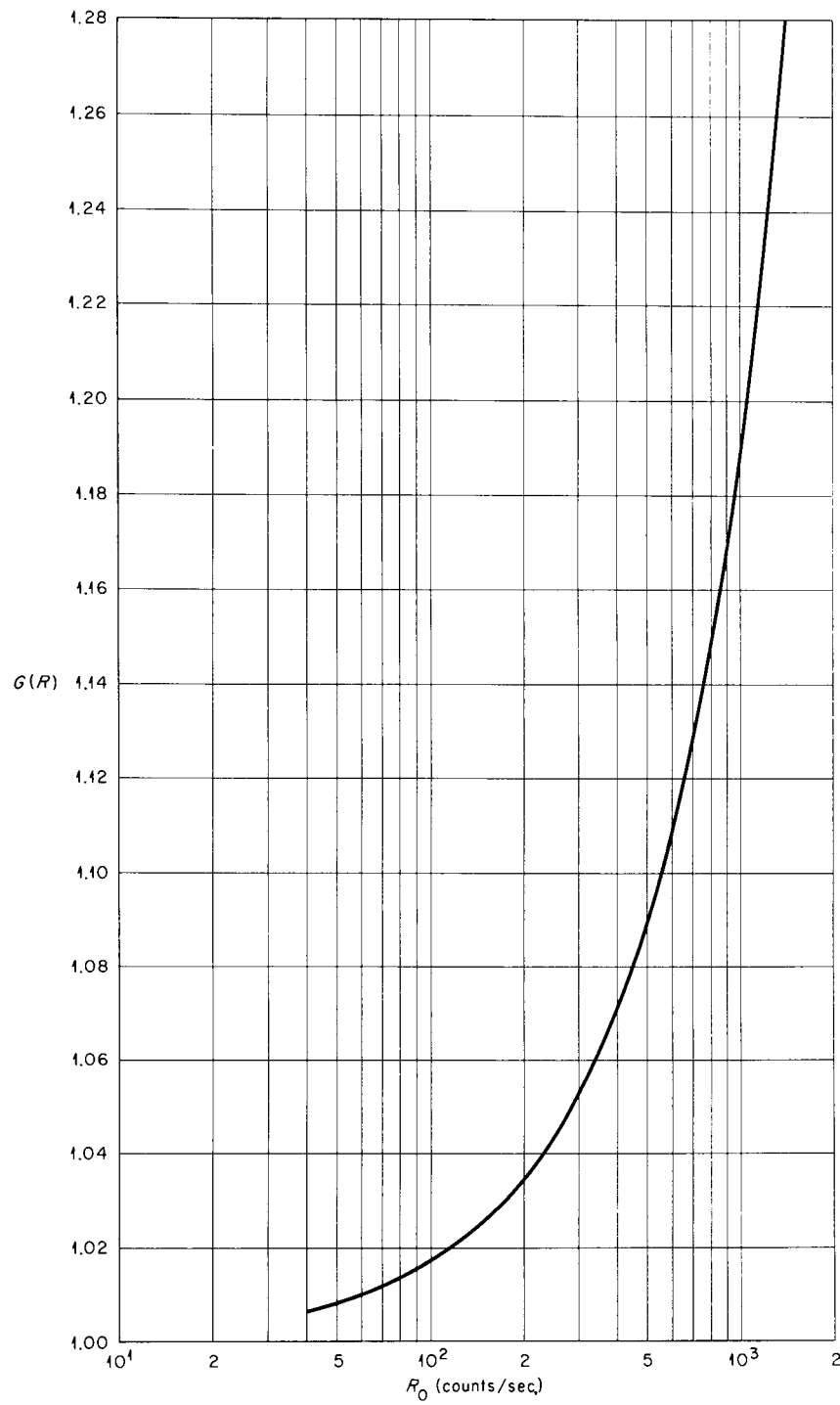


Figure 77. Plot of  $G(R_0) = R_0^4 (\delta\tau)^2 / (1 - R_0\tau)^4$  versus  $R_0$  where  $\delta\tau = 8.3 \times 10^{-6}$  sec. and  $\tau = 4.18 \times 10^{-5}$  sec.

$$S_{21} = (7.33 \pm 0.196) \times 10^6 \text{ neutrons/sec.}$$

#### IV. ACCELERATOR SOURCE STRENGTH

The accelerator was then operated with a target containing 526  $\mu\text{g./cm.}^2$  of tritium on a tungsten backing. The neutron detection rate in the long counters was used to determine the absolute source strength of the accelerator target assuming (1) that the flux at right angles to the beam direction is equal to the mean flux averaged over all solid angles, and (2) that the relative neutron detection efficiency for the 14-MeV. neutrons from the D-T source compared to those from the Am-Be source was  $0.85 \pm 0.075$ .

Assumption (1) is not strictly valid. Strictly, the flux per unit solid angle at  $90^\circ$ , relative to the mean flux per unit solid angle is

$$\frac{\phi(90^\circ)}{\bar{\phi}} = \sqrt{1 - v^2/V_n^2} \quad , \quad (\text{B-3})$$

where  $v$  is the velocity of the center of mass and  $V_n$  is the velocity of the neutrons relative to the center of mass. Now

$$v^2 = \frac{2E_D}{(M_D + M_T)} \quad \text{and} \quad V_n^2 = \frac{2Q}{\left(M_N + \frac{M_N}{M_R}\right)} \quad (\text{B-4})$$

where  $E_D$  is the deuteron energy,  $Q$  is the reaction energy, and  $M_D$ ,  $M_T$ ,

$M_N$ , and  $M_R$  are the masses of the deuteron, target nucleus, neutron, and recoil nucleus, respectively. So

$$\left(\frac{v}{V_n}\right)^2 = \frac{E_D}{Q} \cdot \frac{M_N + (M_N/M_R^2)}{M_D + M_T} . \quad (\text{B-5})$$

In the present case the maximum value of  $E_D$  was 0.3 MeV. With this value the result is:

$$\frac{\phi(90^\circ)}{\bar{\phi}} (\text{D-D}) = 0.986$$

$$\frac{\phi(90^\circ)}{\bar{\phi}} (\text{D-T}) = 0.998 .$$

So the error made by assumption (1) is negligible.

For the purpose of determining the beam-source strengths only the detector Channel II (the more distant) was used since the close channel was subjected to extremely high count rates for which the correction for dead-time was of the same order as the count rate observed.

The contributions to the quoted errors include: (1) the counting statistics including dead-time correction errors, (2) the beam strength uncertainty (taken to be 5 percent, which is the reading error and does not include any systematic errors of the microammeter circuit), (3) the long counter energy response uncertainty of 8.8 percent, and (4) the source calibration error of 2.7 percent. It appeared from the data that there is an increase in the specific yield, i.e., in the number of neutrons produced per second per microampere of beam current at a given beam

energy as the beam current increases. Figure 78 shows this variation. The cause of this phenomenon is not certain but most likely is due to errors in the microammeter calibration in the lowest range, since the curves seem to level out above about 30 microamperes of beam current. Accordingly, the values observed at high-beam currents are used as the correct values in plotting the neutron yield per microamp of beam current as a function of deuteron energy. This is shown in Figure 79, which also includes data taken with a deuterium target. The latter data are very inaccurate since the deuteron concentration on the target was not at equilibrium when the measurements were made. The energy response of the long counters was assumed to be the same for D-D (2.4 MeV.) and D-T (14 MeV.) neutrons. Since the data taken with the highest beam-energy for the D-D target were taken first and the neutron production continued to rise, amounting to an increase of about a factor of two over the time of the data collection, the high-energy points are relatively too low by about this factor. The dotted line in the figure is a rough estimate of the true variation of D-D neutron production with voltage.

#### V. DISTANCE EFFECT OF LONG-COUNTER RESPONSE

With the new-style detector in the long counter at the standard distance of 265 cm. from the target center, at right angles to the beam, the response to D-T neutrons was measured to be:

$(2.77 \pm 0.14) \times 10^{-6}$  long-counter counts per Am-Be neutron produced, and  $(2.35 \pm 0.21) \times 10^{-6}$  long-counter counts per 14-MeV. neutron produced.

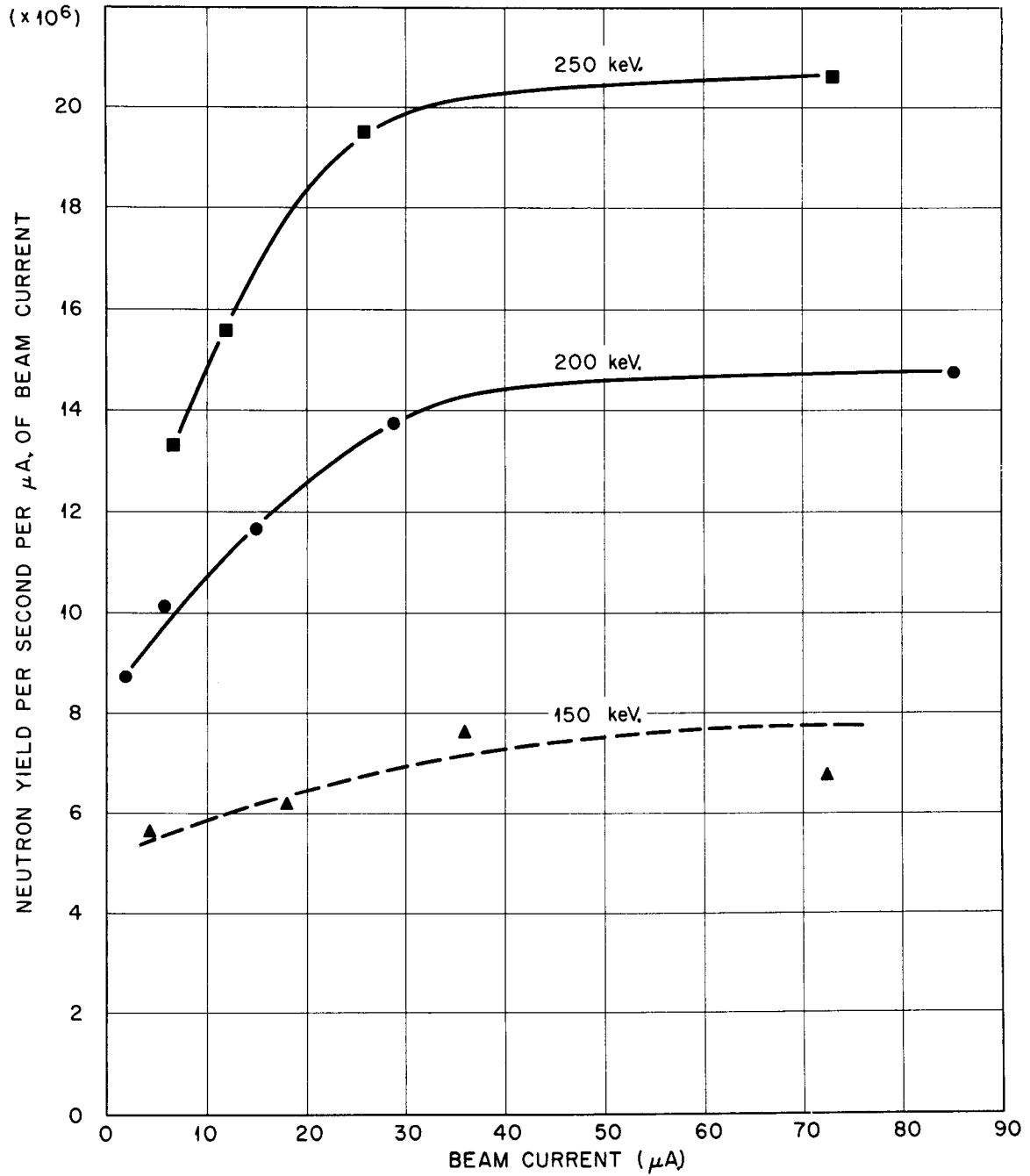


Figure 78. Apparent variation of neutron yield per microampere of beam current for three beam energies.

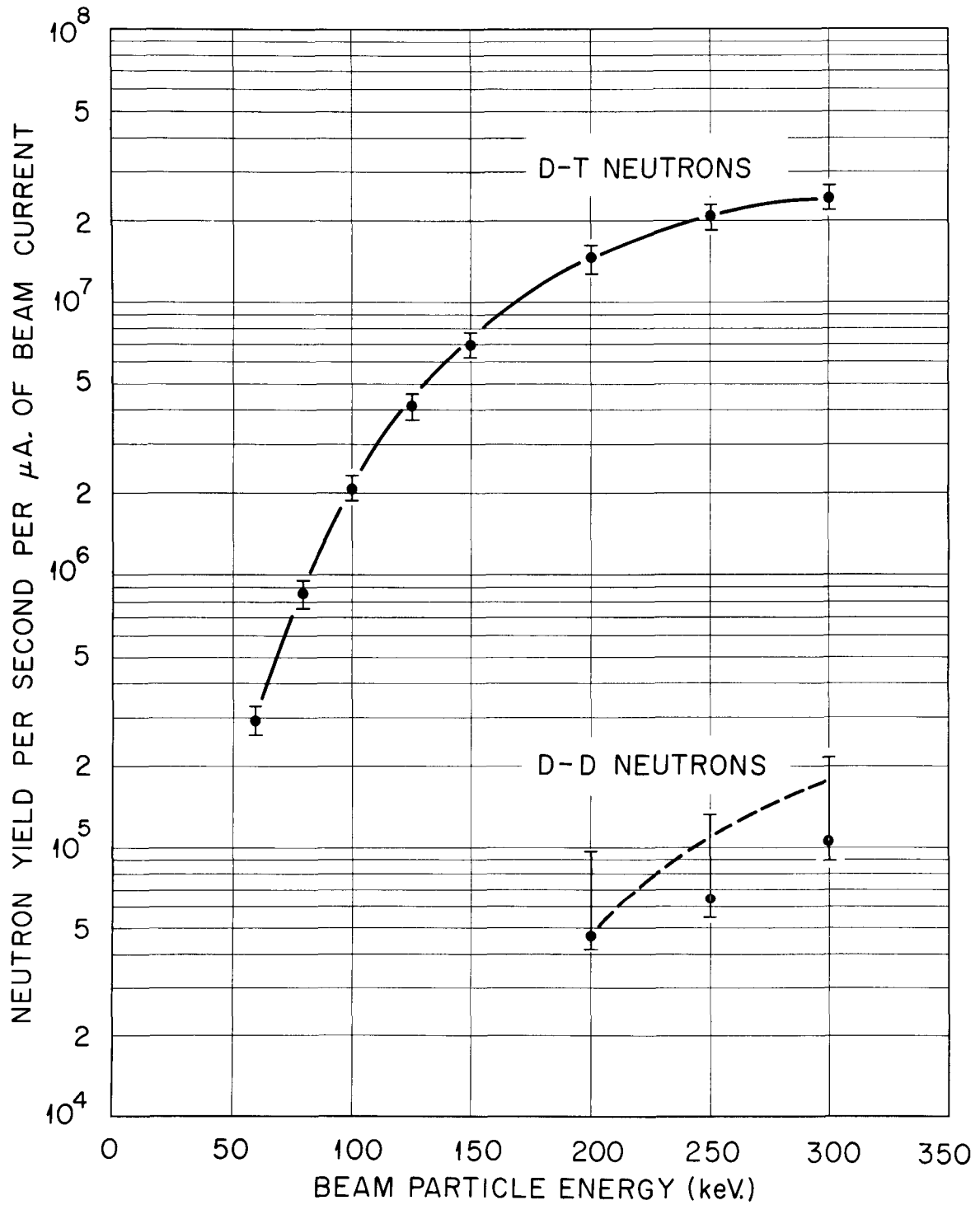


Figure 79. Neutron yield as function of beam energy for tritium and deuterium targets.

In order to facilitate the use of the long counter as an absolute monitor at other locations, data were taken at various distances, always at right angles to the beam direction, and normalized by the use of data from the fixed-position monitor. Figure 80 is a plot of the relative count rate as a function of distance from the source of 14-MeV. neutrons. The distances are measured to the front surface of the long counter. The  $1/R^2$  curve is shown for comparison. The less steep falloff of the actual curve is ascribable to the fact that the center of detection lies several inches behind the front face of the counter, and also to the effect of the divergent geometry of the neutrons when the counter is close to the source.

#### VI. ANGULAR DEPENDENCE OF LONG-COUNTER EFFICIENCY

In order to estimate the effect of misalignment of the long counter on its counting efficiency and to determine the long-counter shield's efficiency in discriminating against scattered neutrons from rearward directions, the angular response was measured. The counter was placed at the "standard" distance of 265 cm. from the target (target center to front face) and then rotated about a vertical axis through the approximate center of gravity of the counter located 286 cm. from the target center. The fixed monitor counter again served to normalize the count rates.

The results are shown in Figure 81. The "hump" around  $90^\circ$  is probably due to the larger surface and the effectively thinner hydrogenous shield which is interposed in this orientation.

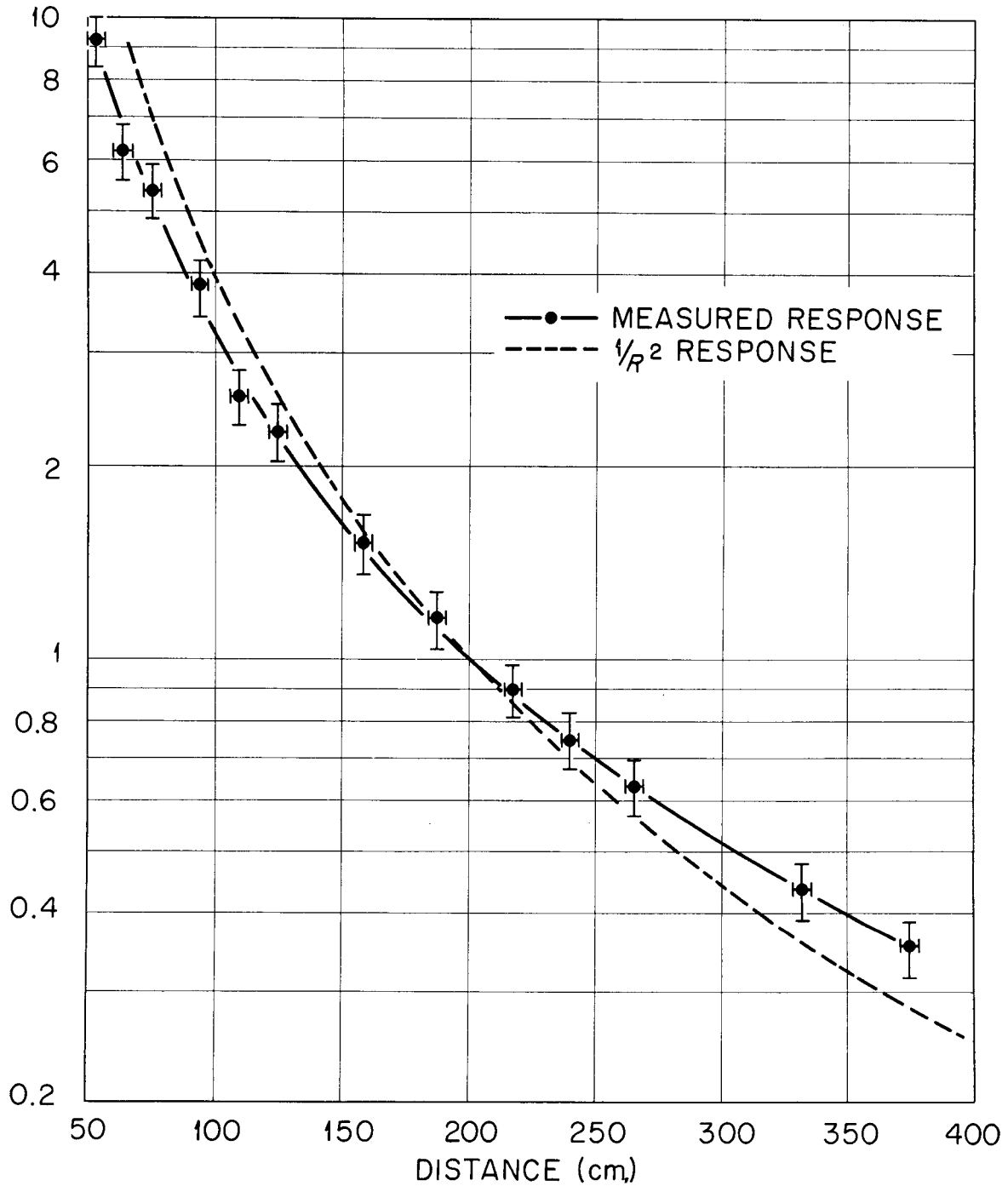


Figure 80. Relative long counter response as a function of the distance between front face of counter and D-T neutron source, at a right angle to D-beam. The  $1/R^2$  curve is shown for comparison. Both curves are normalized to unity at 20 cm. separation.

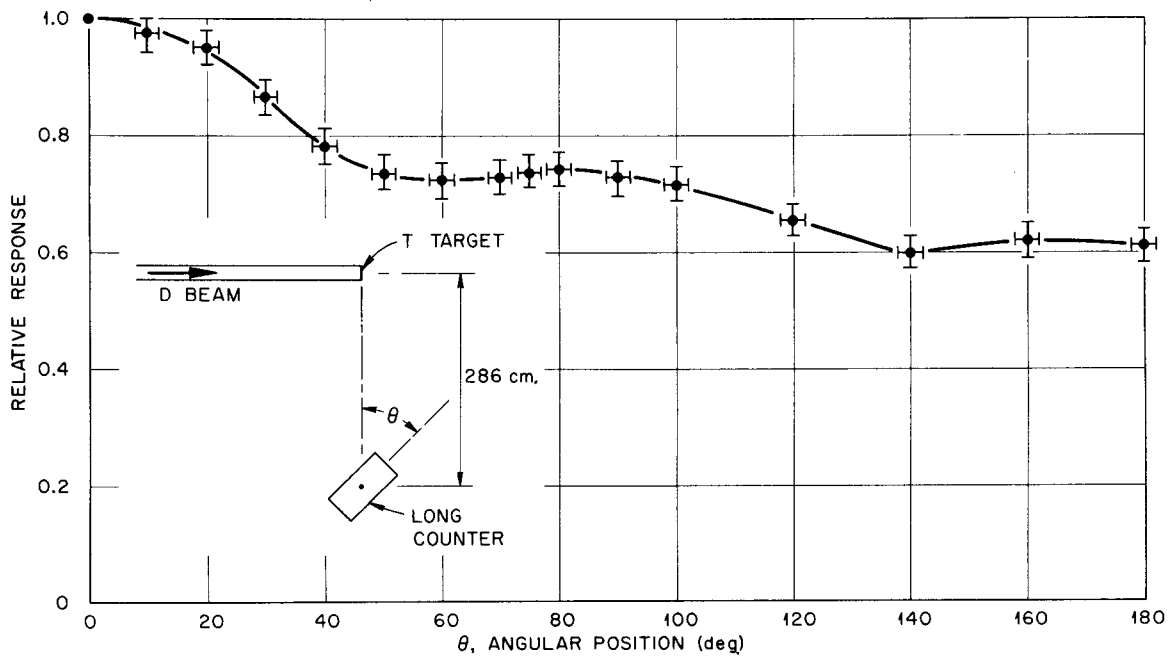


Figure 81. Relative response of long counter as a function of its angular position. At  $\theta = 0^\circ$ , the front of the long counter was 265 cm. from the target center.

APPENDIX C

## APPENDIX C

### TABLES OF MEASURED AND CALCULATED DECAY DATA

Table XIV lists the results obtained in the experiments. In each table the column headed "Observed Counts" gives the total number of counts obtained in each of the eighteen channels by summing the results of the several runs.

The "Calculated Counts" column presents the results of a back calculation using the parameters found by applying the model

$$C_n = P_1 + P_2 e^{-P_3 n \Delta t} + P_4 e^{-P_5 n \Delta t} .$$

The methods used for finding the parameters  $P_1, P_2, \dots, P_5$  are described in Chapter III. In some cases  $P_4$  was found to vanish, within the errors, so that in those cases only three parameters were used in the fit.

The last two columns give the standard deviation, which is just the square root of the number of counts, and the difference between the observed and calculated counts in standard deviation units. That is, the last column gives the quantity

$$\frac{N_o - N_c}{\sqrt{N_o}}$$

where  $N_o$  is the observed count number, and  $N_c$  is the calculated number.

TABLE XIV

MEASURED AND CALCULATED DECAY DATA WITH STANDARD DEVIATIONS  
AND DIFFERENCES IN UNITS OF THE STANDARD DEVIATIONS

| CYLINDER NUMBER 1 |                 | -5 DEGREES CENTIGRADE |                    |                          |
|-------------------|-----------------|-----------------------|--------------------|--------------------------|
| CHANNEL NUMBER    | OBSERVED COUNTS | CALCULATED COUNTS     | STANDARD DEVIATION | ERROR IN STD. DEV. UNITS |
| 1                 | 1104290.        | 1104576.              | 1050.9             | -0.27                    |
| 2                 | 752190.         | 751587.               | 867.3              | 0.70                     |
| 3                 | 509570.         | 510306.               | 713.8              | -1.03                    |
| 4                 | 347340.         | 346030.               | 589.4              | 2.23                     |
| 5                 | 234440.         | 234476.               | 484.2              | -0.06                    |
| 6                 | 158480.         | 158855.               | 398.1              | -0.92                    |
| 7                 | 107080.         | 107654.               | 327.2              | -1.75                    |
| 8                 | 72860.          | 73014.                | 269.9              | -0.55                    |
| 9                 | 49520.          | 49591.                | 222.5              | -0.32                    |
| 10                | 33340.          | 33758.                | 184.0              | 0.49                     |
| 11                | 23240.          | 23059.                | 152.4              | 1.25                     |
| 12                | 15940.          | 15830.                | 126.3              | 0.93                     |
| 13                | 10916.          | 10946.                | 104.5              | -0.29                    |
| 14                | 7679.           | 7646.                 | 87.6               | 0.37                     |
| 15                | 5492.           | 5418.                 | 74.1               | 1.00                     |
| 16                | 3925.           | 3912.                 | 62.6               | 0.20                     |
| 17                | 2862.           | 2895.                 | 53.5               | -0.63                    |
| 18                | 2174.           | 2208.                 | 46.6               | -0.74                    |

TABLE XIV (continued)

MEASURED AND CALCULATED DECAY DATA WITH STANDARD DEVIATIONS  
AND DIFFERENCES IN UNITS OF THE STANDARD DEVIATIONS

| CYLINDER NUMBER 1 |                 | -25 DEGREES CENTIGRADE |                    |                          |
|-------------------|-----------------|------------------------|--------------------|--------------------------|
| CHANNEL NUMBER    | OBSERVED COUNTS | CALCULATED COUNTS      | STANDARD DEVIATION | ERROR IN STD. DEV. UNITS |
| 1                 | 838290.         | 838505.                | 915.6              | -0.24                    |
| 2                 | 578160.         | 577616.                | 760.4              | 0.73                     |
| 3                 | 396580.         | 396917.                | 629.7              | -0.52                    |
| 4                 | 272350.         | 272337.                | 521.9              | 0.03                     |
| 5                 | 186850.         | 186713.                | 432.3              | 0.32                     |
| 6                 | 127380.         | 127987.                | 356.9              | -1.70                    |
| 7                 | 88210.          | 87767.                 | 297.0              | 1.51                     |
| 8                 | 60340.          | 60247.                 | 245.6              | 0.41                     |
| 9                 | 41430.          | 41431.                 | 203.5              | 0.00                     |
| 10                | 28520.          | 28571.                 | 168.9              | -0.27                    |
| 11                | 19730.          | 19785.                 | 140.5              | -0.39                    |
| 12                | 13700.          | 13783.                 | 117.0              | -0.69                    |
| 13                | 9745.           | 9684.                  | 98.7               | 0.63                     |
| 14                | 6827.           | 6884.                  | 82.6               | -0.70                    |
| 15                | 5059.           | 4972.                  | 71.1               | 1.22                     |
| 16                | 3677.           | 3667.                  | 60.6               | 0.17                     |
| 17                | 2788.           | 2776.                  | 52.8               | 0.23                     |
| 18                | 2136.           | 2167.                  | 46.2               | -0.68                    |

TABLE XIV (continued)

MEASURED AND CALCULATED DECAY DATA WITH STANDARD DEVIATIONS  
AND DIFFERENCES IN UNITS OF THE STANDARD DEVIATIONS

| CYLINDER NUMBER 1 |                 | -45 DEGREES CENTIGRADE |                    |                          |
|-------------------|-----------------|------------------------|--------------------|--------------------------|
| CHANNEL NUMBER    | OBSERVED COUNTS | CALCULATED COUNTS      | STANDARD DEVIATION | ERROR IN STD. DEV. UNITS |
| 1                 | 718290.         | 718410.                | 847.5              | -0.14                    |
| 2                 | 497940.         | 498044.                | 705.6              | -0.14                    |
| 3                 | 344810.         | 344404.                | 587.2              | 0.70                     |
| 4                 | 237980.         | 237790.                | 487.8              | 0.40                     |
| 5                 | 163810.         | 164042.                | 404.7              | -0.56                    |
| 6                 | 113180.         | 113139.                | 336.4              | 0.13                     |
| 7                 | 77890.          | 78054.                 | 279.1              | -0.55                    |
| 8                 | 53870.          | 53897.                 | 232.1              | -0.07                    |
| 9                 | 37150.          | 37274.                 | 192.7              | -0.63                    |
| 10                | 25750.          | 25842.                 | 160.5              | -0.57                    |
| 11                | 18000.          | 17982.                 | 134.2              | 0.15                     |
| 12                | 12550.          | 12579.                 | 112.0              | -0.19                    |
| 13                | 8928.           | 8866.                  | 94.5               | 0.65                     |
| 14                | 6419.           | 6314.                  | 80.1               | 1.31                     |
| 15                | 4624.           | 4560.                  | 68.0               | 0.93                     |
| 16                | 3399.           | 3356.                  | 58.3               | 0.75                     |
| 17                | 2534.           | 2528.                  | 50.3               | 0.12                     |
| 18                | 1878.           | 1959.                  | 43.3               | -1.86                    |

TABLE XIV (continued)

MEASURED AND CALCULATED DECAY DATA WITH STANDARD DEVIATIONS  
AND DIFFERENCES IN UNITS OF THE STANDARD DEVIATIONS

| CYLINDER NUMBER 1 |                 | -65 DEGREES CENTIGRADE |                    |                          |
|-------------------|-----------------|------------------------|--------------------|--------------------------|
| CHANNEL NUMBER    | OBSERVED COUNTS | CALCULATED COUNTS      | STANDARD DEVIATION | ERROR IN STD. DEV. UNITS |
| 1                 | 1454520.        | 1454394.               | 1206.0             | 0.10                     |
| 2                 | 1014730.        | 1014531.               | 1007.3             | 0.20                     |
| 3                 | 706570.         | 707252.                | 840.6              | -0.81                    |
| 4                 | 493380.         | 493490.                | 702.4              | -0.15                    |
| 5                 | 345570.         | 345207.                | 587.9              | 0.63                     |
| 6                 | 243150.         | 242543.                | 493.1              | 1.25                     |
| 7                 | 171560.         | 171559.                | 414.2              | 0.00                     |
| 8                 | 122230.         | 122523.                | 349.6              | -0.81                    |
| 9                 | 88460.          | 88671.                 | 297.4              | -0.68                    |
| 10                | 65270.          | 65311.                 | 255.5              | -0.13                    |
| 11                | 49290.          | 49196.                 | 222.0              | 0.45                     |
| 12                | 37960.          | 38081.                 | 194.8              | -0.59                    |
| 13                | 30375.          | 30415.                 | 174.3              | -0.23                    |
| 14                | 25306.          | 25130.                 | 159.1              | 1.10                     |
| 15                | 21513.          | 21486.                 | 146.7              | 0.19                     |
| 16                | 18994.          | 18973.                 | 137.8              | 0.15                     |
| 17                | 17257.          | 17241.                 | 131.4              | 0.12                     |
| 18                | 15963.          | 16046.                 | 126.3              | -0.66                    |

TABLE XIV (continued)

MEASURED AND CALCULATED DECAY DATA WITH STANDARD DEVIATIONS  
AND DIFFERENCES IN UNITS OF THE STANDARD DEVIATIONS

| CYLINDER NUMBER 1 |                 | -85 DEGREES CENTIGRADE |                    |                          |
|-------------------|-----------------|------------------------|--------------------|--------------------------|
| CHANNEL NUMBER    | OBSERVED COUNTS | CALCULATED COUNTS      | STANDARD DEVIATION | ERROR IN STD. DEV. UNITS |
| 1                 | 1183550.        | 1184160.               | 1087.9             | -0.56                    |
| 2                 | 831880.         | 830874.                | 912.1              | 1.11                     |
| 3                 | 582250.         | 582136.                | 763.1              | 0.15                     |
| 4                 | 407700.         | 407655.                | 638.5              | 0.08                     |
| 5                 | 284930.         | 285573.                | 533.8              | -1.19                    |
| 6                 | 200260.         | 200305.                | 447.5              | -0.08                    |
| 7                 | 140750.         | 140822.                | 375.2              | -0.17                    |
| 8                 | 99740.          | 99361.                 | 315.8              | 1.23                     |
| 9                 | 70220.          | 70478.                 | 265.0              | -0.95                    |
| 10                | 50160.          | 50366.                 | 224.0              | -0.90                    |
| 11                | 36260.          | 36366.                 | 190.4              | -0.52                    |
| 12                | 26760.          | 26622.                 | 163.6              | 0.88                     |
| 13                | 20022.          | 19841.                 | 141.5              | 1.28                     |
| 14                | 15272.          | 15122.                 | 123.6              | 1.21                     |
| 15                | 11936.          | 11839.                 | 109.3              | 0.88                     |
| 16                | 9382.           | 9555.                  | 96.9               | -1.79                    |
| 17                | 7934.           | 7966.                  | 89.1               | -0.36                    |
| 18                | 6849.           | 6860.                  | 82.8               | -0.14                    |

TABLE XIV (continued)

MEASURED AND CALCULATED DECAY DATA WITH STANDARD DEVIATIONS  
AND DIFFERENCES IN UNITS OF THE STANDARD DEVIATIONS

| CYLINDER NUMBER 2 |                 | -5 DEGREES CENTIGRADE |                    |                          |
|-------------------|-----------------|-----------------------|--------------------|--------------------------|
| CHANNEL NUMBER    | OBSERVED COUNTS | CALCULATED COUNTS     | STANDARD DEVIATION | ERROR IN STD. DEV. UNITS |
| 1                 | 820920.         | 820043.               | 906.0              | 0.97                     |
| 2                 | 639550.         | 640456.               | 799.7              | -1.13                    |
| 3                 | 498390.         | 499369.               | 706.0              | -1.38                    |
| 4                 | 389070.         | 389001.               | 623.8              | 0.11                     |
| 5                 | 303800.         | 302941.               | 551.2              | 1.57                     |
| 6                 | 236010.         | 235997.               | 485.8              | 0.04                     |
| 7                 | 184410.         | 184020.               | 429.4              | 0.91                     |
| 8                 | 143680.         | 143720.               | 379.1              | -0.09                    |
| 9                 | 112520.         | 112507.               | 335.4              | 0.04                     |
| 10                | 87960.          | 88353.                | 296.6              | -1.30                    |
| 11                | 69750.          | 69672.                | 264.1              | 0.33                     |
| 12                | 55510.          | 55232.                | 235.6              | 1.22                     |
| 13                | 44044.          | 44074.                | 209.9              | -0.14                    |
| 14                | 35225.          | 35455.                | 187.7              | -1.23                    |
| 15                | 28631.          | 28798.                | 169.2              | -0.99                    |
| 16                | 23543.          | 23658.                | 153.4              | -0.75                    |
| 17                | 19802.          | 19689.                | 140.7              | 0.80                     |
| 18                | 16748.          | 16625.                | 129.4              | 0.95                     |

TABLE XIV (continued)

MEASURED AND CALCULATED DECAY DATA WITH STANDARD DEVIATIONS  
AND DIFFERENCES IN UNITS OF THE STANDARD DEVIATIONS

| CYLINDER NUMBER 2 |                 | -25 DEGREES CENTIGRADE |                    |                          |
|-------------------|-----------------|------------------------|--------------------|--------------------------|
| CHANNEL NUMBER    | OBSERVED COUNTS | CALCULATED COUNTS      | STANDARD DEVIATION | ERROR IN STD. DEV. UNITS |
| 1                 | 980140.         | 979010.                | 990.0              | 1.14                     |
| 2                 | 762390.         | 762642.                | 873.1              | -0.28                    |
| 3                 | 590930.         | 594020.                | 768.7              | -4.02                    |
| 4                 | 463880.         | 462786.                | 681.1              | 1.62                     |
| 5                 | 361020.         | 360757.                | 600.8              | 0.45                     |
| 6                 | 282300.         | 281499.                | 531.3              | 1.52                     |
| 7                 | 220870.         | 219968.                | 470.0              | 1.93                     |
| 8                 | 172100.         | 172224.                | 414.8              | -0.29                    |
| 9                 | 134850.         | 135192.                | 367.2              | -0.92                    |
| 10                | 106510.         | 106477.                | 326.4              | 0.11                     |
| 11                | 83920.          | 84217.                 | 289.7              | -1.00                    |
| 12                | 67010.          | 66964.                 | 258.9              | 0.19                     |
| 13                | 53498.          | 53593.                 | 231.3              | -0.41                    |
| 14                | 43132.          | 43233.                 | 207.7              | -0.48                    |
| 15                | 35197.          | 35205.                 | 187.6              | -0.05                    |
| 16                | 28787.          | 28986.                 | 169.7              | -1.17                    |
| 17                | 24281.          | 24169.                 | 155.8              | 0.72                     |
| 18                | 20575.          | 20436.                 | 143.4              | 0.97                     |

TABLE XIV (continued)

MEASURED AND CALCULATED DECAY DATA WITH STANDARD DEVIATIONS  
AND DIFFERENCES IN UNITS OF THE STANDARD DEVIATIONS

| CYLINDER NUMBER 2 |                 | -45 DEGREES CENTIGRADE |                    |                          |
|-------------------|-----------------|------------------------|--------------------|--------------------------|
| CHANNEL NUMBER    | OBSERVED COUNTS | CALCULATED COUNTS      | STANDARD DEVIATION | ERROR IN STD. DEV. UNITS |
| 1                 | 1278870.        | 1277942.               | 1130.9             | 0.82                     |
| 2                 | 1009730.        | 1009775.               | 1004.9             | -0.04                    |
| 3                 | 794230.         | 796480.                | 891.2              | -2.51                    |
| 4                 | 626980.         | 627592.                | 791.8              | -0.77                    |
| 5                 | 495240.         | 494320.                | 703.7              | 1.32                     |
| 6                 | 391220.         | 389428.                | 625.5              | 2.87                     |
| 7                 | 306560.         | 307035.                | 553.7              | -0.84                    |
| 8                 | 242340.         | 242415.                | 492.3              | -0.14                    |
| 9                 | 191710.         | 191795.                | 437.8              | -0.17                    |
| 10                | 152470.         | 152177.                | 390.5              | 0.75                     |
| 11                | 121220.         | 121193.                | 348.2              | 0.09                     |
| 12                | 96630.          | 96973.                 | 310.9              | -1.10                    |
| 13                | 78479.          | 78050.                 | 280.1              | 1.53                     |
| 14                | 63055.          | 63270.                 | 251.1              | -0.86                    |
| 15                | 51149.          | 51729.                 | 226.2              | -2.57                    |
| 16                | 42560.          | 42719.                 | 206.3              | -0.77                    |
| 17                | 35760.          | 35686.                 | 189.1              | 0.39                     |
| 18                | 30539.          | 30197.                 | 174.8              | 1.96                     |

TABLE XIV (continued)

MEASURED AND CALCULATED DECAY DATA WITH STANDARD DEVIATIONS  
AND DIFFERENCES IN UNITS OF THE STANDARD DEVIATIONS

| CYLINDER NUMBER 2 |                 | -65 DEGREES CENTIGRADE |                    |                          |
|-------------------|-----------------|------------------------|--------------------|--------------------------|
| CHANNEL NUMBER    | OBSERVED COUNTS | CALCULATED COUNTS      | STANDARD DEVIATION | ERROR IN STD. DEV. UNITS |
| 1                 | 810030.         | 809699.                | 900.0              | 0.37                     |
| 2                 | 645110.         | 643635.                | 803.2              | 1.85                     |
| 3                 | 508360.         | 511196.                | 713.0              | -3.98                    |
| 4                 | 404660.         | 405926.                | 636.1              | -1.98                    |
| 5                 | 323520.         | 322468.                | 568.8              | 1.86                     |
| 6                 | 257190.         | 256432.                | 507.1              | 1.50                     |
| 7                 | 205500.         | 204264.                | 453.3              | 2.74                     |
| 8                 | 163740.         | 163099.                | 404.6              | 1.60                     |
| 9                 | 130370.         | 130648.                | 361.1              | -0.77                    |
| 10                | 104110.         | 105085.                | 322.7              | -3.00                    |
| 11                | 84740.          | 84959.                 | 291.1              | -0.73                    |
| 12                | 69110.          | 69121.                 | 262.9              | -0.03                    |
| 13                | 56771.          | 56661.                 | 238.3              | 0.46                     |
| 14                | 46640.          | 46863.                 | 216.0              | -1.03                    |
| 15                | 39192.          | 39158.                 | 198.0              | 0.17                     |
| 16                | 33205.          | 33101.                 | 182.2              | 0.57                     |
| 17                | 28251.          | 28340.                 | 168.1              | -0.53                    |
| 18                | 24741.          | 24598.                 | 157.3              | 0.90                     |

TABLE XIV (continued)

MEASURED AND CALCULATED DECAY DATA WITH STANDARD DEVIATIONS  
AND DIFFERENCES IN UNITS OF THE STANDARD DEVIATIONS

| CYLINDER NUMBER 2 |                 | -85 DEGREES CENTIGRADE |                    |                          |
|-------------------|-----------------|------------------------|--------------------|--------------------------|
| CHANNEL NUMBER    | OBSERVED COUNTS | CALCULATED COUNTS      | STANDARD DEVIATION | ERROR IN STD. DEV. UNITS |
| 1                 | 1094150.        | 1094462.               | 1046.0             | -0.30                    |
| 2                 | 874810.         | 874274.                | 935.3              | 0.58                     |
| 3                 | 698450.         | 697606.                | 835.7              | 1.01                     |
| 4                 | 554820.         | 556336.                | 744.9              | -2.03                    |
| 5                 | 443330.         | 443664.                | 665.8              | -0.49                    |
| 6                 | 354480.         | 353983.                | 595.4              | 0.84                     |
| 7                 | 282480.         | 282715.                | 531.5              | -0.43                    |
| 8                 | 226420.         | 226149.                | 475.8              | 0.58                     |
| 9                 | 181700.         | 181295.                | 426.3              | 0.97                     |
| 10                | 145820.         | 145756.                | 381.9              | 0.18                     |
| 11                | 117370.         | 117613.                | 342.6              | -0.68                    |
| 12                | 95500.          | 95338.                 | 309.0              | 0.55                     |
| 13                | 77637.          | 77715.                 | 278.6              | -0.28                    |
| 14                | 63808.          | 63775.                 | 252.6              | 0.13                     |
| 15                | 52450.          | 52751.                 | 229.0              | -1.32                    |
| 16                | 43943.          | 44036.                 | 209.6              | -0.44                    |
| 17                | 37127.          | 37146.                 | 192.7              | -0.10                    |
| 18                | 31894.          | 31700.                 | 178.6              | 1.09                     |

TABLE XIV (continued)

MEASURED AND CALCULATED DECAY DATA WITH STANDARD DEVIATIONS  
AND DIFFERENCES IN UNITS OF THE STANDARD DEVIATIONS

| CYLINDER NUMBER 3 |                 | -5 DEGREES CENTIGRADE |                    |                          |
|-------------------|-----------------|-----------------------|--------------------|--------------------------|
| CHANNEL NUMBER    | OBSERVED COUNTS | CALCULATED COUNTS     | STANDARD DEVIATION | ERROR IN STD. DEV. UNITS |
| 1                 | 950020.         | 950455.               | 974.7              | -0.45                    |
| 2                 | 733230.         | 732338.               | 856.3              | 1.05                     |
| 3                 | 563490.         | 563981.               | 750.7              | -0.65                    |
| 4                 | 434930.         | 434374.               | 659.5              | 0.85                     |
| 5                 | 333880.         | 334796.               | 577.8              | -1.57                    |
| 6                 | 258770.         | 258403.               | 508.7              | 0.74                     |
| 7                 | 200070.         | 199864.               | 447.3              | 0.48                     |
| 8                 | 155050.         | 155045.               | 393.8              | 0.02                     |
| 9                 | 120590.         | 120752.               | 347.3              | -0.46                    |
| 10                | 94090.          | 94526.                | 306.7              | -1.40                    |
| 11                | 74720.          | 74477.                | 273.3              | 0.89                     |
| 12                | 59410.          | 59155.                | 243.7              | 1.08                     |
| 13                | 47402.          | 47448.                | 217.7              | -0.21                    |
| 14                | 38241.          | 38504.                | 195.6              | -1.34                    |
| 15                | 31826.          | 31672.                | 178.4              | 0.86                     |
| 16                | 26637.          | 26454.                | 163.2              | 1.12                     |
| 17                | 22494.          | 22469.                | 150.0              | 0.16                     |
| 18                | 19278.          | 19426.                | 138.8              | -1.06                    |

TABLE XIV (continued)

MEASURED AND CALCULATED DECAY DATA WITH STANDARD DEVIATIONS  
AND DIFFERENCES IN UNITS OF THE STANDARD DEVIATIONS

| CYLINDER NUMBER 3 |                 | -25 DEGREES CENTIGRADE |                    |                          |
|-------------------|-----------------|------------------------|--------------------|--------------------------|
| CHANNEL NUMBER    | OBSERVED COUNTS | CALCULATED COUNTS      | STANDARD DEVIATION | ERROR IN STD. DEV. UNITS |
| 1                 | 733320.         | 733937.                | 856.3              | -0.72                    |
| 2                 | 570230.         | 569222.                | 755.1              | 1.34                     |
| 3                 | 441660.         | 441232.                | 664.6              | 0.66                     |
| 4                 | 341190.         | 342043.                | 584.1              | -1.45                    |
| 5                 | 264970.         | 265327.                | 514.8              | -0.68                    |
| 6                 | 206200.         | 206083.                | 454.1              | 0.27                     |
| 7                 | 160980.         | 160384.                | 401.2              | 1.49                     |
| 8                 | 125030.         | 125164.                | 353.6              | -0.36                    |
| 9                 | 97720.          | 98040.                 | 312.6              | -1.02                    |
| 10                | 77150.          | 77160.                 | 277.8              | -0.02                    |
| 11                | 61050.          | 61094.                 | 247.1              | -0.14                    |
| 12                | 48800.          | 48735.                 | 220.9              | 0.32                     |
| 13                | 39121.          | 39230.                 | 197.8              | -0.55                    |
| 14                | 32078.          | 31922.                 | 179.1              | 0.87                     |
| 15                | 26385.          | 26304.                 | 162.4              | 0.50                     |
| 16                | 22112.          | 21985.                 | 148.7              | 0.86                     |
| 17                | 18570.          | 18665.                 | 136.3              | -0.69                    |
| 18                | 16038.          | 16113.                 | 126.6              | -0.59                    |

TABLE XIV (continued)

MEASURED AND CALCULATED DECAY DATA WITH STANDARD DEVIATIONS  
AND DIFFERENCES IN UNITS OF THE STANDARD DEVIATIONS

| CYLINDER NUMBER 3 |                 | -65 DEGREES CENTIGRADE |                    |                          |
|-------------------|-----------------|------------------------|--------------------|--------------------------|
| CHANNEL NUMBER    | OBSERVED COUNTS | CALCULATED COUNTS      | STANDARD DEVIATION | ERROR IN STD. DEV. UNITS |
| 1                 | 973930.         | 973393.                | 986.9              | 0.54                     |
| 2                 | 762280.         | 762887.                | 873.1              | -0.68                    |
| 3                 | 597790.         | 597912.                | 773.2              | -0.16                    |
| 4                 | 468080.         | 468822.                | 684.2              | -1.08                    |
| 5                 | 368500.         | 367931.                | 607.0              | 0.95                     |
| 6                 | 289690.         | 289154.                | 538.2              | 1.01                     |
| 7                 | 227290.         | 227687.                | 476.7              | -0.83                    |
| 8                 | 180400.         | 179754.                | 424.7              | 1.54                     |
| 9                 | 141810.         | 142391.                | 376.6              | -1.53                    |
| 10                | 113760.         | 113276.                | 337.3              | 1.44                     |
| 11                | 90520.          | 90595.                 | 300.9              | -0.24                    |
| 12                | 72880.          | 72930.                 | 270.0              | -0.16                    |
| 13                | 58899.          | 59173.                 | 242.7              | -1.13                    |
| 14                | 48291.          | 48462.                 | 219.8              | -0.78                    |
| 15                | 40172.          | 40122.                 | 200.4              | 0.25                     |
| 16                | 33723.          | 33630.                 | 183.6              | 0.51                     |
| 17                | 28555.          | 28576.                 | 169.0              | -0.12                    |
| 18                | 24709.          | 24641.                 | 157.2              | 0.43                     |

TABLE XIV (continued)

MEASURED AND CALCULATED DECAY DATA WITH STANDARD DEVIATIONS  
AND DIFFERENCES IN UNITS OF THE STANDARD DEVIATIONS

| CYLINDER NUMBER 3 |                 | -85 DEGREES CENTIGRADE |                    |                          |
|-------------------|-----------------|------------------------|--------------------|--------------------------|
| CHANNEL NUMBER    | OBSERVED COUNTS | CALCULATED COUNTS      | STANDARD DEVIATION | ERROR IN STD. DEV. UNITS |
| 1                 | 912690.         | 913332.                | 955.3              | -0.67                    |
| 2                 | 723020.         | 720927.                | 850.3              | 2.46                     |
| 3                 | 567360.         | 569086.                | 753.2              | -2.29                    |
| 4                 | 449410.         | 449445.                | 670.4              | -0.05                    |
| 5                 | 354870.         | 355288.                | 595.7              | -0.69                    |
| 6                 | 281880.         | 281257.                | 530.9              | 1.19                     |
| 7                 | 223480.         | 223093.                | 472.7              | 0.82                     |
| 8                 | 177330.         | 177420.                | 421.1              | -0.19                    |
| 9                 | 141500.         | 141572.                | 376.2              | -0.18                    |
| 10                | 113360.         | 113446.                | 336.7              | -0.25                    |
| 11                | 91470.          | 91384.                 | 302.4              | 0.30                     |
| 12                | 73730.          | 74083.                 | 271.5              | -1.29                    |
| 13                | 60502.          | 60517.                 | 246.0              | -0.06                    |
| 14                | 50063.          | 49881.                 | 223.7              | 0.81                     |
| 15                | 41485.          | 41544.                 | 203.7              | -0.29                    |
| 16                | 35168.          | 35009.                 | 187.5              | 0.85                     |
| 17                | 29834.          | 29887.                 | 172.7              | -0.30                    |
| 18                | 25834.          | 25872.                 | 160.7              | -0.24                    |

TABLE XIV (continued)

MEASURED AND CALCULATED DECAY DATA WITH STANDARD DEVIATIONS  
AND DIFFERENCES IN UNITS OF THE STANDARD DEVIATIONS

| CYLINDER NUMBER 4 |                 | -5 DEGREES CENTIGRADE |                    |                          |
|-------------------|-----------------|-----------------------|--------------------|--------------------------|
| CHANNEL NUMBER    | OBSERVED COUNTS | CALCULATED COUNTS     | STANDARD DEVIATION | ERROR IN STD. DEV. UNITS |
| 1                 | 1000020.        | 1000260.              | 1000.0             | -0.24                    |
| 2                 | 767520.         | 766951.               | 876.1              | 0.65                     |
| 3                 | 587670.         | 587889.               | 766.6              | -0.28                    |
| 4                 | 450700.         | 450796.               | 671.3              | -0.13                    |
| 5                 | 345810.         | 346028.               | 588.1              | -0.37                    |
| 6                 | 266020.         | 266073.               | 515.8              | -0.10                    |
| 7                 | 205090.         | 205117.               | 452.9              | -0.05                    |
| 8                 | 159320.         | 158682.               | 399.1              | 1.62                     |
| 9                 | 122850.         | 123331.               | 350.5              | -1.35                    |
| 10                | 96670.          | 96429.                | 310.9              | 0.79                     |
| 11                | 75640.          | 75964.                | 275.0              | -1.15                    |
| 12                | 60650.          | 60400.                | 246.3              | 1.05                     |
| 13                | 48534.          | 48565.                | 220.3              | -0.14                    |
| 14                | 39546.          | 39567.                | 198.9              | -0.11                    |
| 15                | 32535.          | 32728.                | 180.4              | -1.07                    |
| 16                | 27631.          | 27529.                | 166.2              | 0.61                     |
| 17                | 23684.          | 23577.                | 153.9              | 0.69                     |
| 18                | 20515.          | 20574.                | 143.2              | -0.42                    |

TABLE XIV (continued)

MEASURED AND CALCULATED DECAY DATA WITH STANDARD DEVIATIONS  
AND DIFFERENCES IN UNITS OF THE STANDARD DEVIATIONS

| CYLINDER NUMBER 3 |                 | -45 DEGREES CENTIGRADE |                    |                          |
|-------------------|-----------------|------------------------|--------------------|--------------------------|
| CHANNEL NUMBER    | OBSERVED COUNTS | CALCULATED COUNTS      | STANDARD DEVIATION | ERROR IN STD. DEV. UNITS |
| 1                 | 926970.         | 927280.                | 962.8              | -0.32                    |
| 2                 | 726160.         | 725188.                | 852.2              | 1.15                     |
| 3                 | 566480.         | 566930.                | 752.6              | -0.59                    |
| 4                 | 442970.         | 443350.                | 665.6              | -0.56                    |
| 5                 | 346500.         | 347057.                | 588.6              | -0.94                    |
| 6                 | 272610.         | 272149.                | 522.1              | 0.89                     |
| 7                 | 214160.         | 213949.                | 462.8              | 0.47                     |
| 8                 | 168880.         | 168774.                | 411.0              | 0.26                     |
| 9                 | 133660.         | 133735.                | 365.6              | -0.18                    |
| 10                | 106580.         | 106573.                | 326.5              | 0.04                     |
| 11                | 85890.          | 85525.                 | 293.1              | 1.26                     |
| 12                | 69200.          | 69222.                 | 263.1              | -0.05                    |
| 13                | 56147.          | 56597.                 | 237.0              | -1.90                    |
| 14                | 46862.          | 46822.                 | 216.5              | 0.19                     |
| 15                | 39183.          | 39254.                 | 197.9              | -0.36                    |
| 16                | 33399.          | 33397.                 | 182.8              | 0.01                     |
| 17                | 28877.          | 28863.                 | 169.9              | 0.08                     |
| 18                | 25447.          | 25355.                 | 159.5              | 0.58                     |

TABLE XIV (continued)

MEASURED AND CALCULATED DECAY DATA WITH STANDARD DEVIATIONS  
AND DIFFERENCES IN UNITS OF THE STANDARD DEVIATIONS

| CYLINDER NUMBER 4 |                 | -25 DEGREES CENTIGRADE |                    |                          |
|-------------------|-----------------|------------------------|--------------------|--------------------------|
| CHANNEL NUMBER    | OBSERVED COUNTS | CALCULATED COUNTS      | STANDARD DEVIATION | ERROR IN STD. DEV. UNITS |
| 1                 | 1021020.        | 1021143.               | 1010.5             | -0.12                    |
| 2                 | 787950.         | 787531.                | 887.7              | 0.48                     |
| 3                 | 607160.         | 607393.                | 779.2              | -0.29                    |
| 4                 | 468460.         | 468755.                | 684.4              | -0.42                    |
| 5                 | 362030.         | 362213.                | 601.7              | -0.30                    |
| 6                 | 280600.         | 280426.                | 529.7              | 0.34                     |
| 7                 | 217620.         | 217696.                | 466.5              | -0.15                    |
| 8                 | 169890.         | 169612.                | 412.2              | 0.70                     |
| 9                 | 132760.         | 132773.                | 364.4              | -0.02                    |
| 10                | 105020.         | 104560.                | 324.1              | 1.45                     |
| 11                | 82610.          | 82958.                 | 287.4              | -1.19                    |
| 12                | 66210.          | 66423.                 | 257.3              | -0.82                    |
| 13                | 53628.          | 53768.                 | 231.6              | -0.61                    |
| 14                | 44115.          | 44084.                 | 210.0              | 0.15                     |
| 15                | 36712.          | 36673.                 | 191.6              | 0.20                     |
| 16                | 31090.          | 31004.                 | 176.3              | 0.49                     |
| 17                | 26718.          | 26666.                 | 163.5              | 0.32                     |
| 18                | 23297.          | 23347.                 | 152.6              | -0.33                    |

TABLE XIV (continued)

MEASURED AND CALCULATED DECAY DATA WITH STANDARD DEVIATIONS  
AND DIFFERENCES IN UNITS OF THE STANDARD DEVIATIONS

| CYLINDER NUMBER 4 |                 | -45 DEGREES CENTIGRADE |                    |                          |
|-------------------|-----------------|------------------------|--------------------|--------------------------|
| CHANNEL NUMBER    | OBSERVED COUNTS | CALCULATED COUNTS      | STANDARD DEVIATION | ERROR IN STD. DEV. UNITS |
| 1                 | 910000.         | 910251.                | 953.9              | -0.26                    |
| 2                 | 704690.         | 704337.                | 839.5              | 0.42                     |
| 3                 | 546030.         | 545571.                | 738.9              | 0.62                     |
| 4                 | 422180.         | 423253.                | 649.8              | -1.64                    |
| 5                 | 329480.         | 329070.                | 574.0              | 0.72                     |
| 6                 | 257230.         | 256586.                | 507.2              | 1.29                     |
| 7                 | 200230.         | 200819.                | 447.5              | -1.30                    |
| 8                 | 157790.         | 157927.                | 397.2              | -0.33                    |
| 9                 | 125040.         | 124943.                | 353.6              | 0.29                     |
| 10                | 99110.          | 99583.                 | 314.8              | -1.48                    |
| 11                | 80590.          | 80086.                 | 283.9              | 1.79                     |
| 12                | 65200.          | 65099.                 | 255.3              | 0.41                     |
| 13                | 53481.          | 53580.                 | 231.3              | -0.43                    |
| 14                | 44988.          | 44726.                 | 212.1              | 1.24                     |
| 15                | 37793.          | 37921.                 | 194.4              | -0.65                    |
| 16                | 32458.          | 32691.                 | 180.2              | -1.29                    |
| 17                | 28642.          | 28671.                 | 169.2              | -0.17                    |
| 18                | 25705.          | 25582.                 | 160.3              | 0.77                     |

TABLE XIV (continued)

MEASURED AND CALCULATED DECAY DATA WITH STANDARD DEVIATIONS  
AND DIFFERENCES IN UNITS OF THE STANDARD DEVIATIONS

| CYLINDER NUMBER 4 |                 | -65 DEGREES CENTIGRADE |                    |                          |
|-------------------|-----------------|------------------------|--------------------|--------------------------|
| CHANNEL NUMBER    | OBSERVED COUNTS | CALCULATED COUNTS      | STANDARD DEVIATION | ERROR IN STD. DEV. UNITS |
| 1                 | 1112000.        | 1111963.               | 1054.5             | 0.04                     |
| 2                 | 866590.         | 865539.                | 930.9              | 1.13                     |
| 3                 | 672380.         | 674464.                | 820.0              | -2.53                    |
| 4                 | 526420.         | 526435.                | 725.5              | -0.02                    |
| 5                 | 412130.         | 411831.                | 642.0              | 0.47                     |
| 6                 | 324050.         | 323151.                | 569.3              | 1.60                     |
| 7                 | 254340.         | 254558.                | 504.3              | -0.43                    |
| 8                 | 201220.         | 201519.                | 448.6              | -0.65                    |
| 9                 | 161010.         | 160516.                | 401.3              | 1.24                     |
| 10                | 128840.         | 128824.                | 358.9              | 0.07                     |
| 11                | 104240.         | 104331.                | 322.9              | -0.27                    |
| 12                | 85240.          | 85405.                 | 292.0              | -0.54                    |
| 13                | 70781.          | 70782.                 | 266.0              | -0.00                    |
| 14                | 59420.          | 59484.                 | 243.8              | -0.26                    |
| 15                | 50417.          | 50755.                 | 224.5              | -1.50                    |
| 16                | 43703.          | 44012.                 | 209.1              | -1.48                    |
| 17                | 39539.          | 38802.                 | 198.8              | 3.70                     |
| 18                | 34626.          | 34778.                 | 186.1              | -0.82                    |

TABLE XIV (continued)

MEASURED AND CALCULATED DECAY DATA WITH STANDARD DEVIATIONS  
AND DIFFERENCES IN UNITS OF THE STANDARD DEVIATIONS

| CYLINDER NUMBER 4 |                 | -85 DEGREES CENTIGRADE |                    |                          |
|-------------------|-----------------|------------------------|--------------------|--------------------------|
| CHANNEL NUMBER    | OBSERVED COUNTS | CALCULATED COUNTS      | STANDARD DEVIATION | ERROR IN STD. DEV. UNITS |
| 1                 | 919300.         | 919165.                | 958.8              | 0.14                     |
| 2                 | 719060.         | 718912.                | 848.0              | 0.18                     |
| 3                 | 562350.         | 562775.                | 749.9              | -0.57                    |
| 4                 | 440660.         | 441041.                | 663.8              | -0.57                    |
| 5                 | 345980.         | 346132.                | 588.2              | -0.26                    |
| 6                 | 272970.         | 272140.                | 522.5              | 1.59                     |
| 7                 | 214830.         | 214455.                | 463.5              | 0.82                     |
| 8                 | 168900.         | 169484.                | 411.0              | -1.40                    |
| 9                 | 134710.         | 134426.                | 367.0              | 0.79                     |
| 10                | 106980.         | 107095.                | 327.1              | -0.33                    |
| 11                | 85550.          | 85789.                 | 292.5              | -0.81                    |
| 12                | 69300.          | 69180.                 | 263.2              | 0.48                     |
| 13                | 56030.          | 56232.                 | 236.7              | -0.85                    |
| 14                | 46093.          | 46138.                 | 214.7              | -0.21                    |
| 15                | 38366.          | 38269.                 | 195.9              | 0.49                     |
| 16                | 32428.          | 32135.                 | 180.1              | 1.63                     |
| 17                | 27130.          | 27353.                 | 164.7              | -1.35                    |
| 18                | 23652.          | 23626.                 | 153.8              | 0.17                     |

TABLE XIV (continued)

MEASURED AND CALCULATED DECAY DATA WITH STANDARD DEVIATIONS  
AND DIFFERENCES IN UNITS OF THE STANDARD DEVIATIONS

| CYLINDER NUMBER 5 |                 | -5 DEGREES CENTIGRADE |                    |                          |
|-------------------|-----------------|-----------------------|--------------------|--------------------------|
| CHANNEL NUMBER    | OBSERVED COUNTS | CALCULATED COUNTS     | STANDARD DEVIATION | ERROR IN STD. DEV. UNITS |
| 1                 | 782770.         | 782778.               | 884.7              | -0.01                    |
| 2                 | 589670.         | 589271.               | 767.9              | 0.52                     |
| 3                 | 443390.         | 443929.               | 665.9              | -0.80                    |
| 4                 | 334740.         | 334949.               | 578.6              | -0.36                    |
| 5                 | 253160.         | 253337.               | 503.2              | -0.35                    |
| 6                 | 192930.         | 192278.               | 439.2              | 1.49                     |
| 7                 | 146770.         | 146627.               | 383.1              | 0.39                     |
| 8                 | 112310.         | 112513.               | 335.1              | -0.60                    |
| 9                 | 87140.          | 87031.                | 295.2              | 0.40                     |
| 10                | 67920.          | 68002.                | 260.6              | -0.30                    |
| 11                | 53850.          | 53794.                | 232.1              | 0.27                     |
| 12                | 42780.          | 43189.                | 206.8              | -1.94                    |
| 13                | 35397.          | 35273.                | 188.1              | 0.66                     |
| 14                | 29486.          | 29365.                | 171.7              | 0.71                     |
| 15                | 24762.          | 24955.                | 157.4              | -1.23                    |
| 16                | 21738.          | 21665.                | 147.4              | 0.49                     |
| 17                | 19512.          | 19210.                | 139.7              | 2.17                     |
| 18                | 17176.          | 17378.                | 131.1              | -1.54                    |

TABLE XIV (continued)

MEASURED AND CALCULATED DECAY DATA WITH STANDARD DEVIATIONS  
AND DIFFERENCES IN UNITS OF THE STANDARD DEVIATIONS

| CYLINDER NUMBER 5 |                 | -25 DEGREES CENTIGRADE |                    |                          |
|-------------------|-----------------|------------------------|--------------------|--------------------------|
| CHANNEL NUMBER    | OBSERVED COUNTS | CALCULATED COUNTS      | STANDARD DEVIATION | ERROR IN STD. DEV. UNITS |
| 1                 | 1150260.        | 1150060.               | 1072.5             | 0.19                     |
| 2                 | 872760.         | 872368.                | 934.2              | 0.43                     |
| 3                 | 660410.         | 662006.                | 812.7              | -1.96                    |
| 4                 | 503480.         | 502937.                | 709.6              | 0.78                     |
| 5                 | 383200.         | 382815.                | 619.0              | 0.63                     |
| 6                 | 292260.         | 292196.                | 540.6              | 0.13                     |
| 7                 | 224640.         | 223884.                | 474.0              | 1.59                     |
| 8                 | 171880.         | 172418.                | 414.6              | -1.28                    |
| 9                 | 133590.         | 133659.                | 365.5              | -0.19                    |
| 10                | 104270.         | 104479.                | 322.9              | -0.63                    |
| 11                | 82350.          | 82517.                 | 287.0              | -0.58                    |
| 12                | 66130.          | 65989.                 | 257.2              | 0.58                     |
| 13                | 53465.          | 53552.                 | 231.2              | -0.38                    |
| 14                | 44322.          | 44196.                 | 210.5              | 0.60                     |
| 15                | 37330.          | 37157.                 | 193.2              | 0.89                     |
| 16                | 31748.          | 31862.                 | 178.2              | -0.64                    |
| 17                | 27866.          | 27879.                 | 166.9              | -0.07                    |
| 18                | 24875.          | 24882.                 | 157.7              | -0.05                    |

TABLE XIV (continued)

MEASURED AND CALCULATED DECAY DATA WITH STANDARD DEVIATIONS  
AND DIFFERENCES IN UNITS OF THE STANDARD DEVIATIONS

| CYLINDER NUMBER 5 |                 | -45 DEGREES CENTIGRADE |                    |                          |
|-------------------|-----------------|------------------------|--------------------|--------------------------|
| CHANNEL NUMBER    | OBSERVED COUNTS | CALCULATED COUNTS      | STANDARD DEVIATION | ERROR IN STD. DEV. UNITS |
| 1                 | 1065260.        | 1064082.               | 1032.1             | 1.14                     |
| 2                 | 813640.         | 814591.                | 902.0              | -1.05                    |
| 3                 | 622090.         | 624188.                | 788.7              | -2.66                    |
| 4                 | 479840.         | 479065.                | 692.7              | 1.12                     |
| 5                 | 369300.         | 368560.                | 607.7              | 1.22                     |
| 6                 | 284390.         | 284477.                | 533.3              | -0.15                    |
| 7                 | 221130.         | 220533.                | 470.2              | 1.27                     |
| 8                 | 172240.         | 171925.                | 415.0              | 0.78                     |
| 9                 | 134880.         | 134987.                | 367.3              | -0.28                    |
| 10                | 106880.         | 106923.                | 326.9              | -0.13                    |
| 11                | 85720.          | 85605.                 | 292.8              | 0.42                     |
| 12                | 69000.          | 69414.                 | 262.7              | -1.57                    |
| 13                | 56658.          | 57118.                 | 238.0              | -1.94                    |
| 14                | 47912.          | 47781.                 | 218.9              | 0.60                     |
| 15                | 40585.          | 40692.                 | 201.5              | -0.53                    |
| 16                | 35298.          | 35308.                 | 187.9              | -0.06                    |
| 17                | 31330.          | 31221.                 | 177.0              | 0.62                     |
| 18                | 28272.          | 28118.                 | 168.1              | 0.92                     |

TABLE XIV (continued)

MEASURED AND CALCULATED DECAY DATA WITH STANDARD DEVIATIONS  
AND DIFFERENCES IN UNITS OF THE STANDARD DEVIATIONS

| CYLINDER NUMBER 5 |                 | -65 DEGREES CENTIGRADE |                    |                          |
|-------------------|-----------------|------------------------|--------------------|--------------------------|
| CHANNEL NUMBER    | OBSERVED COUNTS | CALCULATED COUNTS      | STANDARD DEVIATION | ERROR IN STD. DEV. UNITS |
| 1                 | 1225750.        | 1226243.               | 1107.1             | -0.45                    |
| 2                 | 943920.         | 942616.                | 971.6              | 1.35                     |
| 3                 | 722660.         | 724123.                | 850.1              | -1.71                    |
| 4                 | 556770.         | 556295.                | 746.2              | 0.64                     |
| 5                 | 428410.         | 427667.                | 654.5              | 1.15                     |
| 6                 | 328990.         | 329247.                | 573.6              | -0.44                    |
| 7                 | 253230.         | 254035.                | 503.2              | -1.58                    |
| 8                 | 196170.         | 196613.                | 442.9              | -0.99                    |
| 9                 | 153410.         | 152806.                | 391.7              | 1.55                     |
| 10                | 119710.         | 119404.                | 346.0              | 0.91                     |
| 11                | 94020.          | 93946.                 | 306.6              | 0.25                     |
| 12                | 74390.          | 74550.                 | 272.7              | -0.55                    |
| 13                | 59800.          | 59776.                 | 244.5              | 0.10                     |
| 14                | 48648.          | 48524.                 | 220.6              | 0.56                     |
| 15                | 39807.          | 39956.                 | 199.5              | -0.75                    |
| 16                | 33134.          | 33433.                 | 182.0              | -1.65                    |
| 17                | 28744.          | 28467.                 | 169.5              | 1.64                     |
| 18                | 24665.          | 24687.                 | 157.1              | -0.14                    |

TABLE XIV (continued)

MEASURED AND CALCULATED DECAY DATA WITH STANDARD DEVIATIONS  
AND DIFFERENCES IN UNITS OF THE STANDARD DEVIATIONS

| CYLINDER NUMBER 5 |                 | -85 DEGREES CENTIGRADE |                    |                          |
|-------------------|-----------------|------------------------|--------------------|--------------------------|
| CHANNEL NUMBER    | OBSERVED COUNTS | CALCULATED COUNTS      | STANDARD DEVIATION | ERROR IN STD. DEV. UNITS |
| 1                 | 1074470.        | 1074715.               | 1036.6             | -0.24                    |
| 2                 | 835370.         | 834892.                | 914.0              | 0.53                     |
| 3                 | 648720.         | 648919.                | 805.4              | -0.24                    |
| 4                 | 504670.         | 504885.                | 710.4              | -0.30                    |
| 5                 | 394220.         | 393439.                | 627.9              | 1.26                     |
| 6                 | 307450.         | 307273.                | 554.5              | 0.33                     |
| 7                 | 240360.         | 240689.                | 490.3              | -0.66                    |
| 8                 | 189190.         | 189259.                | 435.0              | -0.15                    |
| 9                 | 149170.         | 149549.                | 386.2              | -0.96                    |
| 10                | 118840.         | 118894.                | 344.7              | -0.15                    |
| 11                | 95170.          | 95236.                 | 308.5              | -0.20                    |
| 12                | 76640.          | 76979.                 | 276.8              | -1.20                    |
| 13                | 62972.          | 62893.                 | 250.9              | 0.32                     |
| 14                | 52301.          | 52025.                 | 228.7              | 1.21                     |
| 15                | 44123.          | 43642.                 | 210.1              | 2.29                     |
| 16                | 37359.          | 37174.                 | 193.3              | 0.96                     |
| 17                | 32149.          | 32185.                 | 179.3              | -0.20                    |
| 18                | 27965.          | 28337.                 | 167.2              | -2.23                    |

TABLE XIV (continued)

MEASURED AND CALCULATED DECAY DATA WITH STANDARD DEVIATIONS  
AND DIFFERENCES IN UNITS OF THE STANDARD DEVIATIONS

| CYLINDER NUMBER 6 |                 | -5 DEGREES CENTIGRADE |                    |                          |
|-------------------|-----------------|-----------------------|--------------------|--------------------------|
| CHANNEL NUMBER    | OBSERVED COUNTS | CALCULATED COUNTS     | STANDARD DEVIATION | ERROR IN STD. DEV. UNITS |
| 1                 | 510050.         | 510243.               | 714.2              | -0.27                    |
| 2                 | 359830.         | 359375.               | 599.9              | 0.77                     |
| 3                 | 252590.         | 252967.               | 502.6              | -0.74                    |
| 4                 | 178270.         | 178005.               | 422.2              | 0.63                     |
| 5                 | 125310.         | 125241.               | 354.0              | 0.20                     |
| 6                 | 87710.          | 88124.                | 296.2              | -1.38                    |
| 7                 | 62210.          | 62024.                | 249.4              | 0.77                     |
| 8                 | 43640.          | 43677.                | 208.9              | -0.16                    |
| 9                 | 30900.          | 30782.                | 175.8              | 0.69                     |
| 10                | 21690.          | 21721.                | 147.3              | -0.19                    |
| 11                | 15200.          | 15354.                | 123.3              | -1.18                    |
| 12                | 10840.          | 10880.                | 104.1              | -0.34                    |
| 13                | 7816.           | 7738.                 | 88.4               | 0.89                     |
| 14                | 5636.           | 5530.                 | 75.1               | 1.41                     |
| 15                | 3877.           | 3979.                 | 62.3               | -1.63                    |
| 16                | 2935.           | 2889.                 | 54.2               | 0.84                     |
| 17                | 2191.           | 2124.                 | 46.8               | 1.43                     |
| 18                | 1528.           | 1586.                 | 39.1               | -1.47                    |

TABLE XIV (continued)

MEASURED AND CALCULATED DECAY DATA WITH STANDARD DEVIATIONS  
AND DIFFERENCES IN UNITS OF THE STANDARD DEVIATIONS

| CYLINDER NUMBER 6 |                 | -25 DEGREES CENTIGRADE |                    |                          |
|-------------------|-----------------|------------------------|--------------------|--------------------------|
| CHANNEL NUMBER    | OBSERVED COUNTS | CALCULATED COUNTS      | STANDARD DEVIATION | ERROR IN STD. DEV. UNITS |
| 1                 | 492070.         | 492058.                | 701.5              | 0.02                     |
| 2                 | 349610.         | 349697.                | 591.3              | -0.13                    |
| 3                 | 248840.         | 248769.                | 498.8              | 0.16                     |
| 4                 | 176940.         | 177107.                | 420.6              | -0.39                    |
| 5                 | 126430.         | 126172.                | 355.6              | 0.74                     |
| 6                 | 90070.          | 89939.                 | 300.1              | 0.47                     |
| 7                 | 63950.          | 64152.                 | 252.9              | -0.78                    |
| 8                 | 45660.          | 45792.                 | 213.7              | -0.57                    |
| 9                 | 32590.          | 32716.                 | 180.5              | -0.66                    |
| 10                | 23470.          | 23402.                 | 153.2              | 0.46                     |
| 11                | 16860.          | 16766.                 | 129.8              | 0.77                     |
| 12                | 12090.          | 12038.                 | 110.0              | 0.53                     |
| 13                | 8592.           | 8669.                  | 92.7               | -0.83                    |
| 14                | 6281.           | 6268.                  | 79.3               | 0.17                     |
| 15                | 4571.           | 4558.                  | 67.6               | 0.20                     |
| 16                | 3350.           | 3339.                  | 57.9               | 0.20                     |
| 17                | 2456.           | 2470.                  | 49.6               | -0.27                    |
| 18                | 1848.           | 1851.                  | 43.0               | -0.07                    |

TABLE XIV (continued)

MEASURED AND CALCULATED DECAY DATA WITH STANDARD DEVIATIONS  
AND DIFFERENCES IN UNITS OF THE STANDARD DEVIATIONS

| CYLINDER NUMBER 6 |                 | -45 DEGREES CENTIGRADE |                    |                          |
|-------------------|-----------------|------------------------|--------------------|--------------------------|
| CHANNEL NUMBER    | OBSERVED COUNTS | CALCULATED COUNTS      | STANDARD DEVIATION | ERROR IN STD. DEV. UNITS |
| 1                 | 700030.         | 700022.                | 836.7              | 0.01                     |
| 2                 | 506340.         | 506215.                | 711.6              | 0.18                     |
| 3                 | 365010.         | 365634.                | 604.2              | -1.03                    |
| 4                 | 264610.         | 263878.                | 514.4              | 1.44                     |
| 5                 | 190040.         | 190336.                | 435.9              | -0.67                    |
| 6                 | 137460.         | 137242.                | 370.8              | 0.60                     |
| 7                 | 98760.          | 98940.                 | 314.3              | -0.55                    |
| 8                 | 71340.          | 71325.                 | 267.1              | 0.09                     |
| 9                 | 51190.          | 51423.                 | 226.3              | -0.99                    |
| 10                | 37260.          | 37083.                 | 193.0              | 0.97                     |
| 11                | 26680.          | 26754.                 | 163.3              | -0.44                    |
| 12                | 19400.          | 19314.                 | 139.3              | 0.65                     |
| 13                | 13900.          | 13957.                 | 117.9              | -0.48                    |
| 14                | 10099.          | 10099.                 | 100.5              | 0.00                     |
| 15                | 7332.           | 7321.                  | 85.6               | 0.13                     |
| 16                | 5359.           | 5320.                  | 73.2               | 0.53                     |
| 17                | 3863.           | 3880.                  | 62.2               | -0.27                    |
| 18                | 2834.           | 2843.                  | 53.2               | -0.17                    |

TABLE XIV (continued)

MEASURED AND CALCULATED DECAY DATA WITH STANDARD DEVIATIONS  
AND DIFFERENCES IN UNITS OF THE STANDARD DEVIATIONS

| CYLINDER NUMBER 6 |                 | -65 DEGREES CENTIGRADE |                    |                          |
|-------------------|-----------------|------------------------|--------------------|--------------------------|
| CHANNEL NUMBER    | OBSERVED COUNTS | CALCULATED COUNTS      | STANDARD DEVIATION | ERROR IN STD. DEV. UNITS |
| 1                 | 813020.         | 813037.                | 901.7              | -0.02                    |
| 2                 | 591860.         | 591678.                | 769.3              | 0.24                     |
| 3                 | 429820.         | 430123.                | 655.6              | -0.46                    |
| 4                 | 312790.         | 312444.                | 559.3              | 0.64                     |
| 5                 | 225970.         | 226844.                | 475.4              | -1.82                    |
| 6                 | 165370.         | 164644.                | 406.7              | 1.80                     |
| 7                 | 119600.         | 119479.                | 345.8              | 0.36                     |
| 8                 | 86740.          | 86703.                 | 294.5              | 0.15                     |
| 9                 | 62680.          | 62926.                 | 250.4              | -0.97                    |
| 10                | 45610.          | 45683.                 | 213.6              | -0.34                    |
| 11                | 33050.          | 33181.                 | 181.8              | -0.68                    |
| 12                | 24360.          | 24117.                 | 156.1              | 1.59                     |
| 13                | 17579.          | 17547.                 | 132.6              | 0.24                     |
| 14                | 12716.          | 12785.                 | 112.8              | -0.61                    |
| 15                | 9385.           | 9334.                  | 96.9               | 0.52                     |
| 16                | 6743.           | 6833.                  | 82.1               | -1.09                    |
| 17                | 5018.           | 5020.                  | 70.8               | -0.03                    |
| 18                | 3737.           | 3707.                  | 61.1               | 0.49                     |

TABLE XIV (continued)

MEASURED AND CALCULATED DECAY DATA WITH STANDARD DEVIATIONS  
AND DIFFERENCES IN UNITS OF THE STANDARD DEVIATIONS

| CYLINDER NUMBER 6 |                 | -85 DEGREES CENTIGRADE |                    |                          |
|-------------------|-----------------|------------------------|--------------------|--------------------------|
| CHANNEL NUMBER    | OBSERVED COUNTS | CALCULATED COUNTS      | STANDARD DEVIATION | ERROR IN STD. DEV. UNITS |
| 1                 | 850060.         | 849605.                | 922.0              | 0.49                     |
| 2                 | 629720.         | 629744.                | 793.5              | -0.03                    |
| 3                 | 465060.         | 466412.                | 682.0              | -1.97                    |
| 4                 | 345430.         | 345283.                | 587.7              | 0.26                     |
| 5                 | 256180.         | 255566.                | 506.1              | 1.23                     |
| 6                 | 189160.         | 189176.                | 434.9              | -0.01                    |
| 7                 | 140370.         | 140081.                | 374.7              | 0.78                     |
| 8                 | 103490.         | 103794.                | 321.7              | -0.92                    |
| 9                 | 77320.          | 76984.                 | 278.1              | 1.24                     |
| 10                | 57430.          | 57181.                 | 239.6              | 1.07                     |
| 11                | 42520.          | 42556.                 | 206.2              | -0.15                    |
| 12                | 31550.          | 31758.                 | 177.6              | -1.13                    |
| 13                | 23591.          | 23786.                 | 153.6              | -1.26                    |
| 14                | 17779.          | 17900.                 | 133.3              | -0.91                    |
| 15                | 13603.          | 13555.                 | 116.6              | 0.41                     |
| 16                | 10214.          | 10348.                 | 101.1              | -1.32                    |
| 17                | 8176.           | 7981.                  | 90.4               | 2.16                     |
| 18                | 6229.           | 6234.                  | 78.9               | -0.06                    |

TABLE XIV (continued)

MEASURED AND CALCULATED DECAY DATA WITH STANDARD DEVIATIONS  
AND DIFFERENCES IN UNITS OF THE STANDARD DEVIATIONS

| CYLINDER NUMBER 7 |                 | -5 DEGREES CENTIGRADE |                    |                          |
|-------------------|-----------------|-----------------------|--------------------|--------------------------|
| CHANNEL NUMBER    | OBSERVED COUNTS | CALCULATED COUNTS     | STANDARD DEVIATION | ERROR IN STD. DEV. UNITS |
| 1                 | 911700.         | 913400.               | 954.8              | -1.78                    |
| 2                 | 608260.         | 604923.               | 779.9              | 4.28                     |
| 3                 | 399590.         | 400165.               | 632.1              | -0.90                    |
| 4                 | 264480.         | 264539.               | 514.3              | -0.10                    |
| 5                 | 173930.         | 174827.               | 417.0              | -2.13                    |
| 6                 | 115330.         | 115538.               | 339.6              | -0.61                    |
| 7                 | 76000.          | 76379.                | 275.7              | -1.35                    |
| 8                 | 50580.          | 50524.                | 224.9              | 0.27                     |
| 9                 | 33400.          | 33458.                | 182.8              | -0.30                    |
| 10                | 22370.          | 22195.                | 149.6              | 1.22                     |
| 11                | 14970.          | 14763.                | 122.4              | 1.77                     |
| 12                | 9890.           | 9858.                 | 99.4               | 0.40                     |
| 13                | 6677.           | 6622.                 | 81.7               | 0.67                     |
| 14                | 4609.           | 4487.                 | 67.9               | 1.80                     |
| 15                | 3043.           | 3078.                 | 55.2               | -0.63                    |
| 16                | 2135.           | 2149.                 | 46.2               | -0.31                    |
| 17                | 1544.           | 1535.                 | 39.3               | 0.22                     |
| 18                | 1091.           | 1131.                 | 33.0               | -1.21                    |

TABLE XIV (continued)

MEASURED AND CALCULATED DECAY DATA WITH STANDARD DEVIATIONS  
AND DIFFERENCES IN UNITS OF THE STANDARD DEVIATIONS

| CYLINDER NUMBER 7 |                 | -25 DEGREES CENTIGRADE |                    |                          |
|-------------------|-----------------|------------------------|--------------------|--------------------------|
| CHANNEL NUMBER    | OBSERVED COUNTS | CALCULATED COUNTS      | STANDARD DEVIATION | ERROR IN STD. DEV. UNITS |
| 1                 | 1131060.        | 1133114.               | 1063.5             | -1.93                    |
| 2                 | 769200.         | 765073.                | 877.0              | 4.71                     |
| 3                 | 513710.         | 514747.                | 716.7              | -1.44                    |
| 4                 | 345950.         | 345550.                | 588.2              | 0.69                     |
| 5                 | 230650.         | 231654.                | 480.3              | -2.07                    |
| 6                 | 155250.         | 155190.                | 394.0              | 0.17                     |
| 7                 | 103250.         | 103946.                | 321.3              | -2.14                    |
| 8                 | 69080.          | 69645.                 | 262.8              | -2.14                    |
| 9                 | 46770.          | 46702.                 | 216.3              | 0.33                     |
| 10                | 31490.          | 31365.                 | 177.5              | 0.72                     |
| 11                | 21560.          | 21115.                 | 146.8              | 3.07                     |
| 12                | 14290.          | 14266.                 | 119.5              | 0.24                     |
| 13                | 9889.           | 9692.                  | 99.4               | 1.98                     |
| 14                | 6778.           | 6636.                  | 82.3               | 1.72                     |
| 15                | 4573.           | 4595.                  | 67.6               | -0.32                    |
| 16                | 3256.           | 3232.                  | 57.1               | 0.42                     |
| 17                | 2269.           | 2321.                  | 47.6               | -1.10                    |
| 18                | 1661.           | 1713.                  | 40.8               | -1.29                    |

TABLE XIV (continued)

MEASURED AND CALCULATED DECAY DATA WITH STANDARD DEVIATIONS  
AND DIFFERENCES IN UNITS OF THE STANDARD DEVIATIONS

| CYLINDER NUMBER 7 |                 | -45 DEGREES CENTIGRADE |                    |                          |
|-------------------|-----------------|------------------------|--------------------|--------------------------|
| CHANNEL NUMBER    | OBSERVED COUNTS | CALCULATED COUNTS      | STANDARD DEVIATION | ERROR IN STD. DEV. UNITS |
| 1                 | 691120.         | 692228.                | 831.3              | -1.33                    |
| 2                 | 475860.         | 473829.                | 689.8              | 2.95                     |
| 3                 | 323970.         | 323952.                | 569.2              | 0.04                     |
| 4                 | 220920.         | 221318.                | 470.0              | -0.84                    |
| 5                 | 150830.         | 151136.                | 388.4              | -0.77                    |
| 6                 | 102530.         | 103191.                | 320.2              | -2.04                    |
| 7                 | 70350.          | 70459.                 | 265.2              | -0.40                    |
| 8                 | 48160.          | 48124.                 | 219.5              | 0.19                     |
| 9                 | 33070.          | 32886.                 | 181.9              | 1.03                     |
| 10                | 22720.          | 22494.                 | 150.7              | 1.56                     |
| 11                | 15610.          | 15407.                 | 124.9              | 1.63                     |
| 12                | 10590.          | 10574.                 | 102.9              | 0.25                     |
| 13                | 7199.           | 7279.                  | 84.8               | -0.94                    |
| 14                | 4993.           | 5032.                  | 70.7               | -0.55                    |
| 15                | 3491.           | 3501.                  | 59.1               | -0.16                    |
| 16                | 2422.           | 2456.                  | 49.2               | -0.70                    |
| 17                | 1761.           | 1744.                  | 42.0               | 0.39                     |
| 18                | 1264.           | 1259.                  | 35.6               | 0.14                     |

TABLE XIV (continued)

MEASURED AND CALCULATED DECAY DATA WITH STANDARD DEVIATIONS  
AND DIFFERENCES IN UNITS OF THE STANDARD DEVIATIONS

| CYLINDER NUMBER 7 |                 | -65 DEGREES CENTIGRADE |                    |                          |
|-------------------|-----------------|------------------------|--------------------|--------------------------|
| CHANNEL NUMBER    | OBSERVED COUNTS | CALCULATED COUNTS      | STANDARD DEVIATION | ERROR IN STD. DEV. UNITS |
| 1                 | 565560.         | 565770.                | 752.0              | -0.28                    |
| 2                 | 392210.         | 391476.                | 626.3              | 1.18                     |
| 3                 | 270310.         | 271035.                | 519.9              | -1.39                    |
| 4                 | 187950.         | 187731.                | 433.5              | 0.52                     |
| 5                 | 129730.         | 130077.                | 360.2              | -0.95                    |
| 6                 | 90280.          | 90157.                 | 300.5              | 0.44                     |
| 7                 | 62460.          | 62508.                 | 249.9              | -0.15                    |
| 8                 | 43750.          | 43353.                 | 209.2              | 1.92                     |
| 9                 | 29950.          | 30082.                 | 173.1              | -0.75                    |
| 10                | 20840.          | 20885.                 | 144.4              | -0.28                    |
| 11                | 14460.          | 14512.                 | 120.2              | -0.38                    |
| 12                | 10150.          | 10095.                 | 100.7              | 0.62                     |
| 13                | 7009.           | 7034.                  | 83.7               | -0.30                    |
| 14                | 4886.           | 4912.                  | 69.9               | -0.38                    |
| 15                | 3404.           | 3442.                  | 58.3               | -0.66                    |
| 16                | 2453.           | 2423.                  | 49.5               | 0.61                     |
| 17                | 1672.           | 1717.                  | 40.9               | -1.09                    |
| 18                | 1263.           | 1227.                  | 35.5               | 1.02                     |

TABLE XIV (continued)

MEASURED AND CALCULATED DECAY DATA WITH STANDARD DEVIATIONS  
AND DIFFERENCES IN UNITS OF THE STANDARD DEVIATIONS

| CYLINDER NUMBER 7 |                 | -85 DEGREES CENTIGRADE |                    |                          |
|-------------------|-----------------|------------------------|--------------------|--------------------------|
| CHANNEL NUMBER    | OBSERVED COUNTS | CALCULATED COUNTS      | STANDARD DEVIATION | ERROR IN STD. DEV. UNITS |
| 1                 | 1390320.        | 1392699.               | 1179.1             | -2.02                    |
| 2                 | 996050.         | 993033.                | 998.0              | 3.03                     |
| 3                 | 709540.         | 707241.                | 842.3              | 2.74                     |
| 4                 | 501750.         | 503318.                | 708.3              | -2.20                    |
| 5                 | 356340.         | 358027.                | 596.9              | -2.82                    |
| 6                 | 255750.         | 254617.                | 505.7              | 2.25                     |
| 7                 | 179670.         | 181068.                | 423.9              | -3.30                    |
| 8                 | 128710.         | 128784.                | 358.8              | -0.18                    |
| 9                 | 91450.          | 91629.                 | 302.4              | -0.57                    |
| 10                | 64980.          | 65232.                 | 254.9              | -0.98                    |
| 11                | 46780.          | 46481.                 | 216.3              | 1.42                     |
| 12                | 33490.          | 33163.                 | 183.0              | 1.84                     |
| 13                | 23881.          | 23704.                 | 154.5              | 1.15                     |
| 14                | 17024.          | 16987.                 | 130.5              | 0.28                     |
| 15                | 12372.          | 12217.                 | 111.2              | 1.39                     |
| 16                | 8953.           | 8830.                  | 94.6               | 1.29                     |
| 17                | 6491.           | 6425.                  | 80.6               | 0.81                     |
| 18                | 4495.           | 4717.                  | 67.0               | -3.32                    |

TABLE XIV (continued)

MEASURED AND CALCULATED DECAY DATA WITH STANDARD DEVIATIONS  
AND DIFFERENCES IN UNITS OF THE STANDARD DEVIATIONS

| CYLINDER NUMBER 8 |                 | -5 DEGREES CENTIGRADE |                    |                          |
|-------------------|-----------------|-----------------------|--------------------|--------------------------|
| CHANNEL NUMBER    | OBSERVED COUNTS | CALCULATED COUNTS     | STANDARD DEVIATION | ERROR IN STD. DEV. UNITS |
| 1                 | 560090.         | 560505.               | 748.4              | -0.55                    |
| 2                 | 369235.         | 368538.               | 607.6              | 1.15                     |
| 3                 | 243385.         | 243262.               | 493.3              | 0.25                     |
| 4                 | 160975.         | 161233.               | 401.2              | -0.64                    |
| 5                 | 107548.         | 107400.               | 327.9              | 0.45                     |
| 6                 | 71676.          | 72018.                | 267.7              | -1.28                    |
| 7                 | 48311.          | 48740.                | 219.8              | -1.95                    |
| 8                 | 33876.          | 33415.                | 184.1              | 2.51                     |
| 9                 | 23308.          | 23321.                | 152.7              | -0.08                    |
| 10                | 16676.          | 16670.                | 129.1              | 0.04                     |
| 11                | 12214.          | 12288.                | 110.5              | -0.67                    |
| 12                | 9455.           | 9400.                 | 97.2               | 0.57                     |
| 13                | 7573.           | 7496.                 | 87.0               | 0.88                     |
| 14                | 6300.           | 6241.                 | 79.4               | 0.74                     |
| 15                | 5451.           | 5414.                 | 73.8               | 0.49                     |
| 16                | 4845.           | 4869.                 | 69.6               | -0.35                    |
| 17                | 4485.           | 4510.                 | 67.0               | -0.36                    |
| 18                | 4203.           | 4273.                 | 64.8               | -1.08                    |

TABLE XIV (continued)

MEASURED AND CALCULATED DECAY DATA WITH STANDARD DEVIATIONS  
AND DIFFERENCES IN UNITS OF THE STANDARD DEVIATIONS

| CYLINDER NUMBER 8 |                 | -25 DEGREES CENTIGRADE |                    |                          |
|-------------------|-----------------|------------------------|--------------------|--------------------------|
| CHANNEL NUMBER    | OBSERVED COUNTS | CALCULATED COUNTS      | STANDARD DEVIATION | ERROR IN STD. DEV. UNITS |
| 1                 | 441220.         | 442956.                | 664.2              | -2.61                    |
| 2                 | 305384.         | 301404.                | 552.6              | 7.20                     |
| 3                 | 203227.         | 204564.                | 450.8              | -2.97                    |
| 4                 | 138148.         | 138712.                | 371.7              | -1.52                    |
| 5                 | 93733.          | 94111.                 | 306.2              | -1.23                    |
| 6                 | 63727.          | 63980.                 | 252.4              | -1.00                    |
| 7                 | 43691.          | 43661.                 | 209.0              | 0.14                     |
| 8                 | 30138.          | 29974.                 | 173.6              | 0.94                     |
| 9                 | 20651.          | 20762.                 | 143.7              | -0.78                    |
| 10                | 14569.          | 14565.                 | 120.7              | 0.03                     |
| 11                | 10601.          | 10398.                 | 103.0              | 1.98                     |
| 12                | 7628.           | 7596.                  | 87.3               | 0.37                     |
| 13                | 5828.           | 5712.                  | 76.3               | 1.51                     |
| 14                | 4510.           | 4446.                  | 67.2               | 0.96                     |
| 15                | 3635.           | 3595.                  | 60.3               | 0.66                     |
| 16                | 2971.           | 3023.                  | 54.5               | -0.97                    |
| 17                | 2538.           | 2639.                  | 50.4               | -2.01                    |
| 18                | 2375.           | 2381.                  | 48.7               | -0.11                    |

TABLE XIV (continued)

MEASURED AND CALCULATED DECAY DATA WITH STANDARD DEVIATIONS  
AND DIFFERENCES IN UNITS OF THE STANDARD DEVIATIONS

| CYLINDER NUMBER 8 |                 | -45 DEGREES CENTIGRADE |                    |                          |
|-------------------|-----------------|------------------------|--------------------|--------------------------|
| CHANNEL NUMBER    | OBSERVED COUNTS | CALCULATED COUNTS      | STANDARD DEVIATION | ERROR IN STD. DEV. UNITS |
| 1                 | 580200.         | 580319.                | 761.7              | -0.16                    |
| 2                 | 397312.         | 397324.                | 630.3              | -0.02                    |
| 3                 | 273232.         | 272783.                | 522.7              | 0.86                     |
| 4                 | 187465.         | 187716.                | 433.0              | -0.58                    |
| 5                 | 129741.         | 129462.                | 360.2              | 0.78                     |
| 6                 | 89208.          | 89498.                 | 298.7              | -0.97                    |
| 7                 | 61761.          | 62049.                 | 248.5              | -1.16                    |
| 8                 | 43448.          | 43179.                 | 208.4              | 1.29                     |
| 9                 | 30171.          | 30199.                 | 173.7              | -0.16                    |
| 10                | 21143.          | 21267.                 | 145.4              | -0.85                    |
| 11                | 15122.          | 15119.                 | 123.0              | 0.02                     |
| 12                | 10877.          | 10886.                 | 104.3              | -0.09                    |
| 13                | 8148.           | 7972.                  | 90.3               | 1.95                     |
| 14                | 5963.           | 5965.                  | 77.2               | -0.02                    |
| 15                | 4602.           | 4583.                  | 67.8               | 0.29                     |
| 16                | 3614.           | 3631.                  | 60.1               | -0.29                    |
| 17                | 2947.           | 2975.                  | 54.3               | -0.51                    |
| 18                | 2513.           | 2524.                  | 50.1               | -0.22                    |

TABLE XIV (continued)

MEASURED AND CALCULATED DECAY DATA WITH STANDARD DEVIATIONS  
AND DIFFERENCES IN UNITS OF THE STANDARD DEVIATIONS

| CYLINDER NUMBER 8 |                 | -65 DEGREES CENTIGRADE |                    |                          |
|-------------------|-----------------|------------------------|--------------------|--------------------------|
| CHANNEL NUMBER    | OBSERVED COUNTS | CALCULATED COUNTS      | STANDARD DEVIATION | ERROR IN STD. DEV. UNITS |
| 1                 | 603020.         | 603354.                | 776.5              | -0.43                    |
| 2                 | 419921.         | 419153.                | 648.0              | 1.18                     |
| 3                 | 291314.         | 291732.                | 539.7              | -0.77                    |
| 4                 | 203455.         | 203333.                | 451.1              | 0.27                     |
| 5                 | 141564.         | 141881.                | 376.2              | -0.84                    |
| 6                 | 99377.          | 99098.                 | 315.2              | 0.88                     |
| 7                 | 69099.          | 69282.                 | 262.9              | -0.69                    |
| 8                 | 48565.          | 48486.                 | 220.4              | 0.36                     |
| 9                 | 33975.          | 33975.                 | 184.3              | -0.00                    |
| 10                | 23766.          | 23845.                 | 154.2              | -0.51                    |
| 11                | 16759.          | 16771.                 | 129.5              | -0.09                    |
| 12                | 11840.          | 11831.                 | 108.8              | 0.07                     |
| 13                | 8384.           | 8381.                  | 91.6               | 0.03                     |
| 14                | 5980.           | 5971.                  | 77.3               | 0.12                     |
| 15                | 4386.           | 4287.                  | 66.2               | 1.49                     |
| 16                | 3037.           | 3110.                  | 55.1               | -1.34                    |
| 17                | 2348.           | 2289.                  | 48.5               | 1.23                     |
| 18                | 1675.           | 1714.                  | 40.9               | -0.97                    |

TABLE XIV (continued)

MEASURED AND CALCULATED DECAY DATA WITH STANDARD DEVIATIONS  
AND DIFFERENCES IN UNITS OF THE STANDARD DEVIATIONS

| CYLINDER NUMBER 8 |                 | -85 DEGREES CENTIGRADE |                    |                          |
|-------------------|-----------------|------------------------|--------------------|--------------------------|
| CHANNEL NUMBER    | OBSERVED COUNTS | CALCULATED COUNTS      | STANDARD DEVIATION | ERROR IN STD. DEV. UNITS |
| 1                 | 665800.         | 666461.                | 816.0              | -0.81                    |
| 2                 | 479919.         | 478389.                | 692.8              | 2.21                     |
| 3                 | 343165.         | 343749.                | 585.8              | -1.00                    |
| 4                 | 246801.         | 247321.                | 496.8              | -1.05                    |
| 5                 | 178417.         | 178240.                | 422.4              | 0.42                     |
| 6                 | 128928.         | 128739.                | 359.1              | 0.53                     |
| 7                 | 93317.          | 93263.                 | 305.5              | 0.18                     |
| 8                 | 67736.          | 67836.                 | 260.3              | -0.38                    |
| 9                 | 49186.          | 49610.                 | 221.8              | -1.91                    |
| 10                | 36707.          | 36544.                 | 191.6              | 0.85                     |
| 11                | 27150.          | 27178.                 | 164.8              | -0.17                    |
| 12                | 20783.          | 20463.                 | 144.2              | 2.22                     |
| 13                | 15558.          | 15650.                 | 124.7              | -0.73                    |
| 14                | 12284.          | 12198.                 | 110.8              | 0.77                     |
| 15                | 9631.           | 9724.                  | 98.1               | -0.95                    |
| 16                | 7958.           | 7950.                  | 89.2               | 0.09                     |
| 17                | 6696.           | 6679.                  | 81.8               | 0.22                     |
| 18                | 5735.           | 5767.                  | 75.7               | -0.42                    |

TABLE XIV (continued)

MEASURED AND CALCULATED DECAY DATA WITH STANDARD DEVIATIONS  
AND DIFFERENCES IN UNITS OF THE STANDARD DEVIATIONS

| CYLINDER NUMBER 9 |                 | -5 DEGREES CENTIGRADE |                    |                          |
|-------------------|-----------------|-----------------------|--------------------|--------------------------|
| CHANNEL NUMBER    | OBSERVED COUNTS | CALCULATED COUNTS     | STANDARD DEVIATION | ERROR IN STD. DEV. UNITS |
| 1                 | 877300.         | 878292.               | 936.6              | -1.06                    |
| 2                 | 586134.         | 584152.               | 765.6              | 2.59                     |
| 3                 | 388367.         | 388623.               | 623.2              | -0.41                    |
| 4                 | 258029.         | 258623.               | 508.0              | -1.17                    |
| 5                 | 171904.         | 172180.               | 414.6              | -0.67                    |
| 6                 | 115363.         | 114695.               | 339.7              | 1.97                     |
| 7                 | 76021.          | 76465.                | 275.7              | -1.61                    |
| 8                 | 51017.          | 51040.                | 225.9              | -0.10                    |
| 9                 | 33907.          | 34130.                | 184.1              | -1.21                    |
| 10                | 22661.          | 22884.                | 150.5              | -1.48                    |
| 11                | 15665.          | 15404.                | 125.2              | 2.09                     |
| 12                | 10347.          | 10429.                | 101.7              | -0.80                    |
| 13                | 7356.           | 7120.                 | 85.8               | 2.76                     |
| 14                | 4930.           | 4919.                 | 70.2               | 0.15                     |
| 15                | 3503.           | 3455.                 | 59.2               | 0.81                     |
| 16                | 2582.           | 2482.                 | 50.8               | 1.98                     |
| 17                | 1841.           | 1834.                 | 42.9               | 0.15                     |
| 18                | 1301.           | 1404.                 | 36.1               | -2.84                    |

TABLE XIV (continued)

MEASURED AND CALCULATED DECAY DATA WITH STANDARD DEVIATIONS  
AND DIFFERENCES IN UNITS OF THE STANDARD DEVIATIONS

| CYLINDER NUMBER 9 |                 | -25 DEGREES CENTIGRADE |                    |                          |
|-------------------|-----------------|------------------------|--------------------|--------------------------|
| CHANNEL NUMBER    | OBSERVED COUNTS | CALCULATED COUNTS      | STANDARD DEVIATION | ERROR IN STD. DEV. UNITS |
| 1                 | 718270.         | 718954.                | 847.5              | -0.81                    |
| 2                 | 490123.         | 488385.                | 700.1              | 2.48                     |
| 3                 | 331149.         | 331982.                | 575.5              | -1.45                    |
| 4                 | 225403.         | 225791.                | 474.8              | -0.82                    |
| 5                 | 153646.         | 153644.                | 392.0              | 0.00                     |
| 6                 | 104411.         | 104607.                | 323.1              | -0.61                    |
| 7                 | 71556.          | 71266.                 | 267.5              | 1.08                     |
| 8                 | 48813.          | 48594.                 | 220.9              | 0.99                     |
| 9                 | 33198.          | 33173.                 | 182.2              | 0.14                     |
| 10                | 22610.          | 22684.                 | 150.4              | -0.49                    |
| 11                | 15432.          | 15549.                 | 124.2              | -0.94                    |
| 12                | 10657.          | 10695.                 | 103.2              | -0.37                    |
| 13                | 7349.           | 7393.                  | 85.7               | -0.51                    |
| 14                | 5185.           | 5147.                  | 72.0               | 0.53                     |
| 15                | 3656.           | 3618.                  | 60.5               | 0.63                     |
| 16                | 2667.           | 2578.                  | 51.6               | 1.71                     |
| 17                | 1850.           | 1871.                  | 43.0               | -0.50                    |
| 18                | 1356.           | 1390.                  | 36.8               | -0.91                    |

TABLE XIV (continued)

MEASURED AND CALCULATED DECAY DATA WITH STANDARD DEVIATIONS  
AND DIFFERENCES IN UNITS OF THE STANDARD DEVIATIONS

| CYLINDER NUMBER 9 |                 | -50 DEGREES CENTIGRADE |                    |                          |
|-------------------|-----------------|------------------------|--------------------|--------------------------|
| CHANNEL NUMBER    | OBSERVED COUNTS | CALCULATED COUNTS      | STANDARD DEVIATION | ERROR IN STD. DEV. UNITS |
| 1                 | 600010.         | 601085.                | 774.6              | -1.39                    |
| 2                 | 420594.         | 418906.                | 648.5              | 2.60                     |
| 3                 | 292924.         | 292304.                | 541.2              | 1.15                     |
| 4                 | 203268.         | 204157.                | 450.9              | -1.97                    |
| 5                 | 142449.         | 142702.                | 377.4              | -0.67                    |
| 6                 | 99609.          | 99817.                 | 315.6              | -0.66                    |
| 7                 | 70007.          | 69869.                 | 264.6              | 0.52                     |
| 8                 | 48616.          | 48946.                 | 220.5              | -1.50                    |
| 9                 | 34368.          | 34324.                 | 185.4              | 0.24                     |
| 10                | 24137.          | 24102.                 | 155.4              | 0.22                     |
| 11                | 16913.          | 16956.                 | 130.0              | -0.33                    |
| 12                | 11988.          | 11959.                 | 109.5              | 0.27                     |
| 13                | 8818.           | 8464.                  | 93.9               | 3.77                     |
| 14                | 6015.           | 6020.                  | 77.6               | -0.06                    |
| 15                | 4355.           | 4311.                  | 66.0               | 0.67                     |
| 16                | 3031.           | 3116.                  | 55.1               | -1.53                    |
| 17                | 2206.           | 2280.                  | 47.0               | -1.56                    |
| 18                | 1723.           | 1695.                  | 41.5               | 0.68                     |

TABLE XIV (continued)

MEASURED AND CALCULATED DECAY DATA WITH STANDARD DEVIATIONS  
AND DIFFERENCES IN UNITS OF THE STANDARD DEVIATIONS

| CYLINDER NUMBER 9 |                 | -65 DEGREES CENTIGRADE |                    |                          |
|-------------------|-----------------|------------------------|--------------------|--------------------------|
| CHANNEL NUMBER    | OBSERVED COUNTS | CALCULATED COUNTS      | STANDARD DEVIATION | ERROR IN STD. DEV. UNITS |
| 1                 | 507980.         | 507982.                | 712.7              | -0.00                    |
| 2                 | 357781.         | 357825.                | 598.1              | -0.07                    |
| 3                 | 252512.         | 252385.                | 502.5              | 0.25                     |
| 4                 | 177965.         | 178192.                | 421.9              | -0.54                    |
| 5                 | 126382.         | 125909.                | 355.5              | 1.33                     |
| 6                 | 88646.          | 89026.                 | 297.7              | -1.28                    |
| 7                 | 63039.          | 62986.                 | 251.1              | 0.21                     |
| 8                 | 44406.          | 44591.                 | 210.7              | -0.88                    |
| 9                 | 31681.          | 31592.                 | 178.0              | 0.50                     |
| 10                | 22517.          | 22403.                 | 150.1              | 0.76                     |
| 11                | 16052.          | 15906.                 | 126.7              | 1.15                     |
| 12                | 11180.          | 11312.                 | 105.7              | -1.25                    |
| 13                | 8027.           | 8063.                  | 89.6               | -0.40                    |
| 14                | 5762.           | 5765.                  | 75.9               | -0.04                    |
| 15                | 4201.           | 4140.                  | 64.8               | 0.95                     |
| 16                | 2941.           | 2990.                  | 54.2               | -0.90                    |
| 17                | 2169.           | 2177.                  | 46.6               | -0.17                    |
| 18                | 1618.           | 1601.                  | 40.2               | 0.41                     |

TABLE XIV (continued)

MEASURED AND CALCULATED DECAY DATA WITH STANDARD DEVIATIONS  
AND DIFFERENCES IN UNITS OF THE STANDARD DEVIATIONS

| CYLINDER NUMBER 9 |                 | -85 DEGREES CENTIGRADE |                    |                          |
|-------------------|-----------------|------------------------|--------------------|--------------------------|
| CHANNEL NUMBER    | OBSERVED COUNTS | CALCULATED COUNTS      | STANDARD DEVIATION | ERROR IN STD. DEV. UNITS |
| 1                 | 845410.         | 845926.                | 919.5              | -0.56                    |
| 2                 | 612897.         | 611453.                | 782.9              | 1.84                     |
| 3                 | 441290.         | 442437.                | 664.3              | -1.73                    |
| 4                 | 320481.         | 320402.                | 566.1              | 0.14                     |
| 5                 | 232436.         | 232181.                | 482.1              | 0.53                     |
| 6                 | 168197.         | 168347.                | 410.1              | -0.37                    |
| 7                 | 121907.         | 122129.                | 349.2              | -0.63                    |
| 8                 | 89082.          | 88648.                 | 298.5              | 1.45                     |
| 9                 | 64185.          | 64387.                 | 253.3              | -0.80                    |
| 10                | 46898.          | 46801.                 | 216.6              | 0.45                     |
| 11                | 33925.          | 34052.                 | 184.2              | -0.69                    |
| 12                | 24757.          | 24807.                 | 157.3              | -0.32                    |
| 13                | 18197.          | 18104.                 | 134.9              | 0.69                     |
| 14                | 13369.          | 13243.                 | 115.6              | 1.09                     |
| 15                | 9710.           | 9717.                  | 98.5               | -0.07                    |
| 16                | 6934.           | 7160.                  | 83.3               | -2.71                    |
| 17                | 5486.           | 5305.                  | 74.1               | 2.44                     |
| 18                | 3921.           | 3960.                  | 62.6               | -0.62                    |

TABLE XIV (continued)

MEASURED AND CALCULATED DECAY DATA WITH STANDARD DEVIATIONS  
AND DIFFERENCES IN UNITS OF THE STANDARD DEVIATIONS

| CYLINDER NUMBER 10 |                 | -5 DEGREES CENTIGRADE |                    |                          |
|--------------------|-----------------|-----------------------|--------------------|--------------------------|
| CHANNEL NUMBER     | OBSERVED COUNTS | CALCULATED COUNTS     | STANDARD DEVIATION | ERROR IN STD. DEV. UNITS |
| 1                  | 417260.         | 421639.               | 646.0              | -6.77                    |
| 2                  | 267700.         | 268143.               | 517.4              | -0.85                    |
| 3                  | 171360.         | 170861.               | 414.0              | 1.21                     |
| 4                  | 109310.         | 109189.               | 330.6              | 0.37                     |
| 5                  | 69850.          | 70075.                | 264.3              | -0.84                    |
| 6                  | 45250.          | 45251.                | 212.7              | 0.02                     |
| 7                  | 29510.          | 29482.                | 171.8              | 0.21                     |
| 8                  | 19620.          | 19449.                | 140.1              | 1.27                     |
| 9                  | 12970.          | 13052.                | 113.9              | -0.70                    |
| 10                 | 8890.           | 8958.                 | 94.3               | -0.66                    |
| 11                 | 6300.           | 6325.                 | 79.4               | -0.23                    |
| 12                 | 4650.           | 4618.                 | 68.2               | 0.50                     |
| 13                 | 3499.           | 3499.                 | 59.2               | -0.00                    |
| 14                 | 2782.           | 2754.                 | 52.7               | 0.53                     |
| 15                 | 2217.           | 2247.                 | 47.1               | -0.63                    |
| 16                 | 1899.           | 1891.                 | 43.6               | 0.18                     |
| 17                 | 1711.           | 1633.                 | 41.4               | 1.90                     |
| 18                 | 1513.           | 1436.                 | 38.9               | 1.96                     |

TABLE XIV (continued)

MEASURED AND CALCULATED DECAY DATA WITH STANDARD DEVIATIONS  
AND DIFFERENCES IN UNITS OF THE STANDARD DEVIATIONS

| CYLINDER NUMBER 10 |                 | -25 DEGREES CENTIGRADE |                    |                          |
|--------------------|-----------------|------------------------|--------------------|--------------------------|
| CHANNEL NUMBER     | OBSERVED COUNTS | CALCULATED COUNTS      | STANDARD DEVIATION | ERROR IN STD. DEV. UNITS |
| 1                  | 1526260.        | 1529256.               | 1235.4             | -2.42                    |
| 2                  | 1044320.        | 1040539.               | 1021.9             | 3.71                     |
| 3                  | 708730.         | 709159.                | 841.9              | -0.51                    |
| 4                  | 485870.         | 484403.                | 697.0              | 2.11                     |
| 5                  | 330640.         | 331907.                | 575.0              | -2.20                    |
| 6                  | 227790.         | 228385.                | 477.3              | -1.23                    |
| 7                  | 157910.         | 158061.                | 397.4              | -0.37                    |
| 8                  | 110030.         | 110243.                | 331.7              | -0.63                    |
| 9                  | 78080.          | 77686.                 | 279.4              | 1.44                     |
| 10                 | 55490.          | 55480.                 | 235.6              | 0.08                     |
| 11                 | 40130.          | 40298.                 | 200.3              | -0.81                    |
| 12                 | 29900.          | 29885.                 | 172.9              | 0.09                     |
| 13                 | 22636.          | 22712.                 | 150.5              | -0.51                    |
| 14                 | 17862.          | 17743.                 | 133.7              | 0.90                     |
| 15                 | 14356.          | 14274.                 | 119.8              | 0.69                     |
| 16                 | 11862.          | 11829.                 | 108.9              | 0.31                     |
| 17                 | 10054.          | 10085.                 | 100.3              | -0.30                    |
| 18                 | 8767.           | 8821.                  | 93.6               | -0.58                    |

TABLE XIV (continued)

MEASURED AND CALCULATED DECAY DATA WITH STANDARD DEVIATIONS  
AND DIFFERENCES IN UNITS OF THE STANDARD DEVIATIONS

| CYLINDER NUMBER 10 |                 | -45 DEGREES CENTIGRADE |                    |                          |
|--------------------|-----------------|------------------------|--------------------|--------------------------|
| CHANNEL NUMBER     | OBSERVED COUNTS | CALCULATED COUNTS      | STANDARD DEVIATION | ERROR IN STD. DEV. UNITS |
| 1                  | 1388490.        | 1389655.               | 1178.3             | -0.99                    |
| 2                  | 847590.         | 845820.                | 920.6              | 1.93                     |
| 3                  | 517080.         | 517901.                | 719.1              | -1.14                    |
| 4                  | 321540.         | 319893.                | 567.0              | 2.92                     |
| 5                  | 198740.         | 200077.                | 445.8              | -2.98                    |
| 6                  | 127020.         | 127346.                | 356.4              | -0.89                    |
| 7                  | 82620.          | 82991.                 | 287.4              | -1.29                    |
| 8                  | 56090.          | 55758.                 | 236.8              | 1.40                     |
| 9                  | 39030.          | 38873.                 | 197.6              | 0.83                     |
| 10                 | 28440.          | 28258.                 | 168.6              | 1.10                     |
| 11                 | 21640.          | 21457.                 | 147.1              | 1.31                     |
| 12                 | 16810.          | 16990.                 | 129.7              | -1.35                    |
| 13                 | 13940.          | 13961.                 | 118.1              | -0.18                    |
| 14                 | 11773.          | 11830.                 | 108.5              | -0.53                    |
| 15                 | 10160.          | 10268.                 | 100.8              | -1.07                    |
| 16                 | 9100.           | 9076.                  | 95.4               | 0.26                     |
| 17                 | 8124.           | 8129.                  | 90.1               | -0.06                    |
| 18                 | 7418.           | 7352.                  | 86.1               | 0.77                     |

TABLE XIV (continued)

MEASURED AND CALCULATED DECAY DATA WITH STANDARD DEVIATIONS  
AND DIFFERENCES IN UNITS OF THE STANDARD DEVIATIONS

| CYLINDER NUMBER 10 |                 | -65 DEGREES CENTIGRADE |                    |                          |
|--------------------|-----------------|------------------------|--------------------|--------------------------|
| CHANNEL NUMBER     | OBSERVED COUNTS | CALCULATED COUNTS      | STANDARD DEVIATION | ERROR IN STD. DEV. UNITS |
| 1                  | 656440.         | 657596.                | 810.2              | -1.42                    |
| 2                  | 411700.         | 409847.                | 641.6              | 2.90                     |
| 3                  | 255860.         | 256546.                | 505.8              | -1.34                    |
| 4                  | 161950.         | 161587.                | 402.4              | 0.92                     |
| 5                  | 102640.         | 102675.                | 320.4              | -0.08                    |
| 6                  | 65690.          | 66046.                 | 256.3              | -1.35                    |
| 7                  | 42980.          | 43198.                 | 207.3              | -1.05                    |
| 8                  | 28950.          | 28880.                 | 170.1              | 0.43                     |
| 9                  | 19820.          | 19848.                 | 140.8              | -0.19                    |
| 10                 | 14170.          | 14098.                 | 119.0              | 0.68                     |
| 11                 | 10430.          | 10391.                 | 102.1              | 0.46                     |
| 12                 | 8040.           | 7959.                  | 89.7               | 0.99                     |
| 13                 | 6301.           | 6329.                  | 79.4               | -0.35                    |
| 14                 | 5237.           | 5207.                  | 72.4               | 0.42                     |
| 15                 | 4354.           | 4408.                  | 66.0               | -0.82                    |
| 16                 | 3761.           | 3819.                  | 61.3               | -0.94                    |
| 17                 | 3354.           | 3369.                  | 57.9               | -0.27                    |
| 18                 | 3064.           | 3014.                  | 55.4               | 0.92                     |

TABLE XIV (continued)

MEASURED AND CALCULATED DECAY DATA WITH STANDARD DEVIATIONS  
AND DIFFERENCES IN UNITS OF THE STANDARD DEVIATIONS

| CYLINDER NUMBER 10 |                 | -85 DEGREES CENTIGRADE |                    |                          |
|--------------------|-----------------|------------------------|--------------------|--------------------------|
| CHANNEL NUMBER     | OBSERVED COUNTS | CALCULATED COUNTS      | STANDARD DEVIATION | ERROR IN STD. DEV. UNITS |
| 1                  | 1008380.        | 1009560.               | 1004.2             | -1.17                    |
| 2                  | 652340.         | 650018.                | 807.7              | 2.88                     |
| 3                  | 418290.         | 419354.                | 646.8              | -1.64                    |
| 4                  | 271290.         | 271337.                | 520.9              | -0.08                    |
| 5                  | 176800.         | 176320.                | 420.5              | 1.15                     |
| 6                  | 115470.         | 115289.                | 339.8              | 0.54                     |
| 7                  | 75650.          | 76055.                 | 275.0              | -1.47                    |
| 8                  | 50730.          | 50797.                 | 225.2              | -0.26                    |
| 9                  | 34430.          | 34502.                 | 185.6              | -0.36                    |
| 10                 | 24030.          | 23956.                 | 155.0              | 0.48                     |
| 11                 | 17260.          | 17096.                 | 131.4              | 1.27                     |
| 12                 | 12690.          | 12601.                 | 112.6              | 0.84                     |
| 13                 | 9614.           | 9621.                  | 98.1               | -0.07                    |
| 14                 | 7643.           | 7615.                  | 87.4               | 0.33                     |
| 15                 | 6202.           | 6232.                  | 78.8               | -0.39                    |
| 16                 | 5284.           | 5250.                  | 72.7               | 0.47                     |
| 17                 | 4544.           | 4524.                  | 67.4               | 0.30                     |
| 18                 | 4003.           | 3964.                  | 63.3               | 0.61                     |

TABLE XIV (continued)

MEASURED AND CALCULATED DECAY DATA WITH STANDARD DEVIATIONS  
AND DIFFERENCES IN UNITS OF THE STANDARD DEVIATIONS

| CYLINDER NUMBER 11 |                 | -5 DEGREES CENTIGRADE |                    |                          |
|--------------------|-----------------|-----------------------|--------------------|--------------------------|
| CHANNEL NUMBER     | OBSERVED COUNTS | CALCULATED COUNTS     | STANDARD DEVIATION | ERROR IN STD. DEV. UNITS |
| 1                  | 901020.         | 901426.               | 949.2              | -0.43                    |
| 2                  | 558922.         | 558098.               | 747.6              | 1.10                     |
| 3                  | 345754.         | 346222.               | 588.0              | -0.80                    |
| 4                  | 215596.         | 215354.               | 464.3              | 0.52                     |
| 5                  | 134371.         | 134434.               | 366.6              | -0.17                    |
| 6                  | 84085.          | 84332.                | 290.0              | -0.85                    |
| 7                  | 53116.          | 53259.                | 230.5              | -0.62                    |
| 8                  | 34312.          | 33949.                | 185.2              | 1.96                     |
| 9                  | 21919.          | 21918.                | 148.1              | 0.01                     |
| 10                 | 14279.          | 14400.                | 119.5              | -1.01                    |
| 11                 | 9720.           | 9684.                 | 98.6               | 0.36                     |
| 12                 | 6734.           | 6713.                 | 82.1               | 0.26                     |
| 13                 | 4803.           | 4830.                 | 69.3               | -0.40                    |
| 14                 | 3674.           | 3631.                 | 60.6               | 0.72                     |
| 15                 | 2821.           | 2860.                 | 53.1               | -0.74                    |
| 16                 | 2352.           | 2361.                 | 48.5               | -0.18                    |
| 17                 | 2040.           | 2035.                 | 45.2               | 0.12                     |
| 18                 | 1829.           | 1819.                 | 42.8               | 0.23                     |

TABLE XIV (continued)

MEASURED AND CALCULATED DECAY DATA WITH STANDARD DEVIATIONS  
AND DIFFERENCES IN UNITS OF THE STANDARD DEVIATIONS

| CYLINDER NUMBER 11 |                 | -25 DEGREES CENTIGRADE |                    |                          |
|--------------------|-----------------|------------------------|--------------------|--------------------------|
| CHANNEL NUMBER     | OBSERVED COUNTS | CALCULATED COUNTS      | STANDARD DEVIATION | ERROR IN STD. DEV. UNITS |
| 1                  | 1402060.        | 1402296.               | 1184.1             | -0.20                    |
| 2                  | 890988.         | 890057.                | 943.9              | 0.99                     |
| 3                  | 564419.         | 565502.                | 751.3              | -1.44                    |
| 4                  | 359817.         | 359819.                | 599.8              | -0.00                    |
| 5                  | 230205.         | 229429.                | 479.8              | 1.62                     |
| 6                  | 146503.         | 146730.                | 382.8              | -0.59                    |
| 7                  | 94204.          | 94244.                 | 306.9              | -0.13                    |
| 8                  | 61171.          | 60901.                 | 247.3              | 1.09                     |
| 9                  | 39391.          | 39688.                 | 198.5              | -1.49                    |
| 10                 | 26069.          | 26164.                 | 161.5              | -0.59                    |
| 11                 | 17557.          | 17518.                 | 132.5              | 0.30                     |
| 12                 | 12029.          | 11966.                 | 109.7              | 0.57                     |
| 13                 | 8394.           | 8380.                  | 91.6               | 0.16                     |
| 14                 | 5963.           | 6044.                  | 77.2               | -1.05                    |
| 15                 | 4500.           | 4505.                  | 67.1               | -0.07                    |
| 16                 | 3579.           | 3475.                  | 59.8               | 1.74                     |
| 17                 | 2767.           | 2772.                  | 52.6               | -0.10                    |
| 18                 | 2245.           | 2280.                  | 47.4               | -0.73                    |

TABLE XIV (continued)

MEASURED AND CALCULATED DECAY DATA WITH STANDARD DEVIATIONS  
AND DIFFERENCES IN UNITS OF THE STANDARD DEVIATIONS

| CYLINDER NUMBER 11 |                 | -45 DEGREES CENTIGRADE |                    |                          |
|--------------------|-----------------|------------------------|--------------------|--------------------------|
| CHANNEL NUMBER     | OBSERVED COUNTS | CALCULATED COUNTS      | STANDARD DEVIATION | ERROR IN STD. DEV. UNITS |
| 1                  | 1067350.        | 1067622.               | 1033.1             | -0.26                    |
| 2                  | 694909.         | 694578.                | 833.6              | 0.40                     |
| 3                  | 451664.         | 452468.                | 672.1              | -1.20                    |
| 4                  | 296570.         | 295281.                | 544.6              | 2.37                     |
| 5                  | 193339.         | 193178.                | 439.7              | 0.37                     |
| 6                  | 126229.         | 126813.                | 355.3              | -1.64                    |
| 7                  | 83412.          | 83639.                 | 288.8              | -0.79                    |
| 8                  | 55421.          | 55521.                 | 235.4              | -0.42                    |
| 9                  | 37156.          | 37179.                 | 192.8              | -0.12                    |
| 10                 | 25273.          | 25191.                 | 159.0              | 0.52                     |
| 11                 | 17466.          | 17334.                 | 132.2              | 0.99                     |
| 12                 | 12176.          | 12167.                 | 110.3              | 0.08                     |
| 13                 | 8838.           | 8754.                  | 94.0               | 0.90                     |
| 14                 | 6423.           | 6485.                  | 80.1               | -0.78                    |
| 15                 | 4922.           | 4966.                  | 70.2               | -0.62                    |
| 16                 | 3925.           | 3939.                  | 62.6               | -0.23                    |
| 17                 | 3220.           | 3237.                  | 56.7               | -0.29                    |
| 18                 | 2783.           | 2750.                  | 52.7               | 0.62                     |

TABLE XIV (continued)

MEASURED AND CALCULATED DECAY DATA WITH STANDARD DEVIATIONS  
AND DIFFERENCES IN UNITS OF THE STANDARD DEVIATIONS

| CYLINDER NUMBER 11 |                 | -65 DEGREES CENTIGRADE |                    |                          |
|--------------------|-----------------|------------------------|--------------------|--------------------------|
| CHANNEL NUMBER     | OBSERVED COUNTS | CALCULATED COUNTS      | STANDARD DEVIATION | ERROR IN STD. DEV. UNITS |
| 1                  | 1206910.        | 1207784.               | 1098.6             | -0.80                    |
| 2                  | 797187.         | 795265.                | 892.9              | 2.15                     |
| 3                  | 524360.         | 524530.                | 724.1              | -0.23                    |
| 4                  | 345574.         | 346699.                | 587.9              | -1.91                    |
| 5                  | 229835.         | 229770.                | 479.4              | 0.14                     |
| 6                  | 153113.         | 152787.                | 391.3              | 0.83                     |
| 7                  | 101704.         | 102023.                | 318.9              | -1.00                    |
| 8                  | 68814.          | 68484.                 | 262.3              | 1.26                     |
| 9                  | 46240.          | 46271.                 | 215.0              | -0.14                    |
| 10                 | 31615.          | 31516.                 | 177.8              | 0.56                     |
| 11                 | 21820.          | 21681.                 | 147.7              | 0.94                     |
| 12                 | 15065.          | 15097.                 | 122.7              | -0.26                    |
| 13                 | 10482.          | 10667.                 | 102.4              | -1.81                    |
| 14                 | 7620.           | 7668.                  | 87.3               | -0.56                    |
| 15                 | 5686.           | 5624.                  | 75.4               | 0.82                     |
| 16                 | 4216.           | 4219.                  | 64.9               | -0.05                    |
| 17                 | 3314.           | 3244.                  | 57.6               | 1.21                     |
| 18                 | 2524.           | 2561.                  | 50.2               | -0.74                    |

TABLE XIV (continued)

MEASURED AND CALCULATED DECAY DATA WITH STANDARD DEVIATIONS  
AND DIFFERENCES IN UNITS OF THE STANDARD DEVIATIONS

| CYLINDER NUMBER 11 |                 | -85 DEGREES CENTIGRADE |                    |                          |
|--------------------|-----------------|------------------------|--------------------|--------------------------|
| CHANNEL NUMBER     | OBSERVED COUNTS | CALCULATED COUNTS      | STANDARD DEVIATION | ERROR IN STD. DEV. UNITS |
| 1                  | 750110.         | 750244.                | 866.1              | -0.16                    |
| 2                  | 515346.         | 515438.                | 717.9              | -0.13                    |
| 3                  | 354722.         | 354562.                | 595.6              | 0.27                     |
| 4                  | 244509.         | 244267.                | 494.5              | 0.49                     |
| 5                  | 168828.         | 168592.                | 410.9              | 0.57                     |
| 6                  | 116292.         | 116622.                | 341.0              | -0.97                    |
| 7                  | 80701.          | 80893.                 | 284.1              | -0.68                    |
| 8                  | 56281.          | 56299.                 | 237.2              | -0.07                    |
| 9                  | 39384.          | 39342.                 | 198.5              | 0.21                     |
| 10                 | 27628.          | 27632.                 | 166.2              | -0.02                    |
| 11                 | 19583.          | 19527.                 | 139.9              | 0.40                     |
| 12                 | 13855.          | 13904.                 | 117.7              | -0.42                    |
| 13                 | 10145.          | 9991.                  | 100.7              | 1.53                     |
| 14                 | 7159.           | 7260.                  | 84.6               | -1.20                    |
| 15                 | 5402.           | 5347.                  | 73.5               | 0.75                     |
| 16                 | 3943.           | 4001.                  | 62.8               | -0.92                    |
| 17                 | 3052.           | 3049.                  | 55.2               | 0.06                     |
| 18                 | 2383.           | 2372.                  | 48.8               | 0.23                     |

TABLE XIV (continued)

MEASURED AND CALCULATED DECAY DATA WITH STANDARD DEVIATIONS  
AND DIFFERENCES IN UNITS OF THE STANDARD DEVIATIONS

| CYLINDER NUMBER 12 |                 | -5 DEGREES CENTIGRADE |                    |                          |
|--------------------|-----------------|-----------------------|--------------------|--------------------------|
| CHANNEL NUMBER     | OBSERVED COUNTS | CALCULATED COUNTS     | STANDARD DEVIATION | ERROR IN STD. DEV. UNITS |
| 1                  | 762560.         | 762843.               | 873.2              | -0.32                    |
| 2                  | 450462.         | 449735.               | 671.2              | 1.08                     |
| 3                  | 265540.         | 266187.               | 515.3              | -1.26                    |
| 4                  | 158904.         | 158506.               | 398.6              | 1.00                     |
| 5                  | 95130.          | 95255.                | 308.4              | -0.41                    |
| 6                  | 57845.          | 58033.                | 240.5              | -0.78                    |
| 7                  | 36150.          | 36062.                | 190.1              | 0.46                     |
| 8                  | 22911.          | 23034.                | 151.4              | -0.81                    |
| 9                  | 15446.          | 15254.                | 124.3              | 1.54                     |
| 10                 | 10606.          | 10558.                | 103.0              | 0.46                     |
| 11                 | 7640.           | 7679.                 | 87.4               | -0.45                    |
| 12                 | 5825.           | 5873.                 | 76.3               | -0.62                    |
| 13                 | 4709.           | 4704.                 | 68.6               | 0.06                     |
| 14                 | 3894.           | 3918.                 | 62.4               | -0.38                    |
| 15                 | 3423.           | 3362.                 | 58.5               | 1.04                     |
| 16                 | 2920.           | 2950.                 | 54.0               | -0.56                    |
| 17                 | 2583.           | 2628.                 | 50.8               | -0.87                    |
| 18                 | 2406.           | 2365.                 | 49.1               | 0.84                     |

TABLE XIV (continued)

MEASURED AND CALCULATED DECAY DATA WITH STANDARD DEVIATIONS  
AND DIFFERENCES IN UNITS OF THE STANDARD DEVIATIONS

| CYLINDER NUMBER 12 |                 | -25 DEGREES CENTIGRADE |                    |                          |
|--------------------|-----------------|------------------------|--------------------|--------------------------|
| CHANNEL NUMBER     | OBSERVED COUNTS | CALCULATED COUNTS      | STANDARD DEVIATION | ERROR IN STD. DEV. UNITS |
| 1                  | 711120.         | 710960.                | 843.3              | 0.19                     |
| 2                  | 433240.         | 433230.                | 658.2              | 0.02                     |
| 3                  | 264038.         | 264690.                | 513.8              | -1.27                    |
| 4                  | 162779.         | 162333.                | 403.5              | 1.11                     |
| 5                  | 100405.         | 100101.                | 316.9              | 0.96                     |
| 6                  | 61833.          | 62206.                 | 248.7              | -1.50                    |
| 7                  | 39316.          | 39078.                 | 198.3              | 1.20                     |
| 8                  | 24836.          | 24919.                 | 157.6              | -0.53                    |
| 9                  | 16164.          | 16212.                 | 127.1              | -0.38                    |
| 10                 | 10797.          | 10825.                 | 103.9              | -0.27                    |
| 11                 | 7587.           | 7464.                  | 87.1               | 1.41                     |
| 12                 | 5304.           | 5343.                  | 72.8               | -0.53                    |
| 13                 | 3944.           | 3983.                  | 62.8               | -0.62                    |
| 14                 | 3028.           | 3096.                  | 55.0               | -1.23                    |
| 15                 | 2587.           | 2502.                  | 50.9               | 1.68                     |
| 16                 | 2067.           | 2093.                  | 45.5               | -0.58                    |
| 17                 | 1904.           | 1804.                  | 43.6               | 2.29                     |
| 18                 | 1525.           | 1591.                  | 39.1               | -1.70                    |

TABLE XIV (continued)

MEASURED AND CALCULATED DECAY DATA WITH STANDARD DEVIATIONS  
AND DIFFERENCES IN UNITS OF THE STANDARD DEVIATIONS

| CYLINDER NUMBER 12 |                 | -45 DEGREES CENTIGRADE |                    |                          |
|--------------------|-----------------|------------------------|--------------------|--------------------------|
| CHANNEL NUMBER     | OBSERVED COUNTS | CALCULATED COUNTS      | STANDARD DEVIATION | ERROR IN STD. DEV. UNITS |
| 1                  | 921990.         | 923205.                | 960.2              | -1.27                    |
| 2                  | 582984.         | 580709.                | 763.5              | 2.98                     |
| 3                  | 365418.         | 366195.                | 604.5              | -1.29                    |
| 4                  | 232043.         | 231677.                | 481.7              | 0.76                     |
| 5                  | 146123.         | 147200.                | 382.3              | -2.82                    |
| 6                  | 94567.          | 94052.                 | 307.5              | 1.68                     |
| 7                  | 60225.          | 60544.                 | 245.4              | -1.30                    |
| 8                  | 39594.          | 39362.                 | 199.0              | 1.17                     |
| 9                  | 25951.          | 25931.                 | 161.1              | 0.13                     |
| 10                 | 17402.          | 17382.                 | 131.9              | 0.15                     |
| 11                 | 12007.          | 11918.                 | 109.6              | 0.81                     |
| 12                 | 8360.           | 8407.                  | 91.4               | -0.52                    |
| 13                 | 6122.           | 6138.                  | 78.2               | -0.21                    |
| 14                 | 4680.           | 4661.                  | 68.4               | 0.27                     |
| 15                 | 3677.           | 3693.                  | 60.6               | -0.27                    |
| 16                 | 3001.           | 3053.                  | 54.8               | -0.95                    |
| 17                 | 2623.           | 2625.                  | 51.2               | -0.04                    |
| 18                 | 2378.           | 2337.                  | 48.8               | 0.85                     |

TABLE XIV (continued)

MEASURED AND CALCULATED DECAY DATA WITH STANDARD DEVIATIONS  
AND DIFFERENCES IN UNITS OF THE STANDARD DEVIATIONS

| CYLINDER NUMBER 12 |                 | -65 DEGREES CENTIGRADE |                    |                          |
|--------------------|-----------------|------------------------|--------------------|--------------------------|
| CHANNEL NUMBER     | OBSERVED COUNTS | CALCULATED COUNTS      | STANDARD DEVIATION | ERROR IN STD. DEV. UNITS |
| 1                  | 784900.         | 787520.                | 885.9              | -2.96                    |
| 2                  | 504456.         | 502472.                | 710.3              | 2.79                     |
| 3                  | 321624.         | 320891.                | 567.1              | 1.29                     |
| 4                  | 206902.         | 205211.                | 454.9              | 3.72                     |
| 5                  | 130722.         | 131505.                | 361.6              | -2.17                    |
| 6                  | 84581.          | 84534.                 | 290.8              | 0.16                     |
| 7                  | 53574.          | 54591.                 | 231.5              | -4.39                    |
| 8                  | 35537.          | 35493.                 | 188.5              | 0.23                     |
| 9                  | 23168.          | 23304.                 | 152.2              | -0.89                    |
| 10                 | 15341.          | 15514.                 | 123.9              | -1.40                    |
| 11                 | 10584.          | 10527.                 | 102.9              | 0.56                     |
| 12                 | 7519.           | 7325.                  | 86.7               | 2.24                     |
| 13                 | 5300.           | 5260.                  | 72.8               | 0.55                     |
| 14                 | 3947.           | 3919.                  | 62.8               | 0.45                     |
| 15                 | 3093.           | 3039.                  | 55.6               | 0.97                     |
| 16                 | 2435.           | 2454.                  | 49.3               | -0.38                    |
| 17                 | 1986.           | 2055.                  | 44.6               | -1.55                    |
| 18                 | 1795.           | 1776.                  | 42.4               | 0.44                     |

TABLE XIV (continued)

MEASURED AND CALCULATED DECAY DATA WITH STANDARD DEVIATIONS  
AND DIFFERENCES IN UNITS OF THE STANDARD DEVIATIONS

| CYLINDER NUMBER 12 |                 | -85 DEGREES CENTIGRADE |                    |                          |
|--------------------|-----------------|------------------------|--------------------|--------------------------|
| CHANNEL NUMBER     | OBSERVED COUNTS | CALCULATED COUNTS      | STANDARD DEVIATION | ERROR IN STD. DEV. UNITS |
| 1                  | 987010.         | 987288.                | 993.5              | -0.28                    |
| 2                  | 657538.         | 656921.                | 810.9              | 0.76                     |
| 3                  | 437303.         | 437800.                | 661.3              | -0.75                    |
| 4                  | 293261.         | 292333.                | 541.5              | 1.71                     |
| 5                  | 194928.         | 195662.                | 441.5              | -1.66                    |
| 6                  | 130736.         | 131342.                | 361.6              | -1.68                    |
| 7                  | 89232.          | 88487.                 | 298.7              | 2.49                     |
| 8                  | 59666.          | 59888.                 | 244.3              | -0.91                    |
| 9                  | 40628.          | 40769.                 | 201.6              | -0.70                    |
| 10                 | 28183.          | 27962.                 | 167.9              | 1.32                     |
| 11                 | 19499.          | 19361.                 | 139.6              | 0.99                     |
| 12                 | 13538.          | 13572.                 | 116.4              | -0.29                    |
| 13                 | 9665.           | 9662.                  | 98.3               | 0.03                     |
| 14                 | 7026.           | 7014.                  | 83.8               | 0.14                     |
| 15                 | 5169.           | 5213.                  | 71.9               | -0.61                    |
| 16                 | 3908.           | 3984.                  | 62.5               | -1.23                    |
| 17                 | 3084.           | 3141.                  | 55.5               | -1.04                    |
| 18                 | 2662.           | 2561.                  | 51.6               | 1.96                     |

APPENDIX D

## APPENDIX D

### ICE DENSITY MEASUREMENTS

The setup diagrammed in Figure 82 was placed in the freezer. The balance was an "Ohaus" two-pan type capable of an accuracy of 0.05 g. by using auxiliary weights. The weighing liquid was light mineral oil of density

$$P_L(20^{\circ}\text{C}) = 0.82 \pm 0.02 \text{ g./cm.}^3 \quad (\text{D-1})$$

as determined by a hygrometer. At  $-15^{\circ}\text{C}$  the calculated density was

$$P_L(-15^{\circ}\text{C}) = (0.86 \pm 0.025) \text{ g./cm.}^3 \quad (\text{D-2})$$

based on the cubical expansion coefficient of petroleum. Now, if

$W_A$  = weight of specimen in air,

$W_L$  = weight of specimen in oil,

$P_L$  = density of oil,

$P$  = density of specimen, and

$V$  = volume of specimen.

Then

$$W_A = VP; W_L = V(P - P_L) \quad (\text{D-3})$$

which gives

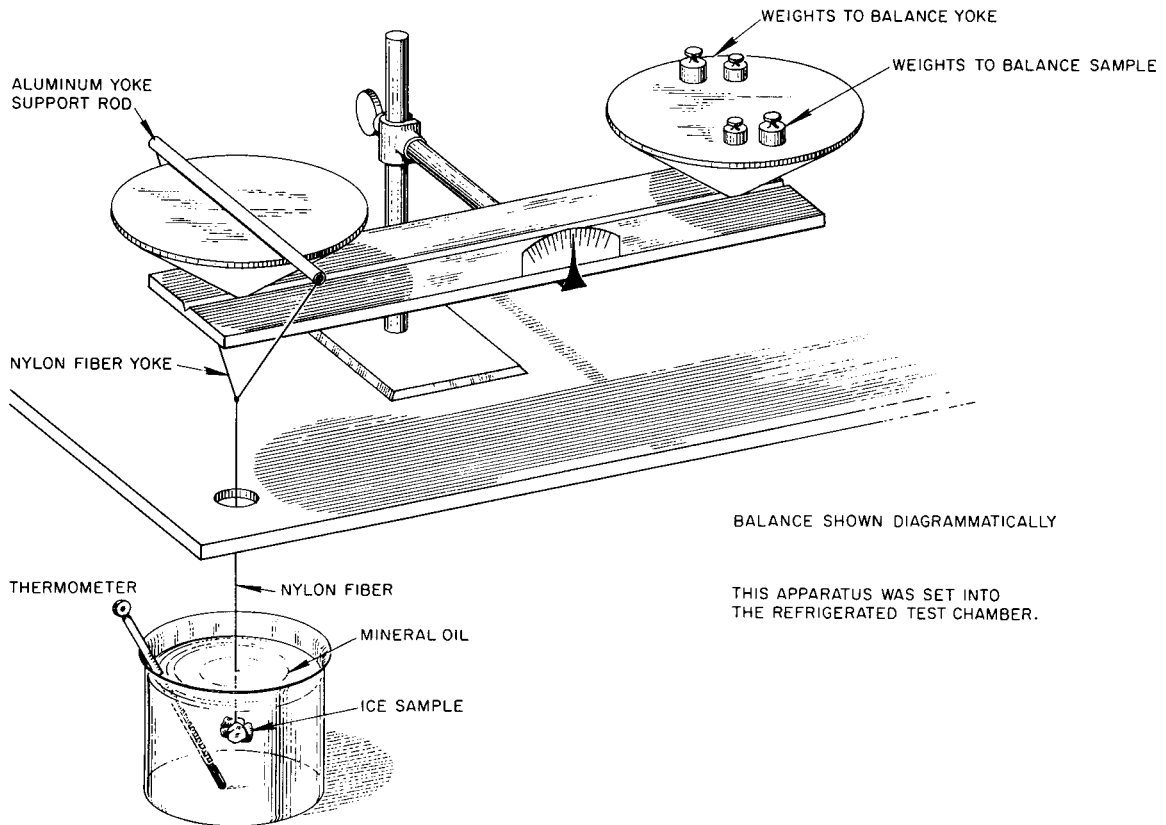


Figure 82. Diagram of apparatus for measurement of ice sample densities.

$$P = P_L \frac{W_A}{W_A - W_L} \cdot \quad (D-4)$$

The uncertainty of the oil viscosity was relatively large, but the relative density of two samples could be determined without this error since:

$$\frac{P(1)}{P(2)} = \frac{W_A(1) [W_A(2) - W_L(2)]}{W_A(2) [W_A(1) - W_L(1)]} \cdot \quad (D-5)$$

The weighing process in liquid was made difficult by the relatively high viscosity of the cold oil which made long balancing times necessary, and by the fact that opening and closing the freezer door always perturbed the balance. However, by careful manipulation of the freezer the results in Table XV were obtained.

The ice samples were suspended from the balance by a thin nylon fiber which was attached to the sample by simply placing a length of wet string (about 1- to 2-cm. long) in contact with the ice specimen. The string immediately froze firmly to the specimen at  $-15^{\circ}\text{C}$ . A drop of water was placed on the string and ice at the contact point to thicken the bonding layer of ice. No remeasurements on a single sample could be performed due to the difficulty of removing the oil after immersion.

The ice specimens came from the following sources:

Sample A: Large piece from central, top portion of cylinder

15-in. diam, 12-in. deep, frozen without pretreatment.

Sample B: Chip from bottom, outside of same cylinder.

Sample C: Place from white-appearing "cone" on axis of same cylinder from  $\approx 2.5$  in. down from top.

TABLE XV  
EXPERIMENTAL RELATIVE AND ABSOLUTE DENSITIES OF ICE SAMPLES

| Sample | Weight<br>(g.) | Absolute Density<br>(g./cm. <sup>3</sup> ) | Density Relative<br>to Sample F |
|--------|----------------|--|---------------------------------|
| A      | 98.7           | not measurable <sup>a</sup>                | <0.90                           |
| B      | 42.1           | 9.12 ± 0.30                                | 0.99 ± 0.01                     |
| C      | 33.3           | 8.39 ± 0.38                                | 0.91 ± 0.01                     |
| D      | 57.0           | 9.10 ± 0.23                                | 0.98 ± 0.01                     |
| E      | 39.9           | 9.12 ± 0.27                                | 0.99 ± 0.01                     |
| F      | 41.6           | 9.24 ± 0.28                                | 1.0                             |

<sup>a</sup>Sample A did not sink in the oil bath, so that its density is less than that of the oil. However, it maintained its location submerged due to the high viscosity. A subjective estimate was made that the density is very close to that of the oil.

Sample D: Chip from top center of a cylinder 10-in. diam, 12-in. high frozen by plug method (see Chapter II).

Sample E: Piece from bottom of same cylinder as Sample D.

Sample F: Piece from center of a small cylinder 4.5-in. diam, 5-in. high, grown by method for small cylinders described in Chapter II.

Within the error limits the densities of the densest samples (Samples B, E, and F) agreed with the theoretical density of ice,  $0.917 \text{ g./cm.}^3$ .

APPENDIX E

## APPENDIX E

APPLICATION OF THE CORNELL METHOD TO THE MODEL  $y = \alpha_0 + \alpha_1 e^{-\beta t}$

The discussion given here is taken from the paper by Cornell, (1956), for the case of a single exponential plus background, assuming also that only one observation of each datum is made.

Let the observed count in the  $i$ th channel be

$$y_i = \alpha_0 + \alpha_1 e^{-\beta t_i} + \epsilon_i, \quad (\text{E-1})$$

where  $\alpha_0$ ,  $\alpha_1$ , and  $\beta$  are the parameters to be fitted,  $t_i$  is the  $i$ th time of observation, and  $\epsilon_i$  is the error of the  $i$ th observation.

It is assumed that the number of observations is an integral multiple of the number of parameters; i.e., since there are three parameters

$$i = 0, 1, 2, \dots, (3n - 1) . \quad (\text{E-2})$$

Further, it is assumed that the times of observation are equally spaced, i.e.,

$$t_i = i(\Delta t); \quad i = 0, 1, 2, 3, \dots, (3n - 1) \quad (\text{E-3})$$

where  $\Delta t$  is the common time interval.

It is also assumed that the  $\epsilon_i$  are normally distributed with equal variances. Note that the latter condition is fulfilled only if the

counting statistics constitute a negligible source of the errors. In fact, this assumption would be strictly true only for an infinite number of counts obtained. However, in the present work the counting errors are very significant, and the Cornell method, therefore, gives too much relative weight to the later channels. However, this applies only to the calculation of the confidence intervals. The calculation of the parameter estimates requires only that the  $\epsilon_i$  are distributed with zero mean and finite variance. Note, however, that if the model is not a perfect fit to the data the mean of the errors need not be zero, and then the error in weight assignment will also affect the calculation of the estimated parameter values. Let

$$S_q = \sum_{i=(q-1)n}^{qn-1} y_i, \quad q = 1, 2, 3, \quad (E-4)$$

and let  $E(y_i)$  be the expected value of  $y_i$ , i.e.,

$$E(y_i) = \alpha_0 + \alpha_1 e^{-\beta t_i}. \quad (E-5)$$

Then

$$E(S_q) = \sum_{i=(q-1)n}^{qn-1} E(y_i), \quad q = 1, 2, 3, \quad (E-6)$$

so

$$\left. \begin{aligned}
 E(S_1) &= \sum_{i=0}^{n-1} \left[ \alpha_0 + \alpha_1 e^{-\beta t_i} \right] = n\alpha_0 + \alpha_1 \sum_{i=0}^{n-1} e^{-\beta t_i} \\
 E(S_2) &= n\alpha_0 + \alpha_1 \sum_{i=n}^{2n-1} e^{-\beta t_i} \\
 E(S_3) &= n\alpha_0 + \alpha_1 \sum_{i=2n}^{3n-1} e^{-\beta t_i} .
 \end{aligned} \right\} \quad (E-7)$$

Defining  $t_i \equiv i(\Delta t)$  and  $A \equiv e^{-(\Delta t)\beta}$ , one gets, setting the expected value equal to the observed value,

$$S_q = n\alpha_0 + \alpha_1 \sum_{i=n(q-1)}^{nq-1} A^i. \quad q = 1, 2, 3 \quad . \quad (E-8)$$

Now

$$\sum_{i=n(q-1)}^{nq-1} A^i = A^{n(q-1)} + A^{n(q-1)+1} + \dots + A^{nq-1} =$$

$$A^{n(q-1)} \left[ 1 + A + A^2 + \dots + A^{n-1} \right] = A^{n(q-1)} \frac{1 - A^n}{1 - A} \quad , \quad (E-9)$$

so

$$S_1 = n\alpha_0 + \frac{\alpha_1(1 - A^n)}{1 - A}; \quad S_2 = n\alpha_0 + \frac{\alpha_1 A^n(1 - A^n)}{1 - A}$$

$$S_2 = n\alpha_0 \frac{\alpha_1 A^{2n}(1 - A^n)}{1 - A} . \quad (E-10)$$

Then

$$S_1 - S_2 = \frac{\alpha_1}{1 - A} [(1 - A^n) - A^n(1 - A^n)] = \frac{\alpha_1(1 - A^n)^2}{1 - A} , \quad (E-11)$$

and

$$S_2 - S_3 = \frac{\alpha_1}{1 - A} [A^n(1 - A^n) - A^{2n}(1 - A^n)] = \frac{\alpha_1 A^n(1 - A^n)^2}{1 - A} . \quad (E-12)$$

Therefore

$$\frac{S_1 - S_2}{S_2 - S_3} = A^{-n} \quad (E-13)$$

or, taking logarithms,

$$-n \ln A = \ln \frac{S_1 - S_2}{S_2 - S_3} , \quad (E-14)$$

so that

$$n\beta\Delta t = \ln \frac{S_1 - S_2}{S_2 - S_3} . \quad (E-15)$$

So, designating the estimated value of  $\beta$  by  $\hat{\beta}$ :

$$\hat{\beta} = \frac{1}{n(\Delta t)} \ln \left( \frac{S_1 - S_2}{S_2 - S_3} \right) . \quad (\text{E-16})$$

To find  $\hat{\alpha}_0$ , note that

$$\begin{aligned} S_1 &= n\alpha_0 + \frac{\alpha_1(1 - A^n)}{1 - A} \\ &= n\alpha_0 + \frac{\alpha(1 - A^n)^2}{(1 - A)(1 - A^n)} \\ &= n\alpha_0 + \frac{S_1 - S_2}{1 - A^n} . \end{aligned} \quad (\text{E-17})$$

But

$$(1 - A^n) = \left( 1 - \frac{S_2 - S_3}{S_1 - S_2} \right) = \left( \frac{S_1 - 2S_2 + S_3}{S_1 - S_2} \right) , \quad (\text{E-18})$$

so

$$S_1 = n\alpha_0 + \frac{(S_1 - S_2)^2}{S_1 - 2S_2 + S_3} . \quad (\text{E-19})$$

and

$$\alpha_0 = \frac{1}{n} \left[ S_1 - \frac{(S_1 - S_2)^2}{S_1 - 2S_2 + S_3} \right] . \quad (\text{E-20})$$

In the same way  $\alpha_1$  is found by use of Equation (E-11) and noting that

$$1 - A = 1 - \left( \frac{s_2 - s_3}{s_1 - s_2} \right)^{1/n} \quad (\text{E-21})$$

and therefore

$$\hat{\alpha}_1 = (s_1 - s_2) \left[ 1 - \left( \frac{s_2 - s_3}{s_1 - s_2} \right)^{1/n} \right] / \left[ \frac{s_1 - 2s_2 + s_3}{s_1 - s_2} \right]^2. \quad (\text{E-22})$$

The variances of the estimates  $\hat{\alpha}_0$ ,  $\hat{\alpha}_1$ , and  $\hat{\beta}_1$  are as follows:

Let

$$s^2 = \frac{1}{3n - 3} \sum_{i=0}^{3n-1} (y_i - \bar{y})^2 \quad (\text{E-23})$$

and let

$$\eta_q = s_q/2 \quad .$$

Then

$$\text{Var } \beta = \frac{s^2}{n} \sum_{q=1}^3 a_q^2, \quad (\text{E-24})$$

where

$$\left. \begin{aligned} a_1 &= \frac{1}{(\Delta t) n(\eta_1 - \eta_2)} \\ a_2 &= \frac{(\eta_1 - \eta_3)}{(\Delta t) n(\eta_1 - \eta_2)(\eta_2 - \eta_3)} \\ a_3 &= \frac{1}{(\Delta t) n(\eta_2 - \eta_3)} \end{aligned} \right\} \quad (\text{E-25})$$

$$\text{Var } \alpha_o = \frac{s^2}{n} \sum_{q=1}^3 b_q^2 \quad (\text{E-26})$$

where

$$\left. \begin{aligned} b_1 &= \frac{(\eta_2 - \eta_3)^2}{(\eta_1 - 2\eta_2 + \eta_3)^2} \\ b_2 &= \frac{2(\eta_1 - \eta_2)(\eta_2 - \eta_3)}{(\eta_1 - 2\eta_2 + \eta_3)^2} \\ b_3 &= \frac{(\eta_1 - \eta_2)^2}{(\eta_1 - 2\eta_2 + \eta_3)^2} \end{aligned} \right\} \quad (\text{E-27})$$

where

$$\left. \begin{aligned}
 c_1 &= \frac{1}{(1-x)^3} \left[ (1-x) x^{1/n} + n(1-3x)(1-x^{1/n}) \right] \\
 c_2 &= \frac{1}{x(1-x)^3} \left[ nx(1-3x)(1-x^{1/n}) - (1-x)(1+x) x^{1/n} \right] \\
 c_3 &= \frac{1}{x(1-x)^3} \left[ (1-x) x^{1/n} - 2nx(1-x^{1/n}) \right] ,
 \end{aligned} \right\} \text{(E-29)}$$

where

$$x = \frac{S_2 - S_3}{S_1 - S_2} .$$

It is seen that the calculation of the parameter estimates is simple, but the calculations of the variances are laborious, though straight-forward.

APPENDIX F

## APPENDIX F

### CONVERGENCE TESTS ON ARTIFICIAL DATA

In order to determine whether the difficulties with convergence of the small-cylinder decay data using five independent parameters were due to the nature of the model to be fitted or to other causes, a set of artificial decay data of known composition was constructed.

The equation used to construct the data was as follows:

$$C_n = P_1 + P_2 \exp [- n(\Delta t) P_3] + P_4 \exp [- n(\Delta t) P_5] \quad . \quad (F-1)$$

The parameters were assigned the following values:

$$P_1 = 2 \times 10^3$$

$$P_2 = 1 \times 10^6$$

$$P_3 = 10 \times 10^3 \text{ sec.}^{-1}$$

$$P_4 = 1.0 \times 10^5$$

$$P_5 = 15.0 \times 10^3 \text{ sec.}^{-1}$$

$$\Delta t = 40 \text{ } \mu\text{sec.}$$

Table XVI gives the values of  $C_n$  and  $\sqrt{C_n}$  obtained using these parameters.

Then a table of normally distributed random numbers, with zero mean and unit variance, (Dixon and Massey, 1952), was used to construct five sets of "data" including statistical errors. The equation used was

$$S_n = C_n + N_R \sqrt{C_n} \quad (F-2)$$

TABLE XVI

## COMPOSITION OF ARTIFICIAL DECAY DATA FOR CONVERGENCE TESTS

| $n$ | $n(\Delta t)P_3$ | $P_2 e^{-n(\Delta t)P_3}$ | $n(\Delta t)P_5$ | $P_4 e^{-n(\Delta t)P_5}$ | $C_n$     | $(C_n)^{\frac{1}{n}}$ |
|-----|------------------|---------------------------|------------------|---------------------------|-----------|-----------------------|
| 0   | 0.0              | 1,000,000                 | 0.0              | 100,000                   | 1,102,000 | 1050                  |
| 1   | 0.4              | 670,320                   | 0.6              | 54,881                    | 727,201   | 853                   |
| 2   | 0.8              | 449,329                   | 1.2              | 30,119                    | 481,448   | 694                   |
| 3   | 1.2              | 301,194                   | 1.8              | 16,530                    | 319,724   | 565                   |
| 4   | 1.6              | 201,897                   | 2.4              | 9,072                     | 212,969   | 461                   |
| 5   | 2.0              | 135,335                   | 3.0              | 4,979                     | 142,314   | 377                   |
| 6   | 2.4              | 90,718                    | 3.6              | 2,732                     | 95,450    | 309                   |
| 7   | 2.8              | 60,810                    | 4.2              | 1,500                     | 64,310    | 253                   |
| 8   | 3.2              | 40,762                    | 4.8              | 823                       | 43,585    | 209                   |
| 9   | 3.6              | 27,324                    | 5.4              | 452                       | 29,776    | 173                   |
| 10  | 4.0              | 18,316                    | 6.0              | 248                       | 20,564    | 143                   |
| 11  | 4.4              | 12,277                    | 6.6              | 136                       | 14,413    | 120                   |
| 12  | 4.8              | 8,230                     | 7.2              | 75                        | 10,305    | 101                   |
| 13  | 5.2              | 5,516                     | 7.8              | 41                        | 7,557     | 87                    |
| 14  | 5.6              | 3,698                     | 8.4              | 22                        | 5,720     | 76                    |
| 15  | 6.0              | 2,479                     | 9.0              | 12                        | 4,491     | 67                    |
| 16  | 6.4              | 1,661                     | 9.6              | 7                         | 3,668     | 61                    |
| 17  | 6.8              | 1,114                     | 10.2             | 4                         | 3,118     | 56                    |

where  $S_n$  is the channel count number, and  $N_R$  is a randomly selected number from the table. The resulting sets of decay data are listed on Table XVII.

Table XVIII gives the results of five-parameter analyses of these five sets of data by the Busing-Levy Least Squares Code (Busing and Levy, 1962). The initial guesses of parameters  $P_1$ ,  $P_2$ ,  $P_3$ , and  $P_4$  were the correct values, and the initial guess for  $P_5$  was set at  $17 \times 10^3 \text{ sec.}^{-1}$ .

It will be observed that in this case, with no effects other than randomly distributed counting statistics, the convergence requires a large number of iterations in some cases, and fails altogether in many instances. When convergence does occur, the values found for the parameters, and in particular for the dominant decay frequency,  $P_3$ , vary significantly from case to case, even though the true data is the same. In the first set, in the analysis of all eighteen channels a cross-over occurred, that is, the dominant decay shifted to parameters  $P_4$  and  $P_5$  whereas it was initially in parameters  $P_2$  and  $P_3$ .

When the same analysis was used with the set of numbers  $C_n$ , i.e., without use of randomly distributed statistical errors, then reasonably rapid convergence was obtained and parameter values very close to the correct ones were obtained. These results are listed at the bottom of Table XVIII.

As stated in the body of the present work, the convergence difficulty was circumvented by performing a series of calculations, holding  $P_5$  fixed for each one at a different value. For this purpose the Busing-Levy code (Busing and Levy, 1962) was modified to perform automatically

TABLE XVII

FIVE SETS OF ARTIFICIAL DECAY DATA INCLUDING RANDOM COUNTING ERRORS

| n  | $S_1$     | $S_2$     | $S_3$     | $S_4$     | $S_5$     |
|----|-----------|-----------|-----------|-----------|-----------|
| 0  | 1,103,137 | 1,100,775 | 1,101,997 | 1,101,235 | 1,101,098 |
| 1  | 726,695   | 726,280   | 726,527   | 726,948   | 727,004   |
| 2  | 480,898   | 482,070   | 482,259   | 481,524   | 483,045   |
| 3  | 319,302   | 320,584   | 320,736   | 319,554   | 319,731   |
| 4  | 212,988   | 212,526   | 213,164   | 212,314   | 214,121   |
| 5  | 141,942   | 141,859   | 142,465   | 141,834   | 142,335   |
| 6  | 95,588    | 95,440    | 95,450    | 94,782    | 94,868    |
| 7  | 64,330    | 64,671    | 64,306    | 64,407    | 64,777    |
| 8  | 43,464    | 43,454    | 43,676    | 43,781    | 43,499    |
| 9  | 29,835    | 29,734    | 29,705    | 29,482    | 29,566    |
| 10 | 20,594    | 20,561    | 20,492    | 20,761    | 20,399    |
| 11 | 14,422    | 14,358    | 14,250    | 14,495    | 14,322    |
| 12 | 10,252    | 10,374    | 10,233    | 10,366    | 10,109    |
| 13 | 7,514     | 7,569     | 7,578     | 7,569     | 7,523     |
| 14 | 5,619     | 5,705     | 5,727     | 5,672     | 5,826     |
| 15 | 4,525     | 4,543     | 4,597     | 4,512     | 4,524     |
| 16 | 3,641     | 3,750     | 3,631     | 3,727     | 3,708     |
| 17 | 3,068     | 3,200     | 3,103     | 3,003     | 3,106     |

TABLE XVIII  
RESULTS OF FIVE-PARAMETER ANALYSES OF THE ARTIFICIAL DECAY DATA

| Data Set | Channels Analyzed | Number of Iterations | $P_1$<br>( $\times 10^3$ ) | $P_2$<br>( $\times 10^6$ ) | $P_3$<br>( $\times 10^4$ ) | $P_4$<br>( $\times 10^5$ ) | $P_5$<br>( $\times 10^4$ ) |
|----------|-------------------|----------------------|----------------------------|----------------------------|----------------------------|----------------------------|----------------------------|
| $S_1$    | 1-18              | 49                   | 0.615                      | 0.006                      | 0.207                      | 11.090                     | 1.042                      |
|          | 1-15              | 69                   | Matrix Singularity         | Occurred                   | No                         | Convergence                |                            |
|          | 2-16              | 9                    | 2.087                      | 1.071                      | 1.016                      | 5.995                      | 6.360                      |
|          | 3-17              | 4                    | 1.988                      | 1.034                      | 1.006                      | 0.683                      | 1.790                      |
|          | 4-18              | 4                    | 1.967                      | 1.023                      | 1.003                      | 0.787                      | 1.692                      |
| $S_2$    | 1-18              | 6                    | 2.092                      | 1.019                      | 1.005                      | 0.798                      | 1.515                      |
|          | 1-15              | 31                   | 1.959                      | 8.711                      | 0.981                      | 2.274                      | 1.269                      |
|          | 2-16              | 57                   | 1.957                      | 3.950                      | 0.917                      | 7.003                      | 1.103                      |
|          | 3-17              | 79                   | Matrix Singularity         | Occurred                   | No                         | Convergence                |                            |
|          | 4-18              | 17                   | 2.112                      | 1.062                      | 1.013                      | 20.808                     | 5.250                      |
| $S_3$    | 1-18              | 5                    | 2.059                      | 1.055                      | 1.012                      | 0.446                      | 1.823                      |
|          | 1-15              | 9                    | 2.139                      | 1.073                      | 1.017                      | 0.265                      | 2.285                      |
|          | 2-16              | 8                    | 2.155                      | 1.058                      | 1.015                      | 0.375                      | 1.629                      |
|          | 3-17              | 7                    | 2.058                      | 1.021                      | 1.006                      | 0.783                      | 1.483                      |
|          | 4-18              | 11                   | 2.053                      | 1.059                      | 1.013                      | 1.013                      | 2.620                      |
| $S_4$    | 1-18              | 66                   | 1.805                      | 2.526                      | 0.853                      | 8.468                      | 1.098                      |
|          | 1-15              | >100                 | No Convergence             | After                      | Maximum                    | Number of                  | Iterations                 |
|          | 2-16              | 64                   | 1.771                      | 2.274                      | 0.841                      | 8.719                      | 1.093                      |
|          | 3-17              | 5                    | 1.985                      | 9.680                      | 0.992                      | 1.411                      | 1.513                      |
|          | 4-18              | 6                    | Matrix Singularity         | Occurred                   | No                         | Convergence                |                            |
| $S_5$    | 1-18              | 4                    | 2.090                      | 1.058                      | 1.014                      | 0.406                      | 1.747                      |
|          | 1-15              | 9                    | 2.192                      | 1.079                      | 1.020                      | 0.202                      | 2.307                      |
|          | 2-16              | 4                    | 2.154                      | 1.067                      | 1.017                      | 0.300                      | 1.741                      |
|          | 3-17              | >100                 | No Convergence             | After                      | Maximum                    | Number of                  | Iterations                 |
|          | 4-18              | 9                    | Matrix Singularity         | Occurred                   | No                         | Convergence                |                            |
| $C_n$    | 1-18              | 21                   | 1.998                      | 0.996                      | 0.999                      | 1.034                      | 1.489                      |
|          | 1-15              | 18                   | 1.994                      | 0.994                      | 0.999                      | 1.058                      | 1.482                      |
|          | 2-16              | 8                    | 1.993                      | 0.991                      | 0.998                      | 1.084                      | 1.472                      |
|          | 3-17              | 7                    | 1.994                      | 0.990                      | 0.998                      | 1.096                      | 1.465                      |
|          | 4-18              | 8                    | 1.997                      | 0.994                      | 0.990                      | 1.055                      | 1.480                      |

the operation of advancing the fixed value of  $P_5$  from case to case by a given amount and for a specified number of cases. The value of  $\Sigma^2$ , the sum of the squares of the residuals was found to vary from case to case depending on the value of  $P_5$ . For each set a minimum value of  $\Sigma^2$  was obtained for one choice of  $P_5$ , and the parameters corresponding to this fit were chosen as best values. In this fashion the results of Table XIX were obtained. It will be seen that with this procedure the convergence was very rapid, and even with the test data, in which the second decay component differed in frequency by only a factor of 1.5 from the main component, the values found for  $P_3$  were close to the true values in most cases. Where the value of  $P_3$  differed from the correct value the statistical weight was also low.

TABLE XIX

RESULTS OF FOUR-PARAMETER ANALYSES OF ARTIFICIAL DECAY DATA, WITH  
PARAMETER SEARCH FOR  $P_5$  TO MINIMIZE SQUARE SUM OF RESIDUALS

| Data Set | Channels Analyzed | Number of Iterations | $P_1$<br>( $\times 10^3$ ) | $P_2$<br>( $\times 10^6$ ) | $P_3$<br>( $\times 10^4$ ) | Weight of $P_3$<br>( $\times 10^8$ ) | $P_4$<br>( $\times 10^5$ ) | Value of $P_5$<br>( $\times 10^4$ ) yielding<br>Minimum $\Sigma^2$ | Minimum<br>Value of $\Sigma^2$ |
|----------|-------------------|----------------------|----------------------------|----------------------------|----------------------------|--------------------------------------|----------------------------|--|--------------------------------|
| $S_1$    | 1-18              | 4                    | 1.971                      | 1.026                      | 1.004                      | 17.9                                 | 7.474                      | 1.70   | 0.27                           |
|          | 1-15              | 4                    | 1.853                      | 0.979                      | 0.993                      | 6.31                                 | 1.220                      | 1.50   | 0.18                           |
|          | 2-16              | 4                    | 1.984                      | 1.028                      | 1.005                      | 7.20                                 | 0.730                      | 1.70   | 0.33                           |
|          | 3-17              | 4                    | 1.989                      | 1.035                      | 1.006                      | 5.68                                 | 0.678                      | 1.80   | 0.33                           |
|          | 4-18              | 4                    | 1.968                      | 1.024                      | 1.003                      | 2.91                                 | 0.783                      | 1.70   | 0.34                           |
| $S_2$    | 1-18              | 4                    | 2.090                      | 1.015                      | 1.005                      | 10.3                                 | 0.832                      | 1.50   | 0.69                           |
|          | 1-15              | 5                    | 1.949                      | 0.843                      | 0.978                      | 1.63                                 | 2.551                      | 1.25   | 0.81                           |
|          | 2-16              | 10                   | 1.960                      | 0.376                      | 0.913                      | 0.14                                 | 0.719                      | 1.10   | 0.78                           |
|          | 3-17              | 4                    | 2.081                      | 1.037                      | 1.008                      | 5.61                                 | 0.727                      | 1.80   | 0.69                           |
|          | 4-18              | 4                    | 2.093                      | 1.052                      | 1.010                      | 8.25                                 | 1.084                      | 2.40   | 0.53                           |
| $S_3$    | 1-18              | 4                    | 2.057                      | 1.054                      | 1.011                      | 21.7                                 | 0.461                      | 1.80   | 0.55                           |
|          | 1-15              | 4                    | 2.131                      | 1.071                      | 1.018                      | 26.5                                 | 0.283                      | 2.25   | 0.33                           |
|          | 2-16              | 4                    | 2.157                      | 1.059                      | 1.015                      | 6.32                                 | 0.361                      | 1.65   | 0.31                           |
|          | 3-17              | 4                    | 2.060                      | 1.024                      | 1.007                      | 2.58                                 | 0.755                      | 1.50   | 0.48                           |
|          | 4-18              | 4                    | 2.045                      | 1.053                      | 1.011                      | 6.95                                 | 0.801                      | 2.25   | 0.48                           |
| $S_4$    | 1-18              | 12                   | 1.808                      | 0.264                      | 0.857                      | 0.38                                 | 8.356                      | 1.10   | 0.95                           |
|          | 1-15              | 5                    | 1.407                      | 1.040                      | 1.062                      | 0.57                                 | 0.593                      | 0.65   | 0.79                           |
|          | 2-16              | 8                    | 1.779                      | 0.851                      | 1.098                      | 0.71                                 | 2.486                      | 0.85   | 0.90                           |
|          | 3-17              | 4                    | 1.983                      | 0.964                      | 0.992                      | 2.59                                 | 1.448                      | 1.50   | 0.95                           |
|          | 4-18              | 4                    | 1.897                      | 0.945                      | 0.985                      | 1.98                                 | 1.794                      | 1.55   | 1.13                           |
| $S_5$    | 1-18              | 4                    | 2.090                      | 1.058                      | 1.014                      | 19.7                                 | 0.404                      | 1.75   | 1.42                           |
|          | 1-15              | 4                    | 2.180                      | 1.076                      | 1.019                      | 23.0                                 | 0.229                      | 2.15   | 1.62                           |
|          | 2-16              | 4                    | 2.155                      | 1.067                      | 1.017                      | 7.96                                 | 0.297                      | 1.75   | 1.62                           |
|          | 3-17              | 4                    | 2.133                      | 1.077                      | 1.020                      | 10.3                                 | 0.379                      | 2.35   | 1.54                           |
|          | 4-18              | 4                    | 2.014                      | 1.082                      | 1.023                      | 2.85                                 | 0.050                      | 0.45   | 1.53                           |
| $C_n$    | 1-18              | 8                    | 2.007                      | 1.011                      | 1.002                      | 10.4                                 | 0.882                      | 1.50   | 0.00                           |
|          | 1-15              | 5                    | 2.000                      | 1.000                      | 1.000                      | 6.26                                 | 1.003                      | 1.50   | 0.00                           |
|          | 2-16              | 4                    | 1.989                      | 0.985                      | 0.997                      | 3.37                                 | 1.151                      | 1.45   | 0.00                           |
|          | 3-17              | 6                    | 1.992                      | 0.986                      | 0.998                      | 2.16                                 | 1.136                      | 1.45   | 0.00                           |
|          | 4-18              | 4                    | 1.997                      | 0.991                      | 0.999                      | 1.65                                 | 1.182                      | 1.50   | 0.00                           |

APPENDIX G

## APPENDIX G

### FORTRAN CODES WRITTEN FOR THE DATA ANALYSIS

Two FORTRAN programs were written by the author and used in the data reduction for this work, and a third code was written for this work by P. Emmett of the Oak Ridge National Laboratory Mathematics Division and subsequently modified by the author. These codes are for the IBM-7090 computer.

The first code, THESDA, was written to produce the table of Appendix C, and to obtain the distribution of the residuals shown in Figure 50. The input consisted of a deck of 1080 data cards, one card for each channel, listing the counts in each channel and a deck of sixty parameter cards listing the channel widths and the parameters found for each decay. Figure 83 is a flow chart for THESDA.

The second code, CALER, was written to compute the errors of the decay parameters, using the equations shown in Chapter IV. Its input consists of a deck of sixty cards listing the values of  $P_3$ , with their variances, for the calculations using (1) all eighteen channels, (2) the even-numbered channels, (3) the odd-numbered channels, (4) channels 1-15, and (5) channels 4-18, for each cylinder and temperature. Figure 84 is the flow chart for CALER. The code called BIFT LEAST SQUARES utilizes an existing code BIFIT as subroutine to calculate the diffusion parameters from the decay frequencies and dimensions. This code will also be shown. Figure 85 is the flow chart for BIFT LEAST SQUARES, considerably simplified.

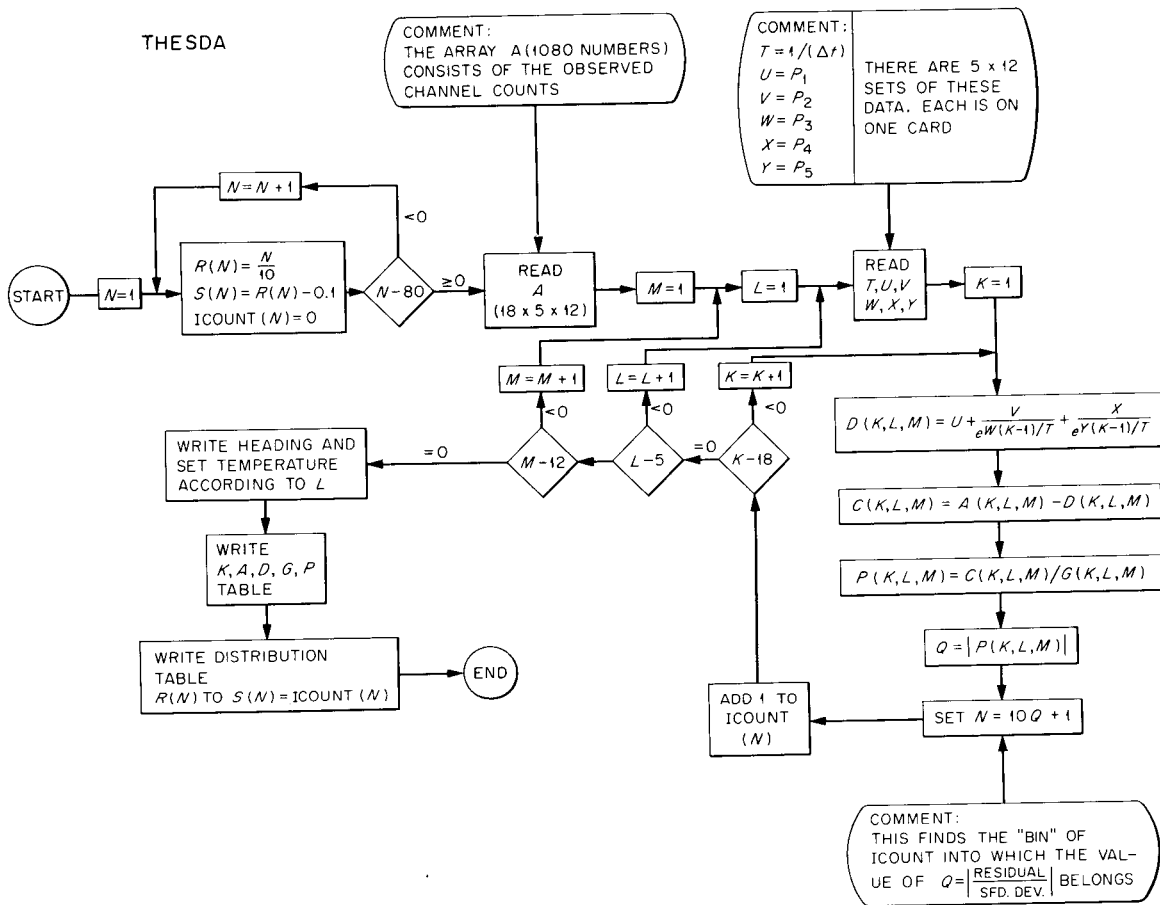


Figure 83. Flow chart of code THESDA.

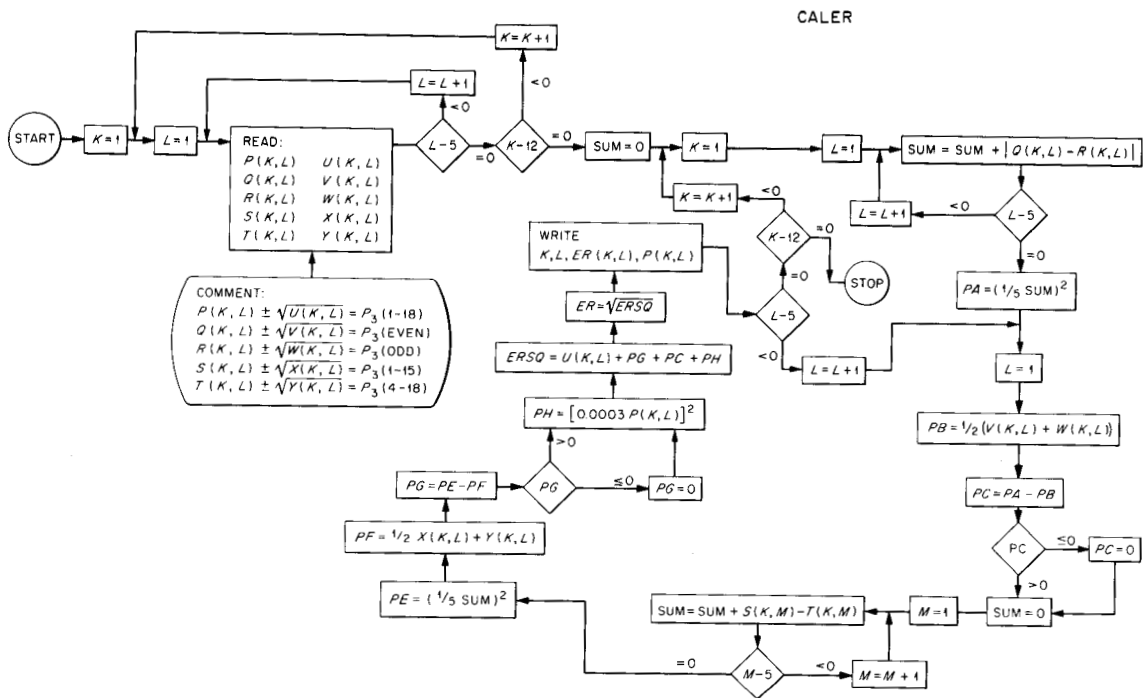


Figure 84. Flow chart of code CALER.

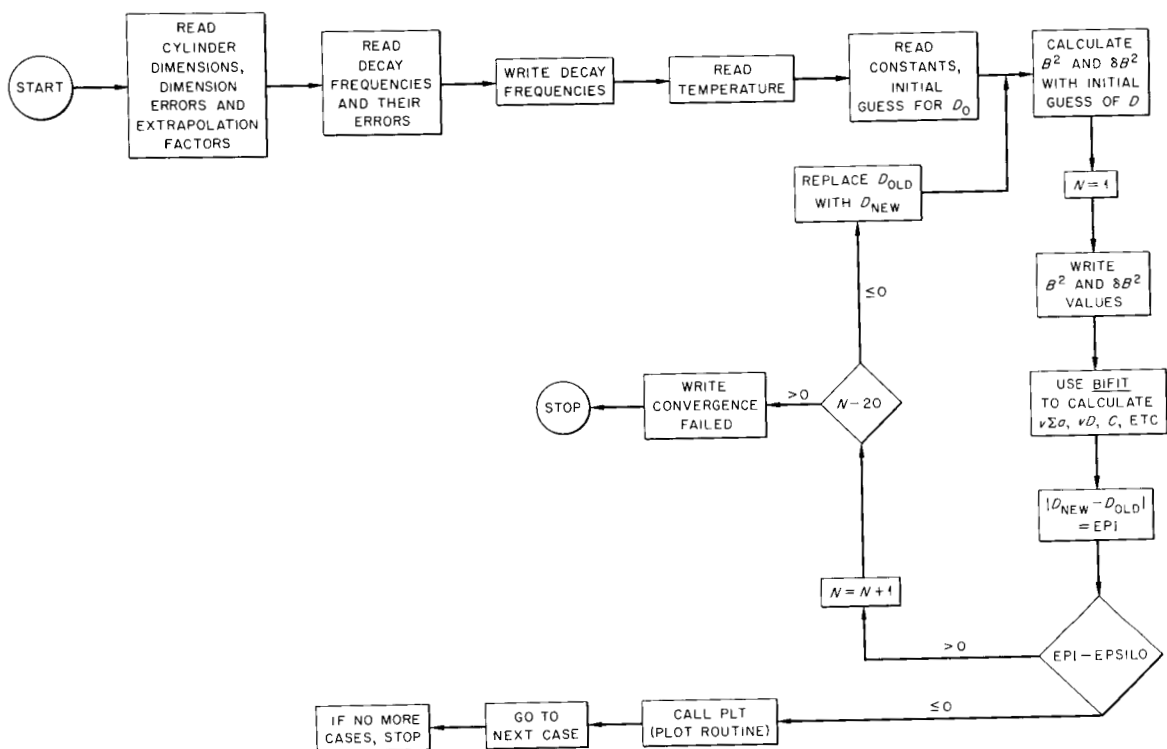


Figure 85. Simplified flow chart of code BIFT LEAST SQUARES.

## FORTRAN CODE THESDA

```

1  DIMENSION  A(18,5,12),  D(18,5,12),  P(18,5,12),  G(18,5,12),  ICOUNT(80)
1      R(80),S(80),  C(18,5,12)

2  FORMAT (30X,E12.5)

3  FORMAT (7E10.5)

4  FORMAT (1H3/      10X,59HMEASURED AND CALCULATED DECAY DATA WITH STAN
1  DARD DEVIATIONS/14X,51HAND DIFFERENCES IN UNITS OF THE STANDARD DE
1  VIATIONS)

5  FORMAT (1H)/16X,15CYLINDER NUMBER, I3, I12, 1X, 18HDEGREES CENTIGRADE/
1  1H)/ 9X, 7HCHANNEL, 3X, 'HOBSERVED, 4X, 10HCALCULATED, 3X, 8HSTANDARD, 3X
1  , 13HERROR IN STD./ 9X, 6HNUMBER, 5X, 6HCOUNTS, 7X, 6HCOUNTS, 5X, 9HDEVIAT
1  ION, 3X, 10HDEV. UNITS)

6  FORMAT (1H0, 9X, I2, 7X, F8.0, 5X, F6.1, 7X, F5.2)

7  FORMAT (1H1/33X, 18HERROR DISTRIBUTION/1H0)

8  FORMAT (15X, F3.1, 4H to , F3.1, I8, 18X, F3.1, 4H to , F3.18)

      DO 9 N=1,80                                (This DO-loop sets up the bins for
      R(N) = (FLOATF(N))*0.10                      calculating the distribution of
      S(N) = R(N) - 0.10                          residuals)

9  ICOUNT(N) = 0

10  READ INPUT TAPE 10,2,A

      DO 50 M = 1,12                               (This double loop reads the
      DO 50 L = 1,5                                 parameter deck)

      READ INPUT TAPE 10,3,T,U,V,W,X,Y

      DO 50 K = 1,18

      D(K,L,M) = U+V/EXPF(W*(FLOATF(K-1))/T)+X/EXPF(Y*(FLOATF(K-1))/T)
      C(K,L,M) = A(K,L,M) - D(K,L,M)    (C(K,L,M) are the residuals)

```

```

G(K,L,M) = SQRTF(D(K,L,M))
P(K,L,M) =C(K,L,M)/G(K,L,M)      (P(K,L,M) are the residuals in units
Q = ABSF(P(K,L,M))              of G(K,L,M), the standard deviations)
N = 10.*Q+1
50 ICOUNT(N) = (COUNT(N)+1      (Here the histogram is "filled")
DO 102 M = 1,12
DO 102 L = 1,5
WRITE OUTPUT TAPE 9,4
IF(L-1) 61,61,62
61 ( = -5
GO TO 100
62 IF(L-2) 63,63,64
63 I = -25
GO TO 100
64 IF(L-3) 65,65,68
65 IF(M-9) 66,67,66              (This IF takes care of labeling the
66 I = -45                      case of Cylinder 9 which was measured
GO TO 100                       at -50°C rather than at -45°C)
67 I = -50
GO TO 100
68 IF(L-4) 69,69,70
69 I = -65
GO TO 100
70 I = -85
100 WRITE OUTPUT TAPE 9,5,M,I

```

```
DO 102 K = 1,18
102 WRITE OUTPUT TAPE 9,6,K,A(K,L,M), D(K,L,M), G(K,L,M),P(K,L,M)
    WRITE OUTPUT TAPE 9,7
    DO 105 N = 1,35                (This DO-loop lists the distribution
                                table)
105 WRITE OUTPUT TAPE 9,8,S(N),R(N),ICOUNT(N),S(N+35),R(N+35),ICOUNT(
1 N+35)
    CALL EXIT
END
```

## FORMAT CODE CALER

```

1  FORMAT (10E8.5)
3  FORMAT (1H0,5X,I6,I6,E8.5,5X,E8.5)
   DIMENSION P(12,5),Q(12,5),R(12,5),S(12,5),T(12,5),U(12,5)
1  V(12,5), W(12,5),X(12,5), Y(12,5), ER(12 5)
   DO 50 K = 1,12                (This double DO-loop reads in the
   DO 50 L = 1,5                  values of P3 and the variances)
50  READ INPUT TAPE 10,1 P(K,L) U(K,L),Q(K,L),V(K,L) R(K,L),
1  W(K,L),S(K,L) X(K,L) T(K,L),Y(K,L)
   SUM = 0
   DO 66 K = 1,12
   DO 52 L = 1,5
52  SUM = SUM+ABSF(Q(K,L) * R(K,L))
   PA = (SUM * 0.1) ** 2
   DO 66 L = 1,5
   PB = (V(K,L)+W(K,L)) * 0.5
   PC = PA - PB                    PC ≡ (Er)2
   IF(PC) 53,53,58
53  PC = 0
58  SUM = 0
   DO 59 M = 1,5
59  SUM = SUM+S(K,M) - T(K,M)
   PE = (SUM * 0.1) ** 2
   PF = (X(K,L) + Y(K,L)) * 0.5

```

```
PG = PE - PF                                PG ≡ (Ep)2
IF(PG) 62,62,63
62 PG = 0
63 PH = (P(K,L) * 0.0003) ** s
64 ERSQ = U(K L) + PG + PC + PH
65 ER(K,L) = SQRTF(ERSQ)
66 WRITE OUTPUT TAPE 9,3, K, L, ER(K,L), P(K,L)
CALL EXIT
END
```

## FORTRAN CODE BIFIT LEAST SQUARES

```

CBIFIT LEAST SQUARES CODE
C   E. G. SILVER PROBLEM
C   UPDATED VERSION. EXTRAPOLATION DIST. CORRECTION PAR-
C   AMETERS ARE CALLED FOR IN BOTH DIMENSIONS.
C   7 NUMBERS ARE REQUIRED ON DIMENSION-DATA CARDS.
   DIMENSION X(100),Y(100),DELX(100),DELY(100),H(100),DE
1 LH(100),R(100),DELR(100),EL(100),CAY(100),S(100),ANS(
28),XRES(100),YRES(100),ELN(8,8),XLAMB(100),ERRM(8,8),
3 STDEP(8),R2(100),DHSQ(100),DNO(100),YC(100),EM(100)
   DIMENSION A(6),Y2(100)
   DIMENSION TABLE(250),TAB(250)
102 READ INPUT TAPE 10,1,I
   NT#0
   1 FORMAT(I4)
   READ INPUT TAPE 10,2,(H(J),DELH(J),EM(J),R(J),DELR(J)
1,EL(J),DNO(J),J#1,I)
   2,J#1,I)
   2 FORMAT(6E10.5,E9.3)
   READ INPUT TAPE 10,9,(Y(J),DELY(J),J#1,I)
9   FORMAT(2E12.5)
   WRITE OUTPUT TAPE 9,104,(Y(J),J#1,I)
104 FORMAT(1H0,10HOBSERVED Y/(1H ,8F12.5))
   READ INPUT TAPE 10,2,T
   READ INPUT TAPE 10,3,D,EPSILO ,C1,C2,C3,C4,C5,J1
   3 FORMAT(7E9.3,I4)
   CSQ3#C3*C3
   CSQ4#C4*C4
   CQ3#CSQ3**2
   CQ4#CSQ4**2
   DO 12 N#1,I
   DHSQ(N) # DELH(N)**2
12  R2(N) # DELR(N)**2
   5 DO 10 N#1,I
   CAY(N)#H(N)+C1*D*EM(N)
   H2#CAY(N)**2
   S(N)#R(N)+C2*D*EL(N)
   S2#S(N)**2
   X(N)#(CSQ3/H2)+(CSQ4/S2)
10  DELX(N)#2.*SQRTF((CQ3/(H2*H2*H2))*DHSQ(N) +(CQ4/(S2*S
12*S2))*R2(N))
   WRITE OUTPUT TAPE 9,101,(X(MI),DELX(MI),MI#1,I)
101 FORMAT(1H0,6X1HX,15X,4HDELX/(1H ,E12.5,6X,E12.5))
   K#J1-1
   CALL BIFIT(X,Y,DELX,DELY,I,K,ANS,WSUM,XRES,YRES,
1 ELN,ERRM,XLAMB, STDEP,NERR)
   IF(NERR)7,6,8

```

```

6 D2#C5*ANS(2)/SQRT(T)
  DO 22 M#1,I
    YC(M)#D.
    DO 22 N#1,J1
22 YC(M)#YC(M)+ANS(N)*(X(M)**(N-1))
    WRITE OUTPUT TAPE 9,205,(YC(M),DNO(M),M#1,I)
205 FORMAT(1H0,12HCALCULATED Y ,10X,10HIDENTIFIER/(1H ,E1
12.5,7X,E12.3))
    WRITE OUTPUT TAPE 9,206,(ANS(L),L#1,J1)
206 FORMAT(1H0,23HCOMPUTED FIT PARAMETERS/(1H ,
18E12.5))
    WRITE OUTPUT TAPE 9,207,(STDEP(L),L#1,J1)
207 FORMAT(1H0,25HCOMPUTED PARAMETER ERRORS/(1H ,8E12.5))
    WRITE OUTPUT TAPE 9,208,D
208 FORMAT(3H0D# E12.5)
    EPI#ABSF(D2-D)/D2
    IF(EPI-EPSILO )20,20,30
30 D#D2
    NT#NT+1
    IF(NT-20)5,5,11
11 WRITE OUTPUT TAPE 9,201
201 FORMAT(35H CONVERGENCE FAILED AFTER 20 TRIES.)
    CALL EXIT
7 WRITE OUTPUT TAPE 9,202
202 FORMAT(21H TOO MANY DATA POINTS)
    CALL FXIT
8 WRITE OUTPUT TAPE 9,203
203 FORMAT(25H THE MATRIX WAS SINGULAR.)
20 GO TO 102
END

```

1

## DISTRIBUTION

- 1-3. E. P. Blizard
4. G. deSaussure
5. F. C. Maienschein
6. J. T. Mihalczko
7. R. W. Peelle
- 8-17. E. G. Silver
18. G. Dessauer (consultant)
19. M. L. Goldberger (consultant)
20. R. F. Taschek (consultant)
- 21-22. Central Research Library
23. Document Reference Section
- 24-50. Laboratory Records Department
51. Laboratory Records, ORNL, R.C.
52. ORNL Patent Office
- 53-67. Division of Technical Information Extension (DTIE)
68. Research and Development Division (ORO)

